ARIZONA DEPARTMENT OF TRANSPORTATION

REPORT NUMBER: AZ92-344

DEVELOPMENT OF SEISMIC ACCELERATION CONTOUR MAPS FOR ARIZONA

Final Report

Prepared by:
Kenneth M. Euge
Bruce A. Schell
Geological Consultants
2333 West Northern Avenue
Phoenix, AZ 85021

Ignatious Po Lam
Earth Mechanics Inc.
17660 Newhope Street
Fountain Valley, CA 92708

September 1992

Prepared for:
Arizona Department of Transportation
206 South 17th Avenue
Phoenix, Arizona 85007
in cooperation with
U.S. Department of Transportation
Federal Highway Administration

Technical Report Documentation Page

1. Report No.	2. Government Accession No.	3. Recipient's Catalog No.
FHWA-AZ92-344		

4. Title and Subtitle	5. Report Date
Development of Seismic Acceleration Contour Maps for Arizona Final Report	September 1992
	6. Performing Organization Code

7. Author	8. Performing Organization Report No.
Kenneth M. Euge, Bruce A. Schell, Ignatious Po Lam	91-106

9. Performing Organization Name and Address	10. Work Unit No.
Geological Consultants Earth Mechanics Inc. 2333 West Northern Avenue & 17660 Newhope Street Phoenix AZ 85021 Fountain Valley CA 92708	11. Contract or Grant No. HPR-PL-1(37) 344

12. Sponsoring Agency Name and Address	13.Type of Report & Period Covered
Arizona Department of Transportation 206 South 17th Avenue Phoenix AZ 85007	Final 14. Sponsoring Agency Code

15. Supplementary Notes
Prepared in cooperation with the U.S. Department of Transportation, Federal Highway Administration

16. Abstract This report documents the research, field investigations and analyses used to compile a fault map and seismic acceleration coefficient contour maps for Arizona. The seismicity of adjacent regions which may potentially impact Arizona are factored into the analysis. Potential earthquake sources were evaluated using ground and airborne geological reconnaissance, photogeological interpretations and subsurface explorations of selected representative fault features. One hundred eighty-six faults or fault zones are identified. These data combined with other geological, seismological and geophysical data define twenty-one seismic source zones influencing Arizona.

Earthquake recurrence relations for each seismic source are derived. Energy release relationships based on slip rates and seismic moment are evaluated. Comparisons with recurrence relations defined by other researchers such as Algermissen, et al (1990) are made. The SEISRISK III computer program is used to conduct a probabilistic analysis to define acceleration coefficients with 90% probability of non-exceedance in 50 years in accordance with AASHTO seismic design guidelines. Additional maps for 90% probability of non-exceedance in 250 years and for peak ground velocity were also prepared.

Ground acceleration coefficient (90-percent non-exceedance in 50 years) levels determined from the research program are higher than those in the existing AASHTO Seismic Guide specification in the northwestern and north-central parts of the state due to the significant number of potentially active faults identified in those regions. Coefficients are also higher in the southwest corner of Arizona due largely to California and Mexico source zones with high recurrence rates. Ground accelerations in the southeastern part of the state are significantly lower than previous estimates. Acceleration levels are essentially comparable to AASHTO guidelines in the remaining parts of the state.

Maps of new seismic acceleration coefficient contours and compiled faults in Arizona have been prepared to a scale of 1:1,000,000. Electronic digital data files are compiled in a format that can be used to support site-specific and regional studies for seismic design. The map of horizontal acceleration with 90-percent probability of non-exceedance in 50 years is recommended to the Arizona Department of Transportation for use in AASHTO-based design of highway bridges.

17. Key Words	18. Distribution Statement	23. Registrant's Seal
faults, earthquakes, seismotectonics, seismic source zones, recurrence relations, attenuation relations, acceleration coefficients, probabilistic analysis, Arizona	Document available through National Technical Information Service Springfield, VA 22161	REGISTERED GEOLOGIST CERTIFICATE NO. 10338 KENNETH M. EUGE Date Signed 9/8/92 ARIZONA, U.S.A.

19. Security Classification	20. Security Classification	21. No. of Pages	22. Price
Unclassified	Unclassified		

PREFACE

This research program was funded by the Arizona Department of Transportation, Arizona Transportation Research Center. The report was prepared in cooperation with the U.S. Department of Transportation, Federal Highway Administration, Region 9.

SI* (MODERN METRIC) CONVERSION FACTORS

APPROXIMATE CONVERSIONS TO SI UNITS

SYMBOL	WHEN YOU KNOW	MULTIPLY BY	TO FIND	SYMBOL
LENGTH				
in	inches	25.4	millimeters	mm
ft	feet	0.305	metres	m
yd	yards	0.914	metres	m
mi	miles	1.61	kilometres	km
AREA				
in^2	square inches	645.2	millimetres squared	mm^2
ft^2	square feet	0.093	metres squared	m^2
yd^2	square yards	0.836	metres squared	m^2
ac	acres	0.405	hectares	ha
mi^2	square miles	2.59	kilometres squared	km^2
VOLUME				
fl oz	fluid ounces	29.57	millimetres	mL
gal	gallons	3.785	litres	L
ft^3	cubic feet	0.028	metres cubed	m^3
yd^3	cubic yards	0.765	metres cubed	m^3
MASS				
oz	ounces	28.35	grams	g
lb	pounds	0.454	kilograms	kg
T	short tons (2000 lb)	0.907	megagrams	Mg
TEMPERATURE (exact)				
°F	Fahrenheit temperature	5(F-32)/9	Celsius temperature	°C

NOTE: *Volumes greater than 1000 L shall be shown in* m^3.

APPROXIMATE CONVERSIONS FROM SI UNITS

SYMBOL	WHEN YOU KNOW	MULTIPLY BY	TO FIND	SYMBOL
LENGTH				
mm	millimetres	0.039	inches	in
m	metres	3.28	feet	ft
m	metres	1.09	yards	yd
km	kilometres	0.621	miles	mi
AREA				
mm^2	millimetres squared	0.0016	square inches	in2
m^2	metres squared	10.764	square feet	ft^2
ha	hectares	2.47	acres	ac
km^2	kilometres squared	0.386	square miles	mi^2
VOLUME				
ML	millilitres	0.034	fluid ounces	fl oz
L	litres	0.264	gallons	gal
m^3	metres cubed	35.315	cubic feet	ft^3
m^3	metres cubed	1.308	cubic yards	yd^3
MASS				
g	grams	0.035	ounces	oz
kg	kilograms	2.205	pounds	lb
Mg	megagrams	1.102	short tons (2000 lb)	T
TEMPERATURE (exact)				
°C	Celsius temperature	1.8C + 32	Fahrenheit temperature	°F

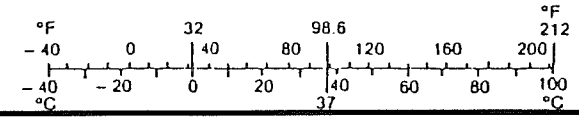

*SI is the symbol for the International System of Measurement (Revised April 1989)

ARIZONA DEPARTMENT OF TRANSPORTATION
ARIZONA TRANSPORTATION RESEARCH CENTER

SI* (MODERN METRIC) CONVERSION FACTORS

FHWA REGION	STATE	PROJECT NUMBER	REPORT NUMBER
9	ARIZ.	HPR-PL-1(37)344	FWHA-AZ92-344

TABLE OF CONTENTS

APPENDICES

LIST OF TABLES

LIST OF FIGURES

LIST OF PLATES

1. INTRODUCTION

a. Purpose and Objectives

This report describes the methods and results of a year-long research project to evaluate seismic hazards in the state of Arizona and to produce a new seismic acceleration contour map to be used in the design of Arizona Department of Transportation (ADOT) facilities. The work was performed by the geological and engineering consulting companies of Geological Consultants of Phoenix, Arizona and Earth Mechanics Inc. of Fountain Valley, California under the direction and guidance of the Transportation Research Center of ADOT.

The investigation comprised six basic tasks:

1) literature review,
2) identification of seismic source zones and faults,
3) preparation of seismic source zone and fault location maps,
4) location of seismic acceleration coefficient contours,
5) preparation of seismic acceleration contour maps, and
6) documentation of methods and results.

The methods employed and the results of these tasks are discussed and described in this report.

b. Background

In 1981, the Applied Technology Council (ATC) published a Federal Highway Administration Report (FWHA/RD-81/081) "Seismic Design Guidelines for Highway Bridges". The 1981 ATC report was adopted by AASHTO and implemented in the AASHTO Guide Specifications for Seismic Design for Highway Bridges (AASHTO, 1983). The document was later adopted as the AASHTO Standard Bridge Design Specification for Bridges (Buckle, 1991) and is currently used by most State Highway Departments for seismic design of highway bridges. The AASHTO Seismic Guide Specification contains a seismic acceleration coefficient contour map of the United States. The acceleration coefficients from this contour map serve as anchor points at zero-second period for the design response spectrum curve in the AASHTO specifications.

The seismic acceleration coefficient contour maps for bridge design have evolved to incorporate more up-to-date research in earthquake hazard studies. The latest map adopted by the AASHTO subcommittee for seismic design of bridges (Buckle, 1991) is the contour map of Horizontal Peak Ground Acceleration for a Probability of 90-percent non-exceedance over a 50-year duration developed by Algermissen et al (1990).

An objective of this project is to incorporate more-recent and/or more-refined local geological and seismological data into the design of highway facilities while preserving the underlying design criteria of the national AASHTO coefficient map. The principal differences between the new seismic acceleration contour maps developed from this project and the AASHTO national

map emanate from the more detailed and up-to-date geological and seismological data compiled and acquired in the course of the project.

c. New Seismic Acceleration Coefficient Contour Maps

The new seismic coefficient contour maps are presented as Plates 2a through 2d of this report. Plate 2a presents the horizontal peak ground acceleration (PGA) contour map with 90-percent probability non-exceedance in 50 years, and it is recommended for use in bridge design by ADOT. The other maps (250 years and A_v maps) were developed so comparisons can be made to other maps developed in prior studies such as Algermissen et al (1990). The probabilistic model and computer program used to produce the new maps are similar to those used for previous maps. In contrast to previous ground-motion contour maps, the new maps are heavily based on detailed geological investigations within and adjacent to the state of Arizona.

Over the past few decades, a substantial body of new data on the location and activity rates of faults in the Arizona region has become available. The present maps are a direct reflection of these new data but also reflect a somewhat different approach to how seismic hazards are defined and how data are incorporated into the evaluation. Most previous seismic-hazard investigations concentrated on historical seismicity with only limited consideration of major late-Quaternary-age faults. These methods may be adequate for areas where the rate of tectonic activity is high (for example, western California), but in an area such as Arizona where rates of tectonism are very slow, the occurrence of just a few new earthquakes can greatly

change the makeup of maps based only on earthquakes. To characterize the seismic potential more completely, a much broader perspective is necessary. This is clearly demonstrated by the poor correlation of historical earthquakes to specific late-Quaternary faults in Arizona. By examining only Quaternary faults or only earthquakes, the potential for future earthquakes cannot be characterized with much certainty. By examining both factors, the understanding of seismic potential is improved, but it may still be lacking in some aspects, as shown by the occurrence of major earthquakes throughout the world where there is no seismicity and no well-known late-Quaternary faults.

To minimize the occurrence of "surprise" earthquakes such as those that occurred in central California (Coalinga) and Idaho (Borah Peak) in 1983, and in the Los Angeles, California area (Whittier) in 1987, this investigation included a broad spectrum of geologic and seismologic data and techniques. For example, instead of using just Holocene-age or late Quaternary-age faults, all faults that have been active during the present tectonic regime (neotectonic) were considered in the analysis. These neotectonic faults were used to define seismic sources capable of generating earthquakes, and then were used to help quantify the seismic potential. Instead of relying solely upon the incomplete historical earthquake record, this investigation directly applied the relatively new geological data on prehistorical earthquakes generated from detailed geomorphic, trenching, and field investigations, to the quantification of earthquake recurrence relationships.

Another important aspect of this investigation is the method of implementation and promulgation of results. The final products are submitted in computer format such that they can be modified and reproduced by ADOT computers at any scale by using readily available computer software such as AutoCAD.

d. Report Organization, Terminology, and Format

The report is organized somewhat in chronological order of the various tasks that were performed.

Measurements within the report are generally in the English system (inch-feet-miles). However, many of the computer programs and mathematical formulae employed in the analysis require units expressed in the metric system; rather than convert all numbers back and forth between the two measurement systems, it is preferable to leave some numbers expressed in the metric system. For example, faulting slip rates are given in millimeters per year (mm/yr). Rates of geologic (tectonic) processes in Arizona are generally very slow, commonly hundredths and thousandths of a millimeter (10^{-2} and 10^{-3}). Such rates are manageable when expressed in mm/yr but as fractions of inches they would be difficult to relate to, even when one is more familiar with the English system.

We attempted to keep esoteric geological terms to a minimum, but to keep discussions as short as possible and the report focused on the important issues it is necessary to use some well-established geological terms. To

help the reader through these discussions, a glossary of selected geological terms used in the report is provided as Appendix B.

Similarly, geological ages are frequently used in the discussions. Appendix C provides a geological time scale to help the reader conceptualize some of the great time spans involved in geological processes as discussed in the report.

e. Participants

Principal participants and their roles in the research project are shown on the project organization chart on Figure 1.

f. Acknowledgements

A project of this magnitude requires the cooperation of numerous individuals both within the project framework and from the geological, seismological and engineering communities at large. Many colleagues, too numerous to mention, contributed by sharing their unpublished work, their opinions, insights and constructive criticism, and we are very grateful. Some particular individuals who contributed were Mr. Larry A. Scofield, P.E., Manager, and Mr. Yee J. Ho, P.E., Project Manager, of the Arizona Department of Transportation Department, Transportation Research Center. Special thanks are also extended to other ADOT representatives including Mr. Charles Deutschlander, Mr. Richard LaPierre and Mr. Mike Hall (Photogrammetry and Mapping) who provided aerial photographs, as well as highway location data,

FHWA REGION	STATE	PROJECT NUMBER	REPORT NUMBER
9	ARIZ.	HPR-PL-1(37)344	FWHA-AZ92-344

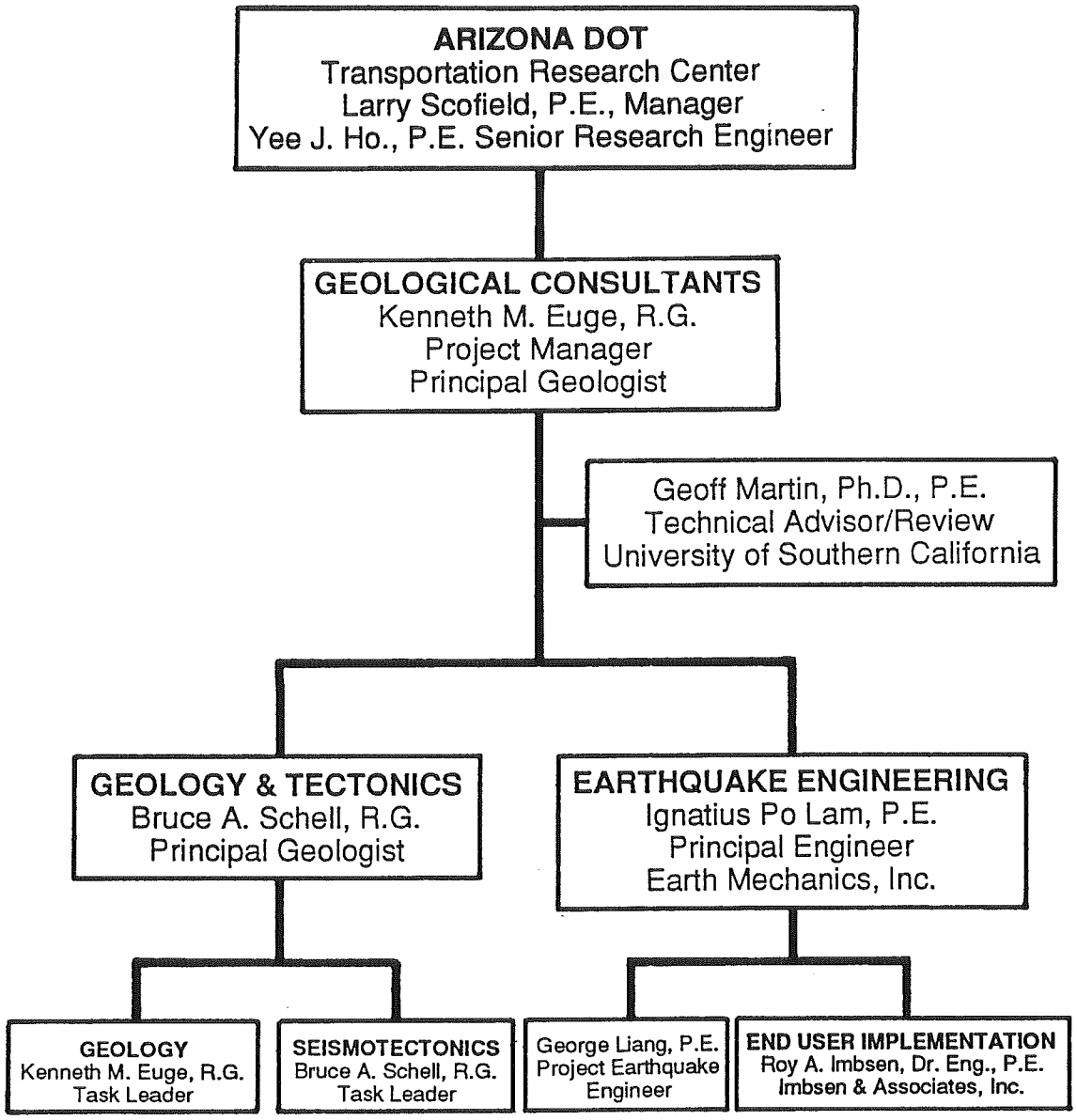

ARIZONA DEPARTMENT OF TRANSPORTATION
ARIZONA TRANSPORTATION RESEARCH CENTER

FIGURE 1
PROJECT ORGANIZATION CHART

and to Mr. Scott Hutchinson (Transportation Planning) who provided the ADOT digital line data files used in base map preparation.

Appreciation is due to Ms. Diane Crawford of the Arizona State Land Department who helped expedite the right-of-entry application required for exploration of the Aubrey Fault. Special thanks are extended to Mr. Merwin Davis, owner of the C.V. Ranch who allowed us access to his land for the Big Chino fault field studies. Mr. Davis' interest and cooperation was most helpful and the people of Arizona are indebted to him.

The valuable technical support of various colleagues, researchers and professionals in the field of geology, seismology and earthquake engineering is acknowledged and appreciated. Special thanks is given to Dr. Larry Fellows and Dr. Phil Pearthree of the Arizona Geologic Survey, Dr. David Brumbaugh of Northern Arizona University, and Dr. David Perkins of the U.S. Geological Survey.

The research team is also indebted to Ms. Sally Atkinson and Ms. Mary Peters for their rapid response, attention and resolution of contract administration matters during the term of the project.

2. LITERATURE REVIEW

a. Scope of Work

The principal scope of work for the literature review task was to review all pertinent geological literature and available unpublished reports and data, and to compile a working data base for the remaining project tasks. Literature and data were compiled from a wide variety of sources including government agencies, local libraries, utility companies, and personal libraries of the research team. This task also included personal contact with geoscientists familiar with the geology and seismology in the area. Pertinent data were compiled and summarized onto maps, tables, and work sheets. The extent and results of these efforts are described further in the subsequent sections of this report.

Although the majority of available information had been collected early in the investigation, data compilation, refinement, and analyses continued throughout the entire project. The investigators evaluated the reliability of most of the data collected and the most reliable data were used throughout the project. Some of the collected data were adequate as they existed but more data were needed for several aspects. The additional data were generated by the principal investigators and the rest came from further discussions with other geoscientists or by more-detailed analysis of the existing literature.

b. Data Collection

The principal type of information needed for this study were data on faults and earthquakes. The literature base that contained the needed information was large and diverse. To keep track of the large amount of data, information was compiled in two formats: 1) data sheets and 2) maps. The final maps of geologic faults is presented as Plate 1. This map shows the location of faults and identifies each fault with a unique reference number. Data on each fault were compiled on fault data sheets. Summaries of the most pertinent data from these data sheets are included in Appendix A.

The principal sources of data and information were:

- State and federal agencies such as the Arizona Geological Survey, Arizona Earthquake Information Center, U.S. Geological Survey, U.S. Bureau of Reclamation, and Utah Geological and Mineral Survey;

- Universities and colleges such as the University of Arizona, Arizona State University, Northern Arizona University;

- Scientific and engineering journals such as the Bulletin of the Geological Society of America, Seismological Society of America Bulletin, and American Society of Civil Engineers Journal;

- Utility companies such as Arizona Public Service Company, Arizona Nuclear Power Project, Southern California Edison Company, San Diego Gas and Electric Company, Salt River Project;

- Scientists and engineers presently conducting research on faults, seismicity, seismic zoning, and earthquake engineering; and

- Special publications such as Arizona Geological Society Digest and various geological society field-trip guidebooks.

3. FIELD INVESTIGATIONS

The field investigations consisted of four principal tasks, photogeology, aerial reconnaissance, ground reconnaissance, and fault trenching.

a. Photogeology

The photogeology task involved detailed and regional evaluation of selected areas. The detailed studies used primarily stereo, black and white, aerial photographs at scales of between about 1:40,000 to 1:60,000. The photographs were obtained from the Arizona Department of Transportation Photogrammetry and Mapping Division. The black and white photographs were augmented with limited color satellite images and photographs.

The aerial-photograph analysis involved documenting geologic features such as faults, folds, lineaments, stratigraphy, and uncertain features. The aerial photographs were used to help identify areas that would yield reliable information on age and rates of neotectonic activity. Interpretations were plotted on 9 by 9 inch mylar overlays taped to alternate photographs. These overlays were also freely annotated with any pertinent information that might help identify significant features during the aerial and field reconnaissance, and with questions that needed to be answered by field checking, field measurement, or aerial reconnaissance. The annotated aerial photographs were then strategically arranged in portable files so as to provide easy and rapid retrieval during the aerial and field reconnaissance.

The aerial photograph interpretations were conducted in stages at various times depending on the nature of questions and the difficulty in the resolution of questions. For example, based on our review of literature, the Mesa Butte area was identified as an area that could provide important data. The first field visit indicated that features needed to be mapped in more detail and over a larger area than was available by published data. Also, better control over relative age data was needed for lava flows displaced by faults. A determination was made that further aerial-photograph analysis would provide the best information, and more photographs were obtained. Further aerial photograph interpretation then resulted in identification of areas where the best or most representative field measurements could be made. These areas were verified and looked at in more detail during the aerial reconnaissance which also provided information on the best access roads to the specific areas. Then the aerial photographs were taken to the field during a second field visit and the identified areas and features were measured, mapped, and otherwise documented in more detail, in the field at the outcrop. Upon return from the field, additional interpretations or refinements of previous interpretations were made under the more-controlled conditions of the office (i.e. better lighting, no wind, rain, etc).

The aerial-photograph analysis and aerial reconnaissance revealed that few of the faults in Arizona occur in areas with young deposits of Quaternary age. The paucity of Quaternary strata rendered trenching studies unsuitable for most faults. This made evaluation of ages of fault displacement and recurrence intervals very difficult. Instead of trenching, aerial-photograph

and geomorphic analyses were found to provide the best results considering the time and budget constraints of this project.

b. Aerial Reconnaissance

Aerial reconnaissance of preselected areas was conducted on 5, 6, and 7 of September 1991. The reconnaissance was by single engine, fixed-wing light airplane with overhead wing without wing struts. Such aircraft are especially well suited for large regional investigations such as this because they provide good visibility, speed, and long range. The aerial reconnaissance concentrated on faults and features identified during the literature review, preliminary aerial photograph-interpretations, and some preliminary field reconnaissance. Maps and aerial photographs which had been previously annotated in the office with questions to be answered about certain features were taken along and used for keeping track of locations and data. Documentation of data during the flyover was by notes on trip logs, aerial photograph overlays, maps, VHS-format video photography, and by 35 mm photographs in both print and transparency format.

The flights departed Phoenix Sky Harbor International Airport at about sunrise. Routes were planned so the areas of interest could be viewed under optimum lighting conditions. The best time for viewing areas with little relief is generally during the early morning when the sun angle is low and shadows accentuate otherwise subtle or obscure fault scarps. The best time for the canyon areas is mid day when the sun is high and illuminates deep into the canyons. Visibility was adequate but commonly less than ideal for

photography due to atmospheric haze, low clouds, and air turbulence. Figure 2 shows the flight paths for the three successive flights. The illustrated flight paths are very generalized. In actuality, the flights were very irregular with frequent course deviations, multiple circling, and back and forth trips to view certain features from various angles, altitudes, and lighting conditions (i.e. morning, mid day, afternoon). Upon return from the flight, the photographs were immediately processed and then annotated with notes and station numbers.

c. Ground Investigations

The ground field investigations consisted of visits by the project geologists to areas of some particular interest. This activity was conducted during several visits generally lasting a few days (5 to 7) during the months of July through December, 1991. Field visits were made at various stages of the investigation depending on the nature of the features or areas to be visited, and on the timing of other activities. Some field checking was conducted during the literature review stage, other features were checked after the aerial flyover, and others after aerial-photograph interpretation. Because most of the areas requiring field checking were in remote areas and generally required travel on primitive dirt trails during rain squalls, four-wheel-drive vehicles were used for transportation. Activities during these visits comprised general reconnaissance, verifying aerial-photograph interpretations, geological mapping, and fault-scarp morphology analysis.

FHWA REGION	STATE	PROJECT NUMBER	REPORT NUMBER
9	ARIZ.	HPR-PL-1(37)344	FWHA-AZ92-344

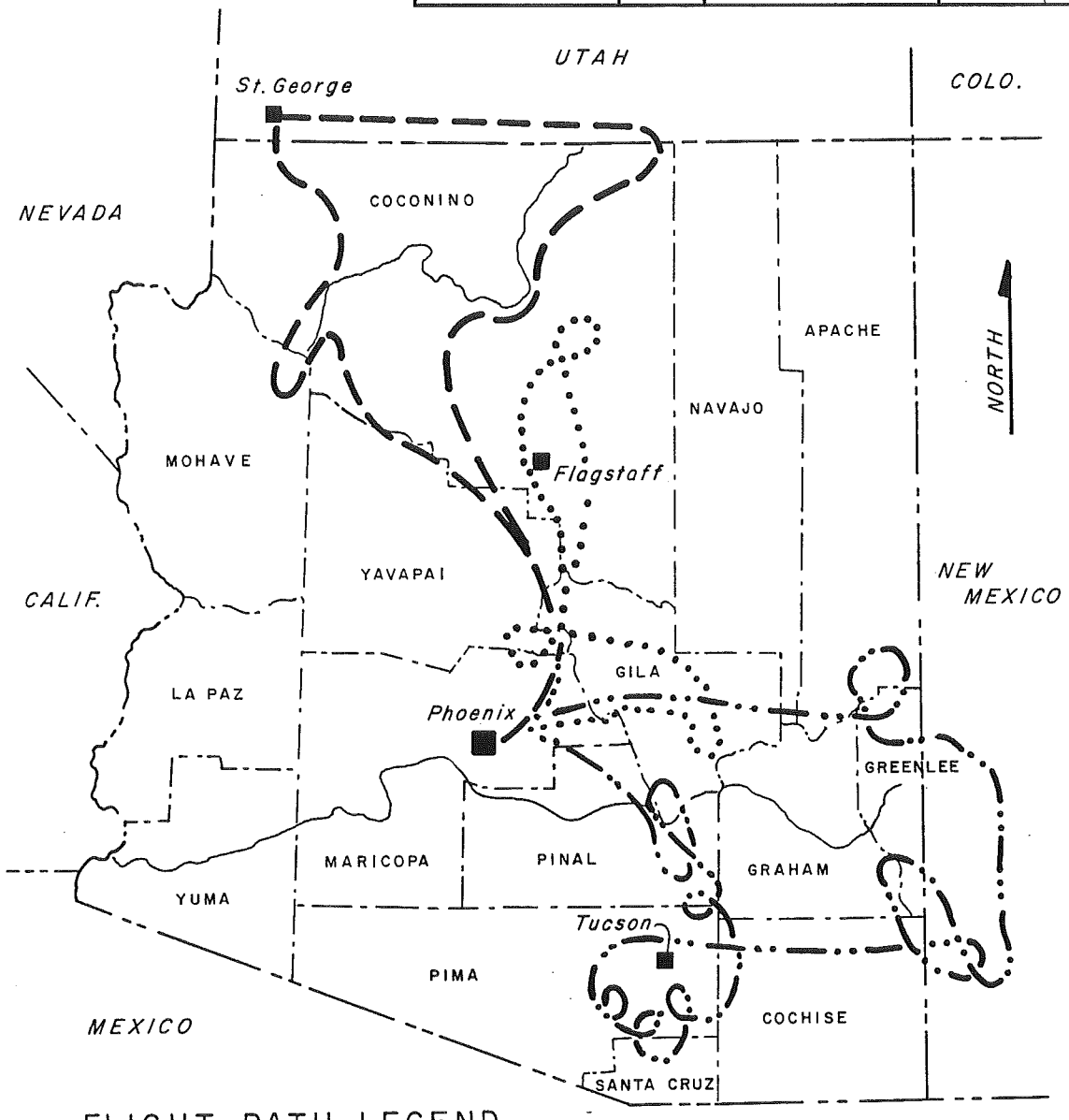

ARIZONA DEPARTMENT OF TRANSPORTATION
ARIZONA TRANSPORTATION RESEARCH CENTER

FIGURE 2
AERIAL RECONNAISSANCE FLIGHT PATH MAP

Features of interest were documented in field notes, maps, and 35 mm photographs. 35 mm photographs were commonly taken in stereo pairs to provide three-dimensional views for future analysis during office work and for detailed comparisons with aerial photographs.

Most of the ground field investigations were conducted in an area extending from the northwest corner of the state to the Tucson area. This is the area with the most young faults and perhaps the least studied. Extensive field checking was conducted in the Aubrey, Big Chino, and Verde valley areas, and the area between the San Francisco Peaks and the Little Colorado River (hereafter referred to as the Mesa Butte area).

Other areas receiving more general reconnaissance-type visits were:

- Arizona-Nevada border area
- Hualapai-Detrital Valley area (northwestern Arizona; Bullhead City-Kingman area to Hoover Dam area),
- Northern Kaibab Plateau (Grand Canyon to Utah border), and
- Northern Toroweap/Hurricane faults area.

Areas such as the central Colorado Plateau did not require any special ground investigations because there is no indication of young faults in that region. The Sonoran Desert and eastern California also were not investigated in detail because they had been looked at in detail by the project geologists and by the Arizona Geological Survey, many times in past few years for various projects, thus, up-to-date information on those areas was already in

hand. Data from southeastern Arizona was available from aerial photographs and aerial reconnaissance, and from published and unpublished investigations by the University of Arizona, Arizona Geological Survey, and the U.S. Geological Survey who investigated that area in detail in recent years.

In addition to the areas investigated by fault trenching, other areas receiving substantial geologic and geomorphological analysis during the ground reconnaissance phase were the Mesa Butte and Verde Valley areas. These investigations are described below:

(1) Mesa Butte Faults

(a) Background: The criterion of using neotectonic faults (late-Pliocene to present) in seismic source evaluations and seismic hazards analysis is problematical, especially for the Colorado Plateau of Arizona which virtually has no stratigraphic deposits younger than Cretaceous (more than about 100 million years old) in the areas where faults are mapped. Due to this lack of young strata, radiometric and stratigraphic age constraints on faulting are rare. In the absence of dateable materials, the ages of many faults were based on geomorphic expression, that is, if a fault has a prominent, linear escarpment such as that shown on Figure 3, it is considered to be a neotectonic feature. To test whether this is a reasonable approach, a detailed evaluation of faulting in the north-central Arizona area just north of San Francisco Mountain was undertaken. This area, referred to as the Mesa Butte area after the longest and most prominent fault in the area (#104), was selected because it has numerous prominent faults in Paleozoic

FHWA REGION	STATE	PROJECT NUMBER	REPORT NUMBER
9	ARIZ.	HPR-PL-1(37)344	FWHA-AZ92-344

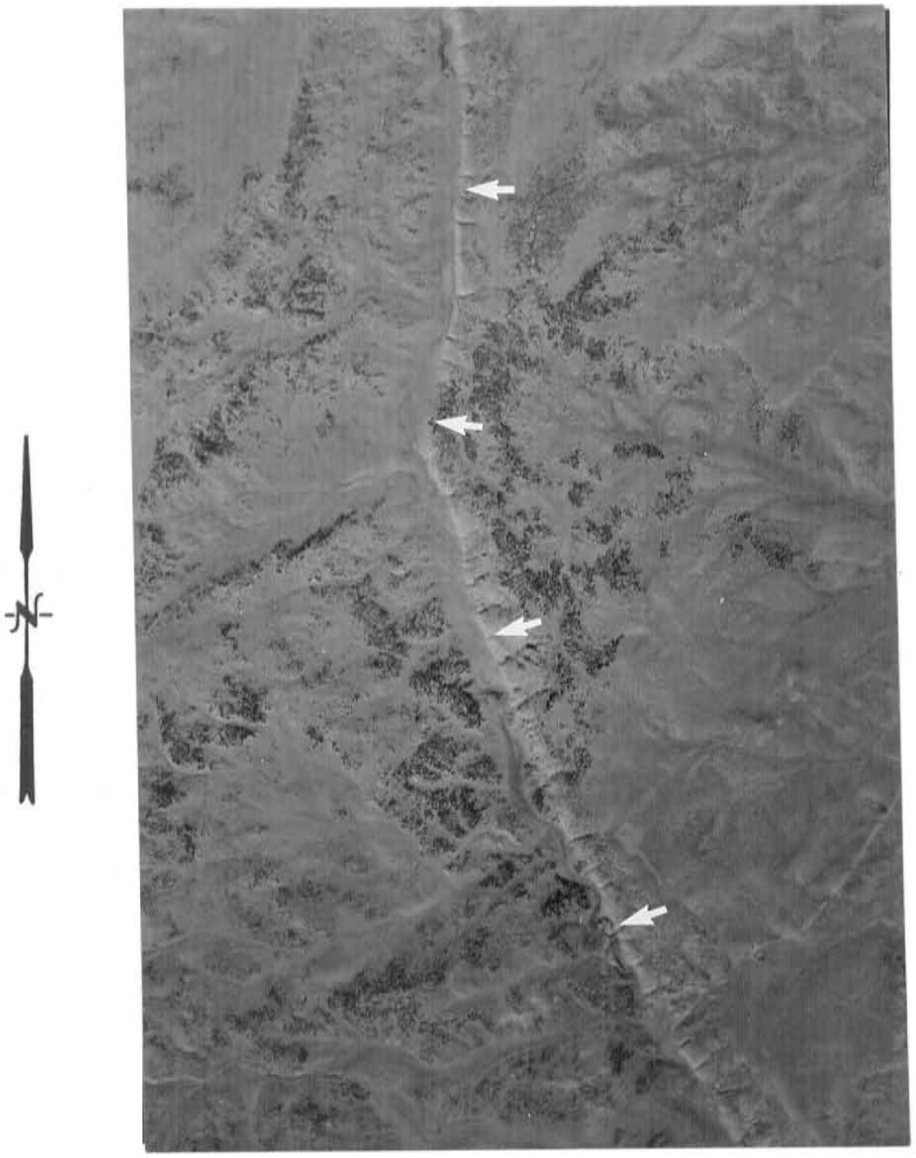

WHITE ARROWS ARE ON THE UPLIFTED BLOCK. LENGTH OF FAULT SHOWN IS ABOUT 6 MILES LONG. OFFSET ROCKS AT GROUND SURFACE ARE PERMIAN-AGE KAIBAB LIMESTONE.

ARIZONA DEPARTMENT OF TRANSPORTATION
ARIZONA TRANSPORTATION RESEARCH CENTER

FIGURE 3
AERIAL PHOTOGRAPH OF ROSE WELL FAULT

and Mesozoic strata which are overlain by dated or correlatable late-Tertiary and Quaternary volcanics (Figure 4). The premise is that if the age of the faults in the Mesa Butte area could be determined, they would provide guidance, by analogy, for estimating the age of faults where stratigraphic age control is lacking.

(b) Methods: Field investigations in the Mesa Butte area consisted of ground checking, aerial reconnaissance, and aerial-photograph analysis. Ground checking included mapping, geomorphic analyses, measuring fault displacements and documenting stratigraphic and age relationships. Geomorphology analyses consisted mainly of assessing the total fault displacements, number of displacements, and displacement per event.

Plate 1 illustrates the great number of surface faults in the Mesa Butte area where there are more than 100 fault zones within a small area of about only 800 square miles. These faults displace Paleozoic and Mesozoic bedrock and several overlapping Quaternary-age volcanic flows. The ages of the volcanic rocks provided important information on the faulting history and thereby helped assess earthquake potential.

Available age information was obtained from published sources. Although there are a large number of age determinations for the San Francisco volcanic area, data in the Mesa Butte area (where faults are most prominent) are relatively scarce. However, with a few key dates such as those of Baksi (1974), Damon et al (1974), and Wolfe et al (1987), a chronology of volcanism

FHWA REGION	STATE	PROJECT NUMBER	REPORT NUMBER
9	ARIZ.	HPR-PL-1(37)344	FWHA-AZ92-344

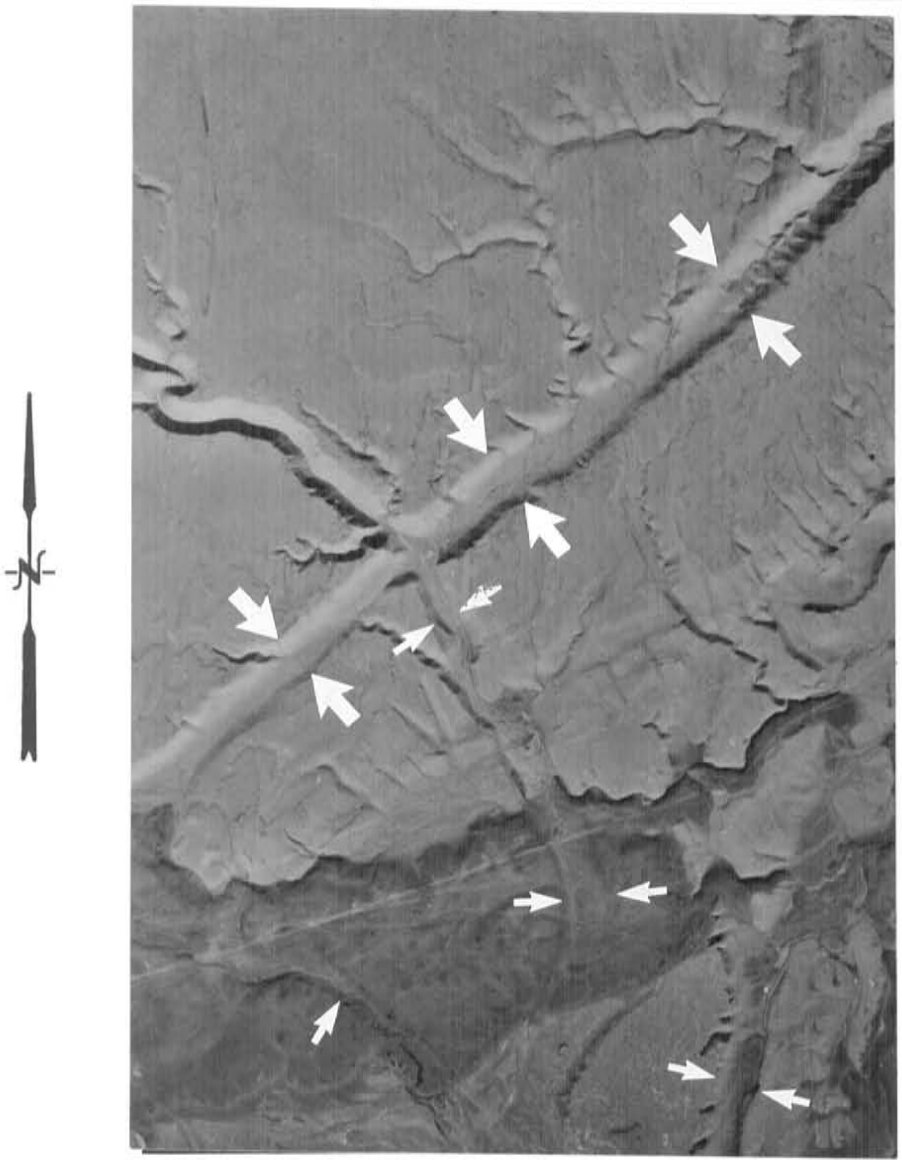

FAULT COMPRISES TWO PARALLEL FAULTS (INDICATED BY LARGER WHITE ARROWS) WITH DOWNDROPPED CENTRAL GRABEN. LIGHT GRAY ROCKS ARE PERMIAN-AGE KAIBAB LIMESTONE; DARK GRAY ROCKS ARE PLEISTOCENE (1.4 MILLION YEARS OLD) LAVA FLOWS WHICH ARE OFFSET BY A NORTHWESTERLY TRENDING GRABEN (SMALLER WHITE ARROWS) THAT DOES NOT APPEAR TO OFFSET MESA BUTTE FAULT. LENGTH OF FAULT ON PHOTOGRAPH IS ABOUT 6 MILES LONG.

ARIZONA DEPARTMENT OF TRANSPORTATION

ARIZONA TRANSPORTATION RESEARCH CENTER

FIGURE 4

AERIAL PHOTOGRAPH OF MESA BUTTE FAULT

and faulting was developed using geomorphology of cones and flows and the geologic principles of stratigraphic superposition and cross-cutting relationships (Figure 5).

A key volcanic unit in the area is the Tappan Wash (TW) basalt flow. The TW flow has a potassium/argon (K/A) age of 530,000 +/- 79,000 years (Damon et al, 1974; Wolfe et al, 1987). The flow is a narrow sinuous feature (Figure 6) that flowed northward, almost like water, from a vent on the east side of Kendrick Peak south of Highway 180 (Wolfe et al, 1987). The TW flow followed existing stream channels and fault troughs, through the Mesa Butte area to the Little Colorado River north of Highway 64, a distance of about 40 miles. There are numerous fault scarps and other lava flows along the flow path. Some of these features were overrun by the TW flow whereas others deflected the flow indicating that they were already well-developed by the time the flow occurred (Figure 6). Other features displace or overlie the Tappan Wash flow showing that they are younger. Another young flow in the area is the SP Crater flow which has been dated at about 71,000 +\- 4,000 years (Baksi, 1974). The SP flow also flowed across faults and older volcanic flows (Figure 5), some of which are the same features that are overlain by the TW flow. Relative ages were estimated by comparing the geomorphic development (preservation of primary flow forms, amount of erosion, soil cover, vegetation, etc), stratigraphic position, and cross-cutting relationships of the common features.

(c) Observations: Some important relationships and conclusions that provide important insights on the history and rates of

FHWA REGION	STATE	PROJECT NUMBER	REPORT NUMBER
9	ARIZ.	HPR-PL-1(37)344	FWHA-AZ92-344

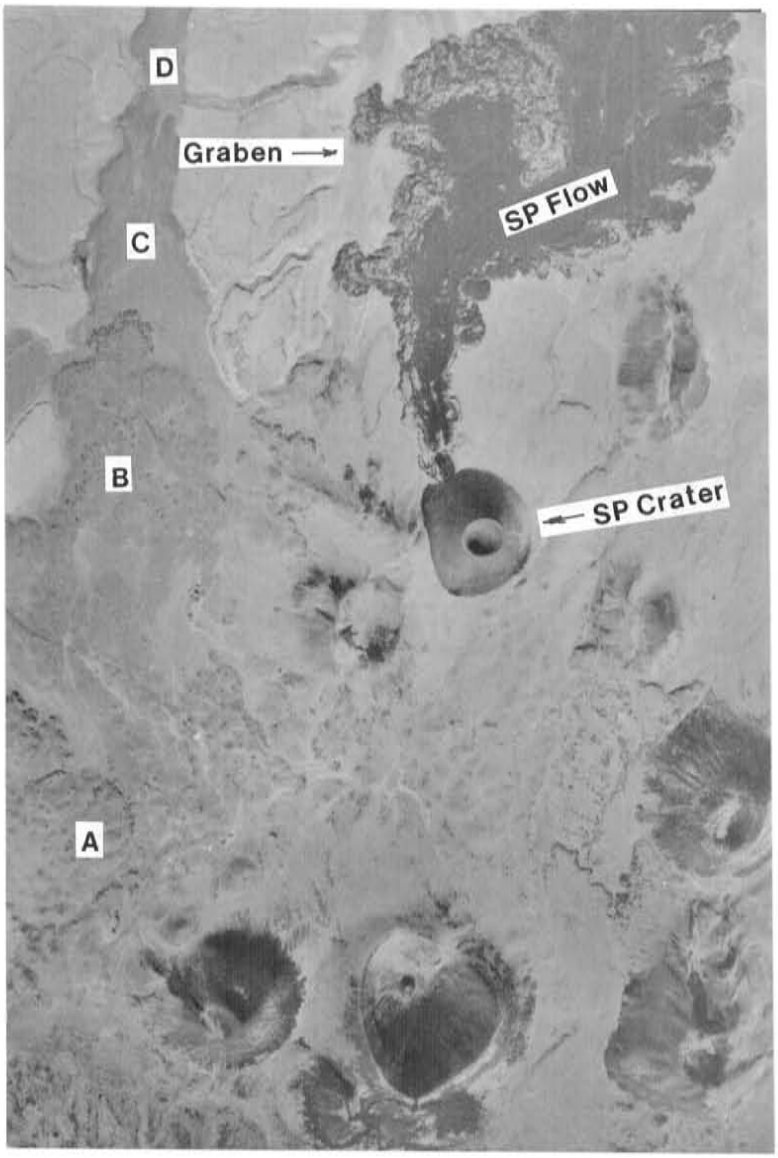

THE BLACK LAVA FLOW EXTENDING NORTHERLY FROM SP CRATER HAS BEEN DATED BY RADIOMETRIC METHODS AT ABOUT 71,000 YEARS. SEVERAL OTHER CRATERS IN THE PHOTOGRAPH ARE MUCH MORE DEGRADED INDICATING THEY ARE OLDER. THE SP FLOW EXTENDS ACROSS A GRABEN FAULT INDICATING THE FAULT IS OLDER THAN THE FLOW. OTHER OLDER FLOWS OVERLIE OTHER FLOWS; FOR EXAMPLE FLOW A OVERLIES FLOW B, B OVERLIES C, AND C OVERLIES D. SUCH SUPERPOSITION, IN CONJUNCTION WITH SURFACE MORPHOLOGY, HELPS ESTABLISH THE RELATIVE AGES OF FAULTS AND VOLCANIC FLOWS.

ARIZONA DEPARTMENT OF TRANSPORTATION
ARIZONA TRANSPORTATION RESEARCH CENTER

FIGURE 5
TYPICAL VOLCANIC LAND FORMS,
MESA BUTTE AREA

FHWA REGION	STATE	PROJECT NUMBER	REPORT NUMBER
9	ARIZ.	HPR-PL-1(37)344	FWHA-AZ92-344

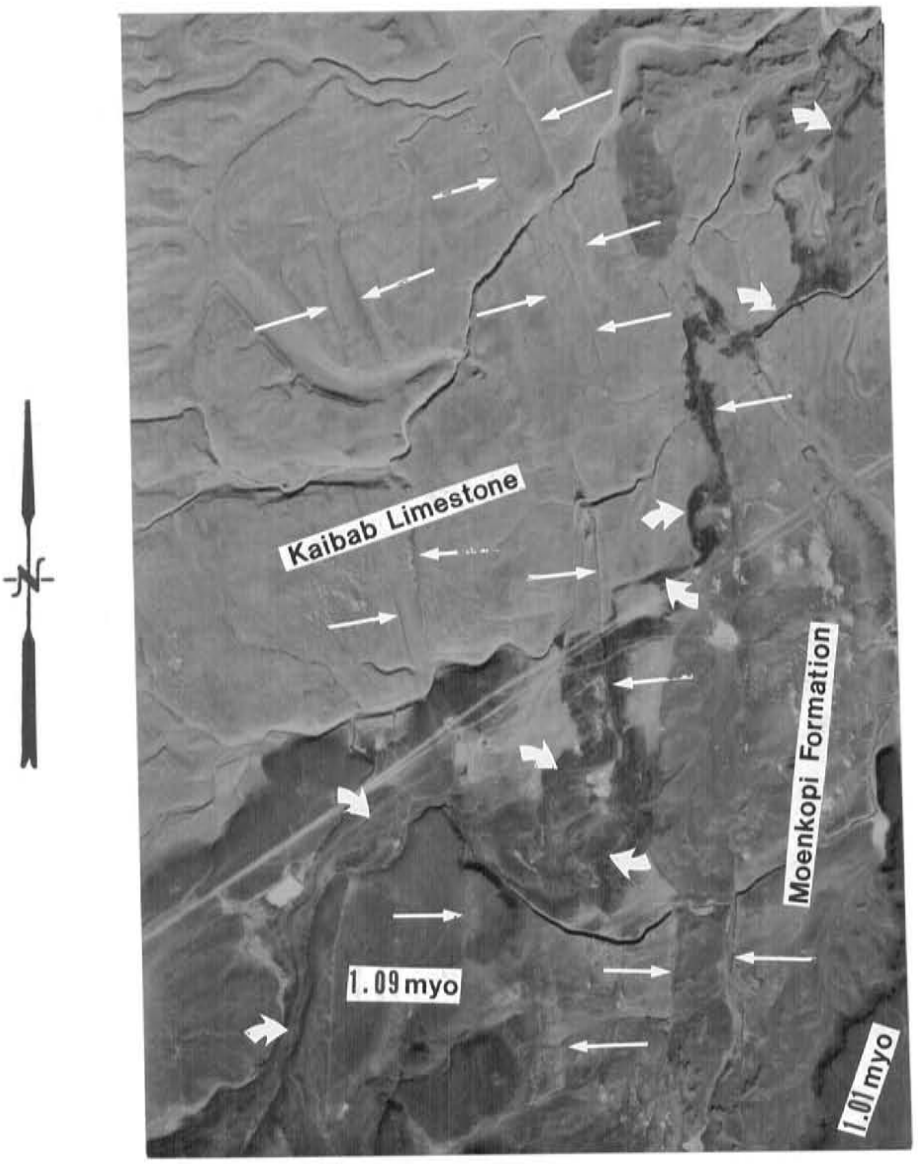

DARK GRAY AREAS ARE PLEISTOCENE-AGE LAVA FLOWS (NUMBERS INDICATE AGE IN MILLION YEARS); LIGHT GRAY AREAS IN UPPER LEFT ARE PERMIAN-AGE KAIBAB LIMESTONE; MEDIUM GRAY AREAS ON RIGHT ARE TRIASSIC-AGE MOENKOPI FORMATION. THIN WHITE ARROWS INDICATE FAULTS. LARGE WHITE ARROWS SHOW SERPENTINE TAPPAN WASH LAVA FLOW (530,000 YEARS OLD).

ARIZONA DEPARTMENT OF TRANSPORTATION
ARIZONA TRANSPORTATION RESEARCH CENTER

FIGURE 6
AERIAL PHOTOGRAPH OF MESA BUTTE AREA

FHWA REGION	STATE	PROJECT NUMBER	REPORT NUMBER
9	ARIZ.	HPR-PL-1(37)344	FWHA-AZ92-344

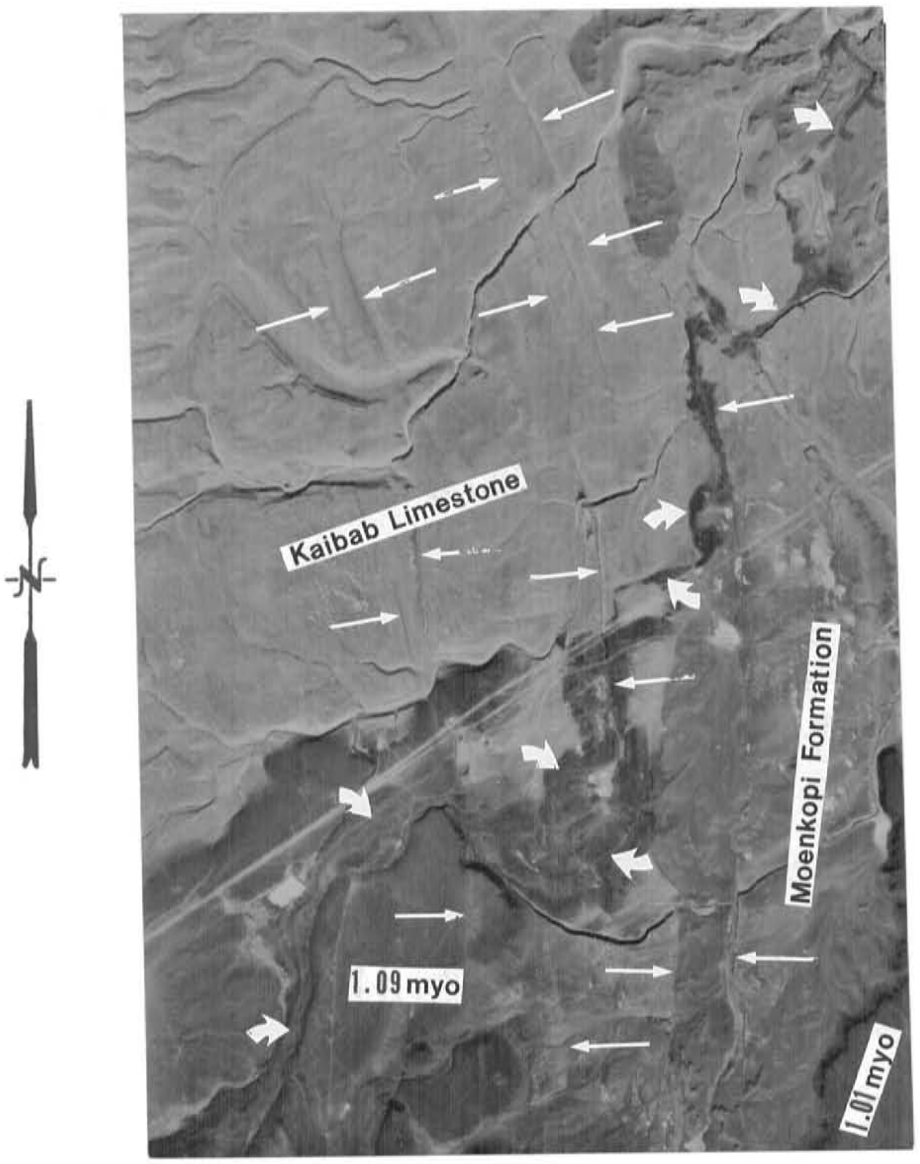

DARK GRAY AREAS ARE PLEISTOCENE-AGE LAVA FLOWS (NUMBERS INDICATE AGE IN MILLION YEARS); LIGHT GRAY AREAS IN UPPER LEFT ARE PERMIAN-AGE KAIBAB LIMESTONE; MEDIUM GRAY AREAS ON RIGHT ARE TRIASSIC-AGE MOENKOPI FORMATION. THIN WHITE ARROWS INDICATE FAULTS. LARGE WHITE ARROWS SHOW SERPENTINE TAPPAN WASH LAVA FLOW (530,000 YEARS OLD).

ARIZONA DEPARTMENT OF TRANSPORTATION
ARIZONA TRANSPORTATION RESEARCH CENTER

FIGURE 6
AERIAL PHOTOGRAPH OF MESA BUTTE AREA

faulting for the Mesa Butte fault are:

- The Mesa Butte fault was well developed before the Mesa Butte cones were formed and before Tappan Wash flow occurred (i.e. more than 500,000 years before present).

- The Mesa Butte cinder cones do not appear to be offset by the Mesa Butte fault thus the fault in the cone area has not been active since the cones formed.

- The southern part of the Mesa Butte fault is overlain by approximately 1 million-year-old lava flows that are not displaced by the Mesa Butte fault (although some smaller cross-faults do appear to displace these flows).

- The Cedar Ranch fault merges with the Mesa Butte fault just north of the Mesa Butte cones, and was active after early Mesa Butte volcanic activity. The fault displaces the 530,000 year-old TW flow by a lesser amount than the 1.04 my-old Mesa Butte flow indicating recurrent displacements. The large amount of displacement of the Mesa Butte and TW flow by the Cedar Ranch fault suggests that the displacement occurred during several events. Several middle to late Pleistocene flows (estimated to be in the 200,000 to 300,000 age range) overlie the Cedar Ranch fault on the south indicating that the Cedar Ranch fault has not moved in late Quaternary time.

- Erosion has significantly deepened the Mesa Butte graben. Although the scarp is more than a thousand feet high in places, the true cumulative fault displacement generally is about 230 to 320 feet on the northwest fault, and net displacement across the graben is more like 100 to 200 feet. Assuming that surface displacements were large (say 10 feet per event) and that they were associated with earthquakes, the Mesa Butte fault could have generated about 10 to 20 large earthquakes. Of course, if the displacements were smaller, a larger number of events with smaller earthquakes would have been required to achieve the total cumulative displacement.

- None of the other faults which strike northwesterly across the Mesa Butte graben appear to significantly affect it, indicating that the Mesa Butte fault is one of the youngest, as well as the major fault in the area.

The Tappan Wash flow provides some of the most conclusive information regarding rate of faulting. The 530,000-year-old flow crosses about 18 fault zones. Eight of these fault zones do not offset the TW flow. Fault offsets occur at 10 locations yielding a minimum average activity rate of 1 event every 53,000 years if the scarps are a result of single-event ruptures. However, most of these events probably occurred over a period much shorter than 530,000 years. Based on lack of fault displacements in the latest Quaternary flows in the region, surface faulting does not appear to have been significant in the past 100,000-200,000 years so the 10 offsets probably

occurred over a time span of no more than 300,000-400,000 years. This would make the average recurrence interval about 30,000-40,000 years. Furthermore, at some of the fault locations, the large cumulative offsets indicate that there were probably more than one offset and this would shorten the average recurrence interval even further. Without more detailed information, most of these age and recurrence estimates are gross calculations and conclusions are rather speculative. However, the lack of evidence for younger displacements of the TW flow would seem to suggest that the rate of faulting diminished in the latest Quaternary and has been considerably slower than during the middle Quaternary.

Some other general observations are:

- Surface faults were present as far back as latest Pliocene (about 2.5 million years ago).

- Most volcanism on the north side of the San Francisco volcanic field is in the 2 million to 200,000-year age-range (includes Sitgreaves, Kendrick, Humphreys, and O'Leary volcanos). More than 90 percent of the cinder cones are in the 700,000-to 100,000-year age range.

- Net cumulative displacements on all the faults are generally small, generally less than 100 feet.

- Many faults have multiple displacements.

- Based on the large number of faults displacing middle Pleistocene flows and the paucity of displacements in latest Quaternary flows, the time of greatest faulting activity appears to have been in the middle Pleistocene.

- There are more than 100 fault zones. If each of these faults had two displacements, there were would have been about 200 surface-rupture events since late Pliocene time. Assuming a time span of 3 million years, the average rate would be one event every 15,000 years. If that rate had continued until today, there should be about 17 faults in the area with evidence of late-Quaternary surface rupture. However, no such late Quaternary ruptures can be documented so the rate of faulting appears to have diminished considerably in latest Quaternary time (i.e. the past 100,000-200,000 years).

- The apparent age-range of the period of most faulting activity is the same as the time of most active volcanism. The volcanism appears to have been episodic, that is, rather than steady continuous activity, volcanism has been characterized by periods of high activity separated by long periods of quiescence. There is no indication of any significant changes in recent times so, just as more volcanic eruptions should be expected, so should more faulting and earthquakes.

- The above observations support Holm's (1987) assertion that one

of the younger documented faults in the area is the Sinagua fault which he interpreted to be more than 250,000 years old.

- The only feature less than 100,000 years old in the Mesa Butte study area is the SP flow. There are several younger flows and cones in the eastern part of the San Francisco volcanic field such as at Sunset and Merriam craters but there are very few faults known in that area. Moore and Wolfe (1987) think that the apparent northwesterly alignment of some cones in the eastern area indicate buried northwest-trending faults.

- Historically, earthquakes have occurred in the area and some (1906, 1910), were in the 5.0 to 6.5 magnitude range (see Section 6. c. (11)). However, in the past few decades, this area does not appear to have been much more seismically active than the Arizona Mountain or Southwestern Plateau Margin zones.

In conclusion, the investigation in the Mesa Butte area indicates that surface faults with prominent scarps in the Paleozoic and Mesozoic rocks are probably neotectonic features. Some of these faults were active as far back as 1 to 2 million years, but many of them continued as active features into the late Quaternary time. However, the paucity of fault displacements in young flows indicates that the activity for the latest Quaternary (the past 200,000+) years is lower than it had been and, consequently, the surface-rupture hazard is also lower. The Mesa Butte fault system is one of the densest fault concentrations in Arizona. The faults occur in close proximity

to young volcanism raising the question of whether the faults are a result of regional tectonic strain or whether they are due to local volcanotectonic activity resulting from crustal swelling and/or collapse over rising or evacuating subsurface magma chambers. The question reduces to whether the volcanism caused the faulting or whether the faults were already there and the volcanism opportunistically used the faults as access routes to the surface. The presence of similar faults throughout the Southwestern Colorado Plateau margin where there is little volcanism seems to favor the latter interpretation, and support the interpretation that the faults are indeed primary tectonic features related to regional tectonic forces rather than to just local volcanic processes..

(2) Verde Fault

The Verde fault is a northwest-striking basin-and-range-type normal fault that forms the boundary between the Black Hills (Mingus Mountain) block and Verde Valley on the northeast. Verde Valley is one of several normal-fault-bounded basins in the Arizona Mountain seismic source zone. These northwesterly trending valleys and their adjacent mountain blocks extend from southwestern New Mexico to the Hurricane and Toroweap faults in northwestern Arizona. The fault-bounded basins and ranges seen today began forming during the Miocene Basin and Range tectonic episode.

Their fault-bounded, tilt-block morphology is quite obvious, but they vary widely in degree of development and preservation. The Verde Valley fault

system, along with the Big Chino Valley and Aubrey Valley systems, is one of the geomorphically more-youthful features suggesting that it has had a higher rate of tectonic activity in Quaternary time than the systems in the southeastern part of the zone such as the San Pedro and San Simon valleys.

Although there may have been some ancient activity along an ancestral Verde fault in both Precambrian and Laramide times (Lundberg, 1986; McKee and Anderson, 1971), Verde Valley appears to have formed primarily since about 10 million years ago based on the distribution and displacement of the Hickey basalts (10-14 million years old). The valley was well developed by 5.5 million years ago when the "Ramp Basalts" (5.5 to 8 million years old) flowed downslope into the valley from the area to the northeast.

Verde Valley had internal drainage until about 2 million years ago when lake beds of the Verde Formation and alluvial deposits filled the valley (Ranney, 1989). Presently, the valley drains southeasterly via the Verde River. With the development of through-flowing drainage, the Verde beds and the overlying alluvium have undergone extensive erosional downcutting and dissection. This downcutting, combined with continued localized deposition of alluvium in the valley has resulted in a complex assemblage of constructive and destructive landforms. Although these geomorphic surfaces provide a means by which to decipher the neotectonic development of the valley, they have not been investigated in detail. Such an investigation would be a major long-term undertaking and is well beyond the scope of the work for this investigation.

However, to assess the earthquake potential of the Verde fault, aerial photographs were analyzed and aerial reconnaissance and ground checking were performed. These investigations revealed that the Verde fault is a complex system of branching, discontinuous fault segments most of which appear to be within bedrock or at the bedrock-alluvium contact. There are at least two major segments and perhaps as many as four. For this investigation, the fault is considered to be composed of two segments, the northern and southern, similar to those designated by Menges and Pearthree (1983). The southern segment extends from the Tule Mesa area in the southeast to the Table Mountain area just northwest of Interstate 17 in the central part of Verde Valley. There does not appear to be a direct connection between the northern and southern segments. In the Table Mountain area, where the two segments overlap, the northern segment is about 2 miles west of the southern segment. The northern segment extends northwesterly, through the mining town of Jerome and into the hills at the northwestern end of Verde Valley. The total length of the fault could be as much as about 55 miles if northwestern and southeastern extensions beyond the valley are included. Considering only the segments of the fault that appear to have been involved in formation of the present Verde Valley, the northern segment would be about 20 miles long and the southern segment about 16 miles long.

The southern segment has the best evidence of late Quaternary displacement. For example, near the town of Camp Verde, a prominent, although short, scarp occurs in stabilized, alluvial-fan surfaces between Ryal Canyon and Allen Canyon. Herein, this scarp is referred to as the Allen Canyon Scarp. The age of these fan surfaces is uncertain but comparison of

their morphology to other similar surfaces suggests great age, certainly several tens of thousands of years and probably more in the 10^5-year age range (see Section 3. d. (1)(c) for discussion of age estimation for fan surfaces). The surfaces are very flat and at first glance they might appear quite young. However, the degree of erosion in some areas indicates that these high-standing flat surfaces are just small remnants of a once-continuous valley-wide bajada. With the advent of through-flowing drainage in Quaternary time extensive downcutting occurred and new alluvial fans formed in the new washes creating a complex situation of nested fans that is difficult to interpret. There appear to be many potentially anomalous conditions with some local parts of the surface surviving much of the erosion. Overview of the valley shows several levels of younger surfaces inset into the higher surfaces supporting the interpretation that these higher surfaces must be quite old; possibly a few hundred thousand years old (200,000 to as much as 500,000). The fact that there is only one or two small fault scarps in such an old surface indicates very long recurrence intervals and very low slip rates for the Verde Fault. The prominent scarp in the high surface at Allen Canyon projects toward younger surfaces and alluvial fans, perhaps a few tens of thousands of years old, which have no apparent offsets. All of these factors suggest localized, minor reactivation of the Verde Valley fault rather than regular, continuous, large-magnitude offsets.

Field examination of the Allen Canyon scarp showed that the maximum height of this scarp in alluvial gravels is about 27 feet. The ground surface is covered with a well-packed, varnished pavement. The scarp crest is rounded and the maximum slope angles are about 15 to 19 degrees with the

average being somewhat less. These relationships suggest the feature is of middle to late Pleistocene age. In one locality, the lower part of the scarp has a 28 degree slope. This steepened lower portion could represent a Holocene- to latest Pleistocene-age displacement of 6 to 7 feet but similar oversteepening was not observed anywhere else along the segment indicating that this short steep slope is a local erosional anomaly. The scarp is below a cluster of large boulders that armors the surface protecting it from erosion at that particular locality.

The fault responsible for the Allen Canyon Scarp is exposed in the steep walls of the unnamed wash north of Allen Canyon where it forms the contact between alluvial gravels and Miocene-age volcanic rocks. The fault zone is about 30 feet wide and strikes an average of about N 20° W and dips about 70 degrees northeast. A younger inset-terrace eroded into one of the walls does not appear to be offset by the fault.

In summary, the field data discussed above, like the aerial photograph interpretations, are inconclusive. Parts of the Verde fault scarp have similarities to scarps that formed within the past 10,000 to 20,000 years. However, there are several indications that the fault may be older, probably of middle or late Pleistocene age. Regardless of when the latest displacement occurred, the long-term average recurrence intervals between large surface-rupturing events appears to be long. Assuming that the 27-foot-high Allen Canyon scarp was formed by 6 to 9 foot displacements would indicate only 3 or 4 displacements since the high-standing alluvial surface formed. Using the ages of the fan surfaces indicated by the surface

geomorphology, the average late-Quaternary recurrence interval would range from 50,000 to 170,000 years. Using the younger age and the maximum displacement yields a conservative slip rate of about 0.03 mm/yr. These numbers are similar to those determined for the Aubrey fault (Section 3.d.(2)).

The slip rates calculated from various other data such as total stratigraphic displacement, valley geomorphology, displacement of Miocene volcanics, fault-scarp morphology, and offset of Quaternary alluvial surfaces have a wide range. The maximum rate is about 0.2 mm/yr and the minimum is about 0.01 mm/yr.

The maximum credible earthquake was estimated by applying empirical fault-length/earthquake-magnitude relationships (Slemmons, 1982; Bonilla et al, 1984) and seismic-moment calculations (Hanks and Kanamori, 1979; Wyss, 1979). These calculations suggest the Verde fault is capable of generating earthquakes in the magnitude 7 + range. For the seismic hazard analysis a magnitude of 7.25 was estimated.

(3) Other Field Reconnaissance Areas

Reconnaissance visits were conducted in the Hualapai, Detrital, Sacramento, and Piute-Eldorado valleys of northwestern Arizona, southeastern California, and southern Nevada. These valleys and their adjacent ranges are unusually linear and relatively parallel for the Arizona area suggesting affinities to modern Basin-and-Range type faulting. The

linear morphology, combined with the presence of a playa (Red Lake) in Hualapai Valley, suggests ongoing fault-controlled subsidence. Aerial photograph analysis, however, does not reveal any Quaternary faulting. Mountain-front tectonic geomorphic analysis indicates highly sinuous mountain fronts suggesting that the ranges have undergone extensive erosion without rejuvenation by tectonic uplift along mountain-front faults. In several northern localities, unfaulted Pliocene volcanic flows occur along valley margins in areas where surface faults would be expected if they had been active in Quaternary times. Rather than being a result of young tectonic activity, the strong linearity of the basins may be inherited from the previous tectonic regime, with enhancement by erosion during Quaternary integration of drainage to the Colorado River at the northern end of the valleys. This integration promotes erosion and provides direct egress of eroded sediments out of the valley thereby channeling the erosion and maintaining valley linearity. In summary, although there could be some ongoing late-stage tectonic subsidence, these basins and ranges do not appear to be very tectonically active so they were included with the Sonoran seismic source zone which is characterized by one of the lowest rates of tectonic activity in the state.

The southwestern margin of the Colorado Plateau is characterized by numerous long faults with prominent surface expression such as the West Kaibab (#3), DeMotte (#41), Muav (#47), and Moquitch (#40) faults (Plate 1). These faults are very obvious on aerial photographs (Figures 3 and 7) but some of the faults are in terrains covered with trees that obscure details. The area was checked by ground reconnaissance to see if any evidence of

neotectonic faulting could be recognized. The DeMotte fault, for example, is expressed as a narrow linear graben up to 400 feet deep in places. Some of this depth may be due to dissolution of the carbonate bedrock in the graben. Evidence of dissolution in the form of sink holes is ubiquitous in the area. As is typical of faults in the southern plateau margin, net displacement is much less than the depth of the graben. Elevations on both sides of the graben are about the same indicating that faulting was primarily extensional with the central block downdropping between two normal faults. Although the bases of the fault scarps commonly had small Quaternary alluvial fans, no evidence of young faulting could be recognized. The morphology suggests that faulting was active in Quaternary time, as does comparison to similar faults in the Mesa Butte area, but fault displacements must be small, slip rates slow, and recurrence intervals long.

Field reconnaissance was conducted in several other areas during the project. Some areas were specifically targeted while others were visited during traverses between other areas. During the course of the project most of the state where neotectonic faults occur, and the margins of the surrounding states, were investigated by at least one of the investigatory methods (aerial photographs, ground reconnaissance, aerial reconnaissance). The only part of the state that didn't receive specific examination was the Sonoran Desert region. However, this area has been examined in detail several times by the project geologists, as well others, during several other projects during the past couple decades. The Research Team is quite confident that no major undiscovered surface faults exist in the area.

FHWA REGION	STATE	PROJECT NUMBER	REPORT NUMBER
9	ARIZ.	HPR-PL-1(37)344	FWHA-AZ92-344

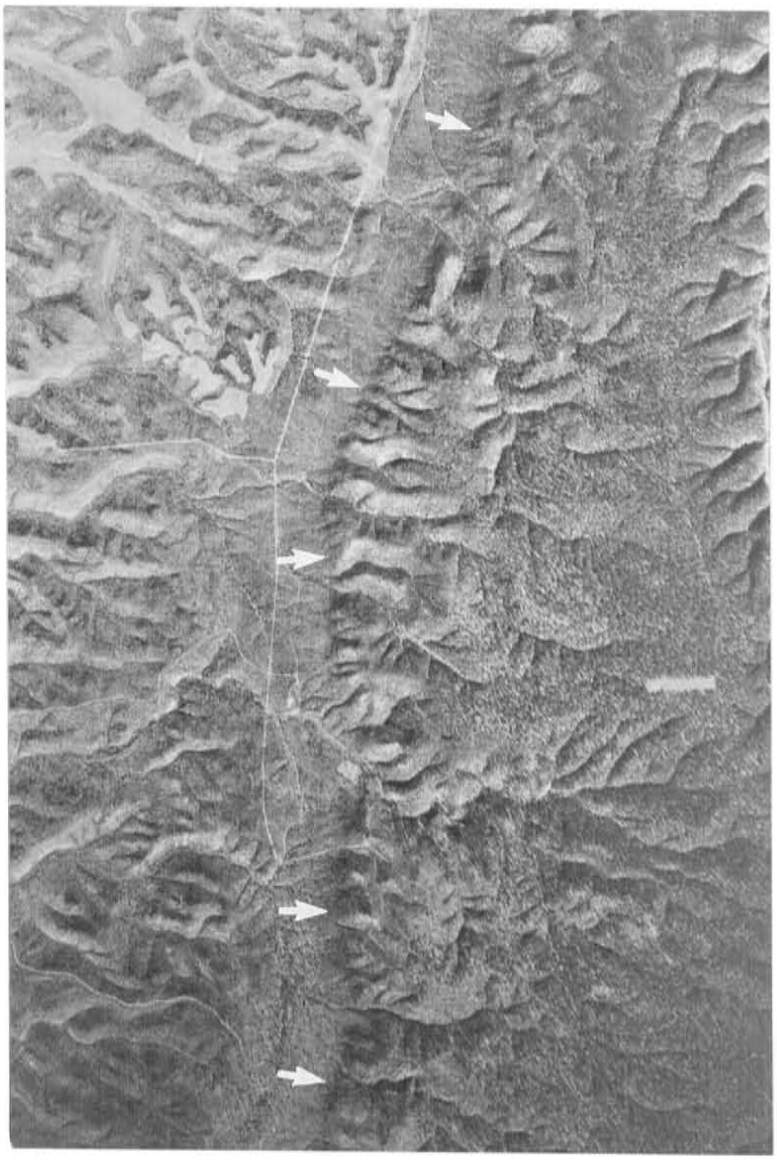

WHITE ARROWS SHOW LOCATION OF MAIN SCARP.

ARIZONA DEPARTMENT OF TRANSPORTATION

ARIZONA TRANSPORTATION RESEARCH CENTER

FIGURE 7

AERIAL PHOTOGRAPH OF WEST KAIBAB FAULT #3

d. Fault Trenching

(1) Big Chino Fault

(a) Background: The Big Chino fault is an important fault for understanding the neotectonics of the north-central Arizona region. The fault is one of several northwest-striking faults in the transition zone (herein referred to as the Arizona Mountain Seismic Source Zone) between the Central Colorado Plateau and the Sonoran Desert (Plate 1). However, unlike some adjacent seismotectonic zones, the Arizona Mountain zone is both seismically active and has several young faults that have ruptured the ground surface in late-Quaternary time such as the Big Chino, Aubrey, Verde, and Horseshoe faults. Of these faults, the Big Chino fault appeared to be the one that ruptured last and had the best characteristics for evaluating recurrence intervals, faulting rates, and earthquake potential.

Three trenches were excavated across the main scarp in Big Chino Valley (Figure 8) to assess the earthquake potential of the Big Chino fault and to acquire details on the nature of faulting such as fault plane orientation, gross displacement, displacement per event, and age of displacements. Also, geologic and geomorphic analyses were conducted. These included terrace and alluvial-fan morphology evaluation, fault-scarp-morphology analysis, aerial-photograph analysis, and field checking of the fault at strategic locations along the surface trace on the ground.

Based on aerial reconnaissance, aerial-photograph interpretation,

review of existing literature, and preliminary ground reconnaissance, an area on CV Ranch in the northern part of Big Chino Valley was selected for Trenching (Figure 8). Trenches were excavated on October 8 through 11, 1991. The fault is characterized by a prominent linear escarpment extending for a distance of about 35 miles. Figure 9 shows the typical surface expression of the Big Chino fault along the southwest flank of Big Black Mesa. The great length and apparent youthfulness of the fault make it a very important feature for evaluating the size and frequency of earthquakes, not only in the Chino Valley area but also for the entire transition zone area between the Colorado Plateau and the Sonoran Desert.

Three trenches were excavated across the trace of the Big Chino fault at an area known to local ranchers as Sheep Camp (Figure 10). The area was deemed to be especially well-suited for deciphering the faulting history because there are several well-developed terraces in the Quaternary alluvium (Figure 11). The occurrence of terraces at several different elevations indicates episodic changes in stream base level and commonly these changes are caused by uplift/subsidence due to vertical fault displacements. However, such terraces can also be the result of changes in stream capacity due to increase in stream flow such as might accompany changes in global climate, local cyclic weather trends, or catastrophic flooding events. At Sheep Camp there are about six levels of terraces that had been postulated to represent faulting events (Soule, 1978) and it was important to determine if they represented individual faulting events, and, if so, what was the frequency of faulting and how much displacement occurred per event. Soule's previous work (1978) was a university masters thesis primarily analyzing

FHWA REGION	STATE	PROJECT NUMBER	REPORT NUMBER
9	ARIZ.	HPR-PL-1(37)344	FWHA-AZ92-344

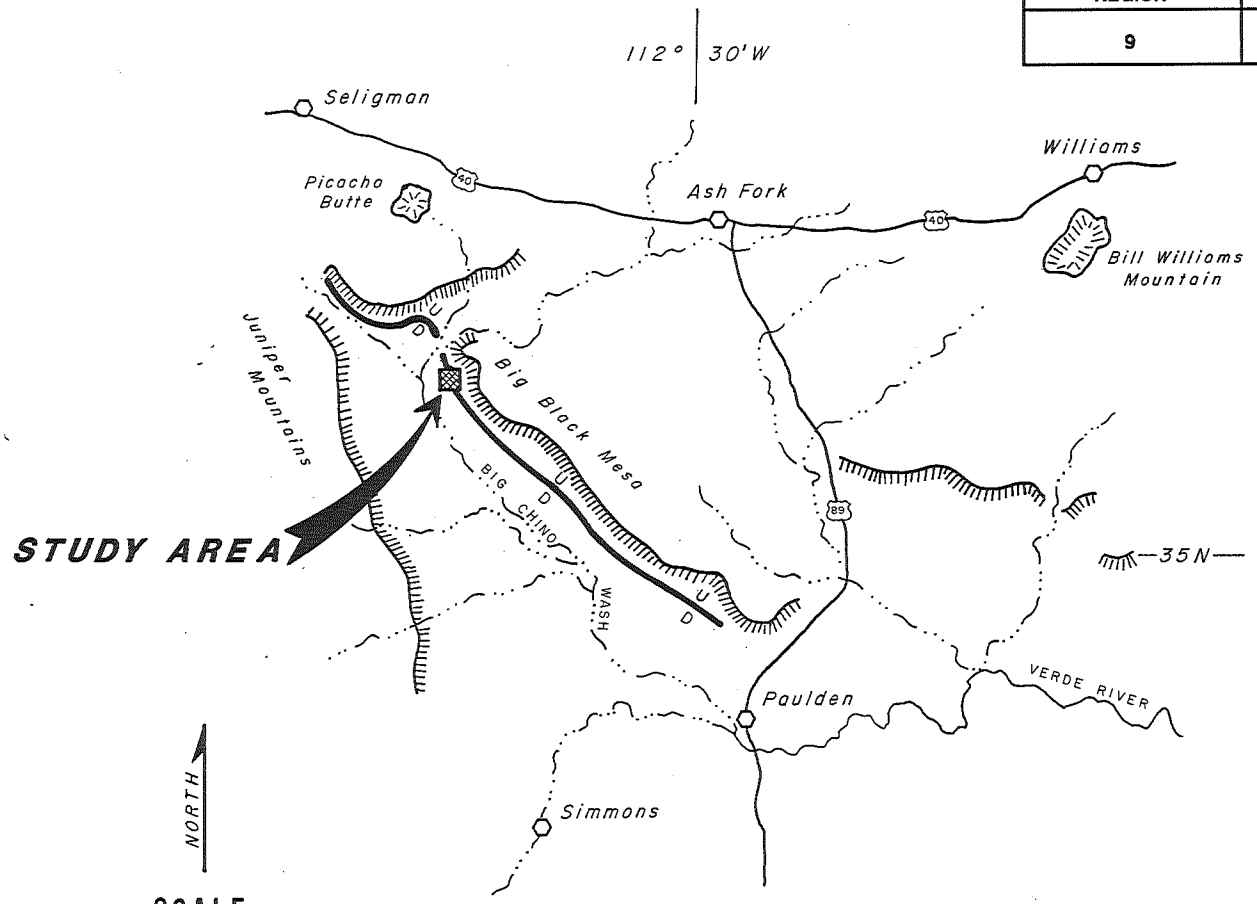

NOTE

BASE MAP MODIFIED FROM SOULE (1978)

KEY

- TOWNS
- US HIGHWAYS
- INTERMITTANT STREAMS
- PERENNIAL STREAM
- CLIFFS
- BIG CHINO FAULT
- SHEEP CAMP STUDY AREA

ARIZONA DEPARTMENT OF TRANSPORTATION
ARIZONA TRANSPORTATION RESEARCH CENTER

FIGURE 8
LOCATION MAP, BIG CHINO FAULT

FHWA REGION	STATE	PROJECT NUMBER	REPORT NUMBER
9	ARIZ.	HPR-PL-1(37)344	FWHA-AZ92-344

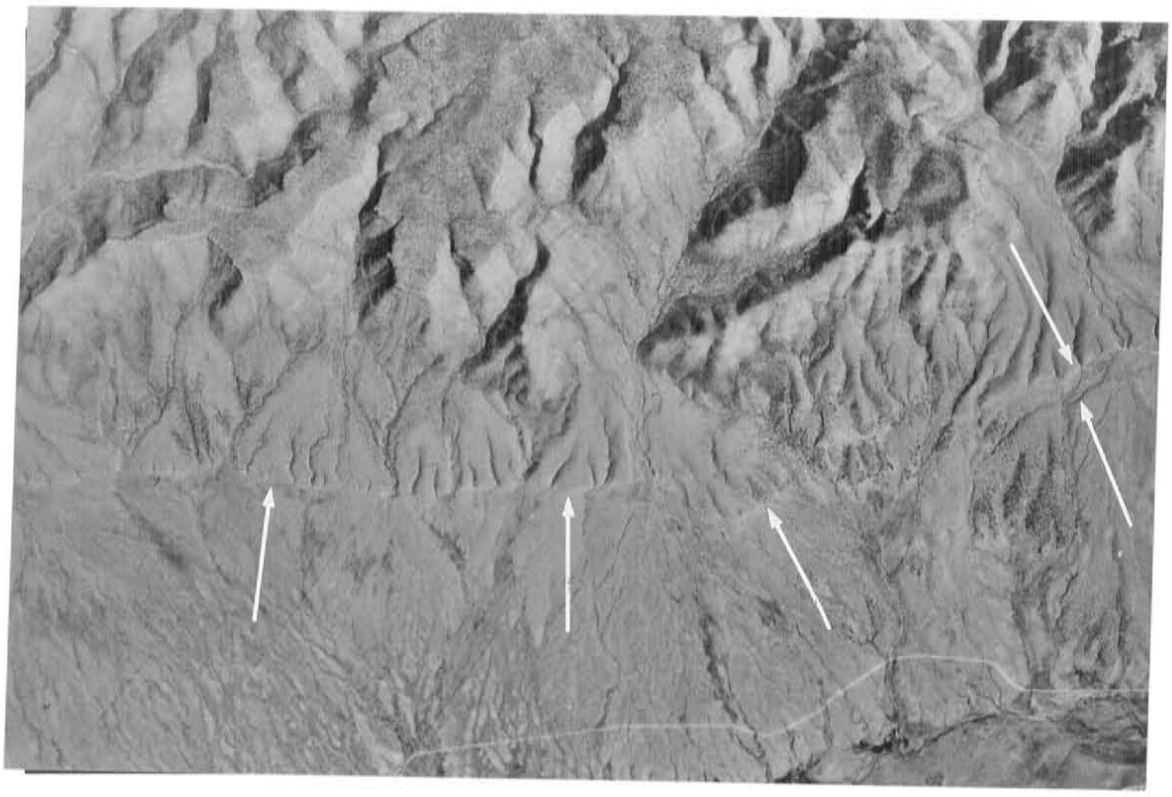

THE FAULT SCARP IS SHOWN BY THE ARROWS. THE AREA TO THE NORTHEAST HAS BEEN UPLIFTED ALONG THE FAULT RELATIVE TO VALLEY ON THE SOUTHWEST. THE MAXIMUM HEIGHT OF THE SCARP ALONG THIS SEGMENT OF THE FAULT AVERAGES ABOUT 80 FEET. ALSO NOTE ALLUVIAL GRABEN AT EXTREME RIGHT EDGE OF PHOTOGRAPH (INDICATED BY DOUBLE ARROWS). THE FAULT SEGMENT SHOWN ON THIS PHOTOGRAPH IS ABOUT 6 MILES LONG.

ARIZONA DEPARTMENT OF TRANSPORTATION

ARIZONA TRANSPORTATION RESEARCH CENTER

FIGURE 9

AERIAL PHOTOGRAPH OF BIG CHINO FAULT
BLACK MESA SEGMENT, CHINO VALLEY, ARIZONA

FHWA REGION	STATE	PROJECT NUMBER	REPORT NUMBER
9	ARIZ.	HPR-PL-1(37)344	FWHA-AZ92-344

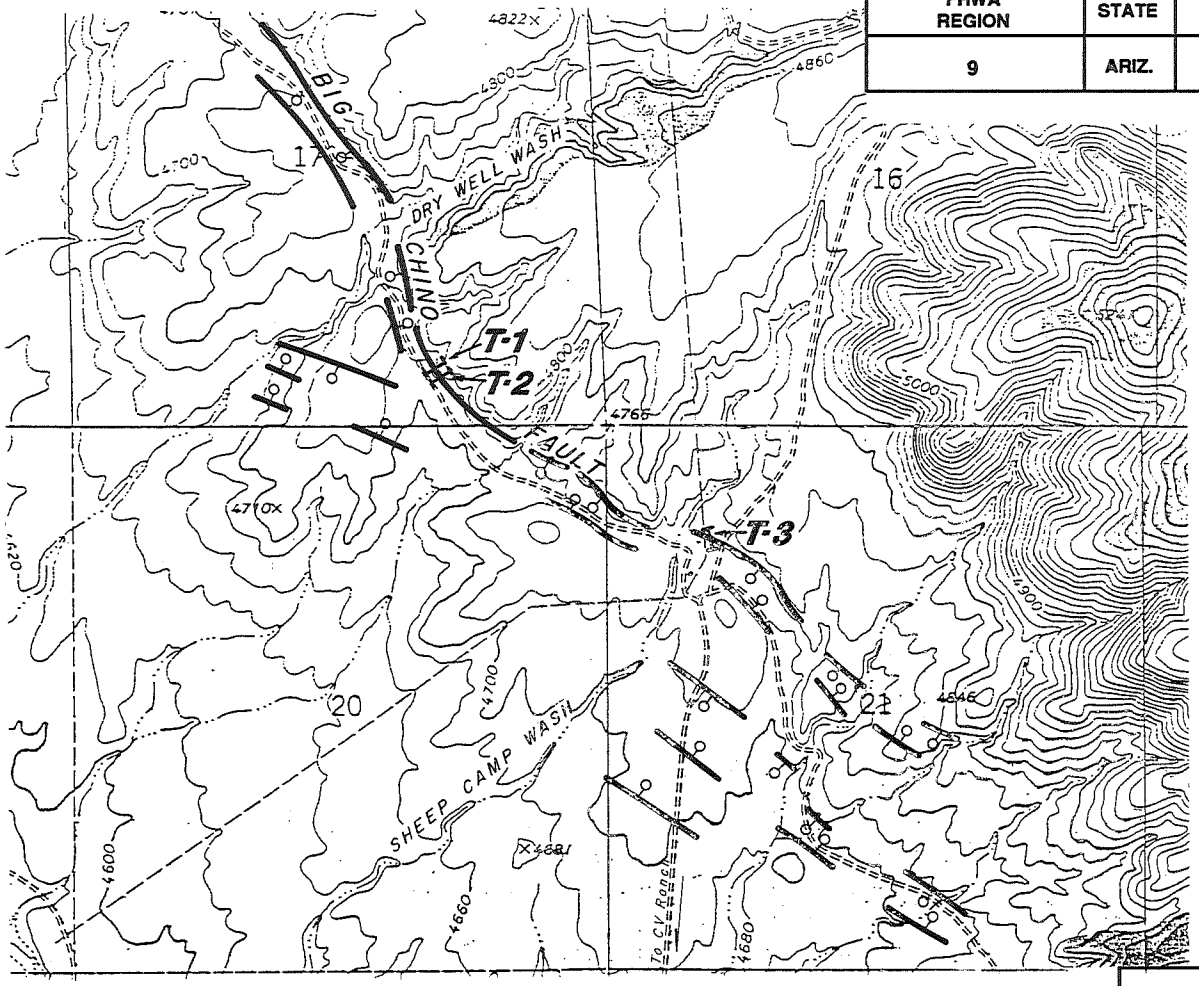

FAULT:
Bar and ball on downthrown side

Exploration trench location and number.
T-3

NOTE:
BASE MAP ENLARGED FROM SOUTH BUTTE 7.5 MINUTE TOPOGRAPHIC QUADRANGLE (USGS, 1973)

SCALE

FEET
1000 0 1000 2000 3000

0 500 1000
METERS

ARIZONA DEPARTMENT OF TRANSPORTATION
ARIZONA TRANSPORTATION RESEARCH CENTER

FIGURE 10
FAULT MAP, SHEEP CAMP AREA
BIG CHINO VALLEY
T20N, R4W, YAVAPAI COUNTY, ARIZONA

FHWA REGION	STATE	PROJECT NUMBER	REPORT NUMBER
9	ARIZ.	HPR-PL-1(37)344	FWHA-AZ92-344

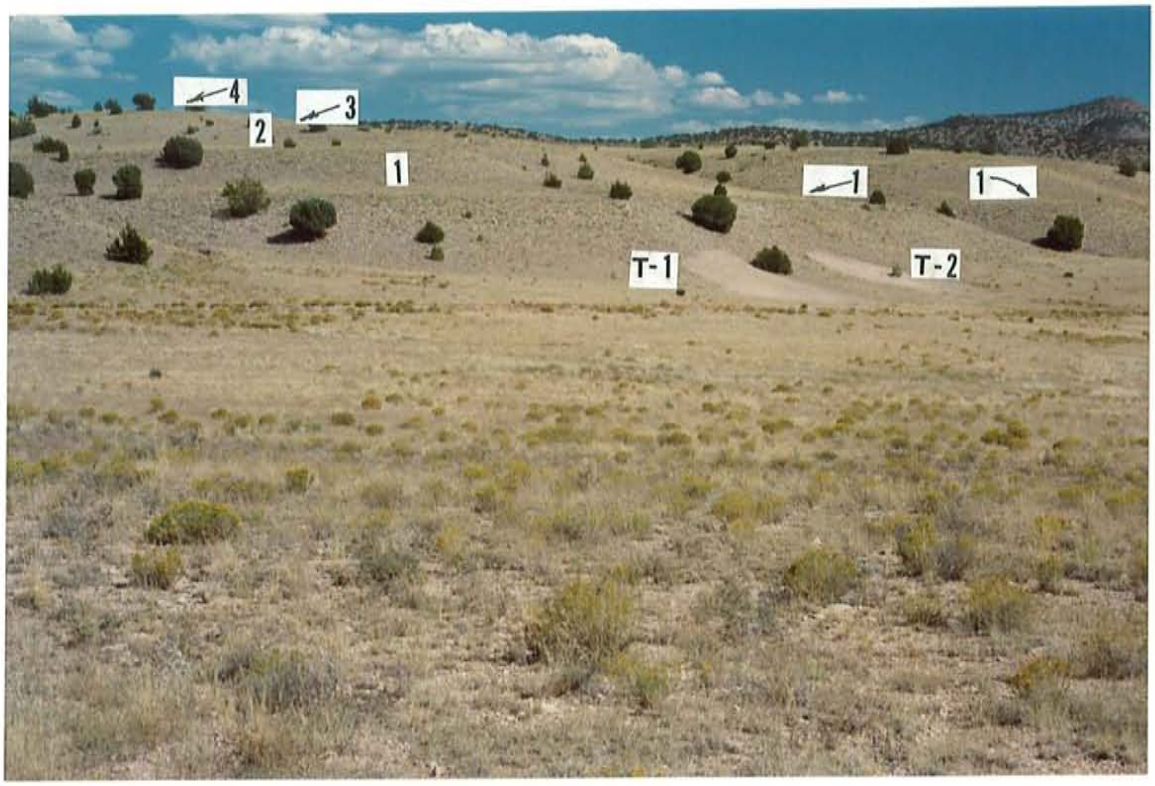

BIG CHINO FAULT IS ALONG THE BASE OF THE SLOPES. FOUR LEVELS OF TERRACES ARE SHOWN ON THIS PHOTOGRAPH. LEVEL 1 IS ABOUT 40 FEET HIGH. THE LIGHT, NON-VEGETATED AREAS ON THE RIGHT SIDE OF THE PHOTOGRAPH ARE THE LOCATIONS OF TRENCHES 1 AND 2. VIEW IS TOWARD THE EAST.

ARIZONA DEPARTMENT OF TRANSPORTATION
ARIZONA TRANSPORTATION RESEARCH CENTER

FIGURE 11
TERRACES ALONG BIG CHINO FAULT
SHEEP CAMP STUDY AREA

FHWA REGION	STATE	PROJECT NUMBER	REPORT NUMBER
9	ARIZ.	HPR-PL-1(37)344	FWHA-AZ92-344

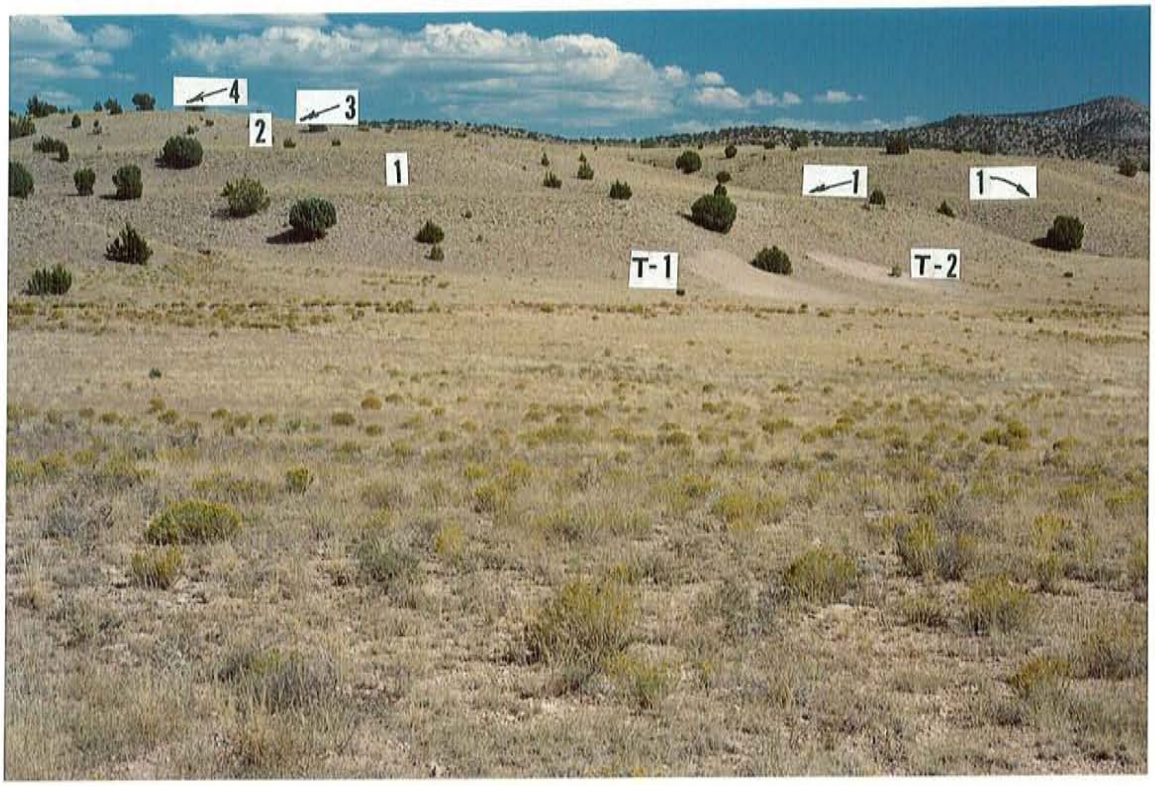

BIG CHINO FAULT IS ALONG THE BASE OF THE SLOPES. FOUR LEVELS OF TERRACES ARE SHOWN ON THIS PHOTOGRAPH. LEVEL 1 IS ABOUT 40 FEET HIGH. THE LIGHT, NON-VEGETATED AREAS ON THE RIGHT SIDE OF THE PHOTOGRAPH ARE THE LOCATIONS OF TRENCHES 1 AND 2. VIEW IS TOWARD THE EAST.

ARIZONA DEPARTMENT OF TRANSPORTATION
ARIZONA TRANSPORTATION RESEARCH CENTER

FIGURE 11
TERRACES ALONG BIG CHINO FAULT
SHEEP CAMP STUDY AREA

surface geomorphology and soil-profile development. Our preliminary analysis indicated that only two or possibly three of the terraces occurred consistently elsewhere along the fault so it was questionable as to whether all of the terraces were tectonically controlled or whether some of them represented local fluvial effects of local creeks.

The three trenches were excavated at two sites which, based on geomorphology, seemed to represent the best locations for unambiguous results. In the selection of trench locations it is important to select sites that will reveal several layers of strata free from local or anomalous erosional or depositional events, and these layers must be shallow enough to be excavated by standard digging equipment such as a backhoe or a bulldozer. At one site, two trenches (T-1 and T-2) were excavated (Figures 10 and 11). Trench 1 was the principal trench. Trench 2 was a confirmatory trench, excavated to ensure that the relationships seen in T-1 were indeed typical and representative of the faulting/depositional regime. T-3 was excavated across a smaller scarp near a drainage referred to herein as Sheep Camp Wash (Figures 10 and 12). The depth of trench excavation depended on three factors: 1) the hardness of the material, i.e. the depth of refusal, 2) the deepest digging capability of the backhoe, or 3) the depths where stratigraphy was adequate to make reliable determinations. The maximum depth capability of the backhoe was about 14 to 15 feet. This depth was needed only in T-3.

The trenches were excavated across the faces of the main fault scarp. The scarp at T-1 and T-2 was about 40 feet high; at T-3 the scarp was about

FHWA REGION	STATE	PROJECT NUMBER	REPORT NUMBER
9	ARIZ.	HPR-PL-1(37)344	FWHA-AZ92-344

VIEW LOOKING NORTHWEST. TRENCH 3 WAS EXCAVATED ACROSS THE SCARP JUST THIS SIDE OF THE BARBED-WIRE FENCE. THE SCARP ON THE RIGHT IS ABOUT 15 FEET HIGH.

ARIZONA DEPARTMENT OF TRANSPORTATION

ARIZONA TRANSPORTATION RESEARCH CENTER

FIGURE 12

BIG CHINO FAULT SCARP AT TRENCH 3 LOCALITY

15 feet high. Smaller scarps are sometimes better for trenching because correlative layers are more likely to be found on each side of the fault thereby allowing better estimates of amounts and timing of displacements. The length of the trenches were 40 feet (T-2), 66 feet (T-1), and 85 feet (T-3). Prior to logging, a level line was established on one wall of the trench for reference purposes. The trenches were logged by the project geologists at a scale of 1 inch to 5 feet (Figures 13 and 14) and 1 inch to 10 feet. Dr. Philip Pearthree (Arizona Geological Survey) visited the trench sites and provided helpful observations and insightful discussions with the project geologists. Dr. Pearthree also made a detailed soil-profile description in T-1 (Figure 13c). Upon completion of logging, the trenches were backfilled and the ground surface was restored to the original natural contour as much as possible.

(b) Trenches: Logs of trenches 1 and 3 are presented as Figures 13 and 14. The fault was clearly revealed in both trenches and appears as a zone of disruption in the otherwise layered alluvial sediments. Shearing was minimal in both trenches, as is typical for normal faults in alluvium. Only Trench 3 had a layer (soil Units 6 and 10) that could be correlated to both sides of the fault (Figure 14). This layer provided good information on the amount and age of faulting. Both trenches had well-developed dipping wedges of alluvium (Figure 13, Units 3-6; Figure 14, Units 2-4, 7, 5). Such wedges, commonly called colluvial wedges, represent detritus eroded from newly formed fault scarps and deposited at the base of the scarp. The number of wedges provides information on the number of surface-rupture events. Generally the bulk of these wedges is deposited

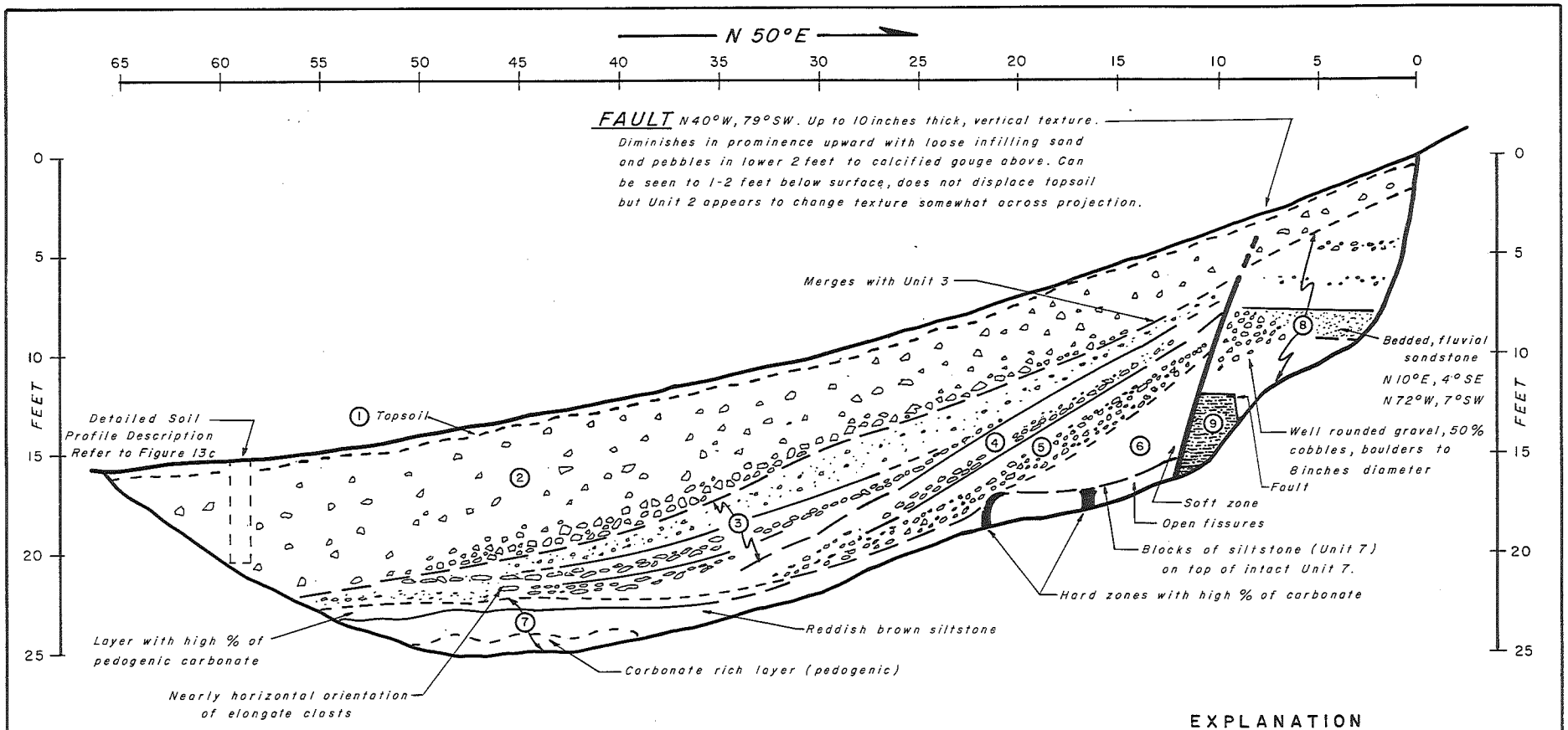

EXPLANATION

(2) - Stratigraphic Unit Designator, refer to detailed descriptions on Figure 13b.

SCALE
5 0 5 10
FEET

FHWA REGION	STATE	PROJECT NUMBER	REPORT NUMBER
9	ARIZ.	HPR-PL-1(37)344	FWHA-AZ92-344

ARIZONA DEPARTMENT OF TRANSPORTATION
ARIZONA TRANSPORTATION RESEARCH CENTER

FIGURE 13a
TRENCH NO. 1 - BIG CHINO FAULT

FHWA REGION	STATE	PROJECT NUMBER	REPORT NUMBER
9	ARIZ.	HPR-PL-1(37)344	FWHA-AZ92-344

Unit No. Description

1) TOPSOIL: Brown (7.5YR 5/2) to dark brown (7.5YR 3/4), gravelly loam, fine-coarse, subangular blocky structure, slightly hard to hard, wavy lower boundary. Thin carbonate coating on some pebbles (see Detailed Soil Description, Figure 13c).

2) GRAVELLY SAND: Pale brown (10YR 6/3), yellowish brown (10YR 5/4), and dark brown (7.5YR 5/4); some mottling. Gravel comprises about 30 percent to 50 percent of unit except for basal layer which is 80% subangular to subrounded pebbles and cobbles. Hard sandy clay matrix. Massive; basal layer is the only noticeable bedding. Clasts range from pebbles to cobbles of 4 - 6 inch diameter. Basal layer has slight imbrication; carbonate occurs as thin strings, lenses, and spots (Stage II); harder than upper part of unit due to better carbonate cementation. Moderately sharp, irregular lower contact (see Detailed Soil Description, Figure 13c).

3) SANDY GRAVEL: Brown to pale brown. Clasts generally in pebble to small cobble (2-inch diameter) size range. Rounded to subangular. Moderately hard to hard depending on carbonate cementation. Poorly bedded, some very slight imbrication of clasts in upper part of unit to moderately well imbricated and weak bedding in lower part of unit. Some discontinuous zones of pedogenic carbonate accumulation with completely coated clasts (Stage II). Gradual to diffuse, irregular lower contact.

4) GRAVELLY SAND/GRAVEL: White to very pale brown. Grades downward from gravelly sand to sandy pebble gravel to pebble-cobble gravel. Clasts in lower layer are generally in pebble to 2 - 3 inch size-range, but some rare cobbles are 6 to 8 inches. Strongly imbricated. Hard, cemented with pedogenic carbonate. Sandy upper part of unit is a completely plugged white carbonate zone; lower part of unit is a gravel with clasts completely coated with carbonate. Tops of clasts have thin films, undersides have irregular buildups to 2mm thick; where clasts are plucked out, a well-developed carbonate rind remains. Moderately sharp, wavy lower contact.

5) GRAVELLY SAND/GRAVEL: (Identical to Unit 5, Unit 4 and 5 could be beds within the same depositional unit).

6) SANDY GRAVEL: Gray to brown; overall color appears gray but zones of brown occur throughout; upper 1 to 1.5 feet is reddish brown. 30 - 40% gravel, 5% silt. Clasts range from pebble to cobble size, 10 - 15% of gravel is cobbles. Clasts are well rounded to subangular (5%), mostly volcanic rocks but some blocks of siltstone similar to Unit 9 are present. Most of these siltstone blocks and fragments are within the upper 1 - 2 feet. Friable, dense, slight cohesion. Poorly bedded, slight imbrication (7° apparent dip). Lower contact is sharp but wavy.

   Upper reddish-brown zone appears to be soil developed on the gray gravel. Clasts in this upper zone have carbonate coating up to 1mm thick on undersides. Matrix has disseminated carbonate.

7) SILTSTONE: Reddish brown (7.5YR 4/6) to white. Scattered and pockets of angular to subrounded pebbles and small cobbles. Vesicular, 5% open root holes. Hard, dry. Both the top and bottom are calcic zones; the bottom calcic zone is completely plugged (Stage III).

8) GRAVEL: Grayish brown, brown to yellowish brown. Predominantly pebbles with small cobbles and few large cobbles with sandy matrix. Well rounded, loose to moderately loose. Poorly bedded but nearly horizontal fabric is obvious in several zones. Middle part of unit is well-bedded, moderately hard, dry, friable, sandstone.

9) SILTSTONE: Very pale brown to reddish brown, with scattered pebbles and beds of silty sand. Moderately well bedded with 2 to 4-inch-thick beds. Slightly moist. Moderately hard but can be disaggregated with difficulty by fingers. Violent reaction to HC1. Very jointed into angular fragments 1 to 2 inches wide. Joint surfaces have black spots and films. Beds near fault plane are bent indicating vertical drag.

ARIZONA DEPARTMENT OF TRANSPORTATION
ARIZONA TRANSPORTATION RESEARCH CENTER

FIGURE 13b
TRENCH NO. 1 - BIG CHINO FAULT
SOIL DESCRIPTIONS

Horizon	Depth (in.)	Color	Structure	Consistency	Texture	Boundary	Carbonate
A	0 - 3	7.5YR 5/4 (dull brown)	Moderate Fine-med	Slightly hard	Gravelly loam	Wavy	Stage IC, Effervescent within discontinuous pebble coatings
		7.5YR 3/4 (dark brown)	Subangular	Slightly sticky Slightly plastic			
Bwk 1	3 - 6.5	7.5YR 5/2 (grayish brown)	Moderate	Slightly hard-hard	Gravelly loam	Wavy	Stage IC, Effervescent, few thin discontinuous pebble coatings
		7.4YR 3/2 (brownish black)	Fine-Coarse sbk	Slightly sticky Slightly plastic			
Bwk 2	6.5 - 12.5	10YR 5/4 (dull yellowish brown)	Weak	Soft-slightly hard	Gravelly loam	Irregular	Stage I-II C, Strong effervescent, thin discontinuous to nearly continuous pebble coatings
		10YR 3/4 (dark brown)	Fine-Med sbk	Slightly sticky Slightly plastic			
Bwk 3	12.5 - 24.5	10YR 6/3 (dull yellow orange)	Weak	Slightly hard-hard	Gravelly loam	Wavy	Stage II C, Violent effervescent, filaments & whitened matrix, soft discontinuous continuous pebble coatings
		10YR 4/3 (dull yellowish brown)	Fine-coarse sbk	Slightly sticky Slightly plastic			
Bwk 4	24.5 - 37.5	7.5YR 5/4 (dull brown)	Moderate	Hard	Very gravelly loam/clay loam	Irregular	Stage II C, Violent effervescent, whitened matrix, harder continuous, discontinuous pebble coatings
		7.5YR 3/4 (dark brown)	Medium-coarse sbk	Slightly plastic Sticky			
Bk	37.5 - 61	7.5YR 6/4 (dull orange)	Massive	Soft	Gravelly sandy loam		Stage I, Strong effervescent, thin, discontinuous pebble coatings
		7.5YR 3/4 (dark brown)		Slightly sticky Slightly plastic	Loam		

Notes: Horizons

A - accumulation of humified organic material mixed with mineral fraction, the latter is dominant.
B - underlies A horizon, little or not evidence of original sediment structure.
Bw - color change or soil structure relative to C horizon, little evidence of clay or silt accumulation.
Bk - accumulation of calcium carbonate.
C - may have weathered material, but otherwise no soil development (parent material)

Abbreviations

sbk - subangular blocky
c - clear
irreg - irregular
sl - slightly
med - medium

Reference: Birkeland, P.W., 1984.

Surface soil at base of scarp, southwest end of trench. Correlative with unfaulted unit in northeastern portion of trench, some colluvial input, but less than closesr to the scarp. (See Figure 13a) for profile location).

FHWA REGION	STATE	PROJECT NUMBER	REPORT NUMBER
9	ARIZ.	HPR-PL-1(37)344	FWHA-AZ92-344

ARIZONA DEPARTMENT OF TRANSPORTATION

ARIZONA TRANSPORTATION RESEARCH CENTER

FIGURE 13c

TRENCH NO. 1 - BIG CHINO FAULT
SOIL PROFILES, UNITS 1 AND 2

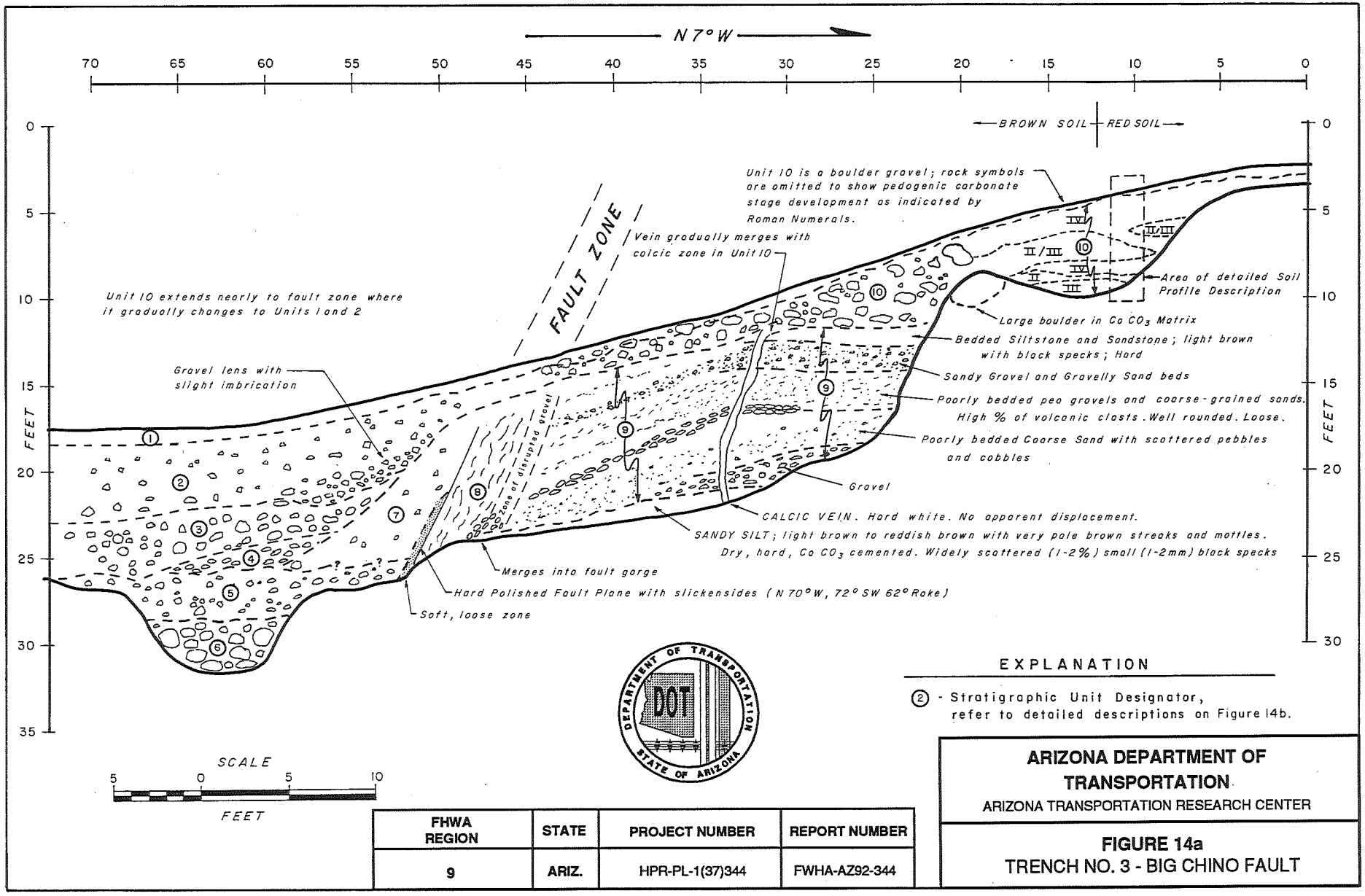

EXPLANATION

② - Stratigraphic Unit Designator, refer to detailed descriptions on Figure 14b.

FHWA REGION	STATE	PROJECT NUMBER	REPORT NUMBER
9	ARIZ.	HPR-PL-1(37)344	FWHA-AZ92-344

ARIZONA DEPARTMENT OF TRANSPORTATION

ARIZONA TRANSPORTATION RESEARCH CENTER

FIGURE 14a

TRENCH NO. 3 - BIG CHINO FAULT

FHWA REGION	STATE	PROJECT NUMBER	REPORT NUMBER
9	ARIZ.	HPR-PL-1(37)344	FWHA-AZ92-344

Unit No. Description

1) TOPSOIL: Dark Brown (7.5YR 3/4), gravelly sandy loam, fine-medium blocky structure, dry, soft and crumbly. Abundant fine rootlets. Gradual-diffuse lower contact. Gravel content increases upslope and soil becomes thinner and less distinct on scarp face where it merges into unit 10.

2) SILTY SAND WITH GRAVEL: Brown to dark brown. (7.5YR 5/4-5/2), 5 to 10% pebbles and small cobbles, subrounded to subangular, size of clasts increases toward bottom of unit. Dry, hard to friable. Lower contact moderately sharp, clear and undulating.

3) BOULDER GRAVEL: Light brown to light gray. Well rounded to subrounded clasts with calcic coatings completely surrounding clasts. All clasts are sedimentary rocks, predominantly limestone but some sandstone and quartzites also are present. Calcic coatings are thin films (< 1mm). Unit appears similar to Unit 2 but is coarser grained and has more advanced carbonate development (Stage II). Lower contact undulating but moderately sharp.

4) GRAVEL: White, hard, dry, tightly cemented with $CaC0^3$. Poorly sorted from granules to boulders in sandy matrix. Small cobbles are most abundant. Well rounded to subrounded clasts of sedimentary rocks clasts are completely coated with calcic rinds, a few rinds appear thicker on top of clast suggesting reworking of older K horizon; calcic nodules up to 1 inch diameter are common in matrix (Stage II-III). Some imbrication of clasts. Lower contact moderately sharp.

5) SILTY SAND AND GRAVELLY SILT: Multicolored; yellowish red (5YR 5/6), pale brown (10YR 6/3), and white. Pebbles and cobbles are widely disseminated to lenticular. Some fine grained areas are white due to high carbonate content. Slightly moist, moderately hard. Vesicular, some vesicles are open, some with calcic lining. Lower contact diffuse.

6) BOULDER GRAVEL: White to pale brown. Poorly sorted clasts of sedimentary rocks, mostly limestone, well rounded to subrounded. Poorly defined bedding, lenticular. All clasts coated with thin (< 1mm) to thick (5mm) calcic rinds (Stage III). Loose to tightly cemented.

7) SANDY SILT WITH GRAVEL: White to very pale brown. Dry, hard, cemented with $CaC0^3$ (Stage IV). Slight imbrication of pebbles and small cobbles.

8) SILT AND SAND WITH GRAVEL: Cemented fault gouge. White to light brown. Dry, hard cemented with $CaC0^3$. Numerous shears, streaks, cracks, carbonate veins and strongly developed fabric with apparent dip of about 70-75 degrees. Southerly contact is abrupt in lower part with striated, polished surface (N 70° W, 72° W; slickensides 62° rake). Northerly contact moderately sharp.

9) SAND, GRAVEL, SANDSTONE, AND SILTSTONE: Gray to light brown. Well-bedded sequence with large percentage of volcanic clasts. Gray color derives from volcanics. Grain sizes comprise silt/clay to small cobbles but these are generally sorted into distinct beds within sub units, 1/2 cm to 2 cm size is most common. Some cross-bedding. Dry, loose to dense, spotty cementation. Disseminated carbonate, no significant calcic coatings. Bedding less defined south of calcic fissure vein.

ARIZONA DEPARTMENT OF TRANSPORTATION
ARIZONA TRANSPORTATION RESEARCH CENTER

FIGURE 14b
TRENCH NO. 3 - BIG CHINO FAULT
SOIL DESCRIPTIONS

10) BOULDER GRAVEL: White with red soil. Dry, hard, with loose zones. Poorly sorted with short discontinuous beds and lenses. Clasts to 1 meter diameter but 30 to 50 cm size is most common, well rounded to subrounded, thick calcic coatings and tightly cemented to loose. Clasts are all sedimentary rocks, mostly limestone with few sandstones. Trench log shows irregular distribution of carbonate development (see detailed soil profile description).

DETAILED SOIL PROFILE DESCRIPTION

Depth (Cm)	Horizon	
0 - 6	A	Strong brown (7.5YR 4/6) when dry; dark brown (7.5YR 3/4) when moist. Loam. Fine to medium granular; soft when dry, friable and slightly sticky when moist. Lower boundary diffuse.
6 - 20	B	Red (2.5YR 4/6) when dry; dark red (2.5YR 3/6) when moist. Silty clay loam with very fine-grained sand. Fine blocky and medium granular. Soft when dry, firm and slightly sticky when moist, slightly plastic when wet. Lower boundary gradual to diffuse. Developed in boulder gravel; pockets of soil extend around and under clasts.
20 - 95	K	White to very pale brown boulder gravel with lenses and layers of sandy pebble gravel. Strongest $CaC0^3$ development is from 20 to 75 cm depth. This stage IV calcic horizon is completely plugged with discontinuous laminae in finer grained layers. These laminae can be broken down by finger pressure with difficulty and can be disaggregated completely with persistent effort. All clasts are completely coated with calcic rinds, maximum thickness on tops of clasts is about 1/2 cm. Rinds on bottoms commonly 1 cm and up to 3 cm where voids occur.
95 - 107		Carbonate development from 95 cm to 107 cm is variable from Stage IV to II depending on grain size and permeability/porosity. In areas below large boulders or impermeable laminae, carbonate development is early Stage II with calcic rinds less than 1 mm thick only on bottom of clasts.
102 - 203		Stage IV zone on west side of trench with laminar horizons and calcic rinds of 0.5 to 1 cm on some clasts. Laminae are discontinuous.

within a few hundred to a thousand or so years after the faulting event, until the scarp is worn back to the angle of repose (about 35 degrees) (see Section 6.a (3)). After that, further deposition is very slow and soils develop on the surface of the wedges until the next rupture occurs when a new scarp is formed and new colluvium is washed over the previous wedge and its soil. The length of time between successive faulting events is important for the development and recognition of these wedges. Faults with long times between surface ruptures will have colluvial wedges with well-developed soils and distinct contacts that can be more-easily differentiated than wedges along faults with short recurrence intervals, where the wedges tend to grade into one another.

It is interesting to note that in Trench 1, the deposits on the northeast side of the fault are not alluvial-fan deposits as was expected. Rather, these deposits were relatively well bedded, nearly horizontal, stream deposits typical of more low-energy, central-valley, depositional processes. Ground checking in the nearby canyons showed similar deposits underlying the entire area indicating these fine-grained deposits are quite extensive and not just a local fault sliver. These deposits indicate that Big Chino Valley had a long quiescent period without substantial surface faulting. Geomorphic analyses of alluvial surfaces in other parts of the valley indicate a long period of erosion and downcutting after the quiescent period, suggesting that the quiescence period probably existed during the early Quaternary, several hundred thousand years to more than a million years ago. The deposit is important because it indicates an episodic nature to the extensional faulting regime. However, such episodic tectonism is not unusual in the Basin and

Range province. The project geologist, as well as others, have documented several cases of similar long-term quiescence in the tectonically more-active central Basin and Range area of Nevada and Utah (Schell, 1982; Schell et al, 1981; Muir et al, 1981; Wallace, 1987; Ryall, 1977).

Soil-profile analysis at Trench 1 revealed that stratigraphic Unit 2 (Figure 13a) which overlies the fault and is unfaulted has moderate reddening, clay alteration, and carbonate accumulations indicative of soil formation since early Holocene to latest Pleistocene time, perhaps in the 8,000 to 10,000 year range. This age is supported by the presence of a small entrenched, but unfaulted, alluvial fan at the mouth of the stream channel just northwest of the trench which overlaps Unit 2 and has a surface geomorphology also indicating an early Holocene age. These data indicate that the latest surface rupture of the Big Chino fault occurred prior to Holocene time. A unit similar to Unit 2 overlies the fault in Trenches 2 and 3 (Figure 14). Although we deduce from this that the latest rupture was pre Holocene, it is uncertain as to how long before Holocene it might have occurred. The soils developed on the colluvial wedges indicate that the time between rupture events was quite long, on the order of at least several thousand years and most likely a few tens of thousands of years. In Trench 1 (Figure 13), the colluvial wedges (stratigraphic Units 3, 4, 5, and 6) all have substantial soil development in the form of reddened B horizons and (or) pedogenic carbonate accumulations typical of soils that have been forming for more than 10,000 years, to as much as several tens of thousands of years.

(c) Tectonic Geomorphology: Although the trenching across the Big Chino fault was successful in documenting several displacements and in quantifying typical amounts of displacements during faulting, the analysis suffers from lack of absolute age control. There are no dated alluvial materials in the Chino Valley area and we uncovered no material that could be dated. However, some general estimates of age and age ranges were estimated by analysis of geomorphic relationships and soil-profile development on alluvial fans and terraces.

Based on comparison of surface geomorphology to alluvial units in other parts of the Basin and Range using the tectonic geomorphology methods such as described by Christenson and Purcell (1985), Schell et al (1981), Muir et al, (1981), Schell and Muir (1982), as well as comparison to other dating studies such as in southern Nevada and New Mexico (Gile et al, 1981; Gile, 1986; Sowers et al, 1988), alluvial surfaces were categorized into order-of-magnitude age categories (e.g. 10^3, 10^4, 10^5, 10^6 years). For example, surfaces which once were flat, coalesced alluvial aprons but which now are dissected such that there are no flat surfaces between stream channels, which have had the soils stripped away by erosion, and which have complex dendritic drainage patterns can be several hundred thousand (10^5) to more than a million years (10^6) old. The erosion generally occurs at a rate dictated by climatic influences but uplift due to faulting can also increase the rate of surface dissection. Highly dissected surfaces with narrow flat areas between channels, wide flat washes, commonly with strong soil carbonate development, advanced soil formation, and closely packed interlocking surface pavements of pebbles and cobbles are typically a few to several hundred thousand years

old (10^5). The degree of development of each of these characteristics narrows the age range within each order-of-magnitude category. For example, the highest alluvial-fan surfaces on the northeast side of Chino Valley fit into the 10^5 category but appear to be of the younger variety between about 200,000 to 400,000 years old. This surface has many similarities to the Jornada I surface in New Mexico that is about 250,000 to 400,000 years old (Gile, 1986). The same type of comparative analyses were used on the other surfaces throughout the entire valley and when the whole system is pieced together, a crude history of alluviation, uplift, and downcutting, presumably related to both climatic and tectonic effects can be deciphered for Big Chino Valley. Although the estimates have large uncertainties, the results do provide some useful age constraints for evaluating the rates of fault displacement and earthquake potential.

(d) Fault Displacements: The best data for determining the amount and age of displacement comes from Trench 3 where, unlike T-1 and T-2, an offset stratigraphic unit with measurable offset on one side of the trench could be matched to its offset counterpart on the other side of the fault. Based on lithologic characteristics and soil development, stratigraphic unit 6 appears to be the downfaulted equivalent of Unit 10 on the upslope side of the fault (Figure 14). This unit, which is about 80,000 to 100,000 years old based on soil-profile (Stage III-IV Calcic horizon) and surface-pavement development is displaced about 25.5 feet. The colluvial wedges in the trench (Units 2, 3, 4, and 7) suggest two or three subsequent displacements. Averaging these displacements over the estimated time span of 80,000 to 100,000 years indicates that the time between events was in the

20,000 to 30,000 year range and that displacements were about 6 to 9 feet per event. The 6- to 9-foot displacement are reasonable figures based on typical Basin-and-Range tectonics and local geomorphology. The thickness and configuration of Unit 5 suggest that prior to its deposition, the scarp was at least 5 feet high which would indicate a minimum offset of about that much.

The total cumulative displacement of the Big Chino fault, based on displacement of the highest-elevation alluvial-fan surfaces, can also provide information on amounts of rupture. Measuring scarp profiles from topographic maps indicates that the average height of the Big Chino Scarp is about 80 feet. Assuming this represents a total displacement of about 80 feet within late Pleistocene time (approximately the past 200,000 years) suggests surface ruptures of about 6 to 11 feet per event. However, these displacements are gross displacements along only the main fault and, as described above, most of the Big Chino fault is paralleled by a subsidiary antithetic (back-dipping) fault. For earthquake magnitude assessments, the net slip should be used and this requires that the slip on the subsidiary back-dipping fault be subtracted from that of the main fault. The back-dipping fault was not trenched but, based on geomorphology of the scarp, its total displacement appears to be about 25 percent of the main scarp, a value typical of Basin-and-Range type normal faults. Subtracting 25 percent of the displacement yields net displacements of about 4.5 to 8 feet per event. None of these estimates of displacement can be completely accepted at face value but they cluster around 4 or 5 to 9 feet which is typical of basin and range faulting

and could very well represent the range of displacements during the prehistoric rupture events on the Big Chino fault.

In Trench 1, stratigraphic units could not be correlated across the fault because the displacements were greater than the depth of the trench. However, the number of colluvial wedges and their soil-profile development suggest 4 or 5 ruptures with similar recurrence intervals in the 20,000- to 30,000-year range.

Surface geomorphology indicates that the Big Chino fault is a normal fault dipping to the southwest with the valley side of the fault displaced downward relative to the mountain side. The trenches revealed a fault-plane dipping 60 to 70 degrees to the southwest (Figures 13 and 14). The surface geomorphology indicates only dip slip but Trench 3 revealed a polished shear surface with well-developed slickensides indicating a right-lateral component of slip of about 30-percent (Figure 15). In other words, as the southwestern or valley fault-block is displaced downward, it moves slightly to the left relative to the rocks on the other side of the fault which are displaced upward and to the right. Although such lateral-slip components are not uncommon in Basin and Range normal faults, just one occurrence of such a slip surface does not provide conclusive evidence that the entire fault has the same sense of slip over its entire length during every event because local geometric variations in fault strike can give apparent lateral components that do not represent the net regional slip.

FHWA REGION	STATE	PROJECT NUMBER	REPORT NUMBER
9	ARIZ.	HPR-PL-1(37)344	FWHA-AZ92-344

BETWEEN STATIONS 50-55 ON TRENCH LOG, TRENCH NO. 3. NOTE GROOVES AND STRIATIONS (SLICKENSIDES) ON SMOOTH POLISHED FAULT-PLANE SURFACE. ARROWS SHOW 60 DEGREE, OBLIQUE ORIENTATION OF SLICKENSIDES. GSA CARD SHOWS SCALE IN INCHES AND CENTIMETERS.

ARIZONA DEPARTMENT OF TRANSPORTATION
ARIZONA TRANSPORTATION RESEARCH CENTER

FIGURE 15
FAULT PLANE OF BIG CHINO FAULT
TRENCH NO. 3

(e) Earthquake Potential: The size of earthquake that probably accompanied the displacements on the Big Chino fault can be estimated by comparison to historical earthquakes on similar faults in similar tectonic environments using fault length and displacements. Analysis of the geomorphology of Big Chino Valley revealed nearly continuous fault scarps along the northeast side of the valley in proximity to the mountain fronts of Big Black Mesa and Picacho Butte. The total length of these fault scarps is about 35 miles. The fault scarps appear to branch out in the Partridge Creek area with one splay extending straight northwesterly and dying out after about 5 miles in older, central-valley, alluvial deposits (Plate 1). The other splay strikes northerly a short distance along Partridge Creek to the mountain front near Picacho Butte then strikes northwesterly to the north end of the valley. On the north, the Big Chino Fault merges with or is transected by east-west trending faults in late Miocene-Pliocene volcanic rocks of the Mount Floyd volcanic field. On the south, the fault gradually dies out near Highway 89, or it may extend into the Paulden volcanics east of the highway.

Subtle differences in the geomorphology between the Big Black Mesa segment and the Picacho Butte segment suggest that the most recent displacement may have been confined to the Big Black Mesa segment from north of Highway 89 to the Partridge Creek area, a distance of about 18 miles (25-30 km). These differences include well-developed, higher, somewhat more distinct scarps and two well developed terrace levels on the Big Black Mesa segment.

(2) Aubrey Fault

(a) Background: The Aubrey study area was located in southern Aubrey Valley (Figure 16). The Aubrey fault is located between the Toroweap and Big Chino faults (Plate 1) in northwestern Arizona and is an important feature for understanding the relationship between the northeasterly striking faults of the Hurricane-Wasatch zone and the northwesterly striking faults of the Arizona Mountain zone. The prominent escarpment of Aubrey Cliffs is a conspicuous landmark along old U.S. Route 66 and had long been suspected of owing its bold cliff face and striking linearity to fault displacement. For example, the Geologic Map of Coconino County (Moore et al, 1960) shows a dotted line, presumably representing a buried fault, in about the same location as the fault shown on Plate 1. Menges and Pearthree (1983) were among the first to actually document the feature as a Quaternary fault. They showed the fault as comprising three segments along the base of the Aubrey Cliffs with a subparallel fault called the Aubrey Valley fault a short distance to the west of the main scarp. Menges and Pearthree assigned an age of Holocene-latest Pleistocene for the latest displacement along the southern part of the fault. To the north, the Aubrey fault merges with several fault splays extending south-southeasterly from the southern Toroweap fault system (Plate 1).

Aubrey Valley has the characteristics of a typical Basin-and-Range-type valley. These characteristics include an asymmetric profile with a gently sloping ramp descending easterly from the southern end of the Hurricane fault escarpment in the Peach Springs Canyon area to the Aubrey Cliffs. Sediments

FHWA REGION	STATE	PROJECT NUMBER	REPORT NUMBER
9	ARIZ.	HPR-PL-1(37)344	FWHA-AZ92-344

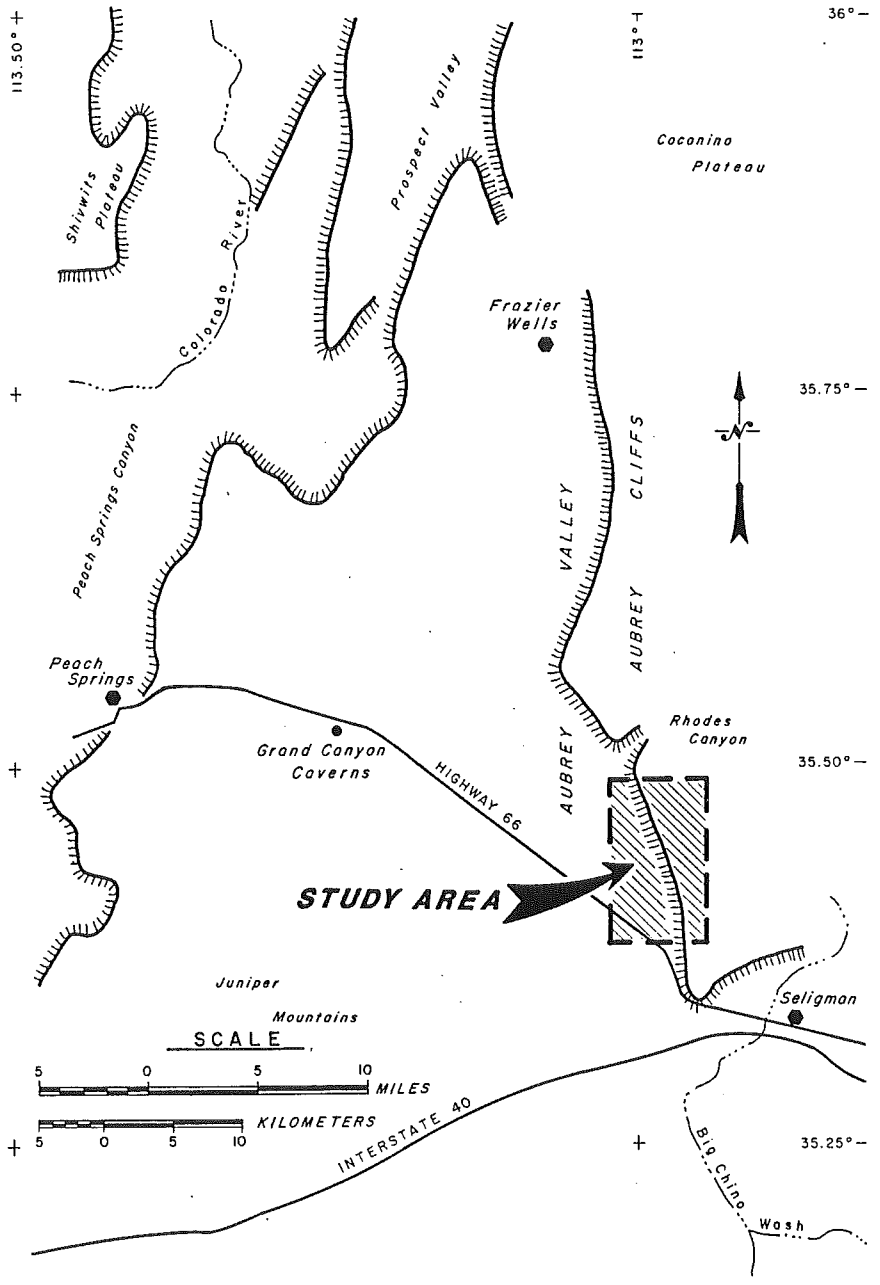

ARIZONA DEPARTMENT OF TRANSPORTATION

ARIZONA TRANSPORTATION RESEARCH CENTER

FIGURE 16

LOCATION MAP - AUBREY VALLEY

eroded from the surrounding mountains have been washed into valley where they are trapped as alluvial valley fill because the valley is an enclosed basin without external drainage. The southern valley is the lowest part of the valley with a sill depth of about 5200 feet elevation. This lower part of Aubrey Valley was the site of a small lake during the late Pleistocene. Remnants of shoreline sand bars can still be recognized on aerial photographs. Based on the degree preservation of these features, the vestiges of this lake appears to have existed until just a few thousand years ago, similar to the glacial (pluvial) lakes in the Basin and Range province of Nevada, Utah, and California. These lakes reached their maximum development in the Basin and Range province about 12,000 to 15,000 years ago. Since that time most of them have dried up because of changing climate. Other subtle escarpments and lake-type deposits in Aubrey Valley extend northwesterly from the southern lake shorelines as shown on Figure 17. Fine-grained deposits in the low areas west of the more-northerly scarps suggest that at one time a smaller lake or catchment area probably existed in this area also. The presence of this lake and the enclosed basin indicate that Aubrey Valley is tectonically subsiding in response to crustal extension and downfaulting along the Aubrey fault at a rate faster than the erosional/depositional rates.

(b) Tectonic Geomorphology: Like most tilt-block Basin-and-Range-type fault valleys, Aubrey Valley has a major fault on one side of the valley (the Aubrey fault - #9 on Plate 1) and several minor faults on the other side (Blue Mountain fault #86; Pica Graben #13; Yampai Graben #14; Audley fault, #15 - see Plate 1). The Aubrey fault, like many of the faults

FHWA REGION	STATE	PROJECT NUMBER	REPORT NUMBER
9	ARIZ.	HPR-PL-1(37)344	FWHA-AZ92-344

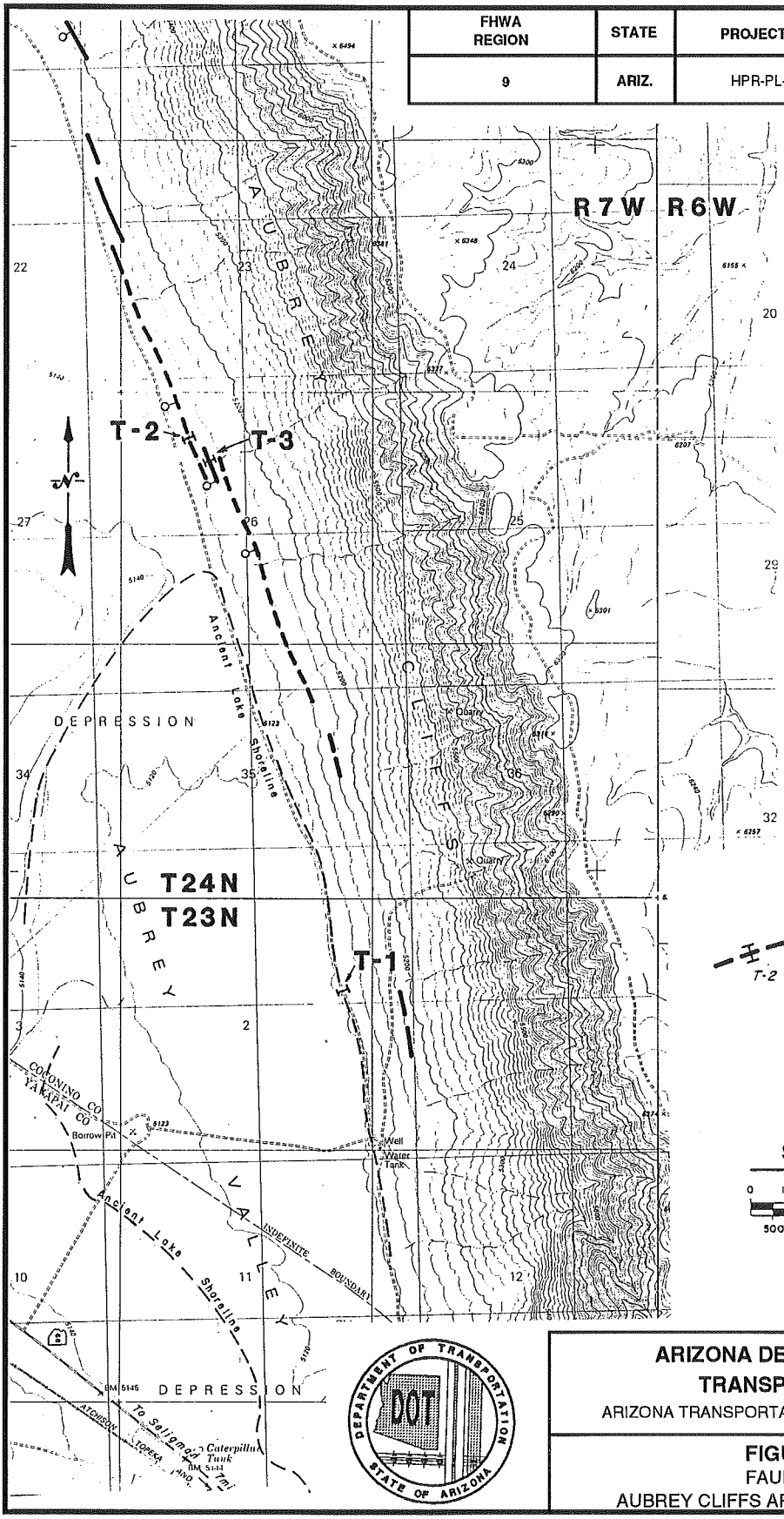

ARIZONA DEPARTMENT OF TRANSPORTATION
ARIZONA TRANSPORTATION RESEARCH CENTER

FIGURE 17
FAULT MAP
AUBREY CLIFFS AREA, AUBREY VALLEY

in northwestern Arizona has a very linear trace, but one that has very distinct changes in orientation. The southern part of the fault strikes northwesterly. About half-way between Seligman and Frazier wells, the fault bends to the northeast; at the northern end, the fault bends again and strikes northerly. Menges and Pearthree (1983) noted these trends and designated three segments, the Southern, Central, and Northern. At the northern end of the northern segment, the fault appears to merge with a prominent east-west trending ridge that appears to be fault-controlled and which merges westerly with the Toroweap fault system. A smaller escarpment extends northwesterly from the intersection of the Aubrey fault and the east-west trending fault. Although no scarps were observed in Quaternary sediments, this northerly extension also appears to be fault-controlled and appears to extend to Prospect Graben (#11), another splay fault of the Toroweap fault. This complex surficial fracture pattern is similar to many faults in this part of the state and is believed to be due to neotectonic reactivation of ancient basement faults as discussed by numerous other geoscientists (for example, Shoemaker et al, 1978; Young et al, 1987; Hamblin and Best, 1979). Reversal of ancient fault displacement along the Aubrey system is evident near milepost 135 at the southern end of the fault (Young et al, 1987).

Aerial reconnaissance, aerial-photograph analysis, and preliminary ground reconnaissance performed during this investigation suggests that Aubrey Cliffs are a fault-line scarp rather than a true fault scarp. The strong alignment of truncated ridge spurs at the base of the cliffs that appear to mark the location of the fault (Figure 18) is probably a result of

nearly horizontal, erosion-resistant Paleozoic strata cropping out along the base of the cliffs below a sequence of softer, less competent strata. In other words, the Aubrey Cliffs might represent a laterally retreating erosional remnant of the principal fault scarp which is recognized by subtle scarps in alluvium about two-thirds of a mile west of the base of the cliffs (Figures 17 and 18). This alluvial fault scarp occurs only along the southern segment of the Aubrey fault system. Alternatively, the escarpment could reflect an older parallel fault that has not ruptured since about middle Pleistocene time. The central and northern segments do not have any good evidence of late Quaternary displacement other than the strong linearity of the cliffs. Although the possibility of a fault being located directly at the base of the cliffs cannot be ruled out and the linearity does suggest control by Quaternary faulting, any alluvial scarps created by fault displacement must have been eroded away. Just how long it might take to remove all trace of such a scarp depends on several factors (height of scarp, climate, erosional regime, resistance to erosion etc.). Scarps in the drier climates of southeastern Arizona are still visible after about 80,000 to 100,000 years; if the rates of erosion are similar in the Aubrey Valley area, the central and northern segments of the Aubrey fault have not suffered any surface rupture in late Pleistocene time (i.e. about the past 100,000 years).

Long periods of inactivity are consistent with the appearance of the Quaternary fault scarps along the southern segment of the Aubrey fault which are very degraded, highly dissected, and rounded. The degree of degradation and low scarp-slope angle, when compared to other scarps in the Basin and

FHWA REGION	STATE	PROJECT NUMBER	REPORT NUMBER
9	ARIZ.	HPR-PL-1(37)344	FWHA-AZ92-344

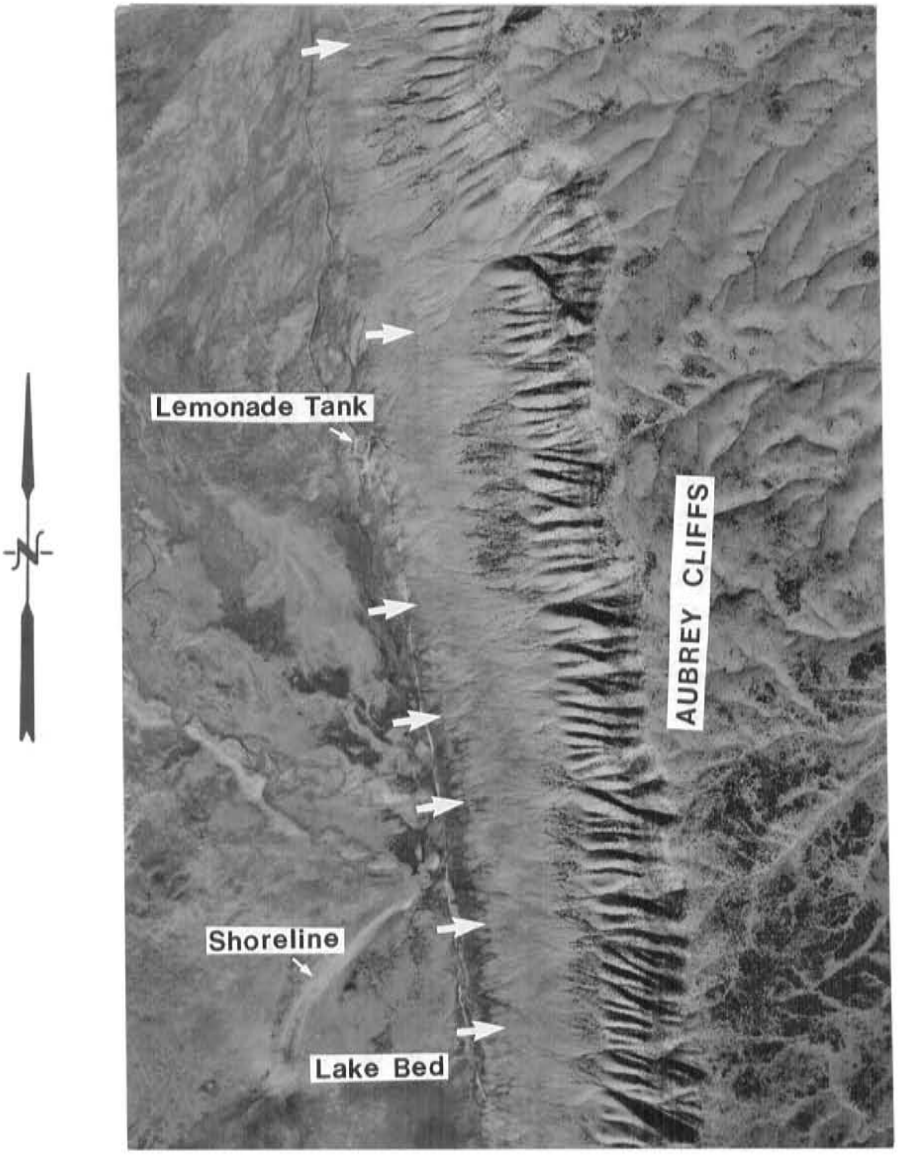

SOUTHERN AUBREY VALLEY; AUBREY CLIFFS ARE ON EAST. WHITE ARROWS INDICATE LOCATION OF QUATERNARY FAULT SCARPS AND LINEAMENTS.

ARIZONA DEPARTMENT OF TRANSPORTATION
ARIZONA TRANSPORTATION RESEARCH CENTER

FIGURE 18
AERIAL PHOTOGRAPH OF AUBREY FAULT

Range province, suggest an age for the latest surface displacement of about 20,000 to 30,000 years before present.

(c) **Trenching:** To evaluate the age and earthquake potential of the Aubrey fault, trenches were excavated across the trace of the southern segment of the fault (Figure 17). Aerial reconnaissance indicated several short, prominent to subtle scarps at the northern end of the south segment just south of Rhodes Canyon. Subsequent field inspection revealed that the alluvial fan gravels along the more prominent of these scarps was thin and underlain by hard Paleozoic-age bedrock. Such hard layers cannot be easily trenched and it was not likely that Paleozoic strata would provide any useful information on neotectonic faulting so these scarps were not considered for trenching. Instead, the trenching activities were conducted across the more-subtle alluvial scarps farther to the south (Figure 17). The trenching methods employed were the same as those discussed in the description of the Big Chino fault (Section 3.d.(1),a) and are not repeated here.

Trench 1 was excavated across the highest and most prominent alluvial scarp along the southern segment (Figure 17). This trench revealed that the scarp was not a fault scarp but a shoreline feature related to the late Pleistocene-age lake described above. Trench 1 (Figure 19A and 19B) conclusively showed unfaulted lake-bed clays overlain by alluvial fan gravels indicating that at one time the lake was larger than the extent indicated by the shoreline shown on Figure 17. Re-examination of aerial photographs after trenching revealed extremely subtle, discontinuous, tonal lineations to the

FHWA REGION	STATE	PROJECT NUMBER	REPORT NUMBER
9	ARIZ.	HPR-PL-1(37)344	FWHA-AZ92-344

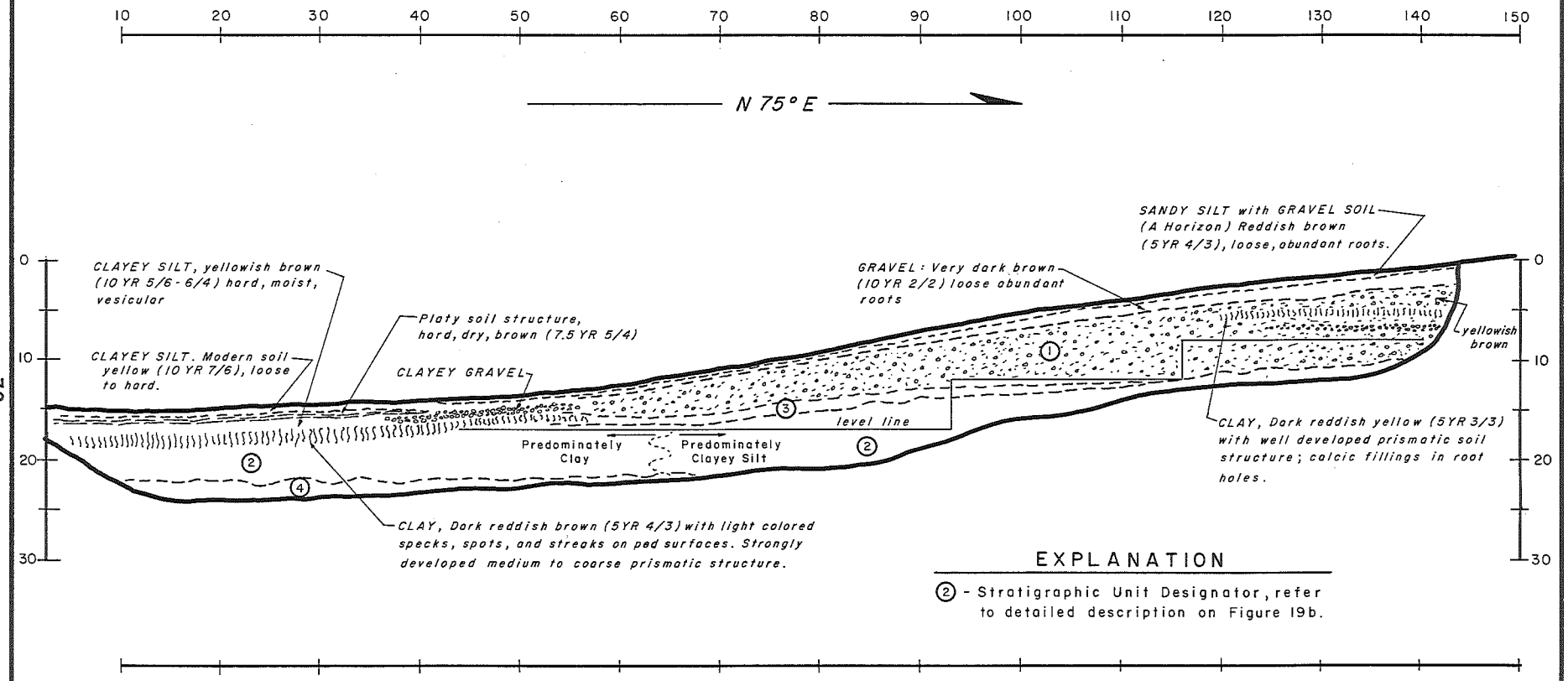

EXPLANATION

(2) - Stratigraphic Unit Designator, refer to detailed description on Figure 19b.

SCALE

10 5 0 10 20

IN FEET

72

ARIZONA DEPARTMENT OF TRANSPORTATION

ARIZONA TRANSPORTATION RESEARCH CENTER

FIGURE 19a

TRENCH NO. 1 - AUBREY FAULT

FHWA REGION	STATE	PROJECT NUMBER	REPORT NUMBER
9	ARIZ.	HPR-PL-1(37)344	FWHA-AZ92-344

Unit No. Description

1) SOIL ARGILLIC B HORIZON: Developed in distal alluvial-fan gravel. Dark reddish brown (5YR 3/4). well-developed clay films on clasts. Most clasts are of pebble size but range from pebbles to small cobbles (1 - 1/2 - inch diameter). Poorly bedded but nearly horizontal attitude is obvious due to lenses of granule-size sand and clayey silt. Several thin layers (about 2 inches) of silty clay with well-developed prismatic soil structure occur northeast of Station 100 (largest one is shown). Hard, dry. Clasts are angular to subangular.

2) SANDY SILT, CLAYEY SILT, CLAY: Multi-colored and mottled. Generally reddish yellow (7.5YR 6/6 to 5YR 6/6) with pale brown and pinkish white (7.5YR 0/2) and black specks, spots, and lenses. Lighter colors due to pedogenic carbonate. Black is manganese oxide. Clay content increases to southwest; northeast of Station 65 unit is predominantly dry clayey silt; southwest of Station 65 unit is predominantly moist clay, with yellowish red (5YR 4/6) to dark reddish brown (5YR 3/4) colors; hard, massive, with more and larger black spots. Northeast of Station 65, unit is generally hard, dry to slightly moist, and porous. Few pores are lined with $CaC0^3$, many have dead roots. Upper part of unit has a few small scattered pebbles, clast content increases with depth. A few short lenses of pebbles and small cobbles occur. Colors darken toward bottom. Contact with Unit 3 is clear but irregular.

3) CLAYEY SAND: Reddish brown, fine-grained sand. Weak to moderately developed prismatic soil structure in scattered lenses. Upper contact abrupt and moderately smooth. Moist, hard.

4) SILTY CLAY: Same as Unit 2 but higher percentage (about 20%) of black manganese oxide as spots, streaks, lenses, and small hard nodules. Upper contact diffused and broken.

ARIZONA DEPARTMENT OF TRANSPORTATION
ARIZONA TRANSPORTATION RESEARCH CENTER

FIGURE 19b
TRENCH NO. 1 - AUBREY FAULT
SOIL DESCRIPTIONS

east of the trench location (Figure 17) suggesting that a fault does extend as far south as the T-1 location but is farther to the east.

Trenches 2 are 3 were excavated farther to the north where scarps are minor, discontinuous features generally no more than about 5 to 10 feet high (Figures 20 and 21). Trench 2 did not show conclusive evidence of surface rupture but did reveal warped gravels, strata thickening, and rudimentary colluvial wedges across a narrow zone (Figure 20). These features are interpreted to be from warping of surficial layers by a subsurface fault that did not quite extend to the ground surface at this specific locality. Strongly developed soil horizons in the alluvial deposits comprise reddish A and argillic B horizons (Unit 1) and strongly developed carbonate (K) soil horizons (Units 2 and 3) indicating the deposits are very old. Generally soils with these characteristics are at least 100,000 years old. The degree of soil-profile development in Unit 5 is indicative of a pre Holocene age (10,000 years). Unit 5 is correlative with Unit 1 but has received added influxes of erosional detritus after the warping event forming a cumulative soil that looks much younger than it is.

Although no dateable material was discovered in Trench 2, the soil-profile development and the fault-scarp morphology indicate that the warping event was pre Holocene, and most likely occurred sometime between a few thousand years ago to tens of thousands of years ago (late Pleistocene).

The main fault was well expressed in Trench 3 and displayed evidence of at least two displacements of Pleistocene alluvial gravels (Figure 21).

FHWA REGION	STATE	PROJECT NUMBER	REPORT NUMBER
9	ARIZ.	HPR-PL-1(37)344	FWHA-AZ92-344

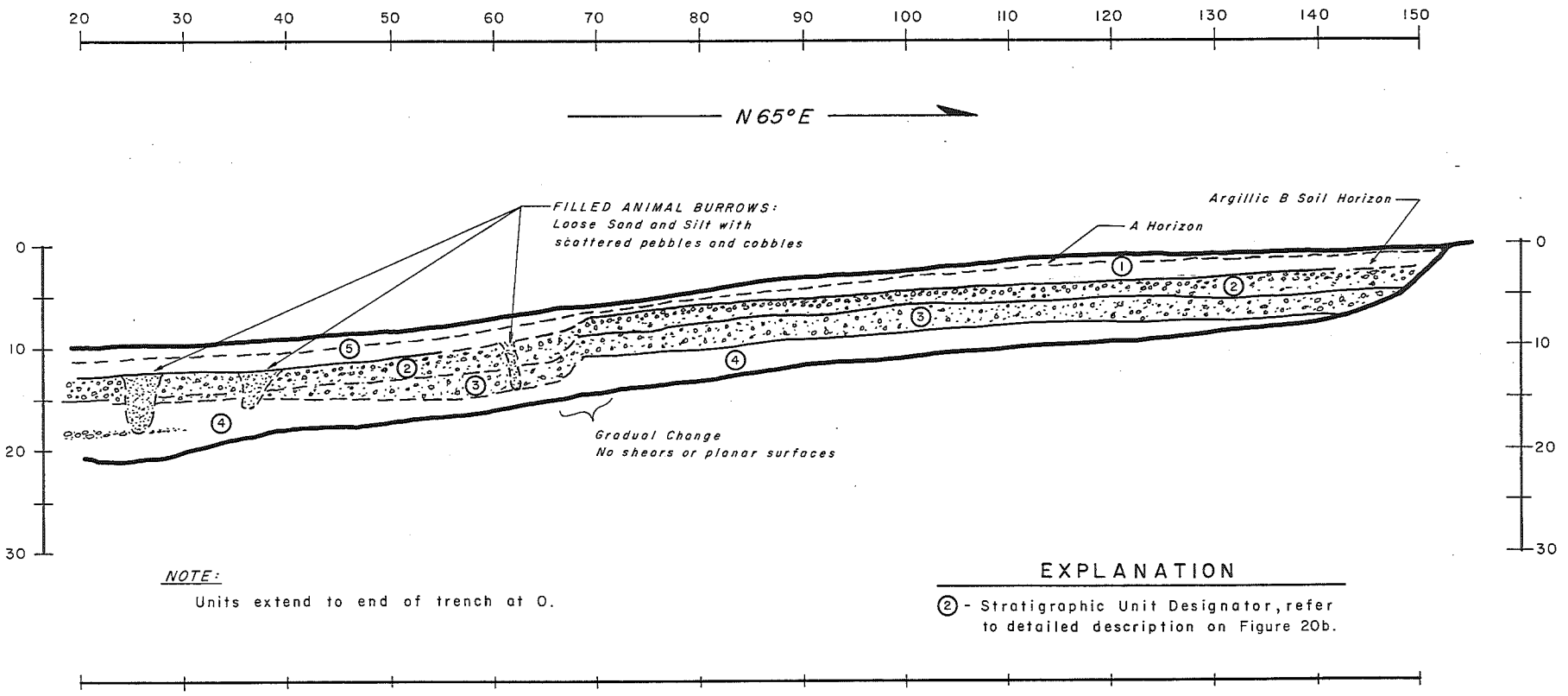

NOTE:
Units extend to end of trench at 0.

EXPLANATION

(2) - Stratigraphic Unit Designator, refer to detailed description on Figure 20b.

SCALE

10 5 0 10 20

IN FEET

ARIZONA DEPARTMENT OF TRANSPORTATION

ARIZONA TRANSPORTATION RESEARCH CENTER

FIGURE 20a

TRENCH NO. 2 - AUBREY FAULT

FHWA REGION	STATE	PROJECT NUMBER	REPORT NUMBER
9	ARIZ.	HPR-PL-1(37)344	FWHA-AZ92-344

Unit No. Description

1) SOIL, GRAVELLY SILT AND SAND:

A - Horizon 0 - 6 inches, reddish brown (5YR 4/4), loose.
B - Horizon dark reddish brown (5YR 3/3);
Argillic B. Moist.

2) GRAVEL: Pedogenic K Horizon, hard, white, Stage IV; large pebbles and cobbles at top tightly cemented in carbonate, grades downward into pea-sized gravel. Some scattered boulders.

3) GRAVEL: Multi-colored, white to yellowish red (5YR 5/8). Lenses of Stage III K horizons.

4) SILT WITH GRAVEL, dark brown (7.5YR 4/6).

5) SOIL, GRAVELLY SILT AND SAND:

A - Horizon 0 - 1 ft., brown (7.5YR 4/4) with abundant roots, loose, dry.
B - Horizon; argillic, yellowish brown (10YR 5/6), hard, dry, moderately developed, medium blocky texture.

ARIZONA DEPARTMENT OF TRANSPORTATION
ARIZONA TRANSPORTATION RESEARCH CENTER

FIGURE 20b
TRENCH NO. 2 - AUBREY FAULT
SOIL DESCRIPTIONS

FHWA REGION	STATE	PROJECT NUMBER	REPORT NUMBER
9	ARIZ.	HPR-PL-1(37)344	FWHA-AZ92-344

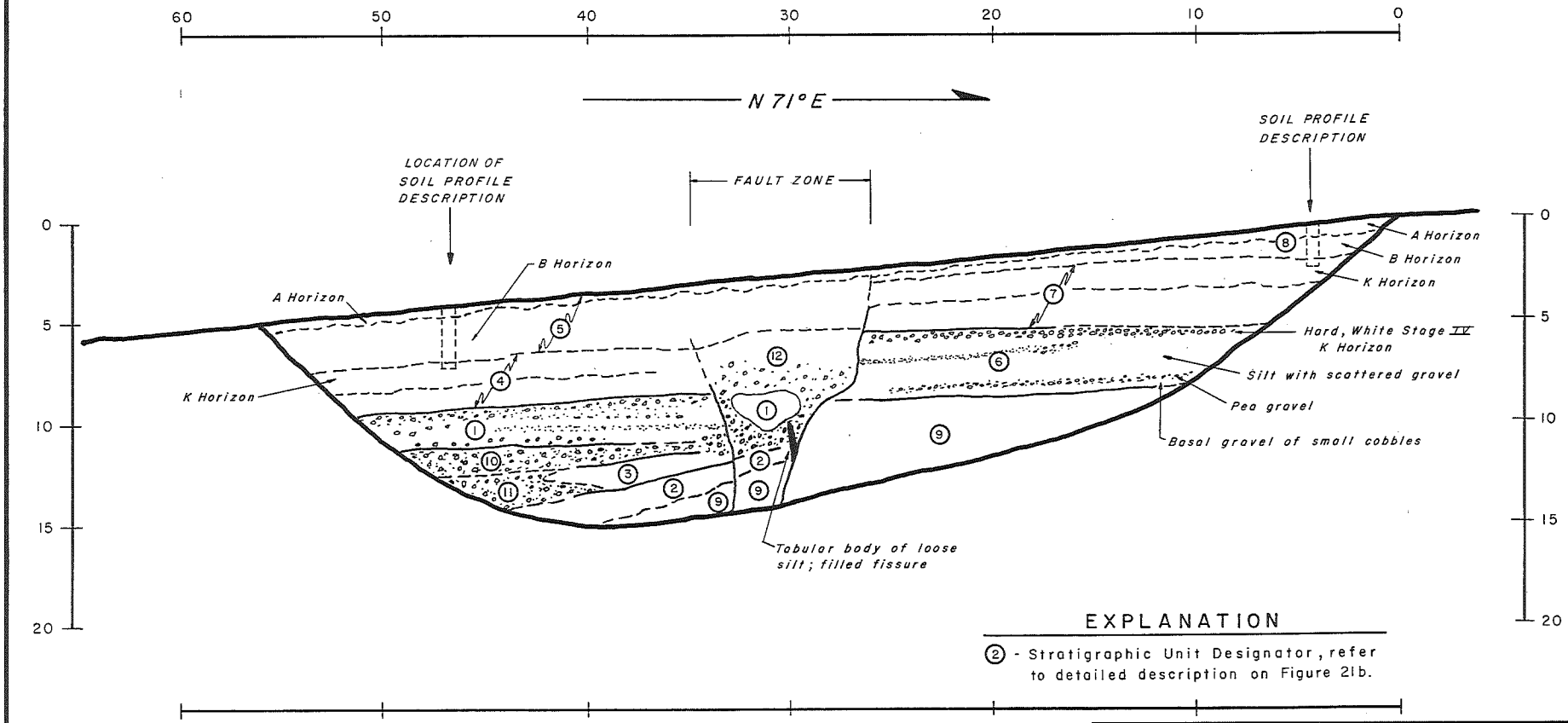

EXPLANATION

(2) - Stratigraphic Unit Designator, refer to detailed description on Figure 21b.

SCALE

5 0 5 10 15

IN FEET

ARIZONA DEPARTMENT OF TRANSPORTATION

ARIZONA TRANSPORTATION RESEARCH CENTER

FIGURE 21a

TRENCH NO. 3 - AUBREY FAULT

FHWA REGION	STATE	PROJECT NUMBER	REPORT NUMBER
9	ARIZ.	HPR-PL-1(37)344	FWHA-AZ92-344

Unit No. Description

1) GRAVEL: Pedogenic K Horizon; white with reddish yellow lenses. Large layer of pebbles at top of unit grades downward into primarily pea-sized gravel at bottom of unit. Pebbles are subrounded to subangular with calcic coatings up to 1/4 inch thick. Hard, dry. Advanced Stage III to early Stage IV. Abrupt, undulating upper contact; clear, undulating lower contact.

2) GRAVEL: Pedogenic K Horizon; white, completely plugged and cemented with CaC03; pebbles completely coated with carbonate. Subrounded to subangular clasts. Hard, dry, Advanced Stage III to early Stage IV. Similar to Unit 6. Gradual, undulating lower contact.

3) GRAVELLY CLAY: Dark reddish brown (5YR 3/3), moist, hard, forms smooth wall. Clear, slightly undulating lower and upper contacts. Grades laterally into gravel of Unit 11.

4) SILT AND SAND LAYERS WITH GRAVEL: Upper 1 to 1.5 feet is hard, white pedogenic K Horizon with advanced Stage III to early Stage IV development. Lower contact of K Horizon is gradual and undulating grading into discontinuous layers, lenses and spots of yellowish red (5YR 5/8) to reddish brown (5YR 4/4) and white silt, sand, and gravel. Becomes less prominent towards fault.

5) CLAYEY SILT AND SAND WITH SCATTERED PEBBLES AND COBBLES (soil developed on alluvial fan deposit):

Horizon	Depth	Color	Structure	Consistency	Boundary	Carbonate
A	0-6"	Strong Brown 7-1/2YR 4/6 Sl. Moist Abundant Roots	fine-med Granules	Loose	Gradual Irreg.	
Bwk_1	6 - 14"	Dark Brown 10YR 4/3 Dry	Medium Subang Weak	Mod. Hard	Gradual Irreg.	Spot & streaks Thin discont. coating Stage I
Bwk_2	14 - 28"	Yellowish Red 5YR 5/6 Dry 5YR 4/6 Wet	Med blocky Mod	Mod. Hard Plastic Non sticky	Gradual Irreg.	Stage I-II Small nodules; Spots, streaks on peds, thin coatings on pebs Stage 1

Porous; can roll into 1/8" thread and bend with some cracking.

6) GRAVEL/SANDY SILT: Pedogenic K Horizon developed on alluvial fan deposits. Upper 2 - 3 feet is hard, white, Stage IV K Horizon in a pebble gravel. Lower part of unit comprises alternating beds of silt, sand, and gravel, moderately well-bedded with variable degrees of pedogenic carbonate development (generally in Stage III). Generally unit is white but a few pinkish and reddish-yellow lenses occur.

7) SAND AND GRAVEL: Alternating reddish brown (5YR 4/4) to yellowish red (5YR 5/8) and white lenses of sand and gravel. Uppermost 1 to 1.5 feet comprises white, completely plugged incipient Stage IV to advanced Stage III, hard, K Horizon developed in a pebble gravel, clasts are subrounded to subangular with calcic coatings up to 1/2 inch thick on bottom of clasts. Lower part of unit comprises discontinuous to continuous coarse sand-pea gravel and small-cobble gravel beds. Predominant gravel size is pebble and pea size but range up to cobble size. Upper contact clear, undulating.

ARIZONA DEPARTMENT OF TRANSPORTATION
ARIZONA TRANSPORTATION RESEARCH CENTER

FIGURE 21b
TRENCH NO. 3 - AUBREY FAULT
SOIL DESCRIPTIONS

FHWA REGION	STATE	PROJECT NUMBER	REPORT NUMBER
9	ARIZ.	HPR-PL-1(37)344	FWHA-AZ92-344

Unit No. Description

8) SOIL SANDY AND GRAVELLY SILT:

A 0 - 6" Sandy silt with scattered pebbles and cobbles with moderate amount of roots and organic debris. Strong brown (7.5YR 4/6). Slightly moist, loose, granular to moderate fine-medium blocky texture in spots. Non-plastic, non-sticky. Gradual, irregular lower contact.

Bwt 6 - 18" Silty gravel; dark yellowish brown (10YR 4/4) when moist, brown (10 YR 5/3) to yellowish brown (10YR 5/4) when dry. Small calcic nodules, spots, and streaks and disseminated carbonate in lower 12" of unit. Dry, hard; moderate, medium blocky texture. Sticky, plastic. Gradual irregular contacts.

9) SANDY SILT WITH SCATTERED PEBBLES AND OCCASIONAL LENS OF GRAVEL: Reddish brown with scattered calcic specks and streaks. Hard, dry, friable.

10) GRAVEL: Reddish brown. Primarily pebble size with scattered small cobbles. Subrounded to subangular clasts.

11) GRAVEL: Reddish brown. Primarily pebble size with scattered small cobbles. Subrounded to subangular clasts. Abrupt, slightly undulating lower contact.

12) GRAVEL/SILT/SAND: Reddish brown (5YR 4/6) to dark brown (7.5YR 4/4). Loose, structureless mixtures of sand, silt and gravel. Gravel sizes range from pebbles to small boulders. Looser with depth.

ARIZONA DEPARTMENT OF TRANSPORTATION
ARIZONA TRANSPORTATION RESEARCH CENTER

FIGURE 21b (cont'd.)
TRENCH NO. 3 - AUBREY FAULT
SOIL DESCRIPTIONS

Units 4 and 7 represent the same stratigraphic unit offset by the fault, as are units 1 and 6. Both of these units have advanced soil-profile development which must have required several tens of thousands of years to develop on each unit. Unit 2 has similar advanced development of pedogenic carbonate which also must have taken several tens of thousands of years to develop. The total time represented by these stratigraphic units appears to represent a large portion of the late-Pleistocene Epoch and might be as old as middle Pleistocene. These relationships indicate that even though there has been recurrent displacement along this fault, the recurrence intervals between events are long and the rate of slip is very slow.

To get a better estimation of the ages involved, a scenario of faulting, erosion, deposition, and soil development is postulated by correlating the major soil horizons to the marine oxygen-isotope chronology of Shackleton and Opdyke (1973). Figure 22 is a diagrammatic reconstruction outlining the sequence of major events interpreted from the wall of Trench 3. On Figure 22, the glacial and interglacial stages refer to the oxygen-isotope stages. The illustrations may appear to represent more-conclusive interpretations than is really intended. Some of the ages given in the scenario may have uncertainties as large as 50 percent. Correlation to the glacial stages suggests that the latest fault rupture occurred about 30,000 years ago and the previous event occurred between about 100,000 and 200,000 years ago.

(d) Fault displacements: The total displacement associated with these events is about 6 feet suggesting a slip rate of about

FHWA REGION	STATE	PROJECT NUMBER	REPORT NUMBER
9	ARIZ.	HPR-PL-1(37)344	FWHA-AZ92-344

A APPROXIMATELY 200,000 YEARS BP

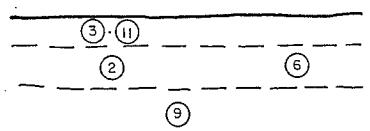

DIAGRAMMATIC SKETCHES - NOT TO SCALE

UNIT 2/6 AND PERHAPS 3/11 DEPOSITED DURING THE COOL WET CLIMATE OF GLACIAL STAGE 8 (>250,000 BP).

SOILS FORM ON THE UPPER PART OF UNITS 2 AND 6 DURING THE DRY WARM INTERGLACIAL STAGE 7 (250,000-200,000 BP). K HORIZON DEVELOPS TO STAGE III/IV.

B

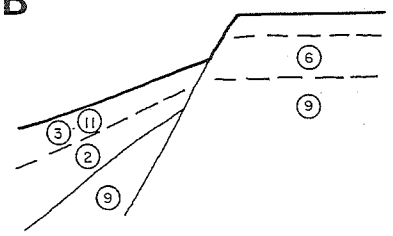

DISPLACEMENT 1 OCCURS (2.5 FT DISPLACEMENT), UNITS 2, 3, AND 9 ARE DOWNFAULTED AND TILTED.

C

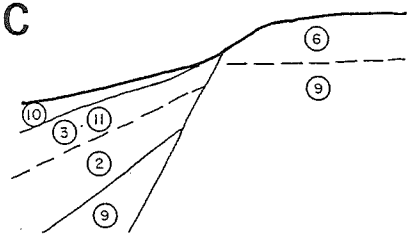

THE FAULT SCARP IS ERODED RESULTING IN DEPOSITION OF UNIT 10 AS COLLUVIAL WEDGE AT BASE OF SCARP. UPPER A/B SOIL HORIZONS OF UNIT 3/11 ARE STRIPPED AWAY BY EROSION. SOIL DEVELOPMENT BEGINS ON UNIT 10 AND REACHES A MODERATE DEGREE OF DEVELOPMENT DURING A TIME INTERVAL OF A FEW THOUSAND YEARS (5,000 TO 15,000 YRS).

D APPROXIMATELY 100,000 YEARS BP

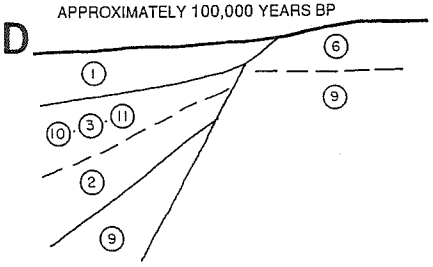

UNIT 1 AND NEW PART OF UNIT 6 ARE DEPOSITED DURING COOL, WET, STAGE 6 GLACIAL PERIOD (125,000-195,000 BP).

SOIL FORMS ON UNIT 1 DURING DRY, WARM, STAGE 5 INTERGLACIAL PERIOD (75,000-125,000 BP). UNIT 1 ACQUIRES STAGE III/IV K HORIZON; EXISTING K HORIZON ON UNIT 6, ALREADY WELL DEVELOPED FROM PREVIOUS CYCLE, CONTINUES TO DEVELOP.

E APPROXIMATELY 65,000 YEARS BP

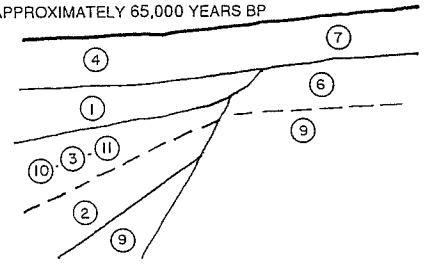

GLACIAL STAGE 4 BEGINS, UNIT 4/7 IS DEPOSITED (65,000-75,000 BP).

SOIL FORMS ON UNIT 4/7 DURING INTERGLACIAL STAGE 3 (30,000-65,000). SOIL-FORMING EPISODE IS LONG ENOUGH TO DEVELOP STAGE III/IV K HORIZON, AN INTERVAL REPRESENTING MOST OF STAGE 3.

F APPROXIMATELY 30,000 YEARS BP

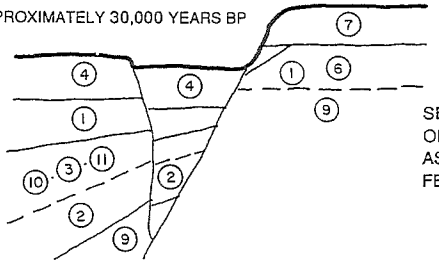

SECOND DISPLACEMENT OCCURS, OFFSETTING UNITS 4/7 AND 1/6, AS WELL AS ALL OTHER EXISTING UNITS, ABOUT 3 FEET.

G PRESENT

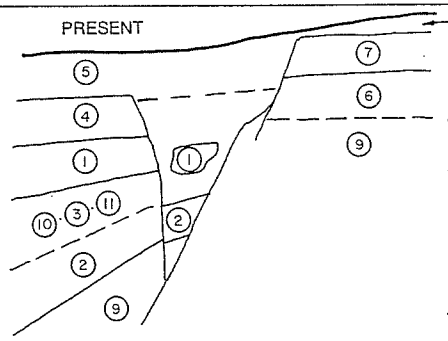

UNIT 5 IS DEPOSITED AS COLLUVIAL WEDGE/GRABEN FILL WITH EOLIAN AND LAKE INFLUENCES DURING GLACIAL STAGE 2 (15,000-30,000 BP).

SOIL FORMS ON UNITS 5/8 DURING INTERGLACIAL STAGE 1 (15,000 TO PRESENT). TIME REQUIRED FOR THIS DEGREE OF SOIL DEVELOPMENT REPRESENTS MOST OF THE PERIOD (I.E., >15,000 YEARS).

ARIZONA DEPARTMENT OF TRANSPORTATION

ARIZONA TRANSPORTATION RESEARCH CENTER

FIGURE 22

FAULTING SCENARIO, AUBREY FAULT

0.01 mm/yr. This is a very slow rate. The surface trace of the southern segment is characterized by several short, en echelon scarps and lineaments (Figures 17 and 18) indicating the faulting is occurring over a broad zone, possibly along sub-parallel faults rather than on one distinct sharp break. The presence of other subparallel scarps and lineaments would suggest that displacement may be partitioned over more than one fault splay and that the rates determined from Trench 3 may not be representative of the total rate for the entire Aubrey fault system. Even though there was no evidence of surface rupture in Trench 2, the ground surface was still displaced about 2 feet. The total slip rate must also account for these apparent displacements in Trench 2, as well as the scarps near Rhodes Canyon which are much larger. The scarps near Rhodes Canyon are up to 15 to 20 feet high. If the total late-Pleistocene displacement is similar to the height of the scarp, the slip rate would be about 0.03 mm/yr.

(e) Earthquake Potential: As discussed above in Subsection (b), the Aubrey fault may consist of several discrete segments and as such is not likely to experience rupture of its entire length during any one event. The total length of the fault, from the south end to the Toroweap fault is about 48 miles. The two most prominent segments, the Southern and the Central, each are about 17 to 18 miles long.

The latest surface rupture, as indicated by alluvial scarps and trenching, was about 12 to 15 miles long. Based on comparison to empirical data, such a rupture length with an average displacement of 3 feet would have been associated with about a magnitude 6.6 earthquake.

Estimates of the maximum credible earthquake based on empirical data such as Slemmons (1982), Bonilla et al (1984), Wyss (1979), and moment-magnitude calculations suggest that the fault is capable of generating an earthquake in the 6.8 to 7.1 magnitude range. For the seismic hazard analysis, the MCE is estimated to be 7.25. Based on age estimates from the trenches, such events appear to be extremely rare and occur only about once every 100,000 years or more.

(f) **Summary:** In summary, trenching investigations of the Aubrey fault have shown that the fault has had recurrent activity in late Quaternary time with the latest displacement occurring about 30,000 years ago and a previous displacement at least 100,000 to as much as 200,000 years before that. These ages suggest long-term average recurrence intervals of at least 100,000 years and slip rates on the order of 0.01 to 0.03 mm/yr. The maximum credible earthquake is estimated to be about 7.25.

4. BASE MAP DEVELOPMENT

The base map for the faults (Plate 1) and seismic acceleration (coefficient contour maps (Plates 2a through 2d) was compiled from various sources.

The small scale (1:1,000,000) base map used for Plates 1 and 2 covers the entire State of Arizona, portions of adjacent states, and northern Mexico. Presentation at this scale will help facilitate regional planning of larger projects. Large scale maps for site-specific engineering design projects can also be produced. In addition to hard copies presented as plates in this report, the data are compiled in AUTOCAD™ format on floppy disk media. This will enable ADOT to produce specific study-area maps at any desired scale.

a. Base Map Data

To minimize inaccuracies associated with map production, we attempted to utilize ADOT in-house electronic digital geographical and roadway data whenever they are available. This information was transmitted to us in the form of digital data files in "Drawing Interchange" file format (DXF™). Computer Aided Design (CAD) programs including both AutoCAD™ and Intergraph MicroStation™ were available in-house for map production. The AutoCAD™ program was chosen for the project due to its widespread usage.

The digital data files transmitted to us included milepost locations

state boundaries and county boundaries. Additional data were superimposed on the ADOT digital data to form the base map. Information was separated into individual layers in the AutoCAD program to facilitate map making by allowing overlaying of any combination of data. The resultant base map consisted of:

- mileposts markers with annotations every ten miles,
- Arizona state boundary,
- county boundaries,
- roadway networks constructed from the milepost data,
- city and geographic locations; these were added based primarily on the "State of Arizona General Highway Map" (dated 1986, Map Scale: 1 to 500,000) prepared by the ADOT Photogrammetry and Mapping Services Department, complemented by the U.S. Geological Survey map, "State of Arizona" (dated 1972, revised 1981; Map Scale: 1 to 500,000).
- Coordinate systems included the Geographic Reference System (latitudes and longitudes) and the Universal Transverse Mercator Reference System (UTM in meters). Coordinate systems were computed using the General Cartographic Transformation Package (GCTP), Version II Program distributed by the U.S. Department of

Commerce, National Oceanic and Atmospheric Administration (NOAA) dated 1987.

In the course of the project, other maps were developed by overlaying data from other sources on the base map. They included the following maps:

- a fault map of Arizona,
- a seismic sources map,
- a seismicity map developed by plotting historical seismicity data supplied by Dr. D. Brumbaugh of Northern Arizona University (1992), and
- several design acceleration coefficient contour maps arising from probabilistic analyses of the seismic hazard potential of Arizona.

The fault map and the seismic sources map originated from maps compiled by the project geologist from existing Arizona Geological Survey and U.S. Geological Survey topographic and geological maps (see Section 5). Additional data were introduced and refinement of the data were made in the course of the project. The resultant fault map was electronically scanned and overlaid on the base map. In addition to hard copies of all the above maps, our deliverables include electronic digital data files (DXF) for use by ADOT in their future work.

b. Accuracy of Developed Maps

Since much of the information on the base map and other project data (including the acceleration contours) were transmitted by or created as computer files, the resultant maps should be accurate to the degree permissible by hardware equipment or more likely, limited by the accuracy of the original sources used to create the data.

The fault map and the seismic source zone map were generated by electronic scanning of existing hand-drawn maps and then overlaid onto the base map. Errors that may arise in the process probably come from the following sources:

- o incompatibility of map projection schemes between the ADOT base map and the original fault map,
- o distortion from reproduction of the original fault map, and
- o limitation of the electronic scanning device.

By comparison of the latitude and longitude markers between the fault map and the base map during our overlay operation, it was observed that incompatibilities between the two maps are within 1 mile (about 2 kilometers).

5. FAULT MAP

a. Description of Map

A map of potentially active faults is presented as Plate 1. The preliminary fault map was hand drawn and compiled on a special topographic base map at a scale of 1:500,000 to provide easy reference for geological analysis and field reconnaissance. The map shown as Plate 1 is the computer-generated final fault map.

Certain published and unpublished compilations of faults were of particular importance for compiling the fault map. These included:

- Report and "Map of Neotectonic (Latest Pliocene-Quaternary) Deformation in Arizona" by Menges and Pearthree (1983).

- Map and report on "Neotectonics of Southwestern Arizona, Eastern California, and Sonora Mexico" by Schell and Wilson (1982).

- Map of "Late Pliocene-Quaternary (Post 4 m.y.) Faults, Folds, and Volcanic Rocks in Arizona" by Scarborough, Menges, and Pearthree (1983 ca).

- "Map showing Quaternary and Pliocene Faults in the Silver City 1 x 2° Quadrangle and the Douglas 1 x 2° Quadrangle, Southeastern

Arizona and Southwestern New Mexico" by Machette, Personius, Menges, and Pearthree (1986).

- "Reconnaissance Photogeologic Map of Young Faults in the Las Vegas 1 x 2° Quadrangle, Nevada, Utah, and Arizona" by Dohrenwend, Menges, Schell, and Moring (1992).

- Map of faults in Utah by Hecker (1992).

- "Fault Map of California with Locations of Volcanoes, Thermal Springs, and Thermal Wells" by Jennings (1975).

Plate 1 shows all faults thought to have been active during the present tectonic regime (neotectonic regime). To compile such a map requires knowledge of when the neotectonic regime began but establishing exactly when that was is very difficult. This difficulty is due to at least four factors:

- Lack of detailed data. The lack of data can be due partly to lack of study and/or to the appropriate information not being preserved in the geologic record.

- Tectonic relations are very complex because they involve a multitude of parameters, some of which are not completely understood by geoscientists.

- There may not be a single unique time. There are several discrete seismotectonic zones in the area and the neotectonic regime may have begun at different times in different zones.

- The transition from ancient tectonic regimes to the neotectonic regime was not instantaneous. The change may have taken place over geologic time spans that might approach up to a few million years.

All of the above difficulties and uncertainties notwithstanding, most of the state of Arizona appears to have entered into its present tectonic regime between latest Miocene and early Pliocene time (i.e. about 4 to 8 million years ago). As discussed by Schell and Wilson (1982), this time appears to be related to major plate-tectonic events along the North American/Pacific plate boundary in the Gulf of California region.

For this investigation the neotectonic regime is considered to include Pliocene, Pleistocene, and Holocene time. There are still uncertainties as to whether all of these faults are still potentially active. There is considerable evidence that some of these faults have not been active for several hundred thousand to a million years so they may not represent significant seismic sources. The faults with good evidence of Quaternary activity (Pleistocene and Holocene Epochs) are shown as the thicker lines on Plate 1 whereas the faults shown as thin lines are either older (Pliocene-Miocene) or do not have good evidence of later movements. The lack of evidence for young fault displacement may be due to actual lack of Quaternary

displacement, or it may be due to poor preservation of evidence. When intervals between episodes of faulting activity are on the order of several thousand years to a hundred thousand years, substantial erosion and concealment of evidence should be expected.

Most faults on Plate 1 are labeled with a circled letter and a number. The number along side the faults refers to the number of the fault tabulated in Appendix A. The letters refer to the suspected age of latest displacement according to the age criteria described on the map explanation. These ages generally are the age of the youngest displaced strata and therefore are the maximum ages of latest displacement. That is, the latest displacement could have occurred shortly after or a long time after the designated age. For example, a fault designated as M (middle Pleistocene) indicates that the fault displaces middle Pleistocene strata. In many cases, there is no way to determine how long after middle Pleistocene that displacement occurred; it could have been middle Pleistocene, late Pleistocene, or Holocene time. Information on the age of latest displacement is given on the fault tables in Appendix A. The major faults on Plate 1 are numbered from 1 to 186. However, not all faults are numbered individually and several large groups of similar faults are included under one number (for example, numbers 94, 95, and 96 along the Utah-Arizona border).

There are many faults around the perimeter of the Colorado Plateau that have prominent surface escarpments (Figures 3 and 7). However, the surficial deposits that these faults displace are old, commonly of Paleozoic age (250 million years) and Mesozoic (150 million years) age. The latest displacement

on these faults could be tens of millions of years old and not neotectonic, but other evidence suggests much-more-recent displacements. This evidence is:

- The prominent surface expression of the faults suggests that the latest surface rupture could be young compared to the age of the surface strata because if the faults have not been rejuvenated by continuous recurrent displacements, the scarps would be eroded away and (or) the downfaulted side of the fault would be filled or covered with erosional detritus making the faults difficult to recognize at the surface. On the contrary, buildup of Quaternary alluvium along the fault scarps is minimal except in the southern part of the state where there are relatively few neotectonic faults, compared to the northwestern part of the state.

- Some of the prominent scarps extend into volcanic rocks of late Tertiary and Quaternary age. Comparison of the relative erosional characteristics of faults in Permian rocks to those in late Tertiary and even Quaternary rocks suggests that the scarps in the Permian rocks are about the same age as those in the Tertiary/Quaternary rocks. This still does not give the true age accurately enough for determination of precise rates of displacement, but it brings the problem into a realm where reasonable assumptions can provide order-of-magnitude estimates that help resolve the relative activity levels of the seismic source zones.

- The areas where most of these faults occur are in the same areas where earthquakes are most frequent. Although no correlations can be made between specific faults and specific historical earthquakes, their mutual proximity suggests subsurface activity is continuing on these faults or on similar subsurface faults.

After literature review, field visits, aerial reconnaissance, and aerial-photograph analysis, the initial fault map was revised and updated to add or remove faults that did or did not fit the neotectonic criteria. From the preliminary fault map and comparison to seismicity data it became apparent that additional data on age of fault displacements, number of displacements, amount of displacement per event would be useful for evaluating the seismic potential of several of the seismic zones.

Because many of the faults shown on Plate 1 do not displace Quaternary sediments, it was not practical to trench them. Our preliminary review of available data resulted in identification of several faults that were considered as candidates for trenching. After preliminary, aerial-photograph interpretation and aerial reconnaissance, we determined that only the Aubrey and Big Chino faults would contribute substantially to the investigation. Other faults like the Verde, Safford, and faults in New Mexico were considered to have only marginal potentials to yield significant results, so investigations concentrated on geomorphic analysis and remote sensing. Other faults such as the Bright Angel, Sinyala, Grand Wash, Mesa Butte, Sonoyta, and Chiricahua were felt not to have much potential for providing significant data.

Although some useful information can generally be obtained from most trenching investigations, trenching most of these faults was judged not to have a reasonable chance of yielding results directly applicable to this investigation, and it was felt that our time, efforts, and budget would be better spent on other types of analyses. Our trenching of the Big Chino fault verified this in that in spite of the fact that it is one of the youngest and most prominent faults in the state, it still did not yield precise age information.

b. Discussion of Fault Trends and Characteristics

The faults shown on the fault map (Plate 1) comprise two basic trends, 1) northerly-northeasterly and 2) northwesterly.

The northerly to northeasterly fault trends predominate in the northwest and southeast corners of the map. The northwest corner of the map is characterized by predominantly north and north-northeast trending, long, continuous faults. Faults in the southeastern corner of the map have similar northerly and northeasterly trends but the individual faults are much shorter and discontinuous than faults in the northwest. Faults in Mexico to the south of the map appear to have predominantly northerly trends and are long and continuous, somewhat similar to faults in the northwest part of the map and in the Basin and Range areas of Nevada and Utah. The best-known fault in southeastern group is the Pitaycachi fault (#161), the source of the 1887 earthquake (M=7.25) and the only fault on the map that has experienced historical ground displacement.

The scattered, somewhat discontinuous faults in the east-central part of the state generally trend northwesterly and appear to connect the two corner regions. Some of the major faults in this group are the Safford (#174), Rim Rock (#169), Mogollon (176), Big Chino (#18), and Verde Valley faults (#22).

The relationships between the northerly trending faults in the northwest and southeast corners of the map and the northwesterly trending faults is not certain. In the southeast corner of the state, the change from the northerly trends to the northwesterly trends is quite obvious both in actual fault traces and in orientation of mountains and valleys. This change approximately coincides with the northern ends of the Hatchet, Animas, Chiracahua, Santa Rita, and Baboquivari mountains. The change from the northwesterly trends to the northerly/northeasterly trends in the northwestern corner of the map is more diffuse. The northwest trends of the central fault belt extend into and intermingle with the northerly trends, commonly with mutually offsetting relationships. Although the northerly trends appear to dominate, some of them (for example, the Hurricane fault, #1) commonly have northwesterly trending segments (see Plate 1). Also, the areas between the major northerly trending faults commonly have numerous northwesterly trending faults (for example #186 and #89). This intermingling is most obvious in the area extending from the San Francisco Volcanic field area to the eastern part of the southern Nevada zone. The intersecting of faults is especially prominent north and west of the San Francisco volcanic field involving faults such as the Kaibab-Sinyala system (# 3 and 4), the

Bright Angel system (# 42), Cataract Creek system (# 44), and the Mesa Butte system (# 104). In Nevada, the fault intersections are not quite as abrupt.

Some faults are combined into groups or clusters and described as fault sets. These faults are located in the north-central part of the state surrounding the San Francisco volcanic field and the area north of the field (Plate 1). These faults are closely spaced and generally well expressed but short and discontinuous, with small displacements. The minor nature of these faults suggests that they may not be major earthquake-generating features. Their trends suggest they may be related to ancient basement faults. However, earthquakes occur in their proximity and some of these faults are of significant length.

Major fault trends outside of the map area are the north-westerly trending San Andreas-San Jacinto system in southeast California and the northerly trending faults of the Rio Grande Rift system in New Mexico, Mexico, and southern Colorado. Showing all of these faults on Plate 1 is not practical, but data were collected on these features and they were considered in the seismic hazard analysis.

6. SEISMIC SOURCES

This section of the report describes the seismic sources defined for this investigation and the methods used to define these sources.

a. Methods Used to Define Seismic Sources

Two types of seismic sources, faults and zones, were defined for this investigation. Generally, the Arizona region has had low to moderate earthquake activity in historical times and earthquakes are somewhat scattered throughout the state. In such seismotectonic environments, seismic-hazard evaluations are generally best conducted using a seismic zone or seismic province approach. However, preliminary geologic investigations suggested that certain faults represent hazards greater than their surrounding zone, and such features are modeled in this analysis as essentially discrete planar seismic sources with a very narrow width at the surface comprising only directly related splay faults. The seismic sources (both zones sources and planar fault sources) used for the seismic hazards model are shown on Figure 23. The methods and parameters used to define these sources are described below.

In general, the method used in this study to subdivide the study area into seismic source zones is similar to the method described by Schell (1978) and Schell et al (1985). The method uses both geological and seismological data to subdivide large regions into zones with similar seismotectonic characteristics. This method differs from other published zonations (such

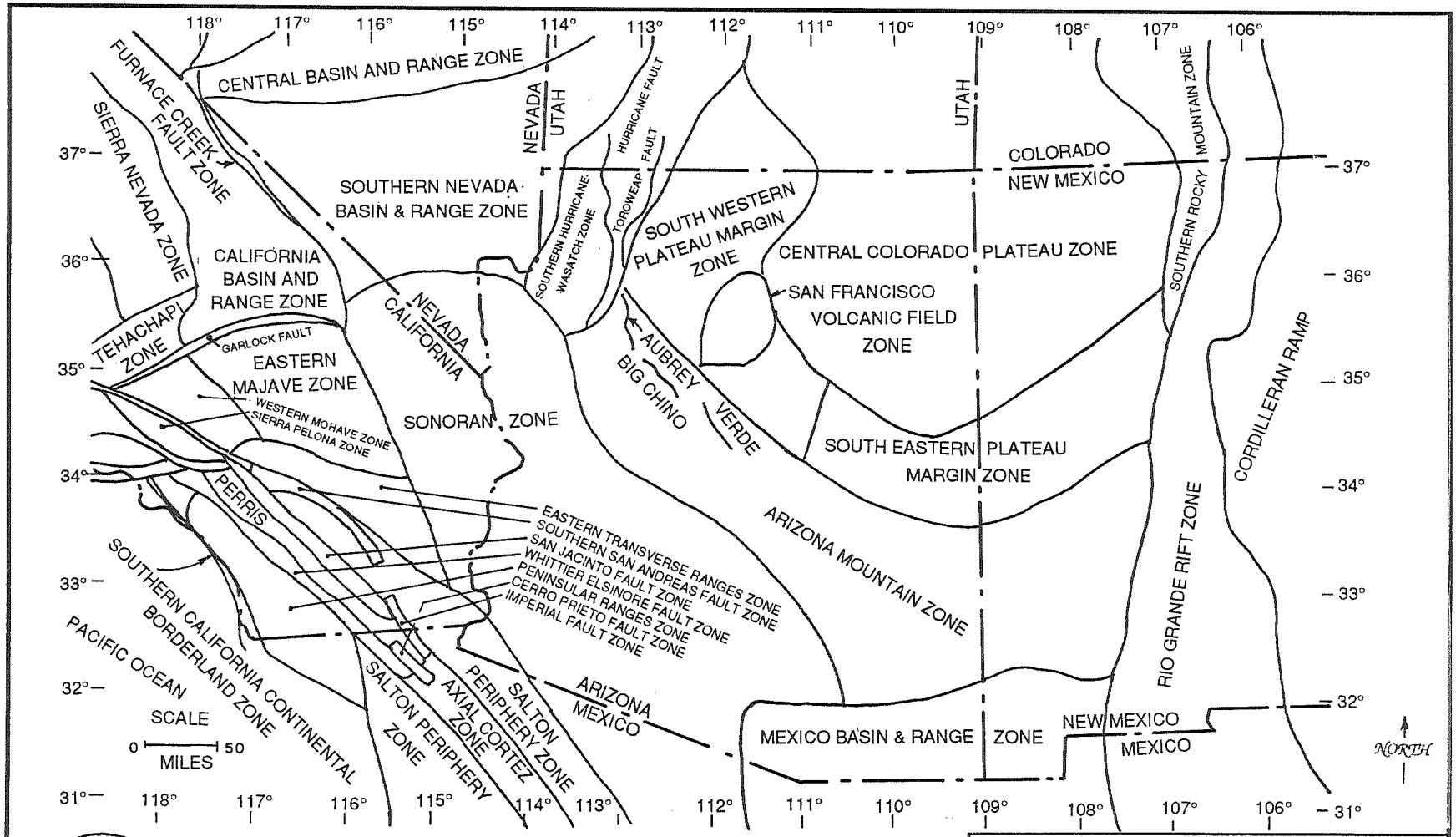

FHWA REGION	STATE	PROJECT NUMBER	REPORT NUMBER
9	ARIZ.	HPR-PL-1(37)344	FWHA-AZ92-344

ARIZONA DEPARTMENT OF TRANSPORTATION
ARIZONA TRANSPORTATION RESEARCH CENTER

FIGURE 23
REGIONAL SEISMIC SOURCE ZONE MAP

use of either seismicity or other types of data, such as geophysical data, which can help characterize the tectonic regime. As with the seismological zonation methods, these geological zonations present valuable data for seismic zoning, but by themselves are based on too few types of data to provide for adequate seismic hazards evaluations.

(1) General Considerations and Methods

A region can be divided into seismic source zones at various levels, ranging from gross regionalization into broad zones (such as the Rocky Mountains, Basin and Range, Cascade Belt, Coast Ranges) to detailed microzones which consider very minor features such as individual faults or soil types. The methods of study are intermediate between these extremes; this study subdivides the study region into zones which have differences that are significant with respect to seismic hazard. For some zones this significance is more subtle than others. For example, in some adjacent zones the maximum earthquakes are the same magnitude, but the frequency with which they occur or their depths or the mode of ground rupture may be the differentiating factor. Other subdivisions or further subdivision of large zones into smaller zones may be possible but the model presented herein is believed to be optimum for the purposes of this investigation. Where appropriate, the zone descriptions given below in Subsection c. discuss the levels of uncertainty.

The basic purpose of seismic source zonation is to subdivide a region into zones or provinces which have an internal consistency with respect to

seismicity and active geologic structures. These zonations are important for realistic seismic-hazard evaluations because of the incompleteness of the seismic record. The geologic processes that lead to earthquakes are very slow by human standards. Most crustal deformational processes occur at rates on the order of tenths to thousandths of inches per year. At these rates it takes hundreds and thousands of years for even the most rapid processes to accumulate enough strain to cause rupture of the rocks or enough deformation to be visible to direct human observation. To approach an understanding of the tectonic regime of a region, a reasonably wide data base must be analyzed. This data base should include the geologic structure, physiography, seismicity, stratigraphy, and various geophysical data such as gravity, magnetics, and heat-flow.

The completeness of the data varies considerably between areas and, therefore, some zones are better defined than others. For example, the rate of seismicity on the San Jacinto Fault is so high that the historical seismicity data appear to be adequate for quantification of its seismic hazard. In comparison, the rates of seismicity in the Great Basin are much lower and, although we probably have a good idea of the maximum size of earthquakes from historical seismicity, our knowledge of how often these maximum earthquakes can occur is poor. Moreover, remote areas such as the Great Basin have not been studied in the detail that the San Jacinto Fault has.

Within these limitations, a seismic source zone map of the Arizona area was constructed (Figure 23 and Plate 1). For completeness, Figure 23 shows

the area from central New Mexico to the Pacific Ocean. Not all of these zones are important to Arizona, especially those west of the San Jacinto/San Andreas fault system because the San Andreas and San Jacinto faults are capable of generating much larger and more frequent earthquakes than the zones and faults farther to the west. The study was not restricted to the Arizona state boundaries because seismicity knows no politics and, in some instances, the part of the source zone outside of the state had the most characteristic or definitive data for that zone. Therefore, the descriptions in this report include references to features outside of the state of Arizona so as to document the most typical characteristics of the zones.

The titles given to the various seismic source zones defined for this investigation were chosen to be readily associated with both the geographic region and/or the primary mode of tectonism. Some names are well established but others are new. For example, the name Arizona Mountain zone includes the area most commonly known as the Transition Zone. A new name was assigned for this area because few publications use the Transition Zone name exactly the same and there is much controversy over where the boundaries are. To avoid getting involved in such disagreements for this zone as well as others, some new names are used. Some zone names are similar to physiographic province names which may encompass the same general area and caution must be exercised by the user not to confuse physiographic provinces with seismic source zones. Furthermore, although the zones outlined in this study are called seismic source zones, they are representative of more than just seismicity. As such, these provinces could just as correctly be termed seismotectonic provinces or neotectonic provinces. Trying to decide on one term that is completely

satisfactory to everyone, is basically a non-productive semantical exercise. Because no term is completely satisfactory, no further discussion or justification is given with respect to choice of terms.

(2) Source Zone Boundaries

The various parameters and combinations of parameters used to differentiate zones can vary along a zone boundary. A zone boundary in one locality, for example, can be based primarily on seismicity and faults, and in another locality on faults and volcanism. Seismotectonic characteristics generally change gradually and, thus, source-zone boundaries cannot be defined precisely by a single line which may represent a map width, depending on map scale, of only a mile or so. The study of the Sonoran province by Schell and Wilson (1982) attempted to quantify the width of province transitions and showed, for example, that the boundary between the Sonoran and Arizona Mountain zones ranged between 2 to 32 miles wide. In some cases, the transition between provinces may be so gradual and wide that it could be considered a separate province characterized by its transitional nature. Such a zone was established by Schell and Wilson (1982) for the seismically quiescent area with few neotectonic faults in the southeastern Arizona Mountain zone. Narrow boundaries are exceedingly rare and generally only occur along active regional faults. For example, the boundary between the Western Mojave and Sierra Pelona zones in California is the San Andreas fault, which is exceptionally narrow and well defined in that area.

In view of the foregoing discussion, the seismic source zone boundary

lines, as shown on the maps, should be considered only as approximate representations of the zone limits, with no particular significance being given to whether a feature might be transected by the line or to whether features are located a short distance on one side of the line or the other.

(3) Geomorphological Parameters

In establishing the zones, primary emphasis is given to seismicity and potentially active (neotectonic) geologic faults. However, physiography or geomorphology can also be an important distinguishing parameter because it is commonly indicative of neotectonic activity. Tectonically active areas most likely are undergoing uplift or subsidence and these processes affect the erosion potential. An area undergoing tectonic uplift will be subject to strong erosion and thus have rugged, immature, or rejuvenated geomorphic features. Areas of tectonic quiescence will have a mature geomorphic character.

Studies during the past couple decades on the effects of tectonics on geomorphic development have led to development of a geologic discipline called tectonic geomorphology. There are several different aspects of tectonic geomorphology that can be useful for deciphering structural geology and seismic potential. Regional aspects include physiography, mountain-front morphology, and erosional/depositional geomorphic surfaces. Local aspects include small-scale erosional and depositional surface development and fault-scarp morphology.

The usefulness of using regional physiography for differentiating seismotectonic zones is well illustrated by comparison of the Central Great Basin, the Mexican Basin and Range, and the Sonoran zones. Although these zones have geologic structures typical of Basin and Range tectonics, the Sonoran zone has a mature physiography indicating that the Basin-and-Range tectonic regime is no longer active. The Sonoran zone has through-flowing drainages indicating that basins are no longer actively subsiding. Also, in contrast to the Central Great Basin and the Mexican Basin and Range zones, the mountain ranges of the Sonoran zone are surrounded by wide aprons of thinly alluviated, planated, bedrock pediments. The presence of these pediments indicates long periods of erosion without uplift and, hence, suggest tectonic quiescence.

Mountain-front geomorphology deals with the impact of local, tectonic, base-level fall on the processes and morphology of stream systems along mountain fronts. Local base-level processes include stream-channel down-cutting in the mountains and erosion or deposition on the piedmont adjacent to the mountain front. These processes are closely related and are responsible for formation of distinctive landforms which can be diagnostic of the relative degree of tectonic activity along the mountain fronts. For example, when compared with inactive mountain fronts of similar relief, climate, and rock type, tectonically active mountain fronts have more convex ridgecrests, steeper slopes at the base of the mountain, narrower and steeper canyons in the mountains, less-sinuous mountain fronts, thicker alluvial deposits next to the mountains, and minimal soil-profile development on the piedmont (Bull and Mcfadden, 1977; Bull, 1974).

One of the most important aspects of tectonic geomorphology relates to the morphology of fault scarps. Fault scarps can reveal important information on the age of faulting according to criteria established by Wallace (1977) and Bucknam and Anderson (1979). The basic premise of fault-scarp morphologic studies is that steep scarp-slope angles are younger than low-angle scarp slopes, and that the time since the scarp formed can be estimated by comparing the slope-angle characteristics of a scarp to other scarps with known ages. The important terms and the process of scarp decline are illustrated in Figure 24.

During the field verification, a number of fault-scarp profile measurements and geomorphic observations were made. These were compared with each other and with the published data to help evaluate fault-scarp ages. These comparisons were made with caution because many of the published studies are academic exercises that make several assumptions of uncertain validity. Techniques of using fault-scarp morphology for dating surface fault ruptures have evolved to include mathematical models and diffusion theory (Nash, 1980; Meyer, 1984; Hanks et al, 1984). Fault-scarp morphology techniques work best with Holocene and latest Pleistocene-aged scarps. The usefulness of mathematical techniques is limited for fault scarps in areas such as Arizona where scarps are commonly the result of multiple ruptures of great age and with long time intervals between ruptures.

Figure 25 shows typical relationships of fault-scarp height plotted against scarp slope angle used to help estimate ages of surface faulting. Lines A, B, and C represent actual normal-fault scarps with well-constrained

FHWA REGION	STATE	PROJECT NUMBER	REPORT NUMBER
9	ARIZ.	HPR-PL-1(37)344	FWHA-AZ92-344

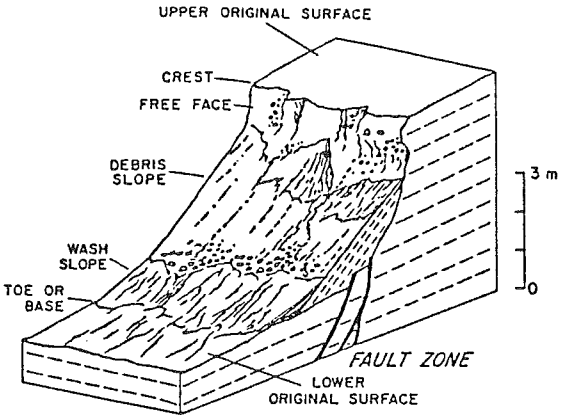

A–BLOCK DIAGRAM OF A FAULT SCARP SHOWING TERMINOLOGY USED IN THIS STUDY.

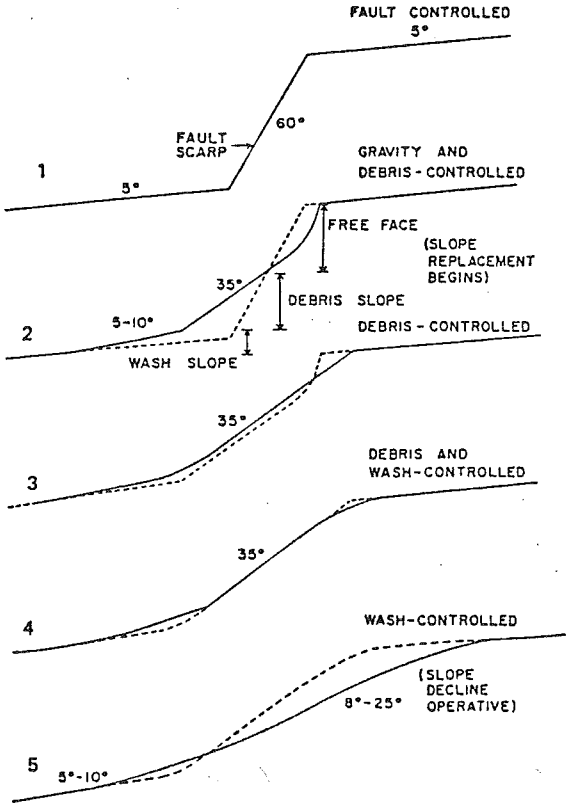

B–SEQUENCE OF FAULT-SCARP DEGRADATION. PROFILES 1 THROUGH 5 SHOW INCREMENTAL CHANGE, DOTTED LINE REPRESENTS SOLID LINE OF PREVIOUS PROFILE.

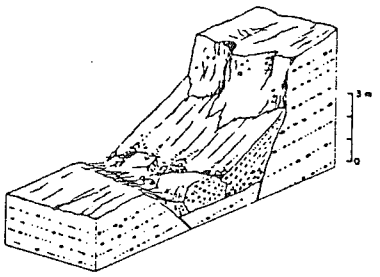

C–NORMAL FAULT SCARP WITH GRABEN.

ARIZONA DEPARTMENT OF TRANSPORTATION

ARIZONA TRANSPORTATION RESEARCH CENTER

FIGURE 24

FAULT SCARP TERMINOLOGY

FHWA REGION	STATE	PROJECT NUMBER	REPORT NUMBER
9	ARIZ.	HPR-PL-1(37)344	FWHA-AZ92-344

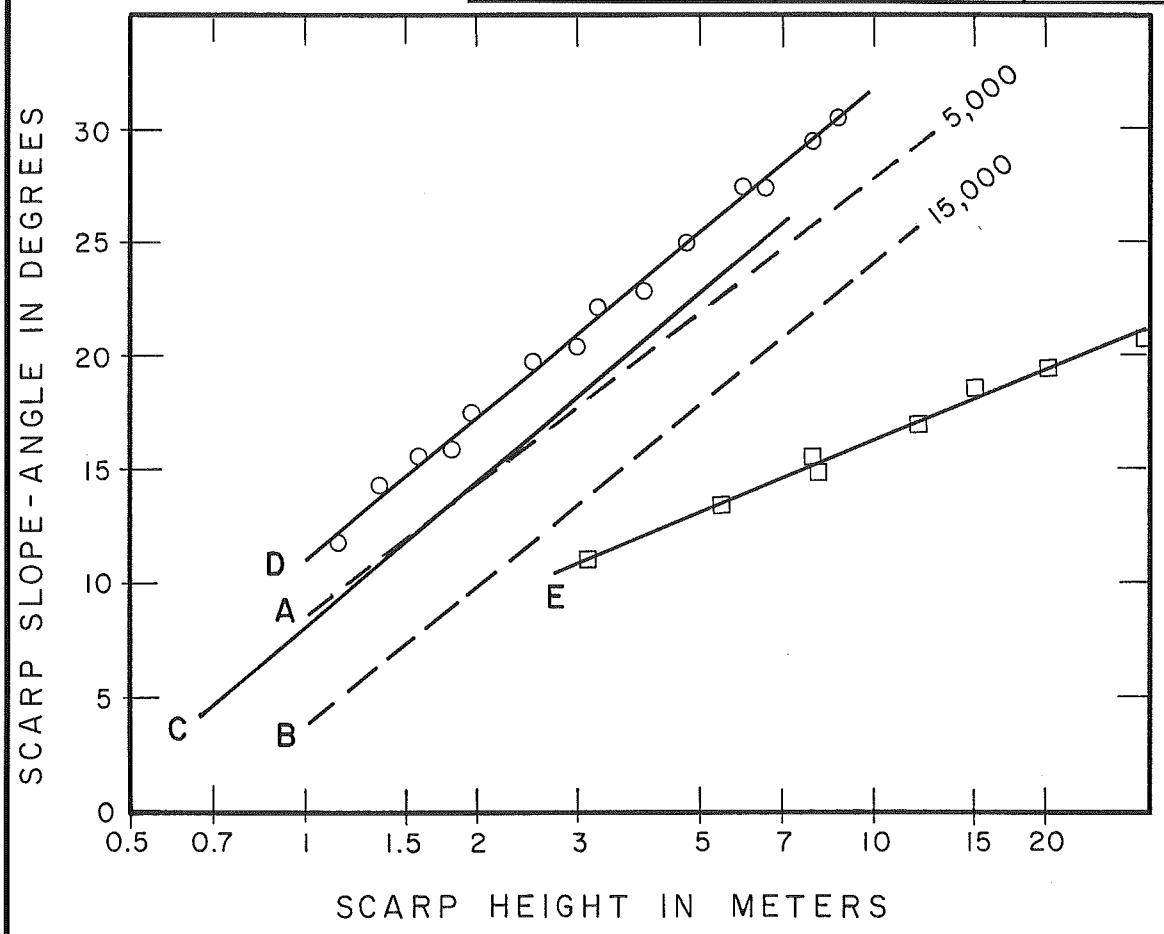

A — — — — — — 5,000 - Cox Ranch and La Jencia Faults, New Mexico

B — — — — — — 15,000 - Lake Bonneville Shoreline

C ——————— 9,000 - Drum Mountain Fault, Utah

D ~~~~~~~~~~ Hypothetical Fault C

E ~~~~~~~~~~ Hypothetical Fault D

PLOT OF FAULT-SCARP SLOPE-ANGLES AGAINST HEIGHT OF SCARP. MODIFIED FROM BUCKNAM AND ANDERSON (1979) AND MACHETTE AND MCGIMSEY (1982).

ARIZONA DEPARTMENT OF TRANSPORTATION
ARIZONA TRANSPORTATION RESEARCH CENTER

FIGURE 25
FAULT SCARP HEIGHT/ANGLE RELATIONSHIP

ages. By comparing similar measurements from fault scarps with unknown ages in Arizona to lines A, B, and C, the relative ages of the unknown scarps can be approximated. The hypothetical scarp represented by line D would be younger than 5,000 to 9,000 years and the hypothetical scarp represented by line E would be older than 15,000 years. If data measured from an actual scarp results in a line that plots between line A and B, its age would be between about 5,000 to 15,000 years.

In view of the uncertainties involved with direct application of these methods to a particular scarp, other factors were used to help constrain the interpretations. In addition to scarp-height and slope-angle measurements, observations of crest sharpness, degree of scarp dissection, type of sediment, and grain size of faulted materials have proven to be important parameters for estimating scarp age. Other parameters such as slope of the original fan surface, orientation, position relative to the mountain fronts and playas, and climate were also considered.

The complex inter-relationships of the various geomorphic, stratigraphic, and climatic parameters make it difficult to devise a model in which all of these variables are included and correctly accounted for. Also there may be other variables that are not yet recognized. The major limitation of using fault-scarp morphology for dating faults appears to be that rates of the degradation process are poorly known and they change as the process advances. For example, the slope of line E on Figure 25 is much lower than the slopes of the lines for the younger scarps (lines A, B, and C). This indicates that the height and slope-angle relationships for scarp E are not

the same as for the other scarps. This difference might be due, for instance, to the scarp being a composite feature, that is, a result of more than one surface displacement. Another possible complicating factor is the difference in rates of degradation due to climatic differences between areas. Although the entire study area is basically an arid environment, there may be important differences between the cooler moister high-elevation areas in the northern part of the state and the lower warmer dryer areas of the southern part of the study area. Lines A and C on Figure 25, for example are quite similar yet one of the scarps is about twice as old as the other. Line C is from the central Great Basin province in Utah whereas line A is from the southern Rio Grande Rift in New Mexico. Due to such uncertainties, not much reliance can be placed on scarp morphology alone but, combined with other data, probable ages of latest movement can be approximated within broad categories such as Holocene, very late Pleistocene, late Pleistocene, middle Pleistocene, and early Pleistocene.

(4) Stratigraphic Parameters

Stratigraphic parameters useful for seismotectonic zonation are those that are related to recent crustal unrest. For example, volcanic rocks can reveal much about deep-seated crustal forces. Volcanic arcs such as the Cascade Volcanic Belt indicate a plate subduction tectonic regime and have major implications regarding stress fields. The type of volcanics can reveal the same type of information; for example, basalts are generally indicative of an extensional tectonic regime. The volcanics along the margin

of the Colorado Plateau show decreasing age and change in composition inward toward the central plateau appearing to document tectonic changes from Tertiary into the Quaternary. Sedimentological aspects of stratigraphic units can also be useful because they provide information on rates of erosion and, hence, uplift and can indicate area of subsidence. The sediments of the east central Arizona document several episodes of basin formation and filling that appear to be due to tectonic processes.

On the other hand, some aspects of stratigraphy and rock type are not relevant to seismotectonic zonation. For example, most deposition, lithogenesis, consolidation, and deformation occurred during previous tectonic (paleotectonic) regimes and, therefore, are generally not relevant to a neotectonic-based analysis such as this investigation. Because of this, seismic source zone boundaries may cross through areas with similar rocks. In the Arizona area, for instance, the Mesozoic sedimentary rocks do not appear to have any significant relationship to neotectonic zones or provinces, and the province boundaries cross them in many places. The ancient basement rocks also do not appear to have much neotectonic significance although they are perhaps most common in the block-faulted Basin-and-Range zones where young downfaulting and deep erosion exposes them in numerous places.

(5) Geologic Structure and Tectonic Parameters

Geologic structures and tectonic elements are of primary importance to differentiation of seismic source zones and generally are given

more weight than most other parameters. Because the geologic processes that form the earth's crust occur over periods of thousands and millions of years, the geologic nature of an area cannot be fully appreciated by short-term parameters (such as seismicity) alone. The major geologic and tectonic parameters used for this seismotectonic analysis are faults, folds, and the tectonic stress fields as indicated by alignment and/or orientation of geologic features.

Faulting is foremost of these parameters. Faults generally tell more about the seismic hazards of an area than any other data because they provide a long-term record of the rock stresses and tectonic activity of a region.

In this regard it is important to differentiate between active faults and inactive faults. For this study, faults are considered active if they have a potential for rupture under the present tectonic stress field. Therefore, a major step in the zoning process was to establish when the present stress fields were initiated. This is an iterative process which requires analysis of geologic history over a period of time long enough to include the time of the last significant change of tectonic regime. Many neotectonic analyses utilize only the Quaternary record but most regions entered into their present seismotectonic (neotectonic) regime long before the Quaternary Period. Some examples of the range in age of initiation of present tectonic regimes are:

Western Transverse Ranges	middle Pleistocene
Salton Trough	early Pliocene
Sonoran	early Pliocene to late Miocene

California Basin and Range	late Miocene
Central Basin and Range	late to middle Miocene
Colorado Plateau	early Tertiary

As indicated by these ages, the Quaternary Period has no special significance with respect to tectonics, although in some areas the Quaternary may represent a period of time that is long enough to be representative of the neotectonic regime.

An extensive analysis of potentially active faults was conducted for this investigation. The analysis consisted of review of published fault maps and literature. These were combined with unpublished data to construct a preliminary map of faults. These faults were analyzed to determine which were well known and could be accepted as seismic sources based on the existing data. Several faults and areas were identified which were not adequately studied and investigations were undertaken to evaluate their seismic potential. These investigations included review of literature, discussions with geoscientists, aerial reconnaissance, aerial-photograph interpretation, field reconnaissance, field mapping, fault-scarp morphology analysis, and trenching. Plate 1, the resulting map of neotectonic faults, is a principal input for defining seismic source zones.

(6) Seismologic Parameters

Various types of seismological data are used for subdividing regions into seismic source zones. The most important data are

the size, distribution, frequency, and focal-mechanisms of earthquakes provided by seismograph networks. In areas with short earthquake records or a low rate of seismic activity, earthquake intensities from historical events that occurred prior to establishment of seismograph networks can help characterize the earthquake potential.

Care must be taken when assigning seismicity to zones for determining recurrence relations. The three main reasons for this are (1) province boundaries are transitional; (2) earthquake sources are commonly dipping planes which may not be obvious from the epicentral locations; and (3) earthquake locations generally are imprecise with some old events having uncertainties of tens of miles.

(a) Types of Data: Seismicity data useful for seismotectonic zoning studies exist in several forms (instrumental, historical, microseismicity). Each of these has strengths and inherent problems with respect to its application in seismotectonic zoning. The following paragraphs discuss some of the strengths and weaknesses of these data.

The best data for defining source-zone boundaries generally are instrumentally located earthquakes recorded within the past 20 to 30 years because they are the most abundant and the most accurately located. The major problem with these instrumental records is that they represent a time period which is too short to adequately represent geologic phenomena which are measured in thousands or even millions of years. To compensate for this

shortcoming, older instrumental data and qualitative historical data and anecdotal accounts were used.

Microseismicity can be useful because it can provide a lot of data in a very short time, and can identify potentially active areas that had no historical records. However, care must be used in the application of microseismicity because it is not clear how it relates to macroseismicity.

Pre-instrumental seismicity comprises earthquakes that occurred prior to the establishment of seismograph networks. The lengths of these pre-instrumental data bases and their completeness vary widely from region to region. Middle eastern and far eastern countries have records of earthquakes that extend a few thousand years back in time, whereas in the western United States the record is only a couple hundred years long at best. The quality of historical records is highly dependent on population density because earthquakes during the 1700s and 1800s were usually recorded only at educational or religious institutions. This results in a distribution of historical earthquakes that is biased towards major cities and towns. Estimates of the intensity or magnitude of pre-instrumental earthquakes are usually based on reports of destruction and loss of life, thus local building practices and foundation conditions probably play a more important role in the intensity assigned than the actual size of the earthquake.

Paleoseismicity refers to earthquakes which occurred prior to historical time. These earthquakes are recognized by analysis of ancient faults and earthquake-induced ground failures such as are caused by

liquefaction. Paleoseismicity studies generally involve analysis of ancient fault scarps by geological, geomorphological and subsurface methods such as trenching. Such studies provide data on the length of ancient fault ruptures, amount of displacement, and frequency of occurrence. These data can then be compared to empirical relationships between fault length/ displacement and earthquake magnitude to estimate the magnitude of the paleoseismic events. Paleoseismic studies conducted for this investigation are discussed in Section 3.

(b) Earthquake Epicenter/Hypocenter Data: Earthquake locations in the study region were compiled from various sources. The principal sources of seismicity data were:

- Historical Seismicity in Arizona, 1830 - 1980 by DuBois et al, 1982.

- Earthquake Catalog of Arizona, 1830 - 1991 by Brumbaugh, 1992.

- Computer files of the U.S. Geological Survey and U.S. Geophysical Data Center; various extracts and catalogs for California, Nevada, Utah, Arizona, New Mexico, Mexico generally covering the period from the 1850s to the late 1980s.

- "Seismicity Map of the State of Arizona" by Stover et al, 1986.

- "Seismicity Map of the State of New Mexico" by Stover et al, 1988.

- "The Relationship Between the Seismicity and Late Cenozoic Tectonics in Arizona" A master thesis by Mokhtar, 1979.

- "Colorado Earthquake Data and Interpretations", 1867 to 1985 by Kirkham and Rogers, 1985.

- Various catalogs of earthquakes in southern Nevada such as Rogers et al, 1981 and Gawthrop and Carr, 1988.

- "Earthquakes in Arizona - 1850 to 1928" by Townley and Allen, 1939.

- "Earthquake History of the United States" by Coffman and Von Hake, 1973.

- "Earthquake History of Arizona and New Mexico, 1850-1966" by Sturgal and Irwin, 1971.

- Catalog of North American earthquakes compiled by the Geological Society of America for Decade of North American Geology (DNAG).

- Files of the project geologists collected from numerous previous projects in the region. The source for these files was mostly

from the U.S. Geological Survey, California Institute of Technology, University of Utah, and University of Nevada, but they have been extensively edited to eliminate duplicate and mislocated events.

- Numerous articles in published journals regarding specific earthquakes or local seismic clusters. These are cited in this report where appropriate; others were reviewed but found not to be especially relevant to this investigation and hence are not listed.

Most of the catalogs listed above have different degrees of completeness and disagree on the locations of several events. The differences are not critical for this investigation because many of the final conclusions were based as much, or more, on paleoseismic and other geologic information. Figure 26 is a seismicity map of the state of Arizona from Brumbaugh (1992) showing the general distribution of earthquakes. Brumbaugh has recently reanalyzed seismicity records and has relocated several of the events along the Arizona-New Mexico border (personal communication, February, 1992).

Although seismicity in the state of Arizona is infrequent and of small magnitude compared to parts of California, Nevada, and Utah, there is a definite trend or belt of seismic activity that extends diagonally from the northwest corner of the state to the southeast corner (Figure 26). This belt of seismicity coincides with the areas with the most abundant Quaternary/neotectonic faults (Plate 1). In spite of this general correlation between

FHWA REGION	STATE	PROJECT NUMBER	REPORT NUMBER
9	ARIZ.	HPR-PL-1(37)344	FWHA-AZ92-344

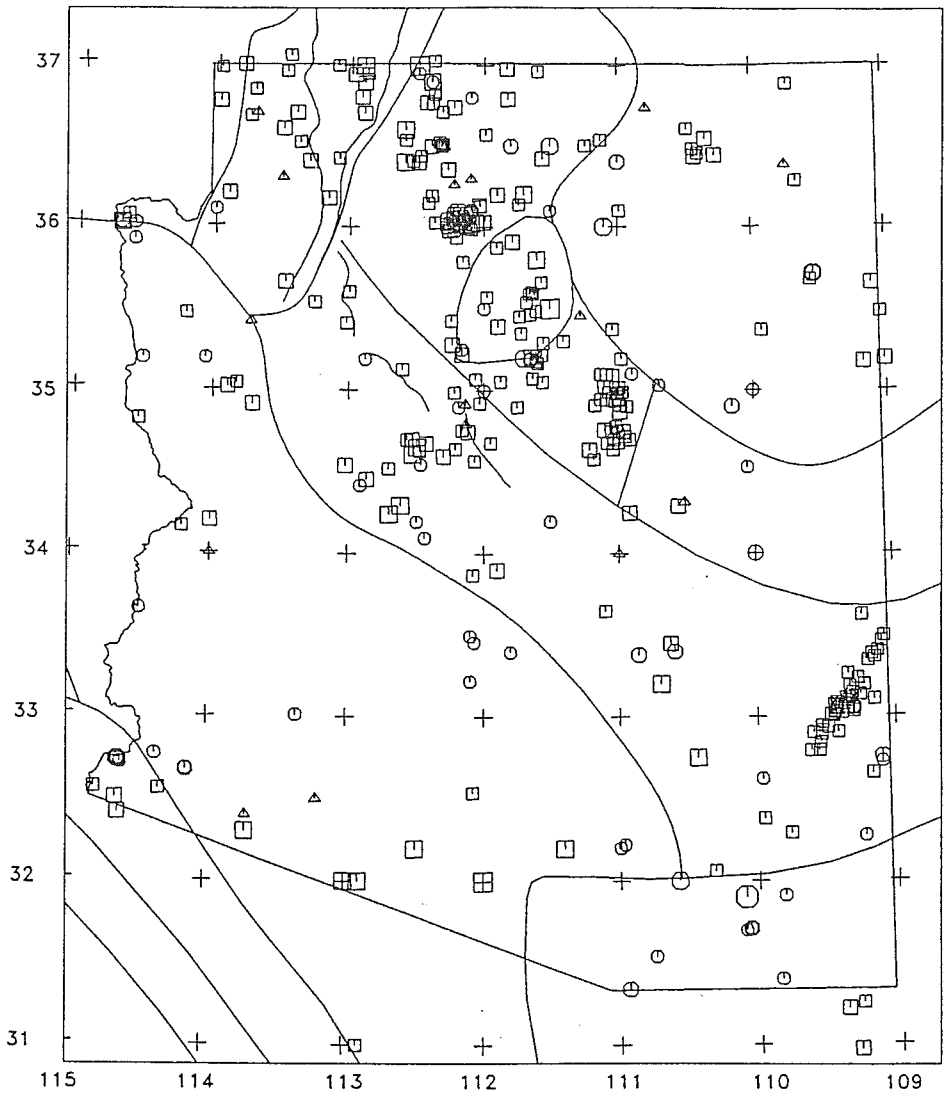

ARIZONA DEPARTMENT OF TRANSPORTATION
ARIZONA TRANSPORTATION RESEARCH CENTER

FIGURE 26
SEISMICITY MAP OF ARIZONA

faulting and seismicity, only the 1887 Sonoran earthquake was associated with a known surface fault. Based on the abundance of faults in the state with evidence of Quaternary displacements, the lack of correlation between seismicity and faults is probably more a function of the slow rate of crustal strain release rather than lack of absolute earthquake potential. In other words, earthquakes should be expected, but they will be infrequent because there is a finite amount of crustal strain in across the region and most of the regional crustal strain-energy release in this area occurs along faults in California, Nevada, and Utah. The small, remaining amount of strain energy must be partitioned among the multitude of faults in Arizona, New Mexico, Mexico, Texas, and Colorado. At the slow rates typical for this region it takes a long time to accumulate enough strain to rupture any one particular fault and the resulting intervals between major earthquakes on these faults are very long.

The relative paucity of seismicity in Arizona does not lend itself well to statistical analysis. Some source zones have less than 10 earthquakes that could be used for statistical analysis. Therefore the probabilistic analysis of earthquake potential for development of the ground-motion contour map required the use of geologic data to construct realistic seismic source zones and to determine recurrence relationships for these zones. Further discussion of how the geologic data and the seismicity data were combined to develop recurrence relations is given in Section 7.

(c) Earthquake Magnitude Scales: The Earthquakes analyzed for this investigation were from a variety of sources that used

several different magnitude scales. The most familiar magnitude scale is probably the one developed by Richter (1935). This scale, denoted by M_L, was developed for southern California earthquakes and is referred to as the Richter magnitude or local magnitude scale.

A more universal magnitude scale for larger shocks and applicable to the whole earth was developed by Gutenberg (1945) for shallow focus (depth 36 miles) earthquakes. This scale is based upon the ground motion of the 20-second surface wave and is denoted by M_S.

Both the M_L and M_S magnitude scales apply to earthquakes which occur at shallow depths. Gutenburg and Richter (1956) introduced a method of sizing earthquakes occurring at depths greater than 36 miles based on amplitudes and periods of body waves. Magnitudes of this scale are denoted by m_b.

Another magnitude scale used for Arizona earthquakes includes the m_bLg scale which is based on the short-period Rayleigh waves. These magnitudes are not based on body waves but use the m_b notation because the Rayleigh waves (Lg) seem to behave, at regional distances, similar to body-wave attenuation.

Some magnitudes are based on the length of time of shaking as measured on seismograms. These magnitudes are called duration magnitudes and are especially useful for small-magnitude events such as those in Arizona (Wallace, T.C., 1992, Personal Communication).

An important aspect of all these instrumental magnitude scales, especially for large California events, is that they exhibit a saturation level with increasing magnitude. That is, the scales converge and do not reflect the true size of earthquakes at magnitudes above about 7.75. For example, consider two great earthquakes, the 1960 Chilean earthquake which may have been the world's largest instrumentally recorded earthquake and the 1906 San Francisco earthquake. The Chilean earthquake ruptured an area comparable to the size of the entire state of California, whereas the San Francisco earthquake ruptured an area less than a third the size of the state. Yet, these two earthquakes had virtually identical surface-wave magnitudes (M_S) of 8-1/4. However, calculations of the energy released during these two events, show that the Chilean event was about 200 times larger than the San Francisco event. The energy released during an earthquake is represented by another scale, the seismic moment magnitude scale (Mw). This scale, developed by Hanks and Kanamori (1979), provides a better representation of the size of large earthquakes than the other scales. The magnitudes of the other scales above which saturation occurs and where M_w becomes a more accurate measure of energy release are M_S 7-1/2, M_L 6-1/4, and m_b 6-1/4 (Heaton and others, 1984). These differences are not likely to have much effect on the analysis in Arizona because few faults in the state appear to be large enough to reach the saturation level. Only the long faults in the Salton Trough such as the San Andreas fault, are likely to be affected.

Some catalogs do not always specify the type of magnitude. Likewise, the type of magnitudes in this report may not always be specified. In many cases, the type of magnitude is not important enough to significantly affect

the seismic hazards. Also magnitude determinations are not unique and different investigators and different recording locations commonly list different magnitudes for the same event, or they compromise by agreeing on some intermediate value. Commonly, other factors such as site characteristics, travel paths, focusing effects, azimuth, depth of earthquake, will have greater impacts on damage than will magnitude. Given these realities, earthquakes with magnitudes differing by one or two tenths of a magnitude unit may be essentially similar and not much relevance can be placed on these differences. The same applies to maximum credible earthquake magnitudes (MCEs). That is, given all the assumptions and inadequacies of the data base, MCEs differing by one or two tenths of a magnitude should be considered similar events.

(d) Earthquake Intensity Scales: Intensity is a subjective measure of the effects of an earthquake and is generally given in Roman numerals. There are two intensity scales commonly given in the literature, the Rossi-Forel scale and the Mercalli scale. The Rossi-Forel intensity scale was developed by de Rossi of Italy and Forel of Switzerland in the 1880s. This scale, with values from I to X, was used for about two decades. In 1902 the Italian seismologist, Mercalli, devised a scale with a range from I to XII. The Mercalli Scale was modified in 1931 by American seismologists to take into account modern structural design (Wood and Neumann, 1931). Unless otherwise noted, the Modified Mercalli Intensity Scale (MMI) is the intensity scale used in this report.

Figure 27 illustrates the approximate relationship between intensity scales and instrumental magnitude scales. Because intensity scales measure effects reported by local observers, they are subject to variations that depend on factors such as distance between the reporting site and the earthquake, stiffness of the building experiencing the earthquake, local soil conditions, and geologic conditions along the travel path between the event and the affected site. For example, for towns at different distances from the source of an earthquake, the nearest town will probably have the highest intensities. Also, towns on alluvium will have higher intensities than towns on solid rock. Because of these variables and the subjectivity of intensity scales, direct conversion between intensity and magnitude is not possible. For this reason, Figure 27 should be used with discretion and only as a general guide to the relative size of earthquakes. The figure should not be used to determine seismic design parameters.

(e) Maximum Earthquakes: Maximum credible earthquakes (MCE) are assigned for each seismic source. The MCE is defined as the largest earthquake that is capable of being produced from a source, structure, or region under the currently known tectonic framework. It is a rational and believable event which can be supported by all know geologic and seismologic data (California Division of Mines and Geology, 1975). This definition dictates that an MCE not be based on, or be dependent on, only seismological data. Seismicity data are adequate for MCE determinations only when the length of the earthquake record equals or exceeds the recurrence time of the largest hypothetical earthquake and, preferably, several cycles should have occurred before much confidence can be placed on using the data.

FHWA REGION	STATE	PROJECT NUMBER	REPORT NUMBER
9	ARIZ.	HPR-PL-1(37)344	FWHA-AZ92-344

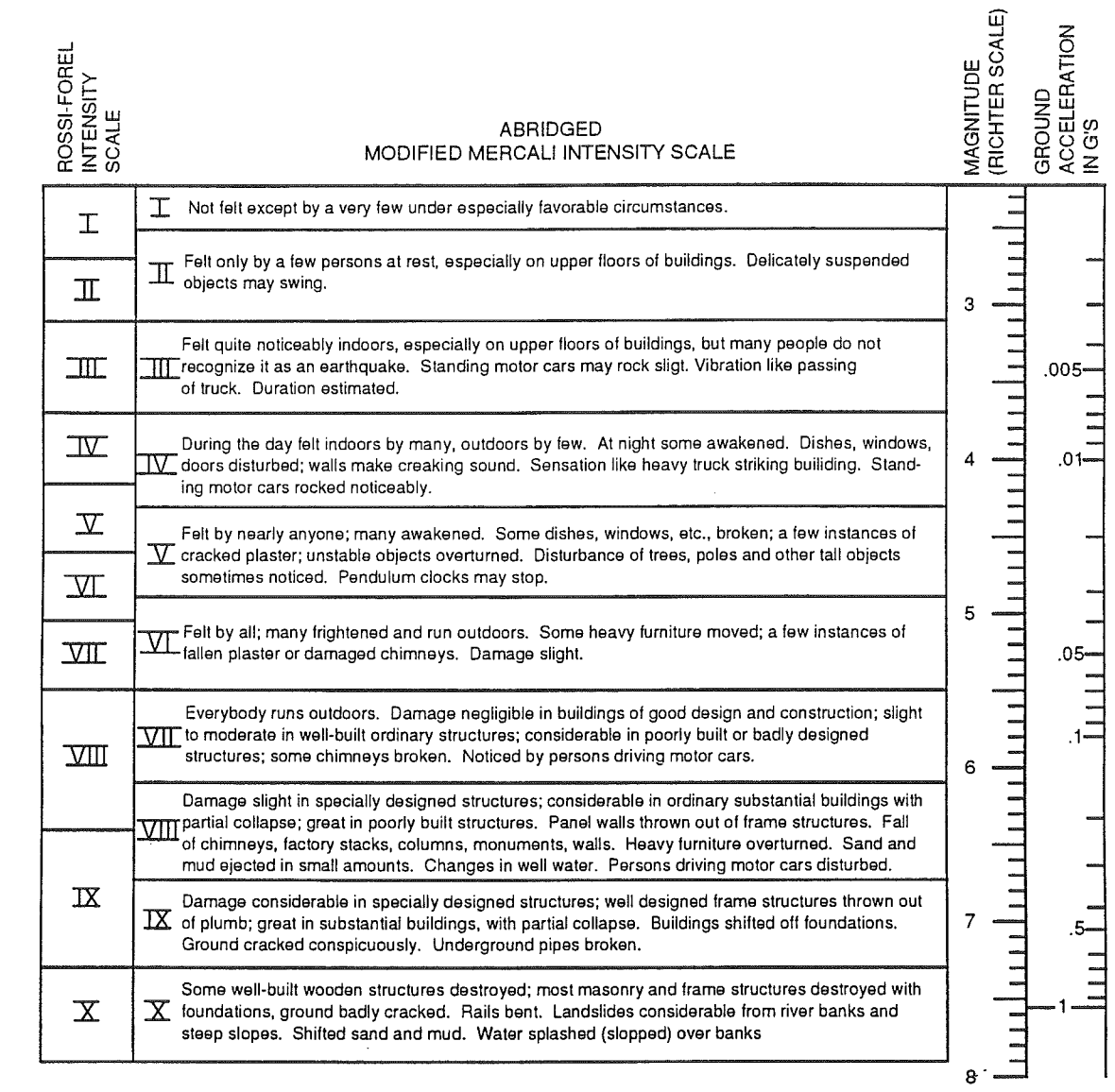

NOTES: THESE RELATIONSHIPS ARE GIVEN TO ILLUSTRATE GENERAL COMPARISONS FOR REGIONAL SCREENING STUDIES AND SHOULD NOT BE USED FOR DESIGN PARAMETERS.

MODIFIED MERCALI INTENSITIES XI AND XII NOT INCLUDED.

ARIZONA DEPARTMENT OF TRANSPORTATION

ARIZONA TRANSPORTATION RESEARCH CENTER

FIGURE 27

RELATIONSHIP BETWEEN EARTHQUAKE INTENSITY AND MAGNITUDE

The maximum earthquake commonly can be determined from historical data in zones with high rates of seismicity and tectonic activity . For example, in the San Jacinto seismic source zone, which has had several moderate to large magnitude earthquakes in historical time, the recurrence time of the maximum earthquake can be estimated. In contrast, most of the seismic source zones in the western United States have rates of tectonic activity that are much less than along the San Jacinto fault. The recurrence intervals for the maximum earthquakes in these other zones can be several thousand to several tens of thousands of years long (Muir et al, 1981; Schell, 1982; Wallace, 1987).

An important aspect in determining maximum earthquakes for some faults is the total length of the fault and the length of rupture per event which are commonly used with empirical length/magnitude relationships to estimate MCEs. Most long faults do not rupture their entire length during any single event (Albee and Smith, 1960; Slemmons, 1982). In recent years some geoscientists have postulated that faults rupture along discrete segments and that these segments have their own characteristic earthquakes, recurrence intervals, and slip rates that are different from adjacent segments on the same fault. Geoscientists have used characteristics such as changes in surface trend, geomorphic anomalies, change in rock type, and various other characteristics (for example, geophysical anomalies) to identify segment boundaries. However, historical earthquakes have repeatedly ignored or ruptured through such "boundaries" (see, for example, Freeman et al, 1986) indicating that, at best, segment identification is a complicated process and, at worst, true discrete segments are exceedingly rare. Another

excellent recent example is the magnitude 7.5 Landers earthquake which occurred in July 1992 during the preparation of this report. Although details are still being collected at the time of this writing, it is quite clear that most of the 40+ miles of surface rupture occurred along several existing mapped faults. Like other earthquakes before it, as discussed by Freeman et al (1986), this event did not "obey" any of the postulated rules of segmentation, casting doubt on the validity of such "rules" and upon the theory of fault segmentation as practiced by many geoscientists. The basic concept is probably valid to some extent, but caution must be exercised when assessing maximum earthquakes for seismic hazard analysis. In view of the historical experience, postulation of short segments does not seem to be conservative and long faults such as the Hurricane and Toroweap probably do not comprise as many discrete seismogenic segments as their irregular surface traces might suggest.

The MCEs assigned to the seismic source zones in this report are based on both geologic and seismologic parameters and are based on a wide variety of data such as comparisons to earthquakes with several magnitude estimates, and thus it is difficult, if not unrealistic, to specify one magnitude scale for all source zone MCEs. However, allowances were made for these uncertainties and the MCE magnitudes given in this report are considered to be moment magnitudes M_w).

In many seismic hazard assessments zones with very low rates of tectonic activity and those that are nearly tectonically stable are commonly assigned MCEs of 5 to 6.5. Even though there is no direct seismological or

geological evidence within these zones that earthquakes this large could occur, these estimates are believed to be reasonable based on comparison to the seismotectonics of other regions. For example, historical earthquake data indicate that even the stable central portion of the United States has occasional earthquakes in the 5 to 5.5 magnitude range and rare events in excess of M = 7 (for example, New Madrid, Missouri). Most of the moderate-magnitude events appear to be random in time and space and are not associated with surface rupture or known geologic structures, therefore, they should be considered capable of occurring anywhere throughout those provinces, and other similar provinces.

In addition to the maximum credible earthquake, characteristic earthquakes are sometimes considered in the hazard models. The characteristic earthquake model states that certain faults have a tendency to generate earthquakes of a specific size or narrow magnitude range greater than the typical Gutenberg-Richter logarithmic relationship would indicate. Figure 28 shows a typical recurrence relationship for a fault that fits the characteristic model. The illustration combines both seismicity data and geological data from paleoseismic studies. The geologic data (displacements of past earthquakes along the fault) provides information on the frequency and size of the larger earthquakes. These were termed characteristic earthquakes by Schwartz and Coppersmith (1984). The slope of a line fitted to the statistical earthquake distribution, as shown on Figure 28, can be assigned a typical number termed the b-value (B on Figure 28). This slope is usually constant within a certain range of magnitudes. Ideally, the slope should be constant up to the maximum earthquake but field geologic studies

FHWA REGION	STATE	PROJECT NUMBER	REPORT NUMBER
9	ARIZ.	HPR-PL-1(37)344	FWHA-AZ92-344

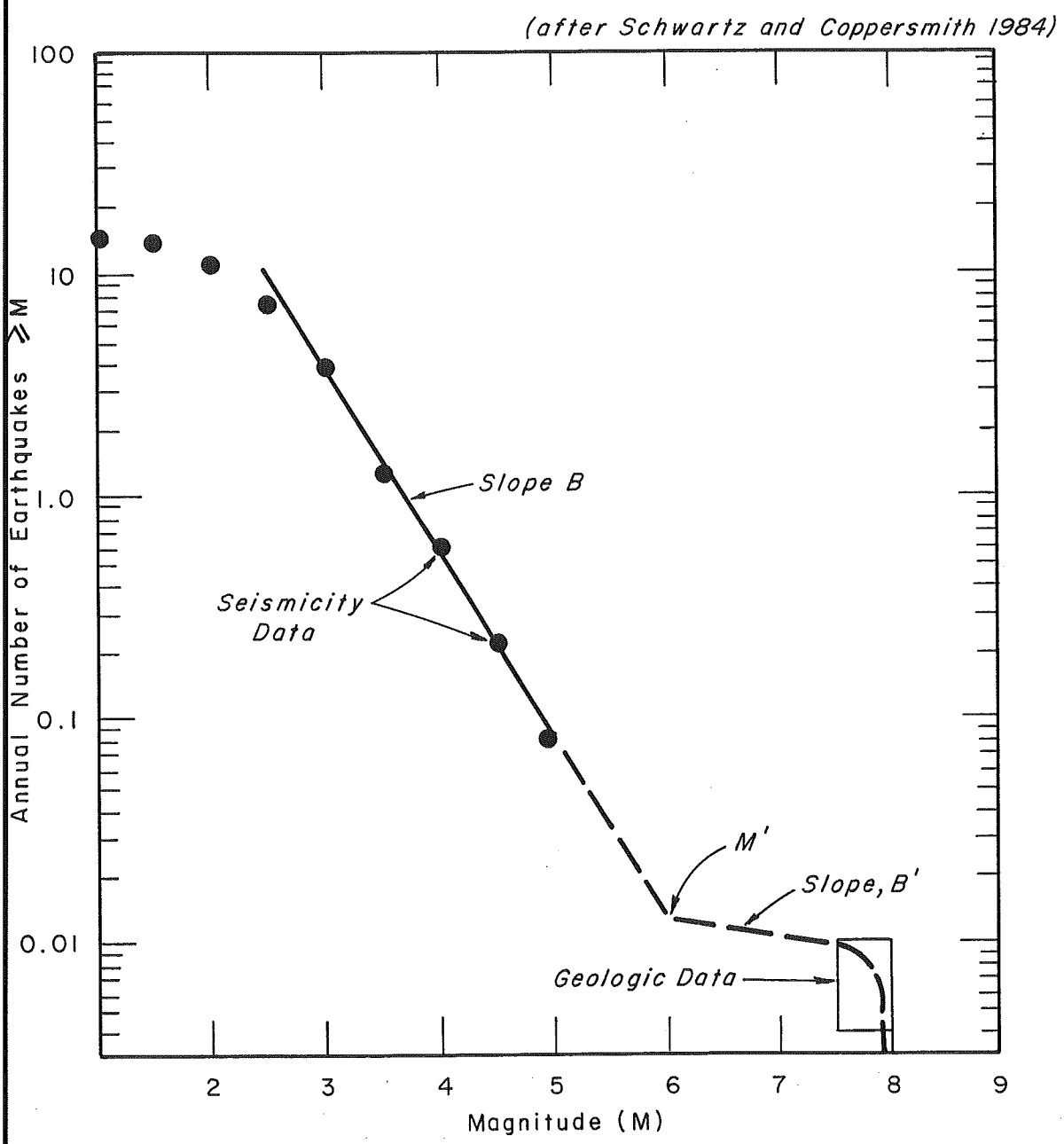

(CHARACTERISTIC EARTHQUAKE MODEL)

ARIZONA DEPARTMENT OF TRANSPORTATION
ARIZONA TRANSPORTATION RESEARCH CENTER

FIGURE 28
RECURRENCE RELATIONSHIP FOR HYPOTHETICAL FAULT

have suggested that some faults typically rupture during a certain narrow magnitude range. The box (labeled "Geologic Data") on Figure 28 represents this characteristic magnitude as determined from geological studies of typical displacements and frequency of events. This box generally does not lie on a straight line extension of the line determined from the smaller earthquakes; a shallower slope (B' on Figure 28) is needed to reconcile the two data sets. The recurrence curve drops off sharply as it approaches the upper end of the characteristic earthquake range. It is not yet known to what extent fault behavior fits the characteristic earthquake model or what the relationship to maximum credible earthquakes is. In some cases they appear equal. Many evaluations conducted by us for other projects do not appear to favor the characteristic model for some faults.

(f) **Random Earthquakes:** In most regions, even those with high rates of seismotectonic activity, earthquakes occasionally occur which cannot be correlated to known geologic structures. Some of these may be due to small displacements on faults with long recurrence intervals and thus with little surface expression. Other fault displacements might occur at great depths and degrade upward into folds and flexures. Still others may exist in areas where geologic structures exist but have not been mapped in detail. To account for such faults, seismic hazards analyses commonly consider a maximum random or floating earthquake which is considered to be capable of occurring anywhere within the source zone. Traditionally such events have not been large because the larger earthquakes were thought to always be associated with known faults. Common practice was to assign a magnitude for

the random event that was consistent with the historical background seismicity. These events were generally in the magnitude 5 to 5.5 range. However, in recent years, a few moderate- to large-magnitude earthquakes have occurred without surface rupture, elevating the importance of random earthquake estimation. For example, the 1983 Coalinga, California earthquake of magnitude M_L = 6.7, the 1987 Whittier, California earthquake of M_L = 5.9, and the 1989 Loma Prieta, California earthquake of M_s = 7.1 all occurred without surface rupture. Subsequent studies revealed surface deformations in the form of uplifts and warping suggesting that in most cases, the larger random shocks can be correlated to geologic structures if the appropriate detailed studies are undertaken. However, the potential for moderate-magnitude (M = 5 to 6.5) events occurring in areas without evidence of geologic structures is still a very real unknown which has to be included in any comprehensive seismic hazard analysis. For this investigation, all zones were assigned maximum random earthquakes of M=6 or larger so the random event problem should be accounted for.

(7) Geophysical Parameters

Geophysics, though generally not directly indicative of tectonic activity, can provide indirect information on tectonic characteristics and thereby help establish seismotectonic zones. For example, gravity and seismic-velocity data can indicate thickness and continuity of the crust and subcrustal parameters; heat flow can indicate crustal weaknesses; and magnetics can indicate subsurface rock types. In

particular, geophysical data can help define province boundaries even though the measured physical parameter may not be characteristic of the entire province.

The Eastern Mojave Province zone provides a good example for the use of geophysical parameters to help locate province boundaries. The eastern boundary of the province is underlain by a change in seismic velocities which indicates an asymmetric ridge or hinge on the Moho (Fuis, 1982). This hinge approximately coincides with the changes in faulting and seismicity and together, these three parameters provide a strong basis for locating the boundary where it is shown (Figure 23). Gravity signatures help define the Sonoran/Arizona Mountain/Plateau margin boundaries. Magnetic anomalies seem to indicate continuity of major faults such as the Mesa Butte and Bright Angel faults. Other geophysical data are discussed in Section 6 under the particular source to which it applies.

b. Seismic Source Map

Figure 23 shows the seismic sources defined for this investigation. The seismic source zones within the state boundaries are also shown on Plate 1. The methods used to define these seismic sources are described above in Section 6.a. The characteristics of each source zone are summarized in the following section.

c. Description of Seismic Source Zones

(1) Arizona Mountain Zone

The Arizona Mountain seismic source zone has an area of about 38,000 square miles (Figure 23). The Aubrey, Big Chino, and Verde faults are considered discrete seismic sources within the Arizona Mountain source zone but for convenience, are discussed under this section so the interrelationships can be better illustrated.

The Arizona Mountain zone forms a somewhat arcuate belt around the southern margin of the Colorado Plateau and Plateau Margin source zones. The Arizona Mountain zone extends from the northwest part of the state to the Rio Grande Rift in New Mexico and the Mexico Basin and Range zone in southeastern Arizona. This zone encompasses a variety of mountain ranges, plateaus, and valleys between the relatively flat, higher elevation Colorado Plateau on the northeast and the lower elevation Sonoran zone on the southwest. The relative proportion of the zone within valleys as opposed to mountains averages about 25 percent of the land area but the relative proportions change substantially to about 50 percent in the southeastern part of the zone. The mountains of this zone were produced primarily by erosion from downcutting related to regional uplift and extensional block faulting, rather than to normal orogenic mountain-building processes (i.e. compressional forces and andesitic-type volcanism).

Elevations and relief vary considerably throughout the zone. From an overview perspective, elevations are highest along the arcuate northeast boundary near the Mogollon Rim where they are generally in the 6000 to 6500 foot range. Elevations decrease southwesterly to the Sonoran zone where they are generally in the 2000 to 3000 foot range. The highest elevations are in the eastern part of the zone where a few peaks exceed 10,000 feet and valleys are 5000 to over 6500 feet high. Elevations generally are lowest in the central part of the province along the Verde River where they are as low as about 1500 feet.

The stratigraphy of the zone can be characterized by two principle domains: the rocks of the mountains and uplands, and the sediments of the valleys. The rocks exposed within the mountains comprise a wide variety with nearly every rock type in the state being represented. The predominant rocks are Precambrian granitic and metamorphic rocks, and Tertiary-Mesozoic volcanics. A simplified picture is one of Tertiary volcanic rocks capping thin flat-lying Mesozoic sedimentary rocks all overlying complexly deformed basement rocks. The wide variety of rocks is a direct result of uplift, extensional faulting, and erosion of the fault blocks exposing the deeper older basement rocks and the overlying stratigraphic sequence. The valleys are generally floored by Quaternary sediments overlying late Tertiary alluvium which was deposited into the basins during an earlier basin-and-range episode (i.e. Miocene).

The Arizona Mountain source zone is largely defined on the basis of its neotectonic regime which is essentially an extensional, block-faulting,

tectonic regime. In typical Basin-and-Range style, the major neotectonic faults lie near the margins of the valleys and separate the down-dropped valley blocks from the uplifted mountain blocks. Also as is typical of Basin and Range tectonic regimes, the Arizona Mountain zone has abundant hot spring activity and a high heat flow (Witcher, 1981). The crustal thickness, however, may be somewhat thicker than normal (Warren, 1969) for Basin-and-Range-type areas. The rate of faulting is slow in this province and the physiography resulting from this tectonic style is more subtle than in other basin-and-range provinces such as those in Nevada and Utah. Major down-faulted block structures are Aubrey Valley, Chino Valley, Verde Valley, Tonto Basin, northern San Pedro Valley, northern San Simon Valley, Lordsburg Basin, and San Augustin Plain. In Arizona, the major faults and their corresponding fault-block structures generally trend north-northwesterly and northwesterly, whereas in the San Augustin Plain region of New Mexico the trends are northeasterly. The major basins of this zone in Arizona form a long northwesterly trend that is quite linear on regional-scale, high-altitude, oblique, satellite photographs and suggestive of a zone of crustal weakness. These valleys also may have a minor left-stepping en echelon arrangement.

Although the zone has common neotectonic characteristics, there are some characteristics across the zone which might indicate some differences in rate and/or style of neotectonic activity. For example, the faults are longest and are associated with more prominent mountain fronts in the northwestern and eastern parts of the zone. Faults in the central region are short, discontinuous, and oriented more randomly, and historical,earthquake activity has been somewhat less in this central region. Considering the low

rate of seismotectonic activity in the region as a whole, it is difficult to assign much importance to the lower local seismicity level. A possible explanation for the apparent differences is that the two extremities, i.e. the northwestern and the eastern ends are in proximity to more-active adjacent zones, the Hurricane-Wasatch in the northwest and the Rio Grande Rift in the east. Changes in crustal strain generally are thought to be gradual so some strain may be "leaking" from these more-active zones across zone boundaries affecting adjacent geologic structures in the Arizona Mountain Zone. Acknowledging these differences and the uncertainties involved, the differences do not appear to be great enough to warrant establishing separate zones for these three subareas, especially because there is little detailed information on many of the faults in the central and eastern parts of the zone to allow more-definitive neotectonic characterization. This uncertainty is typical of areas with low rates of tectonic activity where it is difficult to know whether the present conditions are characteristic of the long-term behavior for just a short-term lull. With recurrence intervals in the thousands and tens of thousands of years, not much relevance can be placed on apparent inactivity at present. The presently inactive areas could "turn on" at any time thereby equalizing them with the apparently more-active areas.

Onset of Basin and Range type faulting may have begun as long as 15 to 20 million years ago (Shafiqullah et al, 1980; Martin, 1990, Muehlberger, 1988; Nations and Brumbaugh, 1992). The present fault-block basins had assumed their present form by 5 to 10 million years ago based on the nature and distribution of basin-fill deposits in Verde Valley (Section 3.c.(2)).

Most of the block-bounding faults in the northwestern part of the Arizona Mountain Zone have been active in Quaternary time, but several of those in the southeast do not show any clear signs of substantial activity in Quaternary time; this may be partly due to slow rates of activity. Where rates of erosion and deposition are greater than rates of tectonic activity, faults tend to be very obscure or buried.

The recurrence intervals between fault displacements in the Arizona Mountain Zone are long. The most recent surface displacement in the zone appears to have occurred on the Big Chino fault (#18). Trenching investigations conducted for this investigation indicated the most recent displacement was probably more than 10,000 to 15,000 years ago and suggested recurrence intervals for large events ($M > 7$) on the order of 20,000 to 30,000 years (section 3.d.(1)). The Big Chino fault has evidence of relatively regular, continuous recurrent activity in late Pleistocene time and is one of the most active faults in the state. This relatively high rate of activity seems much greater than the other faults in the zone so the Big Chino fault is designated as a separate seismic source for the probabilistic analysis. However, the late Quaternary rate of tectonic activity on the Big Chino Fault appears to have been preceded by a long period of tectonic quiescence during the middle or early Quaternary. This situation seems somewhat similar to that in the central Great Basin where faulting appears to be episodic (Section 6.c.(20)), that is, an area may experience several earthquakes within 10^3-year or 10^4-year recurrence intervals and then remain quiescent for 10^5 years.

The other major faults in the zone, the Aubrey (#9) and Verde (#22) faults, also have been active in Quaternary time; the Verde perhaps within the past 20,000 years and the Aubrey about 30,000 years before present (Section 3.d.(1)). The late Quaternary recurrence intervals for the Aubrey and Verde fault appear to be more sporadic than for the Big Chino fault. Trenching across the Aubrey fault indicated that the rupture prior to the latest event could have occurred about 200,000 years ago. This age suggests long-term average recurrence intervals greater than 100,000 years, similar to faults in the Mexico Basin and Range zone. The history of the Verde fault is not as well known but surface geomorphology suggests long recurrence intervals and sporadic activity more like the Aubrey fault rather than the Big Chino fault (Section 3.c.(3)). On the other hand, the Aubrey and Verde faults have some uncertainty on the possibility of several discrete segments and subparallel faults which might add to the seismic hazards. These other segments may be capable of generating additional earthquakes thereby decreasing the average recurrence intervals for the fault zones as a whole. Also, the possibility of episodic faulting discussed in the preceding paragraph must be considered. Because the Big Chino, Aubrey, and Verde faults appear to be larger and perhaps somewhat more active than most of the other faults in the Arizona Mountain source zone, they are considered to be discrete seismic sources each with a separate recurrence relation.

The Arizona Mountain Zone is characterized by numerous other faults that form a band of faults that extends to the southeast. These other faults are generally smaller and appear to be less active than the Aubrey, Big Chino, and Verde faults (Plate 1). With these faults considered separately,

the faulting characteristics for the Arizona Mountain seismic source zone is one of shorter, less-active features scattered throughout the province. Of these remaining faults, the Horseshoe fault (#133) might be considered one of the more active features. The Horseshoe fault experienced two faulting events within the past 300,000 years, but displacements were only about 3 feet (Piety and Anderson, 1991). Although the recurrence history is similar to the Aubrey fault, the Horseshoe fault is much smaller and characterized by smaller displacements, and hence probably is less likely to generate a large earthquake (i.e. M > 7).

The nature of many of the faults in the zone is uncertain. Of these, the Safford fault (#174) stands out. The Safford fault zone extends for almost 20 miles along the east side of the Pinaleno Mountains. It consists of two segments which appear to be discrete features. The northern segment is the most prominent feature and displaces remnants of alluvial deposits and surfaces of early and middle Pleistocene age (Morrison, 1985). The southern segment displaces highly dissected Quaternary-Tertiary age alluvial deposits. Menges and Pearthree (1983 and Machette et al (1986) assigned an age of Holocene to late Pleistocene to the latest displacement of this fault. Our analysis indicates greater ages, certainly no younger that late Pleistocene. In addition, the strong segmentation of this feature indicates that the likelihood of a long rupture associated with a large earthquake (M>7) is quite small.

The Arizona Mountain zone has been one of the most seismically active zones in the state. In total number of events, it ranks first, but a large

number of the events occurred during two swarms of small events. One swarm occurred along the Arizona-New Mexico border in 1962-1963. Although there are mines in the area where the swarm occurred, these events do not seem to be attributable to mine blasts (Racine et al, 1979). Another swarm occurred in the Mogollon Mountains of New Mexico in 1938-1939. Taggart and Baldwin (1982) analyzed the 1938-1939 swarm which consisted of over 400 events with the largest event having a magnitude larger than 5 (M_s = 5.5; mbLg = 5.1). Their analysis suggested that the swarm event represented one of the largest events in New Mexico, even larger than the 1966 Dulce, New Mexico event (M_s= 5.5; mbLg =5.1). For purposes of seismic-hazard analysis, it is common practice to consider swarm activity as one event. Considering these swarms as singular events reduces the apparent seismicity level of the Arizona Mountain seismic source zone to about the same level or a little less than the Southwestern Plateau Margin zone.

Aside from the swarm events described above, seismicity in the zone is about equally scattered throughout the zone with no clustering or correlation to specific faults. The largest earthquake probably was the 1938 event in the Mogollon Mountains of New Mexico described in the preceding paragraph. Other notable events were the 1969 event in the Globe/Miami area with a magnitude M_s = 5.1 (M_L = 4.4), and the Prescott earthquake of M_s = 5.2 (m_b = 4.9) which occurred in 1976. A focal mechanism determined for the 1976 event indicated a northwesterly trending fault with predominantly normal displacement (Eberhart-Phillips et al, 1981). This focal-mechanism solution is compatible with the orientation of faults in the region, but as is typical of the Arizona region, neither the 1976 event nor any of the other

earthquakes in the zone were associated with surface rupture or were even in close enough proximity to known faults such that they could be confidently assigned to one of them. The maximum credible earthquake for the Arizona Mountain seismic source zone (not considering the Aubrey, Big Chino, or Verde faults) is estimated to be $M_w = 6.75$. The maximum credible earthquake for the Big Chino, Aubrey, and Verde seismic sources is $M_w = 7.25$.

The tectonic regime of the zone is clearly one of extensional tectonics but the orientation of deviatoric stress is poorly known due to the paucity of seismological data and variable geologic data. So far, focal-mechanism solutions have been poorly constrained and not diagnostic. Not much confidence can be placed on the orientation of faults to determine stress directions because many of the faults may have inherited their trends from ancient basement faults (Shoemaker et al, 1978). The data basically permit interpretations of extension in E-W, NW-SE, and NE-SW directions. A general east-west orientation seems to be most compatible with the regional tectonic regime. Such a stress field should be expected to cause right normal-oblique displacement on northwest-striking faults. This style of faulting was noted in one trench across the Big Chino fault (section 3.d.(1)) but such data are too few and too localized to be conclusive.

In summary, the Arizona Mountain zone appears to be an area of active block faulting, although of slow rate, where blocks are being split off of and downfaulted from the once-continuous Colorado Plateau. Characteristics that distinguish the Arizona Mountain zone from most of the rest of the state are its higher level of seismicity, abundant Quaternary faults with

northwesterly trends, and physiography.

(2) Axial Cortez Zone

The Axial Cortez zone is within the Salton Province (Figure 23) and is discussed in Subsection 6.c.(13) to better illustrate the interrelationships between this zone and its adjacent zones.

(3) Central Colorado Plateau Zone

The Central Colorado Plateau seismic source zone consists of about 49,000 square miles in the central part of the Colorado Plateau physiographic province. This zone comprises an approximately circular area in northeastern Arizona, southeastern Utah, northwestern New Mexico, and southwestern Colorado (Figure 23). In general terms, the Colorado Plateau is highest around the perimeters and gradually decreases in elevation toward the center of the province. The Central Colorado Plateau zone comprises most of the lower central region. At a smaller scale, the flat plateau aspect is interrupted by large mesas, linear ridges, isolated buttes, and deep canyons. These features primarily are a result of erosional downcutting through flat-lying strata in response to plateau uplift. Relief throughout the zone is generally low except locally where deep canyons have been incised or intrusive igneous bodies occur. In the northern part of the zone, nearly flat-lying and generally undeformed sedimentary strata are deeply incised by the Colorado River and Green Rivers and their tributaries, resulting in the formation of randomly oriented canyons, mesas, and buttes, with local relief

exceeding 4,000 feet. In the southern portion of the province, the absence of a major drainage, coupled with the generally uniform erosion, has left a relatively flat plateau surface.

Stratigraphically, the Central Colorado Plateau zone is characterized by nearly flat-lying Paleozoic, Mesozoic, and early Cenozoic sedimentary strata, disconformably overlying Precambrian metamorphic rocks. One of the most notable aspects of the Plateau is the Mesozoic cross-bedded sandstone formations that comprise a major portion of the surficial strata. Interrupting the flat-lying aspect of the zone are isolated Tertiary intrusive igneous rocks forming prominent mountain peaks with elevations greater than 10,000 feet such as the Abajo Mountains, Navajo Mountain, La Sal Mountains, and the Hopi Buttes. These peaks are testimony to the once-greater thickness of sedimentary strata and the great amount of erosion which accompanied plateau uplift. Quaternary deposits are very limited and primarily occur as alluvium along modern stream channels, colluvium along the margins of small valleys, and as windblown dune sheets.

Structurally, the Central Plateau zone is characterized by a lack of complexity. No major Quaternary faults are known in the zone. The major structures are low-amplitude, monoclines that are generally believed to be of Laramide age (early Tertiary), and related to faults in the Precambrian basement.

Earthquakes in the Central Colorado Plateau zone are relatively infrequent and of small magnitude compared to adjacent seismic source zones.

Geologic evidence suggests that the zone has experienced only broad gentle warping since the Precambrian. Much of the seismicity is near the zone boundaries, where it is probably related to activity in the adjacent tectonically more-active zones. Dense clusters of seismic events in the northwestern part of the zone (Utah) are probably mine blasts. The natural seismic activity in the interior of the zone is minor and widely scattered.

The largest historical earthquake in the zone was the 1976 Crown Point, New Mexico event with an magnitude of 5.0 (M_L = 4.6). The focal depth of this and associated events were about 25 miles deep which is somewhat greater than earthquakes in surrounding zones indicating an unusually thick brittle crust (Dewey, 1982; Wong et al, 1984). Another significant earthquake was the 1966 Dulce, New Mexico event of m_b magnitude 5.5 (M_s = 4.6) (Herrmann and others, 1980) located along the Southern Rocky Mountains seismic zone boundary. This event is not believed to be typical of the Colorado Plateau zone but that possibility cannot be ruled out. From December 1978 to January 1980, a swarm of earthquakes was observed near Capitol Reef National Park, Utah (Humphrey and Wong, 1983). This sequence consisted of 38 events with magnitudes in the 1.0 to 3.6 range. The maximum credible earthquake for the Central Colorado Plateau seismic source zone is estimated to be M_w = 6.0.

In summary, the major difference between the Central Colorado Plateau seismic source zone and adjacent seismotectonic provinces is the zone's tectonic stability as indicated by its relatively undeformed strata; infrequent, small-magnitude earthquakes; and great thickness of underlying crust.

(4) Cerro Prieto Fault Zone

The Cerro Prieto Fault zone is within the Salton Province and is discussed in Subsection 6.c.(13) to better illustrate its inter-relationships with its adjacent provinces.

(5) Eastern Mojave Zone

The Mojave desert is divided into eastern and western seismic source zones. The Eastern Mojave zone occupies approximately 8,000 square miles in southeastern California (Figure 23). The eastern zone is differentiated from the western zone by its higher level of seismic activity and its greater number of long faults.

The Eastern Mojave zone is composed of small rugged mountain ranges separated by wide valleys and flat desert plains. Playas occupy the low parts of many plains and valleys, and alluvial fans and bajadas dominate the mountain pediments. About 75 percent of the zone lies in plains and 25 percent in mountains. The Eastern Mojave province has more-rugged mountain ranges than the Western Mojave with elevations as high as 5,500 to 6,500 feet in the northeastern part of the province, and local relief in excess of 2,000 feet. Elevations gradually diminish southeasterly with the minimum being about 1,000 feet near the southeastern edge of the zone.

Streams are very localized and generally flow only during the rainy winter months. The major stream is the Mojave River which drains northerly

from the San Bernardino Mountains into the central part of the zone near Barstow.

The mountains of the Eastern Mojave zone are principally Mesozoic granitic and late-Tertiary volcanic rocks. Precambrian and Paleozoic metamorphosed igneous and sedimentary rocks, as well as Mesozoic gabbroic rocks, are locally exposed in the mountains of the province, but typically constitute only a minor portion of the total rock mass. Small exposures of very late Tertiary and/or Quaternary basalt flows and cinder cones occur in several places (e.g. Amboy Crater, Black Mountain, Malpais Crater, Newberry Crater, Pisgah Crater).

Although the Eastern Mojave zone has a basin-and-range-type physiography, structural as well as topographic relief is small compared to the Great Basin. The northern, western, and southern boundaries are characterized by continuous mountain fronts uplifted along major faults in adjacent provinces. The eastern boundary is also marked by faulting but these faults are not continuous nor physiographically prominent. The eastern boundary is underlain by subcrustal discontinuities in the Moho (Fuis, 1982).

The major distinguishing feature of the Eastern Mojave zone is the prominence of long northwesterly trending, right-lateral, strike-slip faults, most of which have experienced displacement in Quaternary time. Strike-slip faulting was initiated in the central Mojave in the Pliocene (Dokka and Glazner, 1982). Although these strike-slip faults are long, their cumulative displacements are small, generally no more than 10 to 15 miles (Dibblee,

1980) and possibly less than 5 miles. These faults are generally terminated at both the northern and southern margin of the province by east-west trending faults.

The northeastern corner of the zone has several east-west trending small faults that do not clearly relate to the northwest-southeast trending strike-slip faults. Garfunkel (1974) considered these faults as part of a conjugate strain system. One of the four cases of historic surface rupture on faults within the province was a small left-lateral displacement along one of these faults, the Manix fault.

Regional tectonic models (Garfunkel, 1974; Cummings, 1980; Bohannon and Howell, 1982) postulate that the Mojave block is moving eastward relative to the Sierra and the California Basin and Range zones. This eastward motion appears to be a result of north-south shortening and east-west elongation made possible by slippage on the strike-slip faults, rather than by wholesale translocation of the province as a coherent block. This condition is analogous to toppling a row of books sideways on a shelf.

The Eastern Mojave zone is characterized by moderate to high seismicity. Most of the earthquakes coincide with the area transected by the long northwest-trending faults. The 1947 Manix earthquake (M = 6.2), caused surface rupture in the northeastern portion of the province on an east-west trending, short fault. Other notable events are the 1975 magnitude 5.2 Galway Lake earthquake and the 1979 magnitude 4.9 Homestead Valley-Johnson Valley earthquake, both of which were associated with ground rupture. The

great length of major faults in this province indicate that earthquakes up to about 7.5 magnitude may occur.

During review of the draft report, a sequence of earthquakes occurred in the Johnson Valley-Yucca Valley area in the southern part of the Eastern Mojave zone and the northeastern part of the Eastern Transverse Ranges zone. This sequence began with a M_L = 6.1 earthquake on April 22 of 1992 east of Desert Hot Springs. On 29 June, the M_S = 7.5 Landers earthquake occurred with a 40+ mile-long surface rupture, and was followed a couple hours later by a M_S = 6.6 event near Big Bear Lake to the west in the Eastern Transverse Ranges zone. Earthquake epicenter trends and the surface rupture associated with the Landers event extended in a northwest direction along the Johnson Valley, Homestead Valley, Emerson, and Camp Rock faults. The major activity was in the Mojave zone but some activity occurred in the Eastern Transverse Ranges. At the time of this writing there was not enough information on the depth, distribution, focal mechanism, etc. to evaluate the total impact of the event. However, the magnitudes and frequencies of these events appear typical of the characteristics of the Eastern Mojave and Eastern Transverse Ranges zones as described herein and do not appear to warrant recalculation of statistical parameters (a and b values) for the probabilistic analysis.

In summary, the Eastern Mojave zone can be distinguished from adjacent areas on the basis of its combined physiography, geologic structure, seismicity, and style of tectonic deformation. The style of faulting, represented by long strike-slip faults of small cumulative displacement is

very distinctive and is probably a local result of regional plate tectonic forces.

(6) Eastern Transverse Ranges Zone

The Eastern Transverse Range Seismic Source Zone, consisting of approximately 4,000 square miles, is located in southern California (Figure 23). The Eastern Transverse Ranges zone is characterized by east-west-trending rugged mountain ranges which make up approximately 80 percent of the province. The northern part of the province comprises the San Bernardino and Little San Bernardino mountains. Smaller ranges separated by east-west trending alluvium-filled valleys and washes make up the southern part of the province. These southern ranges include the Pinto, Eagle, Orocopia, and Chocolate mountains. Some of these ranges may have an appearance of trending northwesterly due to the linearity of the southwestern margin which is affected by the San Andreas Fault, but geologic structures within the ranges suggest internal east-west neotectonic trends.

Average elevations range from 7,000 feet in the northern portion of the province, where local relief commonly exceeds 4,000 feet, to 3,000 feet in the southern portion, where local relief is about 1,500 feet. The highest peak in southern California, San Gorgonio Mountain, rises to an elevation of 11,502 feet in the northern part of the province. Minimum elevations are less than 1,000 feet in the valleys of the southern part of the province.

Cretaceous-age granitic rocks are the dominant rock type of the Eastern Transverse Ranges. To the north, in the San Bernardino and Little San Bernardino mountains, approximately 10,000 feet of Paleozoic quartzite and carbonates overlie these crystalline basement rocks. Quaternary sediments comprise small local terrace, lake, and alluvial deposits primarily along the far northern border and within intermontane valleys. The southern mountain ranges are predominantly composed of Precambrian metamorphic and Cretaceous granitic rocks. Tertiary volcanic rocks generally overlie the crystalline basement in this region. The southern area is characterized by smaller ranges and hence has more extensive Quaternary sediments which comprise alluvium in the narrow intra-mountain valleys and washes and around the perimeter of the ranges.

The Eastern Transverse Ranges zone is characterized by complex folding and faulting. Pre-Quaternary formations are generally so complexly folded and faulted that individual folds cannot be traced from one range to the other. The mountain ranges within the province appear to have sustained severe north-south-oriented compressional stresses resulting from shearing along the San Andreas transform fault system along the southwestern margin of the province (Oakeshott, 1971). Northwest-southeast trending faults are common in the southern part of the province but the predominant neotectonic mode of faulting appears to be east-west trending reverse, strike-slip, and left-oblique-reverse faulting.

A major fault system occurs along the northern front of the zone. This fault system is a series of discontinuous reverse faults which is at least

partly responsible for the uplift of the mountains relative to the Mojave zones. Displacement of Pleistocene alluvial fans along the northern mountain front indicates young movement; however, there is no compelling evidence for Holocene activity along this fault system (Allen and Meisling, 1982, Jennings, 1975).

Major left-lateral faults in the province are the Pinto Mountain and Blue Cut faults (Hope, 1969; Dibblee, 1967). The Pinto Mountain Fault, which has the largest displacement in the province, has left-lateral-oblique displacement of about 10 miles, which occurred mostly during Quaternary time (Dibblee, 1967).

Seismicity levels are high in the Eastern Transverse Ranges zone especially in the northern portion. Most historical events occurred at focal depths of less than 12 miles. Until the June 1992 Landers-Big Bear earthquakes (see Section 6.c.(5)), the largest historical event was a magnitude 5.9 earthquake which occurred in 1949 immediately east of the Pinto Mountain Fault. The Big Bear Lake event had a magnitude of 6.6 but was not associated with a surface rupture. The earthquake sequence formed a northeast-trending zone across the dominant east-west trends. At the time of this writing, not enough details are available to fully appreciate how the Big Bear event fits into the zone's regional picture. However, such events are compatible with the characteristics of the zone and this particular event should not alter zone boundaries for the results of the probabilistic analysis.

In summary, the Eastern Transverse Ranges province is a group of east-west-trending mountains adjacent to the Pacific-North American plate boundary located on the west. The province is characterized by east-west fault trends, prominence of left-lateral-reverse faulting, high seismicity, and rugged mountain physiography. Deformation within the province may be related to geometric restrictions of motion along a bend in the plate boundary.

(7) Garlock Fault Zone

The Garlock Fault zone is an east-northeast-trending area of approximately 800 square miles, located in California, extending from the San Andreas Fault in the west to the Avawatz Mountains on the east. The Garlock Fault forms the boundary between the Tehachapi and California Basin and Range zones to the north and the Mojave zones to the south (Figure 23). The zone is primarily a narrow fault zone typified by long linear valleys and troughs occupied by intermittent lakes. The fault zone is generally no wider than 5 to 6 miles. Elevations range from more than 6,000 feet where the Garlock Fault transects the Tehachapi Mountains to less than 1,000 feet near the southern end of Death Valley. Local relief is less than 1,000 feet.

Because the Garlock Fault zone is essentially a fault zone between adjacent blocks, stratigraphy does not apply in the general sense of the word. The fault affects mostly Mesozoic granitic rocks and Quaternary alluvial deposits.

The Garlock fault is a zone of east-northeast-trending, left-lateral, strike-slip faults. Maximum displacement is estimated to be approximately 40 miles along the central reach of the fault (Davis and Burchfiel, 1973). The fault is terminated to the west by the San Andreas fault. To the east the fault merges with northwest striking faults such as the Death Valley fault zone and Quaternary faults along the eastern flank of the Avawatz Mountains. Controversy exists as to whether the Garlock fault is terminated by these faults or whether it continues eastward below the alluvium of valleys to the east. The present data seems to favor termination of the Garlock at the Avawatz Mountains, but even if the fault continues past the Avawatz Mountains, it is not active along that segment.

The Garlock fault appears to be an intracontinental transform fault which accommodates the change from the east-west extension in the California Basin and Range zone on the north to the strike-slip faulting in the Eastern Mojave zone on the south (Davis and Burchfiel, 1973). This motion may have begun as recently as about 5.5 million years ago (Carter, 1982).

Seismicity on the Garlock fault in the last 50 years has been low compared to other major faults in California; the largest event on the Garlock Fault was a magnitude 4.3 earthquake in 1974 (Astiz and Allen, 1983). The Garlock Fault can be divided into two major segments, each with small segments within, and with different seismic behavior. The 90-mile-long western segment adjacent to the Tehachapi zone has exhibited a continuous low level of seismic activity during the past 50 years and well-documented aseismic creep. In contrast, the eastern 70-mile-long segment, adjacent to

the California Basin and Range zone has had very few small earthquakes and no demonstrable creep (Astiz and Allen, 1983).

There is abundant geologic evidence of numerous large displacements along the Garlock Fault during the last 10,000 years suggesting the fault is capable of generating large earthquakes about every 1,000 ($\pm$ 500) years. The Holocene slip rate is about 7 mm/yr. The largest earthquake with this recurrence interval would be of about magnitude 7.3 on the western segment and 7.6 on the eastern segment (Astiz and Allen, 1983). A maximum credible earthquake of magnitude M_w = 7.75 is estimated for the zone.

In summary, the Garlock Fault zone is a major east-northeast striking, left-lateral, strike-slip fault which functions as a transform fault between the Tehachapi-California Basin and Range zones on the north and the Mojave zones on the south. This fault has a potential for generating a great earthquake.

(8) Imperial Fault Zone

The Imperial Fault zone is within the Salton Province and is discussed in Subsection 6.c.(13) to better illustrate the inter-relationships between this zone and its adjacent zones.

(9) Mexico Basin and Range Zone

The Mexico Basin and Range seismic source zone is located

in southeastern Arizona, southwestern New Mexico, and Mexico. In Mexico, the province borders the Sierra Madre Occidental Plateau on the north and west and extends southward to the Gulf of California south of Guaymas, Mexico. The portion of the zone within the United States occupies about 11,000 square miles.

This zone has geomorphic and structural similarities to the central Basin and Range zone and the Hurricane-Wasatch zone of Nevada and Utah in that it is typified by north-south trending, elongate ranges and valleys separated by normal faults with about 50 percent or less of its area comprising basins. In the northern portion of the province the valley floors generally are between 3,000 and 4,500 feet in elevation and the ranges reach maxima of about 9,500 to 10,000 feet; southward the elevations decrease to about 1,000 feet elevation for valleys and 7,500 feet for mountains, but the relative relief remains about the same. In Mexico the mountains are extremely rugged and typically are separated by narrow deep valleys. The part of the province in Mexico has not been studied in detail. Perhaps the most comprehensive study was that of King (1939) who clearly describes the area as one of rugged, linear, flat-topped mountains and alluvial-filled valleys, such as the Eastern and Central Longitudinal Valleys, Tecoripa Graben, and Cedros Valley. These valleys and others formed by recent normal faulting accompanied by basaltic volcanism and hot spring activity, all features typical of the Basin and Range tectonics. Faults are mostly steeply dipping normal faults along valley margins. In the northern portion of the province within the United States, the ranges are shorter and less linear than in Mexico. The northern boundary of the zone is drawn a short distance

north of the Arizona-Mexico border where the north-south oriented mountain and valley trends, as exemplified by the Baboquivari, southern Peloncillo, and Animas ranges, and their intervening valleys, give way to the northwesterly trends of the Galliuro, Pinaleno, and northern Peloncillo mountains, and where the basins have a broader, more-open, geomorphically more-mature nature.

The Mexico Basin and Range zone has two basic stratigraphic domains, the mountain blocks and the valleys. Typical of basin-and-range areas of the western United States, the mountains are composed of older complexly faulted and folded rocks overlain by only slightly deformed Tertiary volcanics. The older rocks are generally quartzite and limestone of Paleozoic and Mesozoic age intruded by plutonic rocks of early Tertiary age (King, 1939). The valley-fill sediments are Quaternary alluvial deposits underlain by late-Tertiary conglomerates. In some places, the Tertiary conglomerate is interbedded with basalts. The zone also contains Holocene and late Pleistocene basalt fields such as those in San Bernardino Valley. These occur in the valleys and near the margins of the mountains. The cinder cones of these young basalts are commonly aligned in a general north-south direction compatible with east-west extension.

The Mexico Basin and Range zone is an area of Quaternary extensional tectonics similar to the Hurricane-Wasatch zone or the central Basin and Range except that its rate of tectonism appears to be less, especially in the northern part of the province within Arizona. Evidence for the Quaternary activity comes from the youthful geomorphology, the late-Quaternary faults,

young volcanics, and historical earthquakes. As with most of the basin-and-range areas of the United States, the older rocks are complexly faulted and folded as a result of Paleozoic and Mesozoic compressional tectonic events. These older structures are transected by high-angle, basin-bounding normal faults from the most-recent extensional tectonic regime. These normal faults are long and continuous south of the international border forming a block-fault terrain typical of basin-and-range tectonics. Little is known about the age of the Quaternary displacements on faults in remote areas of Mexico. The high relief and linear mountain fronts indicate very active late-Quaternary vertical tectonics more similar to the Hurricane-Wasatch province than to the Sonoran or Arizona Mountain zones. The age of faulting is poorly documented but it clearly was active during deposition of the Bucarit formation which is similar to the Gila Conglomerate formation of Arizona. Scattered fossils indicate ages as young as Quaternary for the upper Bucarit and for the overlying younger alluvial deposits (King, 1939). These Quaternary normal faults gradually diminish in continuity northward until, in Arizona and New Mexico, the exposed traces are rarely longer than 10 to 20 miles but the continuity of the basins and ranges suggest much longer subsurface faults. None of the faults in the United States portion of the province have ruptured during historical time, but the Gillespie Mountain (#163) and Washburn Ranch (#165) had surface ruptures in the latest Pleistocene (Machette et al, 1986).

The only known Holocene surface rupture in the zone occurred on the Pitaycachi fault, just south of the border within Mexico in 1887. This event ruptured a 30- to 45-mile-long segment (Goodfellow, 1888; Sumner, 1977; Herd

and McMasters 1982; Bull and Pearthree, 1988). Although the latest rupture was recent, the recurrence interval on this fault is in excess of 100,000 years possibly 300,000 to 500,000 years (Bull and Pearthree, 1988) so it should not be expected to rupture again within the foreseeable future. However, there are other, similar faults in the province that might be capable of similar events and which presumably may be poised for rupture. In addition to the Pitaycachi fault, these other principal faults in the northern part of the province are the Cotton City, Gillespie Mountain, Peloncillo, Santa Rita, and Sierra Vista Faults. Geological and geomorphological investigations of these faults indicate long recurrence intervals typically of several tens of thousands of years to as much as a hundred thousand years or more. For example, the Santa Rita fault appears to have recurrence intervals of about 100,000 years (Pearthree and Calvo, 1987); and the Sierra Vista fault scarp appears more subdued than the Santa Rita scarp suggesting a similar recurrence (Pearthree, personal communication, 1992). In the past 20,000 years, there have been perhaps three surface ruptures events in the northern part of the Mexico Basin and Range Zone suggesting an average recurrence interval of one large event per 6000 to 7000 years within the zone.

Historical seismicity in this province has been relatively infrequent, but this could be partly a result of poor instrumental coverage of this remote area. At least three significant earthquakes occurred within the zone in historical times, in 1830, 1887, and 1923 (DuBois, 1979). The 1830 event in the southern San Pedro valley area had an intensity IX. Little is known about this event. Very little is known about the 1923 event either, but

based on the extent of damage, an event in the magnitude 5 to 6.5 range seems plausible. The 1887 event was one of the largest earthquakes to occur on the North American continent during historical time. The magnitude of the event is unknown because it occurred prior to establishment of seismographic networks, but the surface-rupture length, surface displacement, and estimated seismic moment suggest that this event was similar in size to earthquakes in the 7 to 7½ magnitude range. Dubois and Smith (1980) estimated a magnitude of M_w = 7.25. Based on the length of rupture associated with the 1887 event, the maximum credible earthquake for this source zone is estimated to be M_w = 7.5. Sporadic seismicity still occurs in the area of the Pitaycachi fault and may represent lingering aftershock activity (Wallace et al, 1988; Wallace and Pearthree, 1989). The largest of these were a magnitude 4.0 on 11 June 1988 and a 4.2 on 25 May 1989.

In summary, the Mexico Basin and Range zone is a region of extensional block faulting similar to the Central Basin and Range and the Hurricane-Wasatch zones although with a somewhat reduced rate of activity. The zone is differentiated from adjacent zones on the basis of its Quaternary faulting history and its physiography which is less mature and indicative of a higher rate of Quaternary tectonic activity than adjacent zones to the west and north.

(10) Rio Grande Rift Zone

The Rio Grande Rift zone is an elongate, north-northeast-trending region of approximately 49,700 square miles, extending for more than

700 miles through Colorado, New Mexico, and Texas (Figure 23).

The configuration of the Rio Grande Rift zone is that of a long, flat-floored, north-south trending depression bordered by mountains and mesas to the east and west. This depression extends from a narrow valley in the Colorado Rockies, through central New Mexico, and into Texas and Mexico where it opens into a broad desert plain interrupted by small scattered mountain ranges. In detail, the zone consists of several elongate, en echelon valleys with intervening linear mesas. For descriptive purposes, the province is characterized as three sections with somewhat different physiography. The northern section is the tip of the zone comprising the Arkansas graben and San Luis Valley in Colorado. The central section is set westward of the northern section in proximity to the Embudo fault and Valles Caldera. The central section is made up of several distinct. north-trending basins such as the Tularosa, Journado del Muerto, and Albuquerque basins. The southern section is largely in Mexico but includes the trans-Pecos region of Texas and the Hueco Basin, Salt Basin, and Marfa Plain. This southern section is the widest section at more than 150 miles wide.

Valley elevations in the northern portion of the zone range from approximately 7,500 to 8,000 feet above mean sea level; surrounding mountains range up to 14,000 feet near Leadville, Colorado. In the central portion of the province, elevations of the valley floors range from approximately 4,000 to 6,500 feet, with surrounding mountains as high as 11,000 feet. Valley floor elevations average 3,000 to 5,000 feet and mountains up to 6,500 feet in elevation are typical of the southern portion of the province.

A major feature of the central part of the province is Jemez Mountain, a young (Late Tertiary-Quaternary) volcanic caldera typified by conical morphology. The principal drainage in the zone is the Rio Grande River, with its headwaters originating in the Southern Rocky Mountains and discharging into the Gulf of Mexico.

Rock types in the Rio Grande Rift zone comprise two general domains: the alluvial basins overlying the downdropped structural blocks, and the Precambrian to Cenozoic rocks making up the relatively uplifted structural blocks of the mountains. In the basins, especially in the central and southern portions of the zone, there are extensive and thick deposits of younger alluvium including Miocene to Pleistocene conglomerate, sandstone, mudstone, and interbedded volcanic rock, and Quaternary sands and gravels. Thicknesses of these strata range from hundreds to about 9,000 feet (Cape et al, 1983). The Precambrian crystalline rocks in the mountains consist of thick sequences of metasedimentary and metavolcanic rocks intruded by granitic to gabbroic plutons. Paleozoic and Mesozoic marine and nonmarine sedimentary deposits overlie the Precambrian basement. The combined thickness of the Paleozoic and Mesozoic rocks has been estimated in places to be more than 7,000 feet (Cape et al, 1983).

The Rio Grande Rift appears to be a region of crustal thinning possibly accompanied by an upwelling of magma near Socorro, New Mexico (Towle, 1980). Faults in the Rio Grande Rift zone are primarily normal faults bounding tilted fault-blocks.

More than 100 normal faults of late Quaternary age are located within the Rio Grande Rift province (Nakata and others, 1982). Aeromagnetic data show that the faults are aligned with the structural grain of the basement rocks and many of the faults appear to follow the trend of Laramide, Pennsylvanian (ancestral Rocky Mountains), and possibly earlier uplifts (Cordell, 1978). These faults are due to uplift and extension which began as early as 24 to 28 million years ago. Early activity consisted of caldera formation and low-angle, large-displacement, normal faulting with associated strata-tilting and extension in an east-northeast direction. Modern rift extension characterized by high-angle faulting began about 15 million years ago (Mayer and Foland, 1991) with much of the zone's present physiography forming in latest Miocene (about 9 million years ago) and Pliocene time (Machette and Colman, 1983; Morgan and Seager, 1983). Faulting is still active and the region has a potential for destructive surface rupture but recurrence intervals are long. Typically, faults have very slow rates of slip with recurrence intervals of several tens of thousands of years (Machette, 1978; Golombek, 1981; Gonzales, 1991). There are about 10 faults in the zone with latest displacements within Holocene time (Machette and Colman, 1983).

Occurring mostly in the central and western parts of the Rio Grande Rift province, andesitic volcanism started approximately 20 to 26 million years ago and was followed by bimodal basalt-rhyolite volcanism. Although volcanic activity has been occurring since middle Tertiary time, it accelerated sharply approximately 5 million years ago (Bridwell, 1976). The

rift continues to be geologically active today as indicated by high heat flow, volcanism, and faulting.

A major geothermal anomaly with heat-flow values greater than 2.5 heat flow units coincides with the western part of the province (Reiter and others, 1975) differentiating it from bordering provinces to the west. Surface heat flow of the Rio Grande Rift is 2 to 3 times that of adjacent stable regions (Bridwell, 1976) to the east. The brittle-ductile transition may be less than 6 miles deep (Morgan and Seager, 1983).

In view of the geomorphic and geologic features indicating Holocene tectonic activity, the seismicity of the Rio Grande Rift province is surprisingly low. Historical reports of earthquakes indicate that the most seismically active segment of the Rio Grande Rift province extends southward from Albuquerque through Socorro.

Local seismograph networks in the Jemez Mountain region show frequent small-magnitude activity associated with the Nacimiento Mountains. This activity may be related to the 1966 Dulce earthquake which occurred west of the zone (Cash, 1984). The Jemez Mountains are nearly aseismic but this might be because the high temperature ductile material related to a magma body below the caldera is not brittle enough to store elastic energy (Cash, 1984).

The maximum historical earthquake within the zone was the 1931 earthquake of magnitude 6.4 near Valentine, Texas. The focal mechanism

suggests strike-slip faulting on a northwest trending fault. Historical data indicate recurrence intervals for earthquakes of magnitude 6 within the Rio Grande Rift to be about 100 years (Sanford and others, 1981, 1972). The great length of many of the late-Quaternary faults suggests that much larger earthquakes are possible, and therefore a maximum credible earthquake of about M_w = 7.75 may be more appropriate.

In summary, the Rio Grande Rift zone is differentiated on the basis of its nature as an active crustal rift zone. The zone is distinguished from adjacent provinces by this extensional mode of tectonic activity which manifests itself as a physiographic trough. Features that characterize the province include abundant late Quaternary faulting, recent volcanism, high heat flow, vertical crustal movements, shallow magma bodies, and a thin lithosphere (Cordell, 1978). The province boundaries are generally drawn at major faults identified by prominent escarpments and downdropped valley floors. The northwestern boundary of the central section is more difficult to define precisely because north-south trending normal faults occur west of the physiographic trough. The boundary is drawn to include these faults into the Rio Grande Rift zone. Although historical seismicity has been low, the faults suggest large earthquakes are probable.

(11) San Francisco Volcanic Field Zone

The San Francisco Volcanic Field seismic source zone is an elliptically shaped zone in north-central Arizona (Figure 23, Plate 1). The zone comprises about 2400 square miles of the area around the San Francisco

Peaks. The province boundaries are drawn to include the bulk of the Quaternary volcanic cones and Quaternary faults in the area (Plate 1).

The physiography of the zone includes two extremes, rugged lofty peaks and flat plains. The zone includes the major Pliocene through Quaternary volcanic cones of Bill Williams, Sitgreave, Kendrick, San Francisco Mountain Mount Humphreys Peak, and O'Leary peaks. These cones were extruded onto the flat-lying surface of the Colorado Plateau. The base level of the Plateau surface in the region is about 5000 to 6000 feet in elevation. The highest elevation occurs at Humphreys Peak which has an elevation of about 12,794 feet.

The zone is made up, primarily, of two basic rock groups. The plains are composed of upper Paleozoic and Mesozoic sedimentary rocks and the mountains are composed of bimodal volcanic rocks. The larger peaks are rhyolites and andesites and the smaller peaks are mostly basaltic cinder cones. The young volcanic peaks overlie older Miocene volcanic rocks.

The zone is one of the more poorly defined zones in the state; it is distinguished primarily by its young volcanic rocks, abundant Quaternary faults, and relatively high rate of earthquake activity. In general, the zone is similar to some adjacent zones but a point by point comparison illustrates the differences. For example, the Central Colorado Plateau zone in the northeast has similar rock types but is relatively free of faults, late-Quaternary volcanics, and moderate-magnitude earthquakes. The Arizona Mountain zone to the south does not exhibit the profuse late-Quaternary

volcanism, has fewer and more-widely spaced young faults, but similar levels of historical seismicity. The San Francisco Volcanic Field zone is quite similar to the Southwestern Plateau Margin zone which borders the zone on the northwest and southeast. The differentiating factor is the great abundance of Quaternary faults in the San Francisco Volcanic Field zone and the young volcanism. The Southeastern Plateau Margin zone has young volcanics but far fewer known young faults and earthquakes.

The major fault in the zone is the Mesa Butte fault system. The Mesa Butte fault system was examined in detail and is discussed in Section 3.c.(2). The Mesa Butte fault system, like most of the faults in northwestern Arizona, is part of an orthogonal pattern of intersecting normal faults. The longest, and one of the youngest faults in the system is the northeast-striking Mesa Butte fault (#104) (Figure 4 and Plate 1). Most of the faults in the Mesa Butte system have been active in Quaternary time with the most robust activity occurring in middle Pleistocene time, (1 m.y. to 200,000 yrs B.P.) approximately coincident with the profuse volcanic activity in the San Francisco Mountain area (see Section 3.c.(1)). The main fault, the Mesa Butte fault extends southwesterly under the young volcanic flows surrounding Humphreys Peak. The Williams fault (# 117), which extends southwesterly from below young volcanics on the southwest side of the volcanic pile, may be the southwesterly extension of the Mesa Butte fault (Shoemaker et al, 1978; Wolfe et al, 1987; Holm and Ulrich, 1987).

The San Francisco Volcanic Field seismic source zone may have been the locus of the most frequent moderate-magnitude historical earthquake activity

in the State of Arizona (Figure 26). At least three and perhaps four magnitude 5 to 6+ earthquakes have emanated from the zone. A magnitude 5.0 event occurred near Flagstaff in 1959. The other events occurred in the early part of the century before local seismographic networks were in operation so their magnitudes and locations are uncertain. Three events had Modified Mercalli intensities of VII. Various investigators have assigned magnitudes to these events based on the conversion of the intensity data. Brumbaugh (1991) reanalyzed old seismograph records and estimated the magnitudes as follows:

1906 M_s = 5.8, M_L = 6.2

1910 M_s = 5.6, M_L = 6.0

1912 M_s = 6.1, M_L = 6.2

Both the 1906 and 1910 events are believed to have occurred in the area north of the San Francisco Peaks but there is no evidence of modern surface faulting in the area (Section 3.c.(2)). The 1912 event may have occurred in proximity to the San Francisco Field (DuBois et al, 1982) or much farther north in the Marble Canyon Area (Brumbaugh, 1992). Including these events within the San Francisco Volcanic field zone results in somewhat higher probabilistic ground motions in this area than would result from distributing these events across the northern part of the state. The maximum credible earthquake for this zone is estimated to be M_w = 7.0 but such events would be very infrequent (Section 7).

Few focal-mechanism solutions have been determined for earthquakes in this zone. A solution for the M_L = 3.7 event near Williams in 1971 indicated reverse faulting on a northwest-striking high-angle fault (Brumbaugh, 1980).

In summary, the San Francisco Volcanic Field zone is an area characterized by abundant Quaternary faults and young volcanism, and has been one of the most seismically active zones in the state of Arizona.

(12) Salton Periphery Zone

The Salton Periphery zone is within the Salton Province and is discussed below in Subsection 6.c.(13) to better illustrate the interrelationships between this zone and its adjacent zones.

(13) Salton Province

The Salton Province comprises several seismic source zones in southeastern California and Mexico. These source zones are the San Jacinto, Southern San Andreas, Imperial, Whittier-Elsinore, Perris, Cerro Prieto, Axial Cortez, and the Salton Periphery (Figure 23). For convenience all of these source zones are described together under this heading. However, for the seismic hazard analysis, these zones are considered discrete seismic sources, each with its own recurrence relations (Table 1). In the following discussion, the term Salton Province is used when referring collectively to all the seismic sources.

Within the United States, the Salton province has a width of about 140 miles and a length of about 180 miles. The province widens southward into Mexico. The Salton Province is defined primarily on the basis of its similar tectonic elements. The physiography is quite variable and not really

characteristic except that the province is lower in elevation basically because it is a zone of crustal foundering along the North America/Pacific Plate boundary. The province takes its name from the southern part of the province which is a broad, flat-floored, tectonic depression occupied by the Salton Sea. The Salton Province is bounded on both margins by linear mountain fronts which include the San Bernardino, Little San Bernardino, and Chocolate mountains on the northeast side, and the Santa Ana, Laguna, and Sierra Juarez mountains on the southwest. Southward the Province widens and deepens into the marine basin called the Gulf of California or Sea of Cortez. The central part of the Province in the U.S. is below sea level but is protected from inundation by sea water by alluvial and deltaic sediments of the Colorado River which have accumulated at the head of the Gulf of California, over a crustal upwarp. In the north, the Province narrows into the Coachella Valley and several other narrow, linear fault-controlled valleys between rugged, northwest-trending, subparallel mountain ranges such as the San Jacinto and Santa Rosa mountains. These intervening mountains are topographically high with Mount San Jacinto being the highest at 10,804 feet elevation. The northern boundary of the province coincides with the east-west trending San Gabriel and San Bernardino valleys which lie at the base of the east-west trending Western Transverse Ranges.

The Salton Province contains two basic groups of rocks: the alluvium which fills the subsiding troughs and valleys, and the granitic and metamorphic rocks which make up the mountains. Other minor strata include Mesozoic sedimentary rocks which overlie the crystalline rocks in places. The zone has three late-Quaternary volcanic centers; Obsidian Buttes at the

south end of the Salton Sea, Cerro Prieto south of the international border, and Sierra Pinacate along the province boundary in Arizona and Mexico.

The salient aspect of the Salton Province regarding seismic hazards analysis is its long faults with high rates of seismic activity. The Province is the boundary between the North American and Pacific lithospheric plates and is one of the most seismically active regions in the world. The Province contains several tectonic subdomains which are considered to be separate seismic source zones in this analysis because each may make somewhat different contributions to the overall seismic hazard in Arizona. These tectonic domains are:

- major right-lateral, strike-slip faults such as the San Andreas, San Jacinto, Whittier-Elsinore, Imperial, and Cerro Prieto fault zones;

- the axial rift which comprises numerous, short, crustal spreading centers and transform faults below the Sea of Cortez in the central Gulf of California; and

- peripheral zones of primarily normal or normal-oblique faulting such as the Algodones fault at the eastern edge of the province and the Sierra Juarez and San Pedro Martir faults at the southwestern edge of the province in Mexico.

The bulk of historical seismicity in the Salton province occurs in proximity to the San Jacinto, Imperial, Cerro Prieto and Axial Rift source zones. The Salton Periphery source zone provides significant background seismicity from secondary crustal adjustments. Earthquakes on the Southern San Andreas fault are rare compared to the San Jacinto and Imperial faults indicating that most of the historical plate motion has occurred along the central faults of the province or is stored as elastic strain in the adjacent crust. Although the San Andreas fault has not experienced much seismicity, it has much more cumulative displacement than the San Jacinto-Imperial fault system (about 180 miles vs 15 miles) since inception of the present tectonic regime in Miocene time. Very little plate motion is occurring on the Elsinore fault as indicated by geodetic data (Prescott et al, 1982), by geologic data which shows that cumulative displacements are small compared to the San Andreas and San Jacinto faults, and by a relatively low level of earthquake activity.

Seismicity within the Salton province is most intense in the central portion of the province coincident with the San Jacinto and Imperial faults. Fifteen of the historical earthquakes occurring on the San Jacinto-Imperial fault system have exceeded magnitude 6.0, with the largest being the events in 1934 and 1940 with magnitudes of about 7.0 or 7.1 (Hileman et al, 1973; Coffman and Von Hake, 1973). Earthquakes along the southern San Andreas fault zone have been rare. Moderate-magnitude events occurred on the Banning splay in 1948 and 1986. Small earthquakes occur along the Elsinore fault with the largest being the poorly located 1910 earthquake (M=6). During the late 1970s and early 80s numerous small earthquakes occurred at the south end

of the Salton Sea in the vicinity of the subsurface Brawley and Calipatria faults and in the area between the Imperial fault and the southern end of the San Andreas fault. This activity led to speculation that strain was accumulating on the San Andreas. Small events directly south of the San Andreas fault formed a linear trend suggesting that the San Andreas fault continues southeasterly in the subsurface. However, a focal-mechanism solution (Johnson, 1980) indicated normal faulting with a tensional axis oriented east-west suggesting a normal and/or oblique-normal style of tectonism in the Salton Periphery zone which is consistent with gravity data that indicates subsurface fault blocks below the region.

Like historical seismicity, historical surface faulting has been concentrated along the San Jacinto-Imperial fault system with surface ruptures occurring in 1940, 1968, 1979, and 1987. Geologic data indicates a slip rate of up to 10 millimeters per year on the San Jacinto fault zone. Although there is no historical evidence of major activity on the Southern San Andreas fault, trenching studies near Indio have shown recurrent prehistoric earthquakes. However, these studies also show a decrease in the size of earthquakes and the rate of slip over the past thousand years (Williams and Sieh, 1987). These decreases combined with the present low level of seismicity suggest that the role as major plate-bounding fault may have passed or is passing from the San Andreas to the San Jacinto-Imperial fault system. On the other hand, the time interval since the last surface-rupturing event is only 312 years which is not an unreasonable length between major events compared to other segments of the San Andreas (Sieh et al, 1989). Considering that the recent record may be too short to provide a true

picture San Andreas fault activity, the possibility that the fault may just be storing up energy for the next big earthquake must be given strong consideration. The Working Group on California Earthquake Probabilities (1988) assumed an average recurrence interval of 220 years for the Coachella Valley segment of the San Andreas fault and estimated a 40 percent chance of a M = 8 earthquake in the following 30 years.

For this analysis a maximum credible earthquake of M_w = 8.0 was considered on the San Andreas fault, a M_w = 7.5 for the San Jacinto and Axial Cortez zone, and an M_w = 7.25 for the Imperial and Cerro Prieto faults. The MCE for the Salton Periphery zone is estimated to be about M_w = 6.75.

In summary, the Salton Province comprises several seismic sources making up the boundary between the Pacific and North American plates. The plates are being rifted apart in the Gulf of California, causing the Baja Peninsula to drift northwesterly relative to Arizona. The Salton Trough represents the landward continuation of the rift zone. As the Pacific plate pulls away from the continent, crustal blocks subside and molten material fills the voids with some escaping to the surface. Along with this subsidence, crustal blocks slip laterally or obliquely past one another on the major faults generating large frequent earthquakes. The major sources of the large earthquakes are the San Jacinto, Imperial, and San Andreas faults. Smaller earthquakes emanate from secondary faults, primarily normal or normal-oblique type faults, in the peripheral zones.

(14) San Jacinto Fault Zone

The San Jacinto Fault zone is within the Salton Province and is discussed in Subsection 6.c.(13) to better illustrate the interrelationships between this zone and its adjacent zones.

(15) Sonoran Zone

The Sonoran seismic source zone encompasses approximately 58,900 square miles in southwestern Arizona, southeastern California, and Mexico (Figure 23). The Sonoran zone is characterized by small, scattered mountain ranges and large flat plains and valleys. Some of these ranges and valleys are locally aligned but overall the province has no preferred directional trends. Mountains constitute approximately 20 percent of the total area of the province and are generally surrounded by broad pediments indicating relative geomorphic maturity. Elevations range from approximately 500 to 1,500 feet in the valleys to about 3,000 to 4,000 feet in the mountainous areas. Generally, local relief rarely exceeds 2,500 feet and is generally about 1,000 to 2,000 feet.

Drainage is largely through-going except in some valleys in the northern part of the zone near the boundaries with the Mojave, Eastern Transverse Ranges, and Southern Nevada zones. The major streams are the Gila and Colorado rivers which drain through the province from the Colorado Plateau and Arizona Mountain zones in the northeast. Most other streams are

intermittent and flow only during rainy periods. Sporadic rainfall and resultant flash flooding is a principal mechanism of erosion.

The Sonoran zone has two primary stratigraphic domains, the mountains which are comprised of well-indurated rocks, and the plains or valleys which are underlain by thick deposits of alluvium. The major rock types of the mountains are Precambrian metamorphic and intrusive rocks, and Mesozoic and Tertiary volcanic rocks. Mesozoic metamorphic rocks also crop out in numerous mountain blocks. Late Tertiary volcanic flows commonly cap the ranges forming mesas. The valleys are generally underlain by Quaternary alluvial fan and bolson deposits. These in turn are underlain by Tertiary alluvial deposits that are similar to the Quaternary units but which also include lake deposits from the previous basin-and-range tectonic regime.

A relatively young volcanic field, the Sentinel-Arlington field, has been extruded onto alluvial deposits in the center of the zone. This complex, is chiefly a low-lying Pliocene extrusion. The Pinacate field is a late Pleistocene extrusive vent complex straddling the boundary with the Salton Trough Province.

Although gravity and magnetics do not reveal much about the present degree of tectonic activity, they do help establish the limits of the Sonoran zone. The gravity (West and Sumner, 1973) and magnetic (Sauk and Sumner, 1970) patterns within Arizona show low-amplitude, randomly oriented anomalies in the southwestern part of the state and Sonora, Mexico compared to high amplitude and more-linear patterns in northeastern and southeastern Arizona.

The southwestern edge of the Sonoran zone is marked by linear gravity anomalies identifying the buried boundary of the Salton Trough. Changes in gravity between the northern part of the province and the Great Basin (Eaton et al, 1978) are equally dramatic, but occur over a much broader zone.

The thickness of the brittle seismogenic crust of the Sonoran zone ranges from about 7.5 to 10 miles (Warren, 1969) gradually increasing in thickness northeasterly from the Gulf of California where active rifting occurs and the crust is very thin.

Geodetic data also indicate that the Sonoran province is tectonically stable compared to the tectonically active regions in California (Burford and Gilmore, 1982). The geomorphology of river terraces along the Colorado and Gila Rivers provides longer term verification of this tectonic stability (Schell and Wilson, 1982; Arizona Public Service Company, 1974) indicating no substantial crustal warping during late Quaternary time.

Although the Sonoran zone exhibits basin-and-range-type geologic structure, it has not experienced extensive block-faulting typical of that tectonic regime since Pliocene and possibly late Miocene time (Schell and Wilson, 1982; Menges, 1983). Presently the zone has very little tectonic activity. Earthquakes are rare and of small magnitude (Figure 26) and faults are very minor (Plate 1). The Sonoran zone is relatively aseismic compared to adjacent zones to the northeast and southwest. Seismicity maps show a few small events many of which are in the southwestern part of the province near the Pinacate volcanic field. Detailed examinations of seismograms suggests

that most of these events are probably mislocated and really occurred in the Salton Trough province or were associated with volcanic activity in the Pinacate Field (Schell and Wilson, 1982; Mokhtar, 1979; Arizona Public Service Company, 1974; Brumbaugh, 1992, personal communication). The largest historical earthquake within the Sonoran zone was the magnitude 5.0 event which occurred in the southern part of the province in 1956. Reanalysis of seismogram records discussed by Arizona Public Service Company (1974) suggested that this event should be relocated to the northeast about 40 miles. Brumbaugh's reanalysis (1992) relocated the event about 100 miles to the southeast into Mexico. The maximum credible earthquake is estimated to be magnitude M_w = 6.5 although events this large should be exceeding rare.

In this vast zone there are only a few young faults and these are very minor features. Except for the Sand Tank fault (#36), most of these faults are in proximity to the Colorado River Trough near Blythe, (#33), Needles (#35), and Topock (#34). These faults are short (2 to 8 miles) and discontinuous with low, subtle scarps indicating low rates of activity and small-magnitude earthquakes. For determining the zone recurrence interval in this analysis, earthquakes of magnitude 6 were assumed to have been associated with these surface ruptures. The age of these events are poorly constrained but they appear to have occurred over the latter part of the Quaternary. Assuming that they occurred within the past 10^5 years, the average recurrence for the zone as a whole would be about 1 event every 25,000 years. In addition to such events associated with surface rupture, similar recurrences should be expected for random events.

In summary, the Sonoran zone represents a nearly stable block between tectonically active regions to the northeast and southwest. The zone can be distinguished by its paucity of earthquakes, few short Quaternary faults, mature physiography, thin crust, gravity anomalies, and magnetic trends.

(16) Southern San Andreas Fault Zone

The Southern San Andreas Fault zone is within the Salton Province and is discussed above in subsection 6.c.(13) to better illustrate the interrelationships between this zone and its adjacent zones.

(17) Southeastern Plateau Margin Zone

The Southeastern and Southwestern Plateau Margin seismic source zones form an arcuate belt around the southern margin of the Colorado Plateau from the Hurricane-Wasatch zone to the Rio Grande Rift (Figure 23). In overview, the marginal belt is a relatively flat-lying region with several high-standing young volcanic peaks. The division of the belt into two seismic source zones, the Southwestern zone and the Southeastern zone, was based primarily on the higher level of seismic activity and the greater number of Quaternary faults found in the Southwestern zone (see Subsection 6.c.(18) below).

The zone is characterized by two extremes in topography, flat plains and rugged mountains. The plains comprise the gently ascending Colorado Plateau surface which rises from about 5000 to 6000 feet along the northern

boundary of the zone to about 7000 to 8000 feet along the Mogollon Rim near the southern boundary. The mountains of the zone generally peak in the 9000 to 10,000 feet range but two peaks, Mount Baldy in Arizona and Mount Taylor in New Mexico exceed 11,000 feet in elevation.

Rocks within the zone comprise two general groups, upper Paleozoic-Mesozoic sedimentary rocks and late Tertiary-Quaternary volcanic rocks. The volcanics occur in three major fields, the Springerville, Zuni-Bandera, and Mount Taylor fields. Similar to the Southwestern Plateau Margin, faults in this zone form an intersecting pattern of northeast and northwesterly trending faults. Not many Quaternary faults are known in the zone (Plate 1). This might be partly due to some faults being covered by the voluminous Quaternary volcanic flows of the zone. The abundance of young basaltic volcanic activity suggests that conduits to the mantle have been opened by extensional breakup of the southern margin of the Colorado Plateau.

Historical seismicity within the zone has been low to moderate (Figure 26). The epicenters are most dense in the New Mexico part of the zone and are most abundant close to the Rio Grande Rift. All of the historical seismicity has been of small magnitude; there have been no earthquakes with magnitudes in excess of magnitude 5. The maximum credible earthquake is estimated to be $M_w = 6.5$.

In summary, the Southeastern Plateau Margin zone is characterized by young volcanic activity, a low to moderate level of seismicity, and a few Quaternary faults. These characteristics suggest the zone plays a similar

role as the Southwestern Plateau Margin, but at a lower level of activity, in the extensional breakup of the southern Colorado Plateau margin.

(18) Southwestern Plateau Margin Zone

The base elevations in the Southwestern Plateau Margin zone are fairly constant and range from about 5000 to 6000 feet along the northern boundary to 6000 to 7500 feet along the southern boundary. Although relief is generally very low, the zone is crossed by the Colorado River and contains the Grand Canyon where relief between the river level and the Kaibab Plateau can be more than 5000 feet. The southern margin of the zone is near the Mogollon Rim, a prominent escarpment marking the edge of the Colorado Plateau physiographic province. The northern boundary of the zone merges with the Hurricane-Wasatch zone in Utah (Figure 23) marking the northern extent of abundant neotectonic faults along the Plateau margin.

The rocks of the zone primarily comprise upper Paleozoic and lower Mesozoic sedimentary rocks and volcanics which are of predominantly Pliocene-Pleistocene age.

The Southwestern Plateau Margin zone has numerous neotectonic faults (Plate 1). These faults comprise numerous minor features of short length to several major lengthy faults all with relatively small displacements. Faults form a prominent orthogonal pattern with the vast majority of the faults striking either northeast or northwest. The northeast trending faults appear to be dominant. The largest of these are the Sinyala-West Kaibab system (#

3) and the Bright Angel system (# 42). The northwesterly trending faults are generally shorter and more discontinuous. The most prominent of these is the Cataract Creek system (# 44).

The faults of the zone are enigmatic in that in spite of their prominence and great lengths, they have relatively minor displacements. For example, the Sinyala fault is about 34 miles long and has only about 15 feet of total displacement. Such a displacement could represent only one surface rupture. Many of the faults in the northern part of the zone, near the Utah border (Plate 1),are minor fractures that look more like joints than faults.

The age of the faults is also an enigma. Because most of the surficial strata are of great age (200 million years) and there are no overlying young strata, it is difficult to determine the age of faulting and hence the rates of displacement. In most cases all that is known is that they were active sometime within the past 200 million years. Analysis of the faults in the Mesa Butte area revealed that faults in that area are indeed of Quaternary age, although with very slow rates of activity (see Section 3.c.(2)), and by analogy, other faults around the southwestern plateau margin with similar geomorphic development are also considered to be of Quaternary age.

The Southwestern Plateau Margin seismic source zone has been one of the more seismically active Arizona zones in historical time with about the same number of earthquakes as the Arizona Mountain zone (Figure 26). The largest instrumentally recorded event was the 1959 Fredonia earthquake of M_L = 5.5 to

5.6 (Brumbaugh, 1992; Stover et al, 1986). Another notable event occurred in 1912 somewhere near the Grand Canyon or Marble Canyon before local seismographic networks were in operation so its magnitude and location are uncertain. This event had Modified Mercalli intensities of VII. Brumbaugh's (1991) reanalysis of old seismograph records resulted in a magnitude estimate of M_s = 6.1, M_L = 6.2. DuBois et al (1982) indicate a location just north of the San Francisco volcanic field. Stover et al (1986) mention the possibility of surface rupture associated with the event. Brumbaugh (1992) locates the event east of Marble Canyon in the Central Colorado Plateau Seismic Source zone. Due to the poor location control, the possibility that the event could have been associated with the San Francisco Volcanic Field zone was considered. There is no evidence of modern surface faulting in either the San Francisco Volcanic zone or the Southwestern Plateau Margin zone area. The maximum credible earthquake is estimated to be about M_w = 6.5.

In summary, the Southwestern Plateau Margin seismic source zone is characterized by low-activity Quaternary faults and moderate seismicity. It is differentiated from the Arizona Mountain zone by its physiography and lower rate of faulting activity, and from the Southeastern Plateau Margin zone by its higher seismicity and more-numerous neotectonic faults.

(19) Southern Hurricane-Wasatch Zone

The Hurricane-Wasatch seismic source zone is an elongate, north-northeasterly to north trending zone of approximately 43,300 square miles extending northerly from the northwest corner of Arizona through

central Utah into western Wyoming and southeastern Idaho. Figure 23 shows only the southern part of this zone that was considered in this analysis. The seismic hazard to the north is considerably greater due to the highly active Wasatch Front fault system. However, that fault is too distant to impact Arizona so this analysis only considered the southern part of the zone. The following description also includes the Hurricane and Toroweap faults which occur within the zone but are considered to be discrete seismic sources because they are larger that the typical faults in the zone. They are described here to better illustrate the inter-relationships of all the tectonic elements in the region.

The physiography of the Hurricane-Wasatch province is typified by closely spaced linear ranges and valleys which are a result of late-Cenozoic block faulting. Due to its great length, the zone is best described as three sub areas: the northern area north of the Unita Mountains in Utah and Wyoming (not important to this evaluation); the central portion between the Unita Mountains and Zion Canyon areas; and the southern area.

The Central Hurricane-Wasatch seismic source zone is characterized by a well-developed series of closely spaced, linear, north- to northeast-trending ranges and valleys. The ranges are generally flat-topped and appear to be pieces of the Colorado Plateau that have been uplifted and have drifted away from the main part of the Plateau. Typical ranges are the Sevier, Pavant, Aquarius, and Wasatch plateaus. These plateaus are separated from each other by narrow, linear valleys such as Sevier, San Pitch, Joes, and Long valleys. The eastern boundary is clearly defined by a drop in elevation

and change in physiography to the wide, open, deserts and broad swells of the Central Colorado Plateau.

To the south, in the southern Hurricane-Wasatch seismic source zone, the relief between the plateaus and the valleys is not as dramatic and the physiography is more like a broad staircase of easterly tilted blocks. Here, the principal plateaus are the Shivwitz, Uinkaret, Kanab, and Paunsagunt plateaus. Typical valleys are Mainstreet, Prospect, Tuweep, and Antelope valleys. The western boundary is in proximity to Grand Wash Cliffs and the eastern boundary along the eastern edge of the Paunsagunt and Kanab Plateaus.

The stratigraphy of the Hurricane-Wasatch province is difficult to generalize because of the zone's great length. The strata are generally similar to those in the adjacent central Basin and Range and Central Colorado Plateau zones. In the south, the rocks are primarily Paleozoic and Mesozoic sedimentary rocks which are locally overlain by late Tertiary and Quaternary volcanics such as the Grand Wash and Uinkaret volcanic fields. The Uinkaret/Toroweap volcanic field has about 150 cinder cones and numerous flows generally younger than a million years.

Structurally, the Hurricane-Wasatch zone is characterized by long, north-northeasterly striking, potentially active, normal faults. Major faults are the Hurricane, Wasatch, Toroweap, and Sevier faults. These and other normal faults form a series of tilt blocks between the Colorado Plateau and the central Basin and Range provinces. The Hurricane and Toroweap faults are the major active faults in the southern part of the zone and the ones of

most concern for the Arizona area. The Hurricane fault extends for 160 miles from north of Cedar City, Utah to the Peach Springs area of northern Arizona. The average trend of the fault is north-south but closer inspection reveals that the fault is composed of northeast and northwest striking segments which is characteristic of most faults in the zone, and is believed to be controlled by ancient basement faults (Shoemaker et al, 1978). The Toroweap fault appears to merge with the Sevier fault in Utah for a combined length of about 250 miles. Although the total lengths of the Hurricane and Toroweap-Sevier faults are great, their segmented nature makes it unlikely that the entire lengths will rupture during one event. The geologic record indicates temporal and spatial, episodic, irregular, rupture processes. Structural and geomorphic relationships suggest that faulting began more recently (Pliocene or Pleistocene) in the southern part of the zone (Anderson and Mehnert, 1979).

Although there have been no large earthquakes or surface ruptures along any of the major faults in historical time, numerous large displacements of Quaternary deposits indicate that these faults are capable of generating major earthquakes. The Wasatch fault appears to be the most active fault with recurrence intervals ranging from about 1,000 to about 5,000 years on the various segments and an average recurrence interval of about 340 to 415 years for the composite fault (Machette et al, 1989; Hecker, 1992). The faults have smaller displacements and become less active to the south (Hamblin, 1965; Anderson and Christenson, 1989). The most active faults in the south are the Hurricane and Toroweap faults. Although there are abundant geological data on Quaternary activity for the Hurricane fault compared to

most faults in Arizona, conclusive data on recurrence intervals are scarce and recurrence intervals have wide ranges and uncertainties. Synthesis of data collected by several investigators (for example, Anderson and Christenson, 1989; Hecker, 1992; Jackson, 1990; Hamblin et al, 1981) suggest that late-Quaternary recurrence intervals for large, surface-rupturing events are in the 5,000 to 20,000 year range for the Hurricane fault and about 15,000 to 20,000 year range for the Toroweap fault (see detailed discussion in Section 7.b.(1)).

The Hurricane-Wasatch zone is similar to the California Basin and Range zone along the western margin of the Basin and Range province. Both of these zones have long faults, relatively high seismicity, and young volcanism as well as thinner crust and higher heat flow than adjacent provinces. The level of seismicity in the Hurricane-Wasatch zone is among the highest outside of California and includes most of the earthquakes referred to as the Intermountain Seismic Belt (ISB) by Smith and Sbar (1974). The ISB extends from Montana to southern Utah where it splits, one branch extending southwesterly into southern Nevada and the other southeasterly into Arizona (i.e. into the Arizona Mountain and plateau margin seismic source zones). In historical times earthquakes within the zone have been mostly of small magnitude. The largest historical earthquake in the southern part of the zone was probably the 13 November 1901 event near Richfield, Utah which had a Modified Mercalli Intensity of VIII (Coffman and Von Hake, 1973). Although no magnitude was assigned at the time of the event, the magnitude is estimated to have been about 6.5 (Arabasz et al, 1979).

During final preparation of this report (2 September 1992) a magnitude 5.9 (mb = 5.5) earthquake struck the Arizona-Utah boarder area. This event was close to the Washington Fault (#6) and Hurricane Fault (#1) but at the time of this writing not enough information is available to completely assess the event. However, the location and magnitude are typical for the Southern Hurricane-Wasatch seismic source zone as already described herein, and the event does not alter the probability analysis.

The maximum credible earthquake for this seismic source zone is estimated to be a magnitude M_w = 7.75 based on empirical fault/earthquake-magnitude relationships of Slemmons (1982), Bonilla et al (1984), and Wyss (1979). Focal-mechanism solutions indicate a general east-west directed extensional stress field throughout the zone (Smith and Lindh, 1978) but definite data are scarce in the southern part of the zone.

In summary, the Hurricane-Wasatch zone is a transition zone from the relatively stable provinces to the east and the tectonically active central Great Basin province to the west. The zone is differentiated primarily by its potential for more-frequent large earthquakes than adjacent provinces. This zone is one of the most active seismotectonic zones in the western United States as indicated by its high rate of seismic activity; very young, closely spaced, normal faults of great length; and young volcanic activity. However, both the historical seismicity and the capability to generate frequent large earthquakes decrease southward. Geologic data indicate that the recurrence intervals for large earthquakes are about an order of magnitude less in the southern part of the province than in the central.

(20) Southern Nevada Basin and Range Zone

The Southern Nevada seismic source zone is a triangular area of approximately 22,600 square miles, located primarily in southern Nevada, but extending slightly into southern Utah and southeastern California (Figure 23). Rugged mountains with intervening areas of relatively low elevation and flat desert topography characterize the southern Nevada zone. Elongate north-trending and slightly arcuate mountain ranges with elevations of about 7000 to 8000 feet and valleys near 4500 feet characterize the eastern portion of the province. To the west, the topography is slightly less rugged, and Tertiary volcanic rocks form more subdued, less-elongate, and often flat-topped mountain ranges. As a whole, the physiographic trends in this zone are more randomly arranged than in the Central Basin and Range province. Valleys in the western portion of the province, such as Sarcobatus Flat and the Amargosa Desert, are broad open valleys oriented northwesterly which is more similar to trends in the Walker Lane zone to the north. Well-developed playas occupy many of the valley floors in the zone.

As with most basin-and-range type areas, the stratigraphy of the Southern Nevada zone can be subdivided into two major domains: the mountain ranges and the valleys. The rock and sediment types are very similar to those in the Central Basin and Range province, but there is a marked decrease in volcanics which are usually found capping the ranges to the north. The mountain ranges on the eastern side of the province are characterized by Precambrian and Paleozoic sedimentary rocks overlain by Mesozoic sedimentary rocks. Quaternary alluvium covers most of the valley floors throughout the

zone generally forming alluvial fans around the margins of the valleys and desert playas in the central basins. A major unit underlying the Quaternary alluvium in the valleys is the Muddy Creek Formation. This formation is composed of late Miocene alluvium. Over much of the eastern part of the zone, the valleys are underlain by a hard Pliocene-Pleistocene carbonate-rich caprock known as the Mormon Mesa caprock. The hardness of this unit may enhance fault-scarp preservation making them appear younger than they really are (Dohrenwend et al, 1992).

The structure of the Southern Nevada zone is similar to the typical basin-and-range-type, extensional, fault-block regime. Typically, the basin-and-range structure comprises long, linear, northerly-oriented, subparallel, mountain ranges and valleys separated by normal faults. These fault blocks generally are asymmetrical with a major normal fault and steep mountain front on one side of the valley, and minor antithetic faults on the other side. The density and orientation of young faulting varies widely within the zone (Dohrenwend et al, 1992). Two of the major departures from the typical regime are the northwesterly trending faults in the western part of the province, such as the Las Vegas Valley Shear Zone described by Longwell (1960), and northeasterly trending faults in the eastern part of the province, such as the Lake Mead Shear Zone described by Bohannon (1979). Both of these structural zones were active, perhaps as shear zones, in Miocene time (more than 10 million years ago) under previous tectonic regimes and are no longer active. The abundance of northeasterly and northwesterly trending faults appears to represent a continuation of the orthogonal fault pattern common in northwestern Arizona. One of the most prominent of these

features is the Pahranagat Shear Zone (#74) which is primarily a tertiary feature, but which may have experienced some minor late-Quaternary tectonic activity.

The Southern Nevada zone is obvious on seismicity maps because of its abundant seismicity. However, much of the seismic activity is artificially induced. The seismicity appears to be a southwesterly branch of the Intermountain Seismic Belt (ISB). The northern portion of the zone is characterized by a belt of seismicity that extends approximately east-west subparallel to the northern province boundary. Toward the western end of this belt is a dense cluster of seismic events around the Nevada Test Site. These events are largely the result of nuclear testing and crustal adjustments following test explosions (Rogers, 1977). Nuclear blasts can usually be differentiated from natural earthquakes by their expression on seismograms and by their regular time of occurrence. Most nuclear blasts are detonated on the hour. However, it is virtually impossible or very difficult to distinguish between small natural earthquakes and small post-blast adjustments induced by stresses incurred during the blasting. At least some of the seismicity in this northwestern area may be of tectonic origin. Another cluster of seismic events is located near Lake Mead at the southern boundary of the zone. These events are predominantly reservoir-induced events related to impoundment of Lake Mead behind Boulder Dam (Rogers and Lee, 1976).

Although much of the seismicity is artificially induced, the province still appears to be more seismically active than the Central Great Basin

province to the north and the Sonoran zone to the south. The largest historical seismic event in this source zone is the magnitude 6.1 earthquake which occurred in 1966 in the Clover Mountains near the Utah-Nevada border. A cluster of small earthquakes (maximum magnitude 3.9) occurred in eastern part of the zone in the vicinity of the Pahranagat Shear Zone in 1979, but it is not clear whether this activity was associated with the young north-south-trending normal faults or with the older northeasterly trending faults.

Based on the past level of seismicity, as well as on the length of Quaternary faults and the amounts of associated displacements, the estimated maximum credible event for this zone is M_w = 7.75. These events can be expected to occur at long recurrence intervals. No faults of unequivocal Holocene age have been identified in the zone. Except for the area around Reno, Nevada which has been very seismotectonically active during historical time, the basin and range province is characterized by episodic faulting and large infrequent earthquakes widely spaced in time and location. Seismotectonic activity may occur for a period in one area and then become inactive while the activity moves to another area (Ryall, 1977; Van Wormer and Ryall, 1980; Wallace, 1987). Geologic investigations of paleoseismicity in the basin and range province indicate average long-term recurrence intervals for large earthquakes are commonly in excess of 15,000 years with several tens of thousands of years between events not unusual (Schell, 1981, 1982; Wallace, 1987; Muir et al, 1981).

Focal mechanisms for earthquakes in the zone are ambiguous in that they indicate both normal and strike-slip faulting. These mechanisms do not

indicate any dominant stress orientation. Harmsen and Rogers (1986) suggest the stress field is axially symmetric, that is, that the principal stress axes interchange with depth.

In summary, the Southern Nevada province has many of the characteristics of surrounding basin and range source zones, but can be differentiated by its unusual combination of physiography, seismicity, geologic structure, and tectonic stress regime. The structure is basically basin-and-range type, but it has imprints of previous tectonic regimes which may affect the present-day response of faults to the northwest-southeast extensional stress field that pervades the western United States.

(21) Whittier-Elsinore Fault Zone

The Whittier-Elsinore Fault zone is within the Salton Province and is discussed in Subsection 6.c.(13) to better illustrate the inter-relationships between this zone and its adjacent zones.

d. Description of Fault Sources

The fault sources are described above in section c with the zones to which they are most closely related. This section primarily provides references to those sections to better help the reader find the descriptions.

(1) Aubrey Fault

The Aubrey Fault seismic source zone is discussed in Section 6.c.(1) to better illustrate its inter-relationships with similar faults within the Arizona Mountain zone.

(2) Big Chino Fault

The Big Chino Fault seismic source zone is discussed in Section 6.c.(1) to better illustrate its inter relationships with similar faults within the Arizona Mountain zone.

(3) Hurricane Fault

The Hurricane Fault seismic source zone is discussed in Section 6.c.(19) to better illustrate its inter-relationships with similar faults within the Southern Hurricane Wasatch zone.

(4) Toroweap Fault

The Toroweap Fault seismic source zone is discussed in Section 6.c.(19) to better illustrate its inter-relationships with similar faults within the Southern Hurricane Wasatch zone.

(5) Verde Fault

The Verde Fault seismic source zone is discussed in Section 6.c.(1) to better illustrate its inter-relationships with similar faults within the Arizona Mountain zone.

7. RECURRENCE RELATIONS

a. General Approach

The recurrence interval of an earthquake is the average time between earthquakes of the same magnitude. The relationship between the number of earthquakes of a certain magnitude are plotted as straight lines on x-y plots on semi-logarithmic graph paper according to the equation:

$$\log N = a - bM \qquad \text{(Equation 7-1)}$$

where N is the number of events per year greater than or equal to magnitude, M_w, and a and b are constants. Magnitude is generally shown on the x axis and the number of events on the y axis. Generally, the number of events are normalized as an annual rate per area. The b-value represents the relative proportion of events of different magnitude, that is, a line with a slope of -1.0 represents a recurrence relationship which for every magnitude 5 event per year, there will be one magnitude 6 event every 10 years, and one magnitude 4 every 0.1 year (or 10 magnitude 4 events every year). The a-value is the intercept of the recurrence line at M=0. When b values are the same, lines with higher a-values occur higher on the graph and represent higher levels of seismicity. By convention, and in the discussion that follows, the lines on the x-y plots are commonly referred to as curves because they would be curved if plotted arithmetically. Figure 29 is a composite plot of the recurrence relations for all seismic source zones considered in this investigation. Table 1 lists the various recurrence parameters for the seismic sources in the study region. The recurrence relationships were estimated using three different techniques: 1) historical

FHWA REGION	STATE	PROJECT NUMBER	REPORT NUMBER
9	ARIZ.	HPR-PL-1(37)344	FWHA-AZ92-344

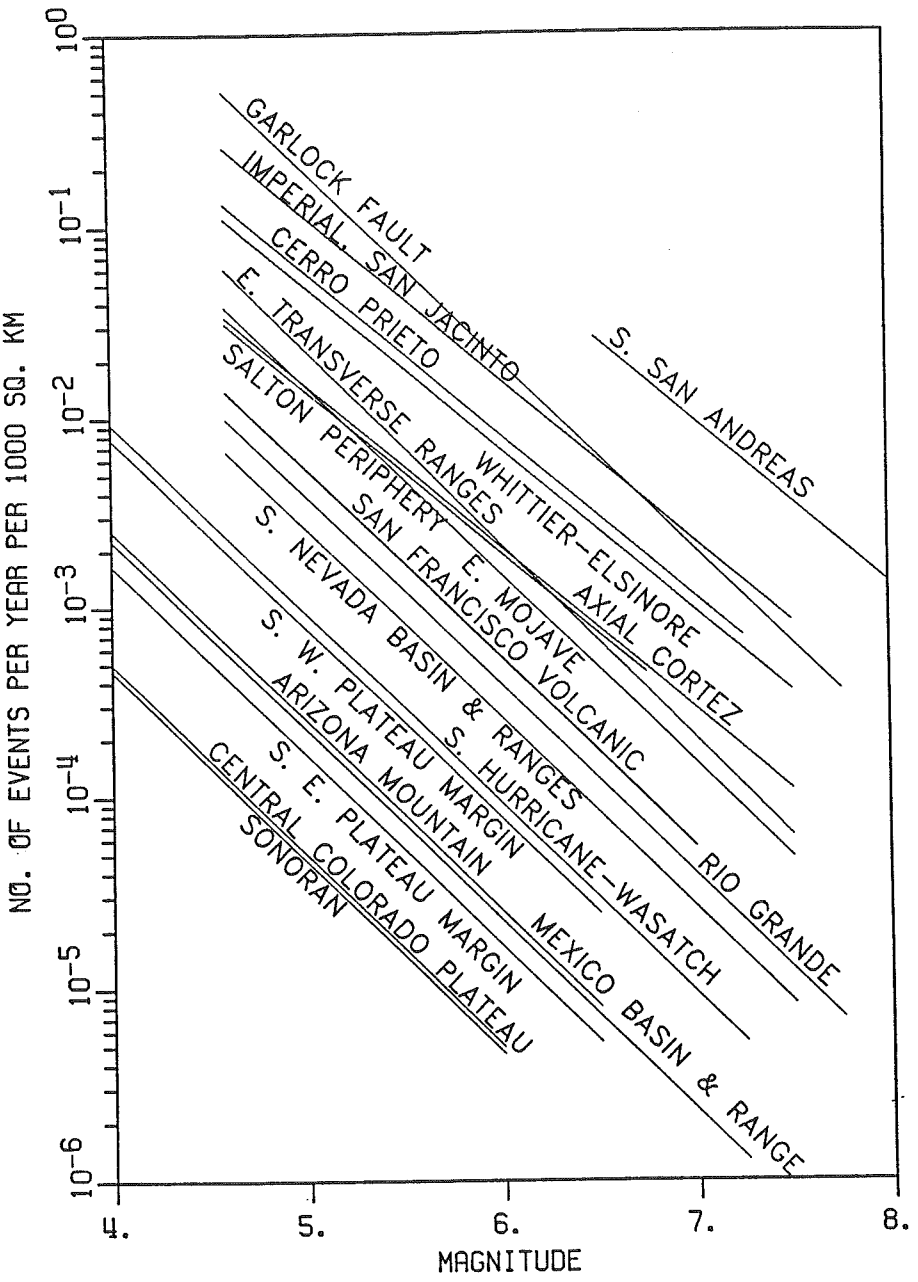

ARIZONA DEPARTMENT OF TRANSPORTATION
ARIZONA TRANSPORTATION RESEARCH CENTER

FIGURE 29
RECURRENCE RELATIONS OF
ALL SEISMIC SOURCE ZONES

TABLE 1

RECURRENCE RELATIONSHIPS FOR SEISMIC SOURCES

NAME	AREA (KM^2)	a (Total Area)	a' (Per 1,000 Km^2)	b VALUE	MAGNITUDE M_{min}	M_{max}
ARIZONA MOUNTAIN	98,466	3.398	1.405	1.00	4.6	6.5
AUBREY FAULT*	N/A	1.863	N/A	1.00	4.6	7.25
AXIAL CORTEZ	7,379	3.352	2.484	0.86	4.6	7.5
BIG CHINO FAULT*	N/A	2.432	N/A	1.00	4.6	7.25
CENTRAL COLORADO PLATEAU	126,571	2.800	0.698	1.00	3.0	6.0
CERRO PRIETO FAULT	714	2.931	3.077	0.86	4.6	7.25
EASTERN MOJAVE	20,933	4.500	3.180	1.00	4.6	7.5
EASTERN TRANSVERSE RANGES	10,355	4.532	3.520	1.03	4.6	7.5
GARLOCK FAULT	1,973	4.600	4.305	1.00	4.6	7.75
HURRICANE FAULT*	N/A	3.057	N/A	1.00	5.0	7.75
IMPERIAL FAULT	698	3.209	3.366	0.86	4.6	7.25
MEXICO BASIN & RANGE	88,154	3.301	1.356	1.00	4.6	7.25
RIO GRANDE RIFT	128,723	4.704	2.594	1.00	4.6	7.75
SAN FRANCISCO VOLCANIC	6,184	3.530	2.739	1.00	4.6	7.0
SALTON PERIPHERY	22,328	3.800	2.451	0.86	4.6	6.75
SAN JACINTO FAULT	3,903	3.957	3.366	0.86	4.6	7.5
SONORAN	152,319	2.845	0.662	1.00	3.0	6.5
SOUTHEASTERN PLATEAU MARGIN	40,167	2.824	1.220	1.00	3.0	6.5
SOUTHWESTERN PLATEAU MARGIN	43,350	3.530	1.890	1.00	4.6	6.5
SOUTHERN HURRICANE WASATCH	26,929	3.400	1.970	1.00	4.6	7.25
SOUTHERN NEVADA BASIN & RANGE	58,165	4.187	2.42	1.00	4.6	7.5
SOUTHERN SAN ANDREAS	1,874	4.274	4.001	0.86	6.5	8.0
TOROWEAP FAULT*	N/A	2.580	N/A	1.00	5.0	7.75
VERDE FAULT*	N/A	2.139	N/A	1.00	4.6	7.25
WHITTIER-ELSINORE FAULT	4,767	3.678	3.00	0.86	4.6	7.5

Note: * Modeled as line sources; all others are area source zones.

seismicity, 2) geologic data, and 3) slip-rate constraints on seismic energy release. Generally, these parameters were calculated from a wide variety of sources using all available data, commonly with several variations on each type of data. All of the results were then synthesized to derive the final recurrence relations used for the probabilistic analysis discussed in Section 8. The following discussion only presents examples of the analyses and representative types of factors used as guides to arrive at the final numbers. We want to emphasize that rarely was any data taken at face value; all inputs were heavily scrutinized and the final results were commonly affected by professional judgements to minimize the impacts of inadequate data bases.

Common practice for determining recurrence curves is to count the recorded number of seismic events of different magnitudes over an interval of time and within a specific area. In this method the areal extent of seismic source zones is defined and measured, and all events within that area are tabulated to derive the recurrence relationships.

Recurrence intervals can also be estimated from detailed geologic information for faults with evidence of surface-faulting events. The resulting recurrence estimate may be valid only at the location where the measurements were made and not necessarily for the entire fault length. For a recurrence relation representative of the entire fault, the recurrence at the one location must be extrapolated to the entire fault length. A better estimate can be derived if several locations are investigated and the results are found to be similar at each location. Commonly, the data from a few localities are averaged to represent the entire fault.

The third method of evaluating recurrence combines the principles of seismology with geologic constraints on energy release based on fault slip-rates. The concept is based on the premise that a fault can release only an amount of earthquake energy that is consistent with the long-term geologic rate of slip on the fault. This concept is consistent with world-wide observations that the faults with the highest rates of slip historically have released the greatest earthquake energy. The energy released during an earthquake can be expressed by the formula (Brune, 1968)

$$M_o = d\ A\ u \qquad \text{(Equation 7-2)}$$

where: M_o is the seismic moment (energy release),
d is the average displacement,
A is the area of fault-plane rupture, and
u is the shear modulus of the rock.

If all of the slip on a fault is the result of earthquakes releasing stored energy, then the past seismicity on that fault is directly related to the seismic moment. Brune (1968) expressed equation (7-1) in terms of slip rate as follows:

$$\dot{M}_o = S\ A\ u \qquad \text{(Equation 7-3)}$$

where: $\dot{M}_o$ is the rate of seismic-moment release,
S is the slip rate, and
2A and u are as described above.

Anderson (1979) established the relationship between total rate of seismic moment release and the recurrence of given magnitude earthquakes on a fault using the following equation:

$$\dot{M}_o = \frac{10^c}{(1-d)\ \ln_e 10}\ 10^{(1-d)\gamma}\Big|_{\gamma_{min}}^{\gamma_{max}} \qquad \text{(Equation 7-4)}$$

where: $d = 2/3\ b$,

$c = a + 16d - \log_{10}(3/2)$,

$\gamma = 16.0 + 1.5\ M$ (M is earthquake magnitude), and

a and b are constants defined below.

For a particular fault, the earthquake recurrence is obtained from the above equations as follows. First, γ_{min} and γ_{max} are computed by substituting the minimum and maximum earthquake magnitudes for the fault into the above equation for γ. The earthquake magnitudes are estimated from geologic data such as fault length, displacement, slip per event, area of rupture, etc. using empirical relationships (e.g. Slemmons, 1982; Bonilla et al, 1984; Wyss, 1979; Hanks and Kanamori, 1979). The maximum value is generally the maximum credible earthquake or characteristic earthquake and the minimum value is generally arbitrarily selected from a typical small event. Next, a value of b is assumed and used to compute the constant, d, which in turn, is substituted into equation (7-4). The value of M_o in equation (7-4) is computed from equation (7-3). Thus, the only unknown in equation (7-4) is the constant, c, for which a unique value is obtained by algebra. The resulting value of c is substituted into the above equation, $c = a + 16d - \log_{10}(3/2)$, which is then solved for the constant, a.

The constants, a and b, are the values needed for the standard recurrence equation (Equation 7-1). Because the historical seismicity data in the Arizona area are generally incomplete, b values derived from simple statistical counts of historical events were considered inadequate. Worldwide averages of earthquake data generally fall with the -0.9 to -1.0

range (Reiter, 1990). For this study, the constant b was assumed to be -1.0 unless there was abundant seismicity data to indicate otherwise. In the final analysis, the b-value of -0.86 from seismicity within the Salton Province was used for zones within the Salton Province and a b-value of -1.0 was used for zones in Arizona (Table 1). These values provided a unique value of the constant a for each seismic source zone and fault source zone defined in this study. The differences between a -0.9 and -1.0 b value are not large but the higher b value results in less frequent events in the higher magnitude ranges. Considering the extremely long recurrence intervals for large events in the Arizona region, the choice of b (0.9 verses 1.0) value will not have a significant effect on the final ground motions. Comparisons to test the sensitivity of the b value assumption resulted in numbers that seemed consistent with the available earthquake and geological data.

A key input for equation 7-4 is the rate of slip for earthquake faults. This slip rate is obtained from field geological and paleoseismic investigations. Such information is scarce and many faults have had slip rates determined at only one location. Such data are of limited precision because slip rates may vary depending on the location of the measurement. If the trenched location is not typical, an anomalous slip rate might be obtained. Figure 30 shows how some slip rates may vary along strike of a particular fault or between faults. There are characteristics that geologists have learned to recognize which increase the chances of excavating a successful trench, but in some cases it may be a trial and error process. The Aubrey Valley experience with Trench 1 is a good example of how surface relations may be misleading (Section 3.d.(2)). Figure 30 shows two hypothetical displacement histories. Note how faults with greatly different

displacement characteristics can yield the same long-term-average slip rate. Faults in the Arizona region appear to be more typical of the irregular displacement histories such as shown in Figure 30, characteristics of A. Geologic data obtained from a fault with the characteristics of B will generally be representative of the fault, whereas a fault with characteristics of A can generate anomalous slip rates if the trench is excavated across a portion of the fault that does not reveal average values. Some published investigations have slip rates determined from just one locality along a fault, and in some cases elaborate theories of increasing or decreasing rates of faulting and regional tectonics have been proposed to explain the data, when in reality, the postulated changes may only be a result of incomplete sampling.

All recurrence relations determined for this investigation were based on a combination of both seismological data and geological data, but more emphasis may have been placed on one parameter depending on the particular situation. For several of the source zones in California (e.g. San Jacinto fault zone, Eastern Transverse Ranges zone, Eastern Mojave zone) the historical seismicity data appeared to be adequate so the seismicity-determined recurrence relations were given priority over those based on geological data. Seismicity data for the Arizona area, however, were commonly marginal to inadequate for determining realistic recurrence relationships, primarily because the earthquake record is short and perhaps incomplete, especially in the smaller and larger magnitude ranges. The smaller events are incomplete because of the inadequacy of seismograph networks to record them, and the large ones are incomplete because recurrence intervals for large events are much longer than the historical record. In addition to an incomplete earthquake record, the "inadequacy" is also partly

FHWA REGION	STATE	PROJECT NUMBER	REPORT NUMBER
9	ARIZ.	HPR-PL-1(37)344	FWHA-AZ92-344

Modified from Wallace, 1987

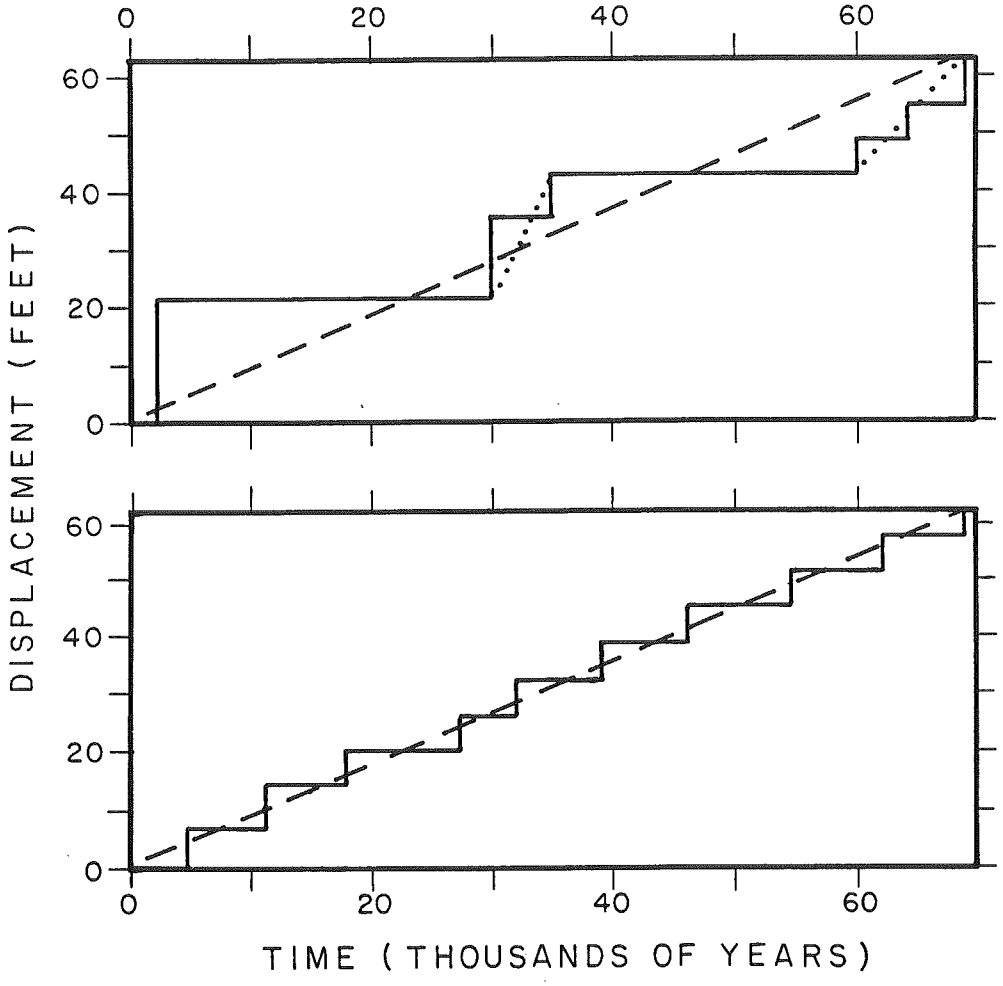

HYPOTHETICAL FAULT DISPLACEMENT TIME HISTORIES SHOWING TWO DIFFERENT FAULTS WITH DIFFERENT SLIP CHARACTERISTICS. SOLID LINES REPRESENT ACTUAL DISPLACEMENT HISTORIES; DASHED LINES REPRESENT LONG-TERM AVERAGE SLIP RATES; DOTTED LINES REPRESENT SHORT-TERM AVERAGE SLIP RATES. THE AVERAGE LONG-TERM SLIP RATE IS THE SAME FOR BOTH FAULTS.

A. FAULT CHARACTERIZED BY IRREGULAR DISPLACEMENT AMOUNTS AND IRREGULAR RECURRENCE INTERVALS WITH EVENTS TYPICALLY SEPARATED BY LONG QUIET PERIODS.

B. FAULT CHARACTERIZED BY MORE-REGULAR DISPLACEMENT AND RECURRENCE INTERVALS.

ARIZONA DEPARTMENT OF TRANSPORTATION
ARIZONA TRANSPORTATION RESEARCH CENTER

FIGURE 30
TYPICAL FAULT DISPLACEMENT HISTORIES

a result of the generally low rate of tectonic activity in the state. That is, the rate of crustal strain appears to be low, and thus it takes a long time for strain to accumulate, and therefore, frequent earthquakes should not be expected. Much of the state is located between tectonically more-active regions of the North American-Pacific plate boundary in California, the Nevada-Utah Basin and Range province, and the Rio Grande Rift in New Mexico. Earthquake recurrence is highest (i.e. earthquakes are most frequent) in the Salton Trough region of adjacent southern California where faults such as the San Jacinto and Imperial faults are among the most seismically active in the world. As discussed in Section 6, the San Jacinto-Imperial system has experienced about 15 earthquakes larger than about magnitude 6 in this century. Although the Basin and Range area (which includes parts of California, Nevada, Utah, Idaho, and Montana) has experienced several large earthquakes ($M > 7$) in this century, the overall level of tectonic activity is generally less than in southern California. Except perhaps in the Central Nevada Seismic Belt in the Reno, Nevada area, the majority of faults in the Basin and Range province generally have recurrence intervals longer than about 15,000 years with intervals as long as 100,000 years or more (Schell et al, 1981; Muir et al, 1981; Schell, 1982; Wallace, 1987). Although the Rio Grande Rift has not experienced any large earthquakes ($M > 7$) in historical time, geologic data indicate several faults capable of such events with recurrence intervals similar to the Basin and Range province of Nevada and Utah. Arizona, which lies between these areas both in geographic location and in rate of seismotectonic activity, has a few faults (e.g., Hurricane and Toroweap faults) with recurrence intervals similar to the more-active Basin and Range faults but the vast majority of faults have not been active in Holocene time, and generally for much longer periods.

Fortunately for seismic hazard analyses, a number of the faults in Arizona have had detailed geologic studies (trenching, tectonic geomorphology, etc) in the past few years. Considering the overall low rate of tectonic activity and relatively small number of faults, this makes the state one of the better areas in the western U.S. for using geologic data to estimate earthquake recurrence relations. Recent geologic data (for example, Menges and Pearthree, 1983; Schell and Wilson, 1982; Bull and Pearthree, 1988; Demsey and Pearthree, 1990; Pearthree and Calvo, 1987; Jackson, 1990; Piety and Anderson, 1990) were augmented by additional tectonic geomorphological studies and trenching conducted for this study (see Section 3) to characterize all recognized tectonic regimes in the state. These data were combined with other published and unpublished geological and seismological data to develop recurrence relations for each tectonic regime by using geologic data either directly or by the moment slip-rate method developed by Anderson (1979) as described above. Although there may be some shortcomings to the moment slip-rate method when used alone (Schell, 1991) these shortcomings do not invalidate the method. The integration of the various methods and the new geological data provide results that are a substantial improvement over using only seismicity data and are believed to provide a more-realistic representation of the earthquake hazards in the region.

The general approach consisted of dividing the state and surrounding region into zones with similar seismotectonic relationships (Section 6), and then determining typical recurrence relations for these zones. Section 6 has a discussion of the terminology and the methods for establishing seismic sources (zones and faults). Table 1 lists the recurrence information derived for each seismic source and Figure 29 shows the relative relationships of the recurrence curves for all the seismic source zones considered in this

investigation. These relationships were developed through a rather complex iterative process which commonly involved considering dozens of different relationships for each zone. In some cases, the recurrence relations determined from seismicity were similar to those compiled by fault slip rates giving confidence that the estimated relations are realistic and characteristic of the true earthquake hazard. In other cases, the recurrence plots were quite different (e.g. one or two orders of magnitude) and judgements were required to reconcile the data and to evaluate which, if any, was the best. The process can be very long and complicated, therefore is difficult to describe in detail for all of the 25 seismic sources used in this investigation. To document the process for this report, a few key examples are described in detail below in Subsection b.

The source zones described below were selected to be representative of the various types of determinations made during this investigation. That is, the Mexican Basin and Range is described because it is a zone which has had significant local, high-level, historical seismicity that does not appear to be representative of the level of activity indicated by the geologic data. In other words, use of historical seismicity alone would have resulted in overestimation of the true seismic hazard.

The Arizona Mountain zone also has had significant historical seismicity but of a low to moderate level and more distributed throughout the zone. The constraints presented by such characteristics are quite different from those of the Mexico Basin and Range zone. The recurrence relationship for the Arizona Mountain zone is based on a combination of geologic data and seismicity data.

The Hurricane fault, unlike most of the other seismic sources, is a line source rather than a zone. The Hurricane and Toroweap faults were considered separately from the Hurricane-Wasatch zone because they are larger and possibly more active than the other faults in the zone. To consider them with the zone would tend to homogenize the seismic hazards. The Hurricane fault has had no demonstrated historical seismicity but the geologic data provide abundant evidence of recurrent prehistorical (paleoseismic) activity. For the Hurricane fault source, the a-value for the recurrence relationship was derived primarily by using the moment slip-rate method, constrained by comparison of the results with other similar faults in similar tectonic environments.

The San Jacinto fault is considered a zone source with a high level of seismic activity which appears to satisfactorily characterize the source. The fault is considered a zone source rather than a line source because the fault system consists of a series of overlapping discrete faults located over an area up to 7 or 8 miles wide in places. The recurrence relation for this source was based completely on the historical seismicity using epicenters within about 10 miles of the fault. The seismically determined recurrence relationship was cross-checked against relations derived from the moment slip-rate method and from published references.

The San Andreas fault was also considered as a zone source but is different from the San Jacinto because it has not had any significant historical seismicity. To estimate a recurrence relation for the San Andreas, geological data were applied to the moment-rate method. Comparisons were made with other faults in the Salton Trough area and to other published relations.

The methods used to develop recurrence relations for the other zones and line sources were essentially the same as one of the above sources and thus are not described in detail below. Most pertinent details are given in the general descriptions of the zones and their rates of seismotectonic activity and in the general discussion of the methods (Section 6).

Before describing the specific examples, a description of the general procedure for determining recurrence relations is presented below. This step-by-step description is approximately the same for all the source zones and faults, although different sources require some modifications and different emphasis. The step-by-step procedure typically followed to determine representative recurrence relationships for each source was as follows:

1) The historical seismicity in proximity to the zone or fault was examined. If historical seismicity was present a recurrence relationship with the number of earthquakes per year on the y axis and their magnitudes on the x axis was plotted. In Arizona, these plots generally have low b-values because the earthquake record is incomplete in the small magnitude range (less than M = 4 or 5) so a second plot was generated with a slope (b-value) of -1.0 using the actual moderate earthquakes (M = 4 or 5) as anchor points. Both of these recurrence curves were then used as guides, in conjunction with the geologic data, to help establish the final recurrence relationship.

2) Geologic data related to paleoseismic earthquake activity were compiled. Of particular importance were:

- the age of latest displacement,

- the number of previous displacements,

- the amount of displacement per event (surface displacement and stratigraphic displacement),

- the total stratigraphic displacement,

- the lengths of surface displacements (smallest, largest, typical),

- the ages of displaced stratigraphic units, soil horizons, or geomorphic surfaces,

- the area of rupture, i.e. the length of the rupture surface multiplied by the thickness of the brittle, seismogenic crust,

- the rate of slip (preferably two values, the late-Quaternary rate and the long-term rate (i.e. the rate since the fault became part of the present tectonic regime),

- the time between ruptures, i.e. the geological recurrence interval,

- the rupture characteristics (i.e. Does the fault rupture in segments, with regular periodicity, etc ?). Does it

rupture only with large events (with characteristic earthquakes) or by a range of events (small and/or moderate events only)?

3) All of these data, were then evaluated to derive preliminary recurrence relationships for various sizes of earthquakes. These recurrence relations are in the form of equation 7-4 and are shown on x-y plots. Generally these preliminary plots comprised a family of possible recurrence curves. Further review of seismotectonic data generally reduced the choices to one or two curves that appeared to provide appropriate alternatives.

4) Once all available data were tabulated and analyzed, the source was compared to other sources with more-complete or more-detailed information and with similar characteristics and/or within similar tectonic environments. These comparisons helped to evaluate whether the information collected was representative and reasonable, and it helped to determine how much conservatism, if any, should be invoked.

5) These plots were then compared to the x-y plots of other seismic sources and judgements were made as to whether the relative levels of seismic activity are in accordance with all the data from the entire region. In some cases, these comparisons suggested that the seismic sources were not compatible with some of the other source zones and the entire process was repeated with appropriate adjustments being made to ensure that all of the sources were consistent with each other and with the regional

seismotectonic regime. In the end, one of the alternatives usually emerged as the preferred relationship and this was used in the risk model which led to construction of the seismic acceleration contour map(s) (Plate 2).

The results of the above evaluations for selected sources are summarized below in Section b.

b. Recurrence-Relation Development for Selected Seismic Sources

(1) Hurricane Fault

The Hurricane fault is one of numerous faults within the Southern Hurricane-Wasatch seismic source zone as described in Section 6.c.(19). Both the Hurricane fault and the Toroweap fault were considered as discrete seismic sources in the seismic-hazard analysis because geologic data indicate they are more active than most of the other faults within the Southern Hurricane-Wasatch zone, and that they may be capable of generating larger earthquakes than most of the other faults in the zone. There has been no substantial historical earthquake activity specifically associated with the fault, therefore its potential for generating earthquakes and its recurrence relations must be estimated from geologic data. The process was an iterative process requiring many adjustments and reevaluations at several of the steps described above.

Analysis of seismicity catalogs showed that very little seismic activity has occurred in proximity to the Hurricane fault. The largest

historical earthquake in proximity to the Hurricane fault was the 1901 Richfield, Utah event with a magnitude of about 6.5 (see Section 6.c.(19)). The location of this event is unknown and there are several faults in the area that are capable of generating such an event. The Southern Hurricane-Wasatch zone is characterized by swarms of earthquakes (Anderson and Christenson, 1989). For example, an earthquake swarm occurred in 1942 near the north end of the Hurricane fault which included two earthquakes with magnitudes of about 5.0 (Arabasz and Smith, 1979; Richins and others, 1981).

The great length of the Hurricane fault suggests that it should be capable of generating large earthquakes. Menges and Pearthree (1983) postulated that the fault comprised eight segments; our analysis suggested six or seven segments based on geomorphic trends. Typical segments ranged from about 20 to 40 miles long. Various estimates of fault rupture-lengths (total length, half length, segment length) and displacements were applied to empirical relationships (Slemmons, 1982; Bonilla et al, 1984; Wyss, 1979; Hanks and Kanamori, 1979) to estimate likely maximum earthquake magnitudes. Estimates ranged from 6.5 to 7.75 with an average of about 7.2. For this evaluation, the maximum credible earthquake was estimated to be M_w = 7.75 and the characteristic earthquake M_w = 7.5.

Recurrence intervals for these maximum earthquakes are difficult to estimate because the age and displacement information for the Hurricane fault vary considerably between segments. This variation could be due partly to lack of data, but it also appears to be characteristic of a sporadic, irregular rupture behavior such as shown on Figure 30. Calculated slip rate ranged from a minimum of 0.03 mm/yr to a maximum of about 0.5 mm/yr. Table 2 lists some of the better constrained information.

TABLE 2

GEOLOGICALLY DETERMINED SLIP RATES FOR THE HURRICANE FAULT

OFFSET STRATIGRAPHIC UNIT		AMOUNT OF OFFSET		SLIP RATE
age	type	feet	(meters)	mm/yr
Pliocene[1]	total	3600-4900	(1100-1500)	0.20 to 0.38
1,000,000	alluvium	1000-1500	(310-470)	0.31 to 0.47
290,000	basalt	280	(87)	0.3
50,000	alluvium	65	(20)	0.4
100,000-200,000	basalt	20-25	(6-8)	0.08 to 0.03

Notes: 1) For estimation of slip rate, ages of 4 and 5 million years were used. The offset represents the total stratigraphic displacement on the fault scarp.

Except for the last entry on Table 2, these data are fairly consistent and seem to cluster between 0.3 to 0.5 mm/yr so these values were used for preliminary seismic moment-rate calculations (Figure 31), again using various characteristic rupture lengths, to derive a range of possible relations from which to choose the final a-values.

Typical geologic recurrence intervals for the Hurricane fault source were estimated from:

- the frequency of prehistorical surface ruptures (for example, see Anderson and Christenson, 1989),
- from fault-scarp morphology,
- from the relationship of the amount of displacement per event

relative to the height of fault scarps and/or stratigraphic displacement.

For example, evaluation of compilations of worldwide empirical data such as Slemmons (1982) and Bonilla et al (1984) and from direct comparisons to historical data indicated that a fault such as the Hurricane fault can generate earthquakes greater than magnitude 7. Historically such events worldwide have displaced the ground surface by amounts from between a few inches to about 35 feet. The worldwide average is about 10 feet with most events falling in the 6- to 20-foot range. Jackson (1990) estimated that displacements of 6.5 to 10 feet were likely events for the Hurricane fault. Historical events in the Basin and Range province have ranged from less than 3 feet to about 20 feet. The recurrence interval for large earthquakes was evaluated by using the various estimates of surface rupture and slip rates. For example, at a slip rate of 0.3 mm/yr, it would take 16,667 years to accumulate enough strain to produce a surface rupture of 16 feet, and 10,000 years to accumulate 10 feet of strain. The range of recurrence intervals derived from such analysis is from 4,000 years to 17,000 years. This range is shown on Figure 31 as the box labeled MCE. Geomorphic relations indicate the last rupture was about 8,000 to 10,000 years ago (Anderson and Christenson, 1989).

Synthesis of all the data indicate that the recurrence interval for large surface-rupturing events (i.e. the maximum credible earthquake) ranges from about 4,000 to as much as 50,000 years and more along various segments of the fault. If the zone comprises two discrete seismogenic segments (see discussion of segmentation in Section 6.a.(6)(e)), two events should be considered for the seismic hazard analysis reducing the recurrence interval

FHWA REGION	STATE	PROJECT NUMBER	REPORT NUMBER
9	ARIZ.	HPR-PL-1(37)344	FWHA-AZ92-344

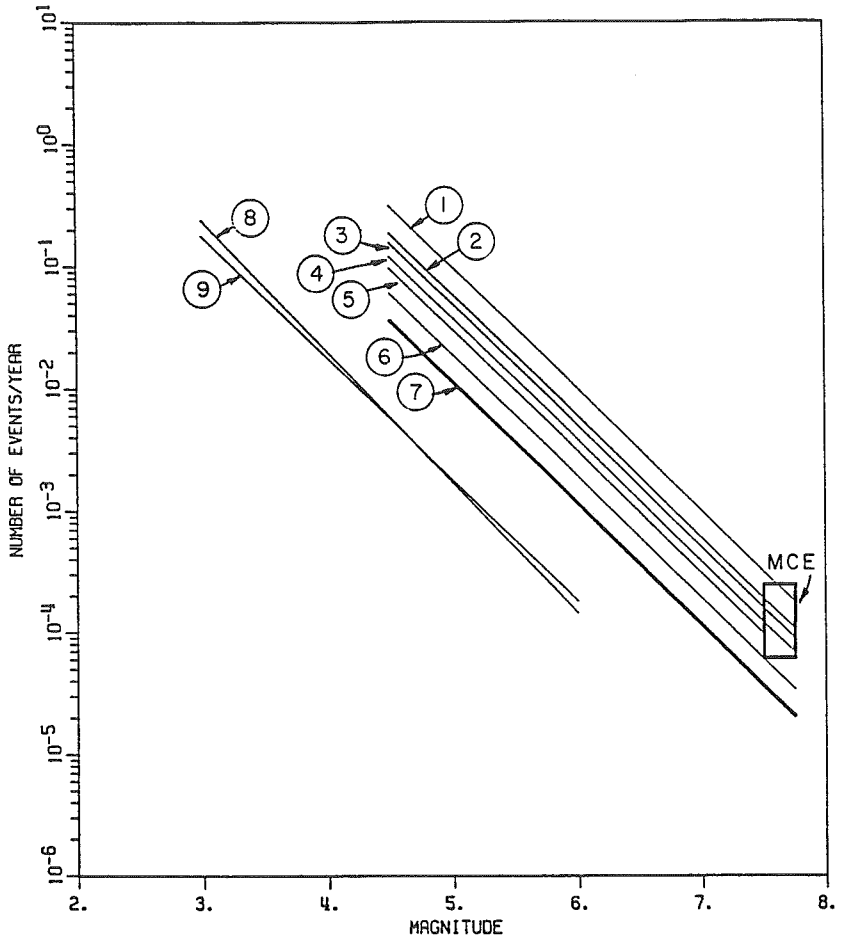

Curve Number	a - value	b - value	Slip rate mm/yr	Rupture Length (Km)	Maximum Magnitude
1	3.995	- 1.0	0.5	260	7.75
2	3.773	- 1.0	0.3	260	7.75
3	3.694	- 1.0	0.5	130	7.75
4	3.580	- 1.0	0.5	100	7.75
5	3.483	- 1.0	0.3	100	7.75
6	3.279	- 1.0	0.5	50	7.75
7	3.057	- 1.0	0.3	50	7.75
8	2.611	- 1.1	Instrumental Seismicity, Stover et. al., 1986		
9	2.255	- 1.0	DNAG Seismicity		

ARIZONA DEPARTMENT OF TRANSPORTATION
ARIZONA TRANSPORTATION RESEARCH CENTER

FIGURE 31
RECURRENCE RELATIONS
HURRICANE FAULT

range to 2,000 to about 20,000 years for the maximum credible earthquake. Our preferred model does not favor postulating a large number of discrete seismogenic segments for the Hurricane fault because the geological data indicate such sporadic, irregular, long-term intervals on the Hurricane fault. The fault becomes less active southward in Arizona and the southernmost section may not have ruptured in Quaternary time.

Figure 31 is an x-y plot of some of the various recurrence relations derived from different combinations of the compiled data. These curves were generated by applying geologically determined slip rates to the moment slip-rate formula (Equation 7-4) discussed in Section 7.a. These recurrence relations and the data used to derive them were compared to other faults in the same seismotectonic environment (Basin and Range). The comparison faults are the Wasatch fault in the central part of the Hurricane-Wasatch province, the Owens Valley fault in the California Basin and Range seismotectonic province, a similar seismotectonic province that occupies a position on the western side of the central Basin and Range similar to the position of the Hurricane-Wasatch does on the eastern side (Schell et al, 1985), and to the Lost River fault in the Idaho Basin and Range area. Table 3 summarizes typical data for these faults.

Numerous combinations of maximum earthquakes, slip rates, rupture lengths, and seismicity were plotted for each of the comparison faults (Figures 32, 33, and 34). These plots were then compared to the Hurricane fault (Figure 31) and examined for trends, similarities, differences, anomalies, etc. to help determine an appropriate a-value for the Hurricane fault source recurrence relationship.

TABLE 3

TYPICAL CHARACTERISTICS OF SOME LARGE FAULTS IN THE BASIN AND RANGE PROVINCE

FAULT	MAX. HIST. EARTHQUAKE	LENGTH (miles)		SLIP RATE (mm/yr)	RECURRENCE INTERVAL (years)
		Total	Segment		
Owens Valley	M_w=7.7	70	None	1.5 to 2	3300-5000[1]
Wasatch	None	200	30	0.6 to 1.5	1000-5000[1]
					2000[2]
					340-415[3]
Lost River	M_s=7.3	85	25	0.3 to 0.4	6000-20,000[1]
Hurricane	None	160	20-40	0.3 to 0.5	4000-17,000[1]

Notes: 1) range for individual segments
2) average for segments
3) average for entire fault zone

The Hurricane fault does not compare well with the Wasatch fault. The most characteristic curves on the Wasatch plot (Figure 32) seem to be curves 1 and 2 which are similar to curves 1 and 2 on the Hurricane fault plot (Figure 31). However, curves 1 and 2 on the Hurricane plot are based on complete rupture of the total length of the fault during one event, an event that does not seem likely based on empirical data (Albee & Smith, 1960, Slemmons, 1982) and the possible segmentation of the Hurricane fault. Also, the Wasatch fault has been much more tectonically active than the Hurricane fault during the Holocene (Anderson and Christenson, 1989). The Wasatch fault has recurrence intervals in the hundreds of years to a few thousand years compared with thousands of years to ten's of thousands of years for the Hurricane fault and the Wasatch fault has significantly more nearby seismic

FHWA REGION	STATE	PROJECT NUMBER	REPORT NUMBER
9	ARIZ.	HPR-PL-1(37)344	FWHA-AZ92-344

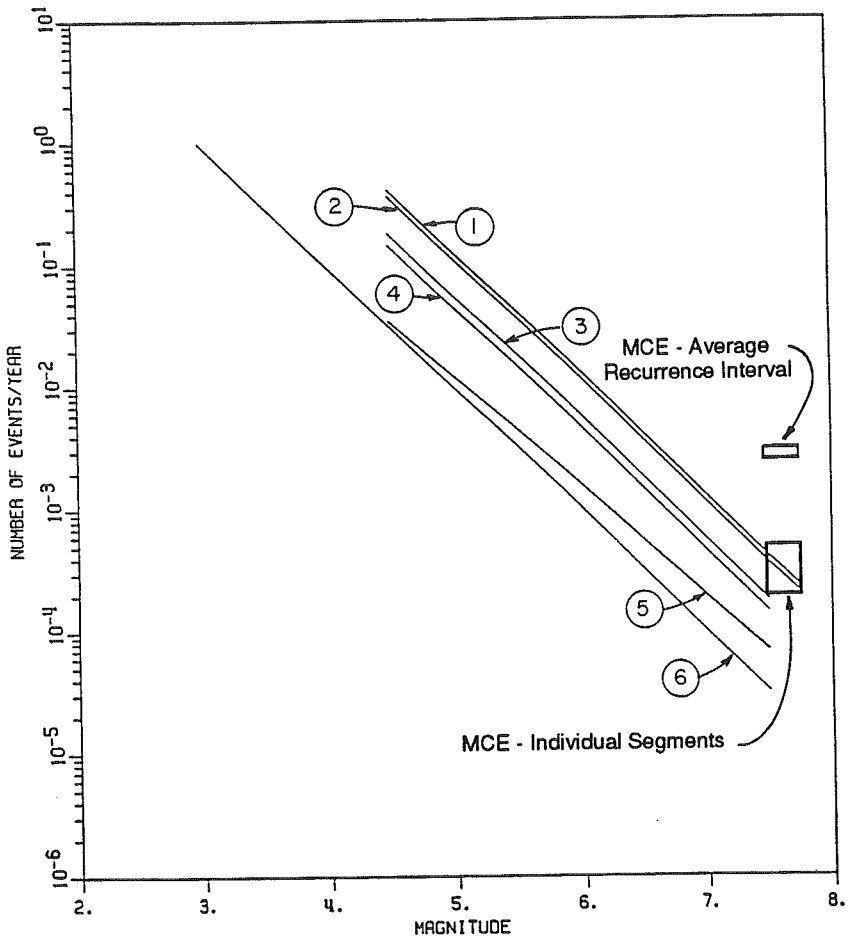

Curve Number	a - value	b - value	Slip rate mm/yr	Rupture Length (Km)	Downdip Width (Km)	Maximum Earthquake
1	4.111	- 1.0	1.7	100	15	7.75
2	4.057	- 1.0	1.5	100	15	7.75
3	3.756	- 1.0	1.5	100	15	7.5
4	3.659	- 1.0	0.6	100	15	7.5
5	2.590	- 0.9	Historical Seismicity, Schwartz and Coppersmith, 1984			
6	3.000	- 1.0	Same as #5 anchored at M = 4.0			

ARIZONA DEPARTMENT OF TRANSPORTATION
ARIZONA TRANSPORTATION RESEARCH CENTER

FIGURE 32
RECURRENCE RELATIONS
WASATCH FAULT

FHWA REGION	STATE	PROJECT NUMBER	REPORT NUMBER
9	ARIZ.	HPR-PL-1(37)344	FWHA-AZ92-344

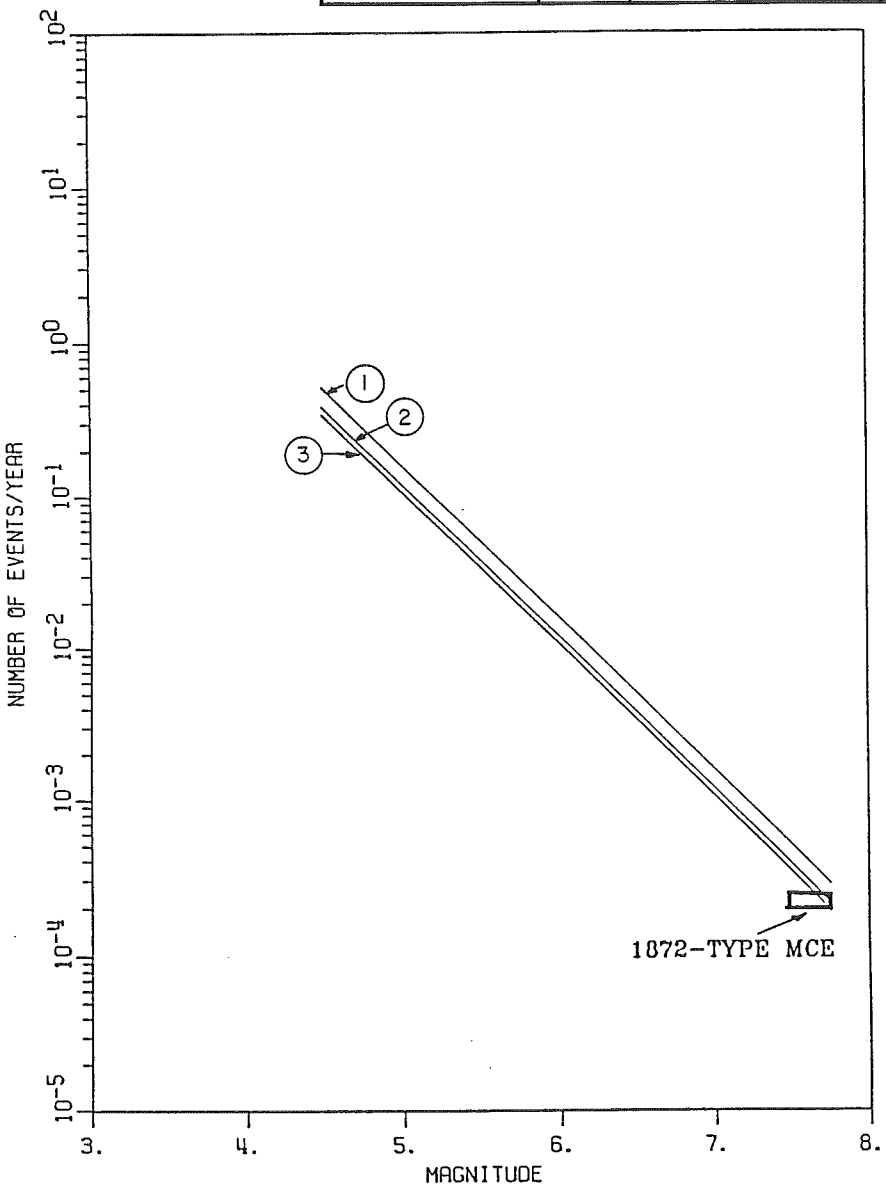

Curve Number	a - value	b - value	Slip rate mm/yr	Rupture Length (Km)	Downdip Width (Km)
1	4.207	- 1.0	2.0	100	15
2	4.082	- 1.0	1.5	100	15
3	4.033	- 1.0	2.0	67	15

ARIZONA DEPARTMENT OF TRANSPORTATION
ARIZONA TRANSPORTATION RESEARCH CENTER

FIGURE 33
RECURRENCE RELATIONS
OWENS VALLEY FAULT

FHWA REGION	STATE	PROJECT NUMBER	REPORT NUMBER
9	ARIZ.	HPR-PL-1(37)344	FWHA-AZ92-344

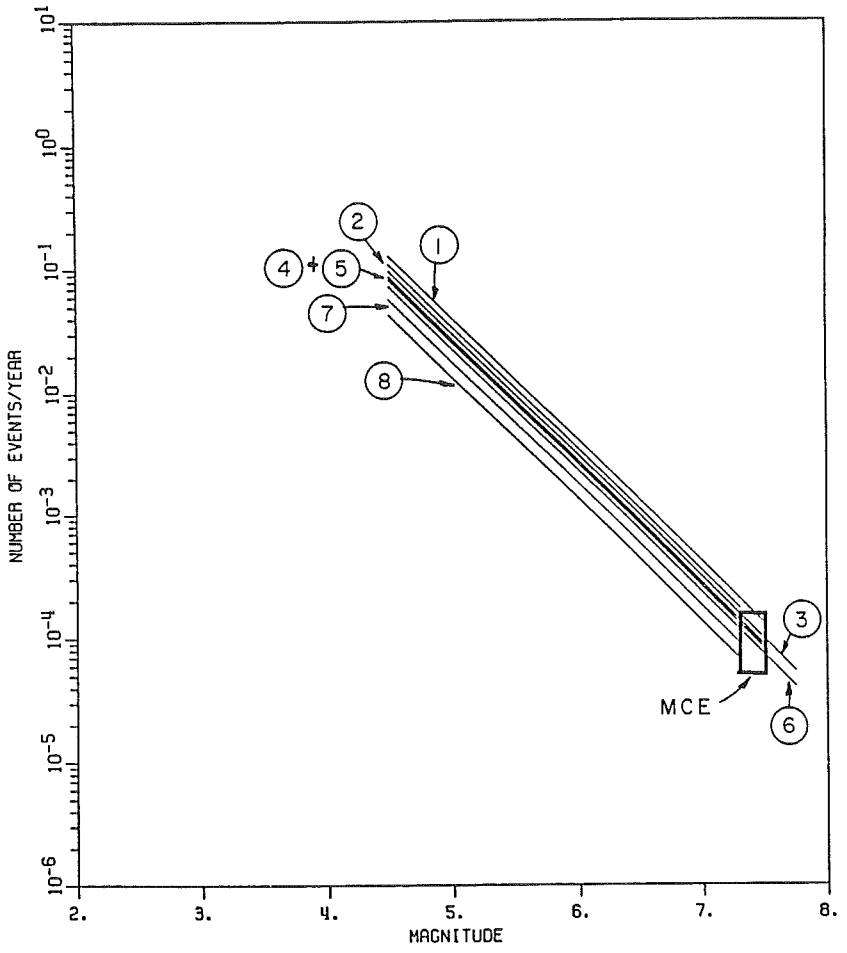

Curve Number	a - value	b - value	Slip rate mm/yr	Rupture Length (Km)	Downdip Width (Km)	Maximum Earthquake
1	3.608	- 1.0	0.4	100	15	7.5
2	3.534	- 1.0	0.4	67	15	7.3
3	3.483	- 1.0	0.4	100	15	7.75
4	3.434	- 1.0	0.4	67	15	7.5
5	3.409	- 1.0	0.3	67	15	7.5
6	3.358	- 1.0	0.3	100	15	7.75
7	3.252	- 1.0	0.4	35	15	7.3
8	3.127	- 1.0	0.3	35	15	7.3

ARIZONA DEPARTMENT OF TRANSPORTATION
ARIZONA TRANSPORTATION RESEARCH CENTER

FIGURE 34
RECURRENCE RELATIONS
LOST RIVER FAULT

activity (even though it has not ruptured the ground surface in historical time) than the Hurricane fault. It appears that the Hurricane fault recurrence relation should be much less than that of the Wasatch fault (Figure 32).

The Hurricane fault does not appear to compare too favorably with the Owens Valley fault either. The Owens Valley fault ruptured during and M_w=7.7 earthquake in 1872 along about a 60-mile length (Figure 33). The Hurricane fault has a much slower slip rate and may be more segmented. Based on these characteristics, the Hurricane fault recurrence relation should be much less than the Owens Valley recurrence relationship.

The Hurricane fault appears to compare most favorably with the Lost River fault, the source of the M_s=7.3 Borah Peak, Idaho earthquake of 1983. Both these faults seem to have similar recurrence intervals, segmentation, and slip rates. The data seem to favor the recurrence relations at the lower levels such as curves 6 and 7 (Figure 34).

After several iterations and calculations, the final numbers for the a-value and b-value to be used in the probabilistic model for the acceleration contour map were a = 3.057 and b = -1.0 (Table 1). At this activity rate, the Hurricane fault would generate earthquakes with magnitudes greater than M = 7.0 on the order of one every 8,000 years.

(2) Mexico Basin and Range Zone

The Mexico Basin and Range source zone is described in Section 6.c.(9). As described in that section, the zone is characterized by

normal faults along the flanks of the mountain ranges. These faults are recognized by discontinuous scarps in alluvial sediments near the mountain-valley boundary. For analyzing the potential seismic hazard and recurrence intervals the surface faults were considered to be part of longer more-continuous fault systems, some of which have not ruptured the surface in late Quaternary time. The linear mountains and valleys were grouped into nine zones based on synthesis of geological, geophysical, seismologic, and geomorphic data. These mountains were considered to be bounded by typical basin-and-range fault systems. Generally basin-and-range fault systems are of tilt-block style with a major fault on one side of the valley and minor faults on the other side. From west to east, the postulated mountain-bounding fault systems are:

Baboquivari,

Santa Rita (includes #150),

Sierra Vista/California Wash (includes #154),

Dragoon/Mule,

Chiricahua/Pedregosa (includes Pedregosa and Joe Glenn Ranch faults, # 157 and 160),

Pitaycachi (includes Bunk Robinson/Outlaw Mtn. fault, # 159),

Peloncillo (includes Washburn Ranch and Grays Ranch faults, # 162 and 165),

Animas (includes Gillespie Mountain and Animas Valley faults, # 163 and 166), and

Hatchet.

Of these systems, three segments have ruptured the ground surface during the Holocene/latest Pleistocene time (the past 15,000 to 20,000 years) (Machette et al, 1986; Menges and Pearthree, 1983). These are the

Pitaycachi, Animas (Gillespie Mtn. segment), and the Peloncillo (Washburn Ranch segment) fault systems. Machette et al (1986) and Menges and Pearthree (1983) also considered the Chiricahua fault as one that ruptured during this time frame, but our analysis could find no evidence of such a recent displacement. Pearthree (1992, personal communication) independently reevaluated the Chiricahua Mountains front and agrees with our interpretation. The geomorphology and the tectonic regime support the notion that there is a Quaternary fault on the east side of the Chiricahua Mountains, but its latest rupture was probably in the middle or early Pleistocene Epoch and any surface scarps formed at that time have been eroded away. The same is assumed to be true for the Baboquivari, Dragoon/Mule, and Hatchet mountain fronts, all of which are relatively linear suggesting neotectonic activity.

Three of the fault systems in the zone that have been examined in detail, the Sierra Vista/California Wash, the Santa Rita, and the Chiricahua/Pedregosa systems, have scarps indicative of only one event in late Pleistocene time indicating recurrence intervals in the 10^5-year range (Section 6.c.(9)). The paucity of composite fault scarps along most of the mountain fronts suggest that 10^5-year recurrence intervals are typical of the Mexico Basin and Range zone. In other words, the time between surface-rupturing events is so long that the scarps are completely eroded away before the next event occurs.

Three fault ruptures within the Mexico Basin and Range zone within the past 15,000 to 20,000 years suggest a zonal average of about one event per 5,000 to 6,667 years. This would be the minimum recurrence interval because it is not certain that a new recurrence cycle has begun; that will not be

known until the next large earthquake occurs. As discussed in Section 6, faulting in the Basin-and-Range tectonic regimes typically is sporadic and tends to cluster in both space and time. If the next large event does not occur for another 5,000 years, then the average recurrence interval range for the zone would be 6,667 to 8,333 years.

Because there have not been any large earthquakes since the establishment of seismograph networks, the size of the large earthquakes must be estimated from geologic data. Using empirical fault-length relationships and seismic-moment calculations (Slemmons, 1982; Bonilla et al, 1983; Wyss, 1979; Hanks and Kanamori, 1979), the faults appear to be capable of generating earthquakes in the 6.75 to 7.5 magnitude range. For this investigation, the characteristic earthquake is estimated to be M_w = 7.25 and the maximum credible event to be M_w = 7.5.

The hypotheses described above indicate that the occurrence of a large magnitude earthquake (1887 type) can be expected in the Mexico Basin and Range zone on the average of no more than once every 5000 to 10,000 years. These values were then used as an anchor point on an x-y plot for the purpose of determining an appropriate recurrence a-value for a line with a slope (b value) of -1.0 (Figure 35). As a check, recurrence curves for the Pitaycachi fault, the source of the 1887 event, using geologically determined slip rates of 0.03 to 0.01 mm/yr are also plotted. A point representing an estimate of the typical recurrence of M > 3 events based on historical seismicity (Wallace et al, 1988) is also plotted to provide a link to actual recorded earthquakes. The final curve used for the probabilistic analysis should also be consistent with this level of activity. The a values of the plotted curves range from 3.500 to 1.881. Inspection of the various relationships

FHWA REGION	STATE	PROJECT NUMBER	REPORT NUMBER
9	ARIZ.	HPR-PL-1(37)344	FWHA-AZ92-344

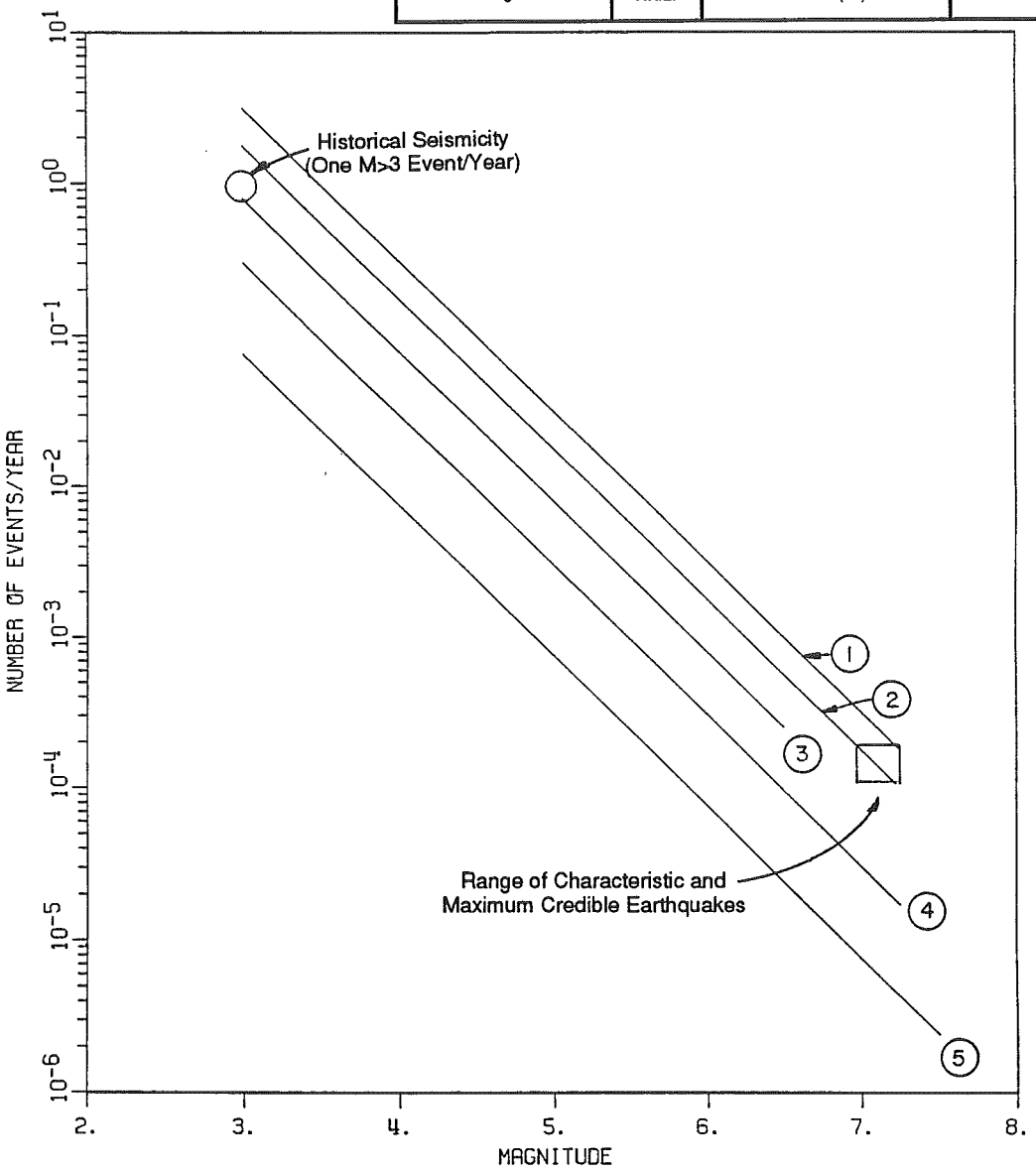

Curve Number	a - value	b - value	Comments
1	3.500	- 1.0	Based on one M = 7.25 event/5000 years
2	3.250	- 1.0	Based on one M = 7.25 event/10,000 years
3	2.901	- 1.0	Based on one M = 6.6 event/5000 years
4	2.483	- 1.0	Pitaycachi Fault: M = 7.25, Sliprate 0.03 mm/yr
5	1.881	- 1.0	Pitaycachi Fault: M = 7.25, Sliprate 0.01 mm/yr

ARIZONA DEPARTMENT OF TRANSPORTATION
ARIZONA TRANSPORTATION RESEARCH CENTER

FIGURE 35
RECURRENCE RELATIONS
MEXICO BASIN AND RANGE ZONE

on Figure 35 indicate that the level of activity represented by curves 4 and 5 are well below what most of the other data indicate. Curve number 1 seems too high because it exceeds the historical seismicity and projects to the higher side of the characteristic/maximum credible earthquake levels. As discussed in Section 6.a.(6)(e), recurrence relationships in most other areas project well below the characteristic earthquake level (Schwartz and Coppersmith, 1984). The most representative recurrence relations seem to be curves 2 and 3. The final recurrence relationship selected to represent the Mexico Basin and Range zone is between curves 1 and 2 which would be conservative but is believed to be representative of the various geologic and seismologic relations without being overly conservative. The a-value for the selected relationship is 3.300 and the b-value is -1.0 (Table 1). As can be seen by the final acceleration contour maps (Plate 2), the selected recurrence relation, even though considered to be conservative, yields considerably lower peak g values than previous ground motion maps. Comparison of these maps is discussed more fully in the Section 7.c.

(3) Arizona Mountain Zone

The Arizona Mountain source zone and the Big Chino, Aubrey, and Verde fault sources are described in Section 6.c.(1). Seismically, the Arizona Mountain source zone is one of the most active zones in Arizona. The zone presents sort of an enigma because its historical seismicity may actually be higher than is suggested by geologic data. There were three M > 5 events within the Arizona Mountain source zone in the past 50 years (1938, 1969, 1976) as well as several M $\geq$ 4 events, and several additional events with Modified Mercalli intensities of V (which are probably equivalent to about magnitude 4 (See Section 6.a.(6)(d)). Recurrence relations based

on this seismic activity have very low b-values (Figure 36, lines 1 and 7) which suggests that either the small-magnitude events are under reported or there were more magnitude 5 events during this time span than is normal. Unfortunately only time will reveal the "truth"; if there are no more magnitude 5 + events in the next hundred years or so, the b-value for the zone would assume a value closer to -1.0 which would be more consistent with worldwide-average seismic behavior. In an attempt to ameliorate any bias due to an inadequate seismic record, the historical seismicity listed in the various earthquake catalogs was analyzed. Sources of earthquake information used in the evaluation are listed in Section 6.a.(6). The earliest reports of seismicity in the province date from about 1830 but the population at that time was so small that many events could have gone unreported. By the 1850s, mining activity, and hence population density, in the zone increased to the level where most of the larger events ($M > 5$) were probably recorded, although with poor accuracy. It seems likely that some events in the 3 to 5 magnitude range might still have gone unreported after the 1850s either because they were not felt or because they were assumed to be caused by mine blasting. By the 1870s, the catalogs have abundant references to small earthquakes suggesting that the catalogs contain most of the events greater than magnitude 4.5, although complete certainty can be expected only for events after the 1960s.

Numerous calculations were performed using the various catalogs and record lengths. A few of the better constrained relationships are shown on Figure 36. All of the catalogs yielded low b-values that probably reflect incomplete records of small magnitude ($M < 4$) events. For example, the DNAG catalog gave an a-value of 1.852 with a b-value of -0.587 (Figure 36). Changing the b-value to -1.0 and anchoring the curve at magnitude 5 resulted

FHWA REGION	STATE	PROJECT NUMBER	REPORT NUMBER
9	ARIZ.	HPR-PL-1(37)344	FWHA-AZ92-344

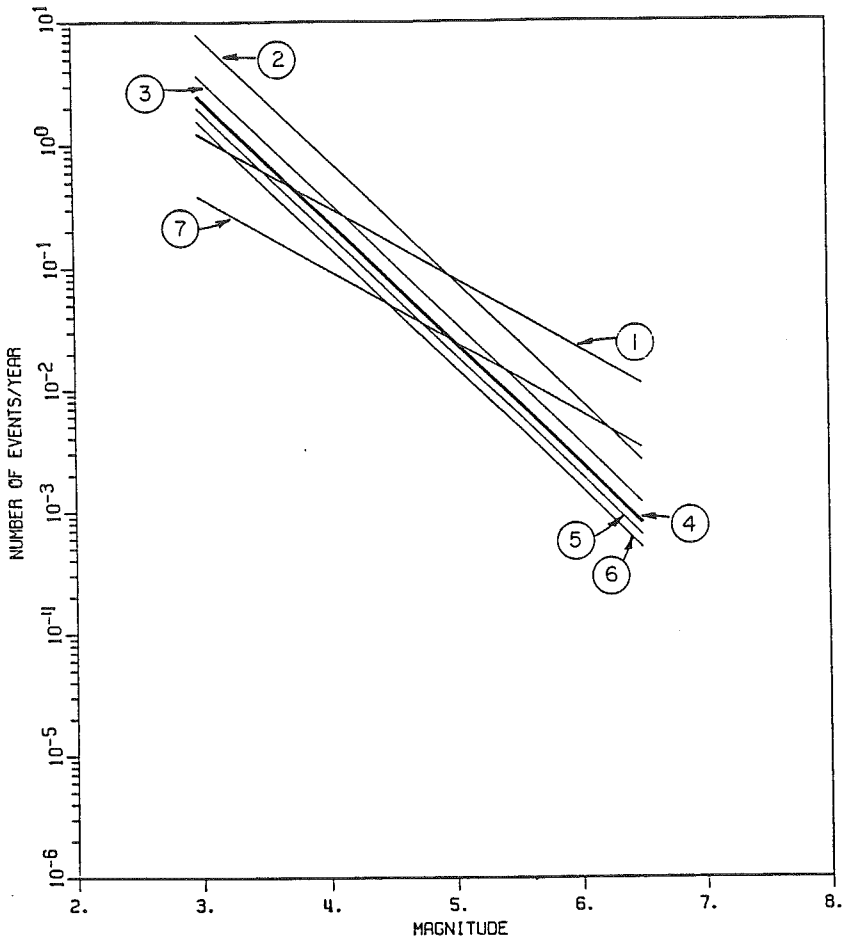

Curve Number	a - value	b - value	Source of Information
1	1.852	- 0.59	Seismicity, 1852-1985; DNAG Catalog
2	3.903	- 1.0	DNAG Seismicity with b = -1 anchored at M - 5
3	3.563	- 1.0	Seismicity representing M > 5 since 1910
4	3.398	- 1.0	Seismicity; Stover et. al. Catalog anchored at M = 5
5	3.301	- 1.0	Seismicity; representing M > 5 in past 150 years
6	3.194	- 1.0	Seismicity; Stover et. al. Catalog achored at M = 4.5
7	1.363	- 0.59	Seismicity; 1870 - 1992; Stover et. al. Catalog modified

ARIZONA DEPARTMENT OF TRANSPORTATION
ARIZONA TRANSPORTATION RESEARCH CENTER

FIGURE 36
RECURRENCE RELATIONS,
ARIZONA MOUNTAIN ZONE

in an a-value of 3.903 which is similar to the level of activity in the source zones of the Salton Trough in California (Figure 29; Table 1). Qualitatively, such a level of activity seems to be too high to be characteristic of neotectonic features in the Arizona Mountain zone. The Stover et al (1986) catalog was edited by eliminating the early part of the catalog and considering only the M > 4 and MMI > V events since 1870. This edited 122-year record resulted in the recurrence relationship shown by curve 7 on Figure 36 with a b-value similar to that from the DNAG catalog but a lower a-value. By using a b-value of -1.0 anchored at M = 5, an a-value of 3.398 was derived which approximately represents a level of seismicity that would yield the Arizona Mountain zone's maximum magnitude of 6.5 on the average of about once every 1250 years, a magnitude 5 every 40 years, and a magnitude 4 event every 4 years. This seems to be conservative and was judged to be reasonably representative of the neotectonic regime so these values were used in the construction of the acceleration coefficient contour map (Plate 2).

(4) Southern San Andreas Zone

The San Andreas fault seismic source zone is described in Section 6.c.(13) under the heading Salton Province. As discussed in that section, there has been little seismic activity along the Southern San Andreas fault. Geologic data suggest that slip-rates and the frequency of large events may be decreasing with time. However, regional plate-tectonic slip-rate budgets cannot be balanced by other faults in the province (such as the San Jacinto and Imperial faults) and, therefore, the San Andreas is considered to be the most likely source of the next great earthquake (Working

Group on California Earthquake Probabilities, 1988). Because of the lack of historical seismicity on the Southern San Andreas, the size and frequency of such a great earthquake can be based only on geological data and comparison to other segments of the fault to the north. Paleoseismicity studies (Sieh et al, 1989; Williams and Sieh, 1987) suggest that past events have ruptured long segments of the Southern San Andreas. Application of empirical earthquake-magnitude/rupture-length relationships (Slemmons, 1982; Bonilla et al, 1984; Wyss, 1979; Hanks and Kanamori, 1979), as well as direct comparison to historical earthquakes on the northern part of the San Andreas system indicate the fault is capable of generating a M_w = 8.0 earthquake.

Determining the recurrence interval for such an event is more difficult. Paleoseismic data indicate that the last three ruptures on the Southern San Andreas fault occurred at increasing intervals of about 150, 230, and 312 years. The variability of these intervals (which is about 50 to 100 percent), as well as the probability that aseismic creep is also occurring (Williams and Sieh, 1987), make determination of a slip rate for moment slip-rate calculations very tentative. The geologic data indicate rates as low as 3.3 mm/yr. If the regional plate-tectonic slip budget is to be balanced, at least 20 mm/yr and possibly as much as 25 mm/yr of slip are required on the Southern San Andreas fault.

To develop the appropriate recurrence relationship several variations of slip rate, rupture length, down-dip width, and b-values were analyzed. The analysis included about twenty different determinations that resulted in unnormalized a-values ranging from as high as 6.400 to as low as 1.588, and b-values ranging from -1.0 to -0.50. A few of the preliminary curves are shown on Figure 37 to illustrate the range of values and relative levels of

FHWA REGION	STATE	PROJECT NUMBER	REPORT NUMBER
9	ARIZ.	HPR-PL-1(37)344	FWHA-AZ92-344

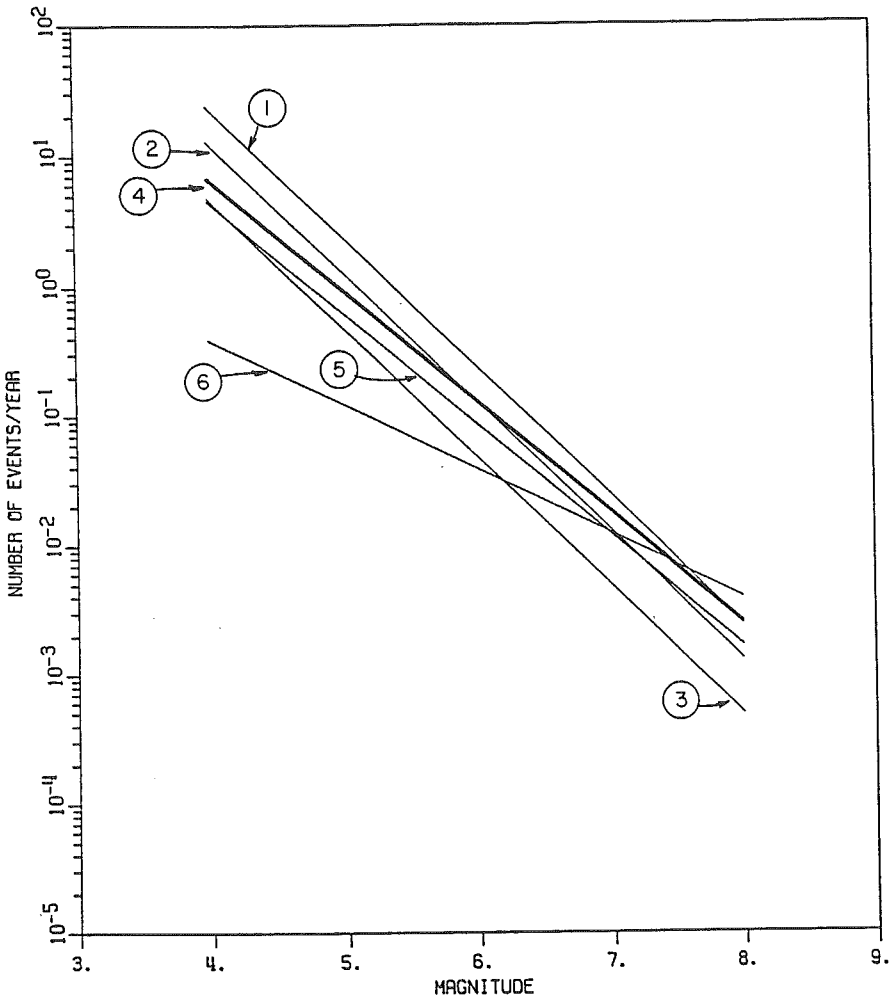

Curve Number	a - value	b - value	Slip rate mm/yr	Rupture Length (Km)	Downdip Width (Km)	Maximum Earthquake
1	5.384	- 1.0	25	170	15	8.0
2	5.111	- 1.0	20	170	10	8.0
3	4.685	- 1.0	15	85	10	8.0
4	4.274	- 0.86	20	170	15	8.0
5	4.098	- 0.86	20	170	10	8.0
6	1.588	- 0.50	20	170	15	8.0

ARIZONA DEPARTMENT OF TRANSPORTATION
ARIZONA TRANSPORTATION RESEARCH CENTER

FIGURE 37
RECURRENCE RELATIONS
SAN ANDREAS FAULT

the relationships. Considering the seismotectonic environment and the geologic information, the most realistic values seemed to be in the 5.300 to 4.800 range (these are not normalized values). However, using such high a-values results in a recurrence relationship with a very large number of small- and moderate-magnitude earthquakes which clearly are not characteristic of the Southern San Andreas fault seismicity. The Southern San Andreas fault, like many of the northern segments (e.g. Mojave, Carrizo), appears to be characterized by large infrequent ruptures and seismic quiescence for long periods of time. The options available to model this characteristic seemed to be either to use a very small b-value or to truncate the minimum magnitude range at a large magnitude. For the final model, the recurrence relationship for the San Andreas was truncated at a minimum magnitude of 6.5 (Figure 29), and a b-value of -0.86 was used (Table 1). The b-value was based on the one calculated from seismicity on the San Jacinto fault.

(5) San Jacinto Fault Zone

As discussed in Section 6.C.(13) under the heading Salton Province, the San Jacinto fault zone appears to have been the source of numerous small to large (M_L7) historical earthquakes. The San Jacinto fault is the most seismically active fault considered in this investigation and as such there is an abundance of information. Figure 38 shows a few of the better constrained relationships. After numerous iterations to test the range of appropriate values and the sensitivities of the various methods and input parameters, the recurrence relation used in the final analysis was based on seismicity from the Caltech earthquake catalog. Compilation of the historical seismicity record yields an a-value of 3.957 and a b-value of -0.861 (Table 1; Figure 29). These values were compared to values generated

FHWA REGION	STATE	PROJECT NUMBER	REPORT NUMBER
9	ARIZ.	HPR-PL-1(37)344	FWHA-AZ92-344

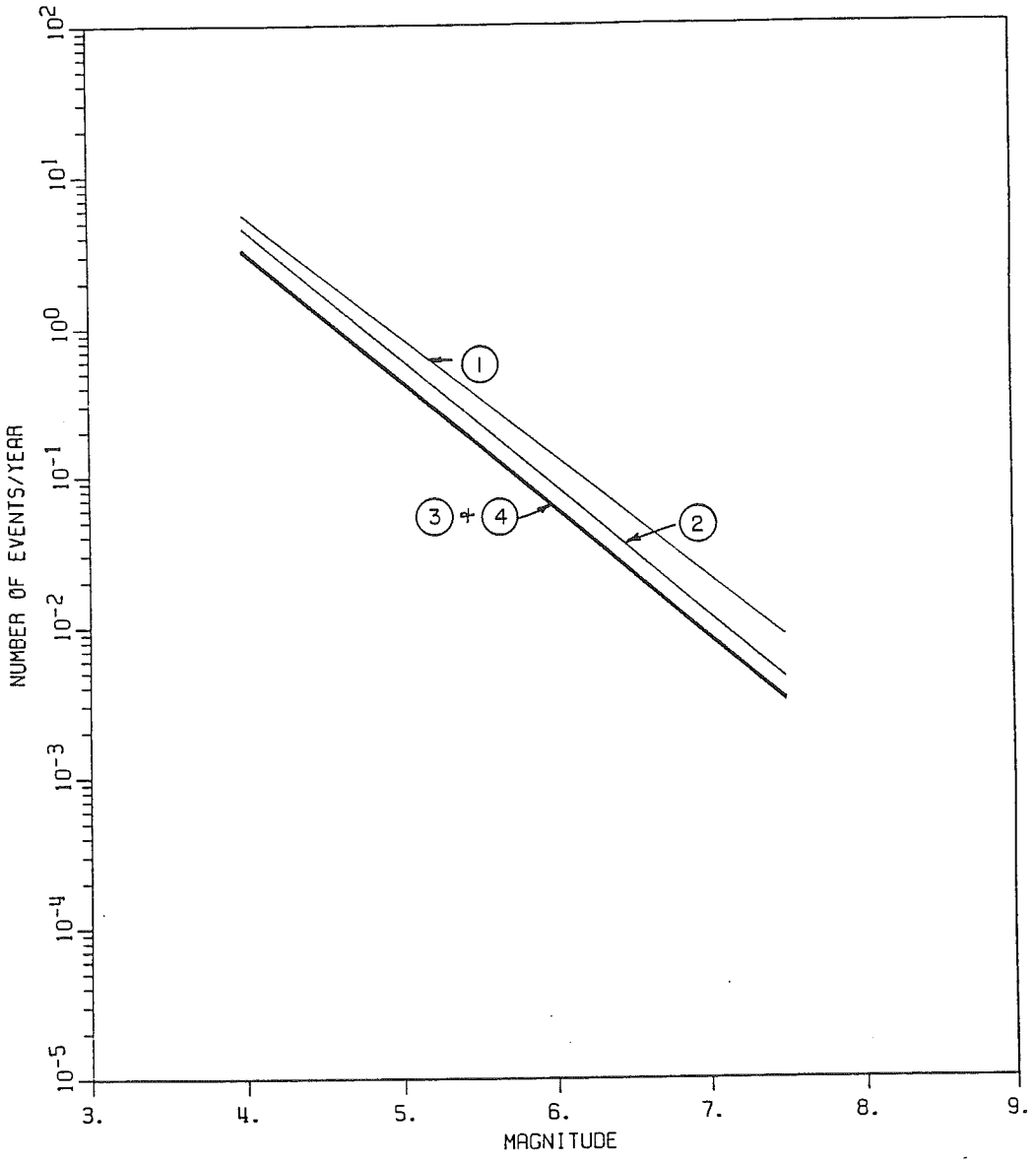

Curve Number	a - value	b - value	Source of Information
1	3.970	- 0.81	Working Group Calif. EQ Probabilities, 1988
2	4.100	- 0.86	Bayesian Analysis
3	3.957	- 0.86	Historical Seismicity
4	3.938	- 0.86	Moment Slip Rate

ARIZONA DEPARTMENT OF TRANSPORTATION
ARIZONA TRANSPORTATION RESEARCH CENTER

FIGURE 38
RECURRENCE RELATIONS
SAN JACINTO FAULT

by numerous other published analyses and numerous calculations from moment slip-rate analyses and for various earthquake catalogs.

The a-value from the preferred moment slip-rate calculation is 3.938. This is the value resulting from using a b-value of -0.86, slip rate of 10 mm/yr, rupture length of 75 km, and downdip width of 15 km. All these values are consistent with abundant geological, geophysical, and seismological data.

Comparisons to the analysis of the Working Group on California Earthquake Probabilities (1988) gives similar results. The Working Group estimated that the probability of at least one M = 7.0 earthquake during the next 30 years was 50 percent. Assuming a Poisson process, the corresponding yearly recurrence rate, N, was computed from the formula $N = -[\ln(1-p)]/30$. The resulting annual rate, 0.0231/yr, was used to establish the a-value in the standard recurrence equation (Equation 7-1) using a b-value of -0.805 which was derived from the National Geophysical Data Center earthquake catalog for events between 1931 and 1987. The resulting a-value was 3.970 (Figure 38, Curve 1).

Campbell (1983) used a Bayesian analysis for extreme earthquake occurrences to estimate recurrence intervals for large-magnitude earthquakes. Using his recurrence relationship of one M = 7.1 event per 100 years yields an a-value of 4.100 when the b-value -0.86 is used (Figure 38, Curve 2) which is consistent with the other data.

A particularly important aspect of the investigation was to verify that the moment slip-rate method could be used to realistically model earthquake hazards on a regional scale. Previous studies had shown some inadequacies

(Schell, 1991). A great deal of time and effort was spent cross-checking and calibrating the method to the San Jacinto seismicity data. The working premise was that the recurrence relation from the abundant seismicity data set available for the San Jacinto fault would provide the best-constrained recurrence relationship available. So, if the moment slip-rate calculations yielded recurrence curves that were similar to those derived from the seismicity data base, the method could be applied to other faults with reasonable confidence. As shown on Figure 38 the two relationships (curves 3 and 4) are nearly identical. This provides confidence that the method can be applied to seismic hazard analyses such as this investigation.

c. Comparisons of Seismic Source Zones and Recurrence Relationships to Other Studies

In the early stages of this investigation it became apparent that the resulting contour map would have some substantial differences from existing maps. To determine what was causing the differences and to evaluate whether those differences were valid, comparisons were made to existing models at various stages of the process.

Most of the comparison studies were directed at the latest maps by Algermissen and his colleagues of the U.S. Geological Survey (Algermissen et al, 1990). Comparison of the final contour maps is discussed in Section 9. This section addresses seismic source zones and recurrence relationships. These are discussed together because changes in source zone boundaries may result in associating different earthquakes to different source zones thereby affecting the recurrence relationships.

(1) Comparison of Seismic Source Zones

Figure 39 shows a portion of the source zones map from Algermissen et al (1982) and Thenhaus et al (1980), hereafter referred to as the Algermissen model. The source zones on this map are essentially the same zones used for the 1990 version of the national contour map (Algermissen, 1991, personal communication; Perkins, 1991, personal communication). Figure 23 shows the seismic sources established for this investigation. At first glance the two maps appear quite different, but more-detailed examination reveals many similarities. For example, most of the zones in California are very similar on both maps. Some minor differences may be partly due to different map projections. In general, the differences are too small to warrant comment.

Perhaps, the major difference in California is the San Andreas fault (Algermissen zone C016 and our Southern San Andreas Fault zone). Zone C016 extends southeasterly to the southwestern tip of Arizona, whereas we terminate the Southern San Andreas zone along the eastern shore of the Salton Sea where the mapped surface trace ends. As discussed in Section 6.c.(13), geology, seismicity, and geophysical data indicate that most of the motion between lithospheric plates steps over to the central part of the Salton Trough, and the area southeast of the surface trace of the San Andreas fault is only a zone of subsidiary vertical block tectonics which we consider to be the Salton Periphery zone. The Algermissen model combined the San Jacinto and the Imperial faults into one zone whereas in this study they are zoned separately but with the same recurrence relationships (Table 1). An important difference involves the two small source zone gaps in the Algermissen model along the California-Mexico border. In our model these two

FHWA REGION	STATE	PROJECT NUMBER	REPORT NUMBER
9	ARIZ.	HPR-PL-1(37)344	FWHA-AZ92-344

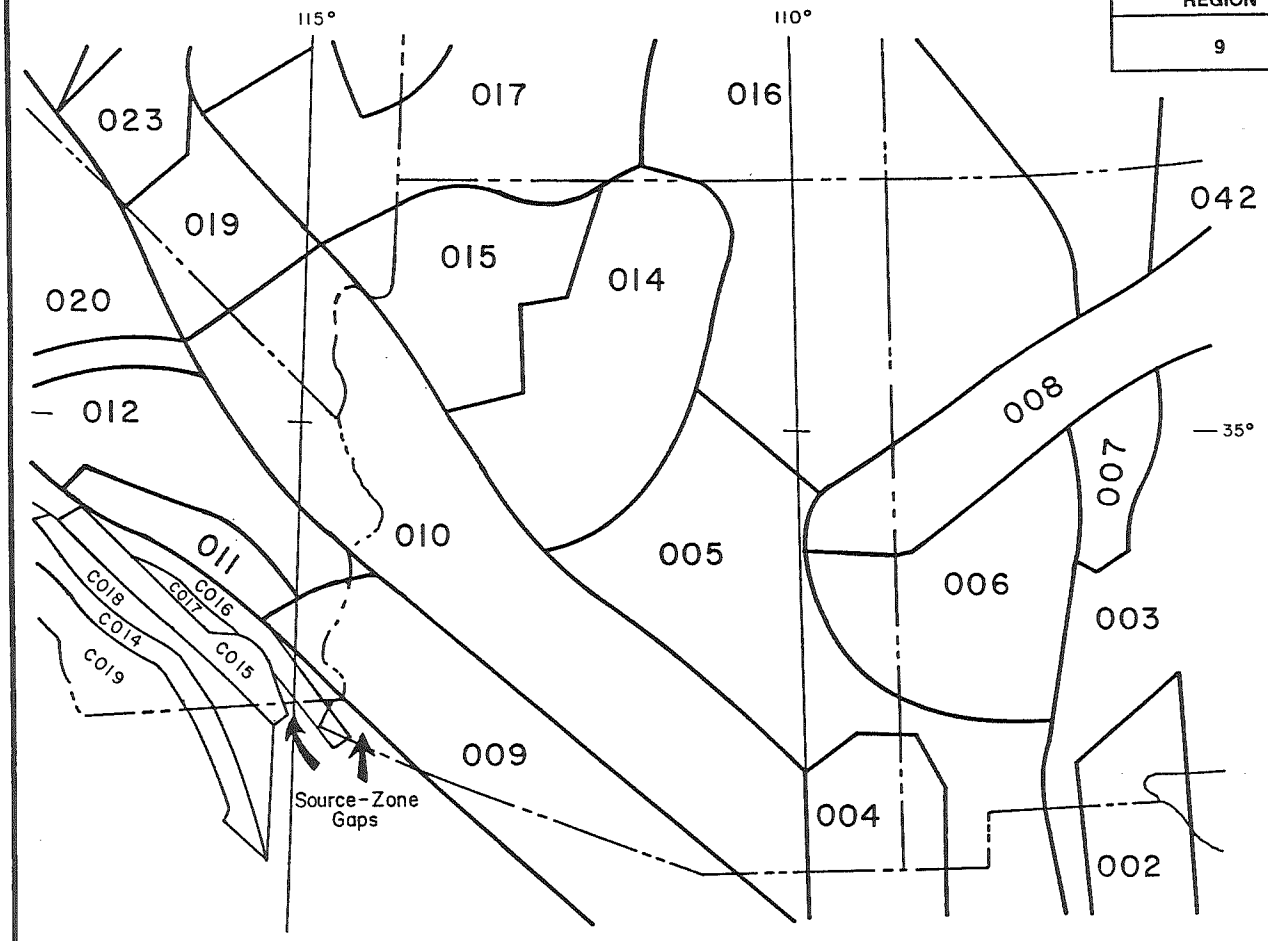

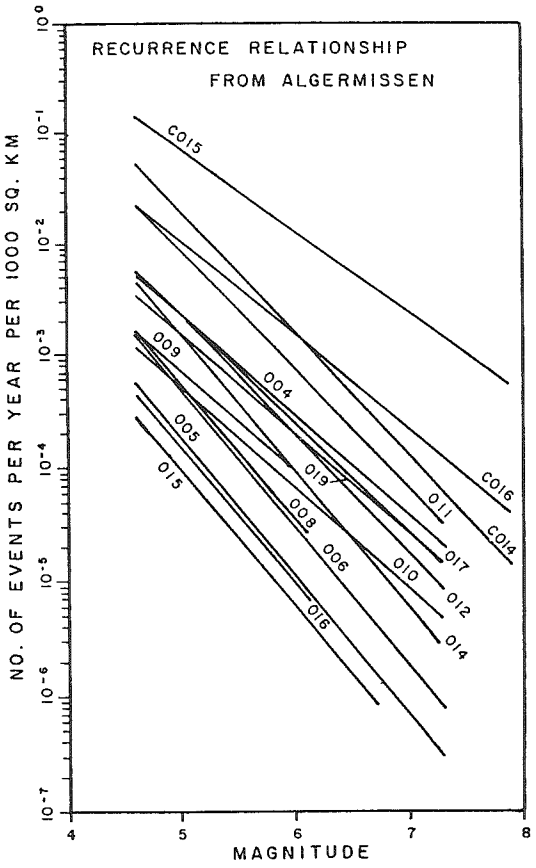

SOURCE: Algermissen, et al., 1982
Thenhaus, et al., 1980

ARIZONA DEPARTMENT OF TRANSPORTATION
ARIZONA TRANSPORTATION RESEARCH CENTER

FIGURE 39
SEISMAC SOURCE ZONES AND RECURRENCE RELATIONS FROM ALGERMISSEN MODEL

gaps have a moderate level of seismicity which may have an important impact on ground-motion contours in southwestern Arizona. Also, our model included earthquakes from northern Mexico.

Within Arizona, the boundary differences are more substantial although the basic rationale for both zonations is similar. The Algermissen model shows the Sonoran zone as two separate zones (009, 010). This is probably a reflection of the presence of more earthquakes in the southwestern part of the Sonoran Desert as shown by some earthquakes catalogs. However, most of these events are poorly located and reanalysis of original seismograms by several researchers (ANPP, 1979; Mokhtar, 1979; Brumbaugh, 1992, personal communication) have suggested that many of these poorly located events really occurred to the southwest in the Salton Trough region. In addition, the validity of relying on so few events (20 to 30) for a statistical analysis is questionable. There are so few events in the Sonoran area that just a couple new events in the northeastern part of the zone would result in a relatively even distribution of seismicity throughout the zone. Both of these aspects, combined with the similarity of neotectonic structures, geologic history, geomorphology, and geophysics (see Section 6.c.(15)) suggest that the Sonoran area is more appropriately regarded as one source zone.

The Algermissen model does not recognize the Mexico Basin and Range area to the same extent as in this study. Their zone (004) basically comprises just a small area around the Pitaycachi fault, the source of the 1887 rupture and its aftershocks. This does not account for the several other Basin and Range frontal fault systems in the area with paleoseismic rupture histories similar to the Pitaycachi fault with recurrence intervals

in the 10^5 years range (see Section 6.c.(9)). Even if zone 004 is appropriate, the areas to the east and west should not be included with the zones 005 and 009; the geology, neotectonics, paleoseismic history, geophysics, and geomorphology are too dissimilar.

Zone 015 of the Algermissen model comprises the Southern Hurricane and Toroweap faults and the surrounding region characterized by numerous long neotectonic faults, many of which have been active in late Quaternary time (Section 6.c. (19)). In this study the area is zoned as the Hurricane-Wasatch zone and includes the area to the northeast in Utah and includes the complete lengths of the Hurricane and Toroweap faults. Although one might agree that the area in Arizona should be separated from the Wasatch Front fault system to the north, the change in neotectonic characteristics is not significant until north of the latitude of Zion Canyon, a much larger area than zone 015. Historically this area has not had much earthquake activity but the geology indicates some of the most abundant prehistorical (paleoseismic) activity in the state and our zone is based on these faulting characteristics rather than only historical seismicity.

Some of the largest differences between the Algermissen model and the model presented herein are in their zones 014, 005, 006, and 008. These four zones coincide with the Arizona Mountain, Southwestern Plateau Margin, and Southeastern Plateau Margin zones (Figure 23). Zone 014 includes the most abundant historical seismicity and as such may be appropriate for a seismicity-based model. However, there are significant differences in geologic characteristics which led to definition of the zones as shown on Figure 23. Primarily, the Arizona Mountain zone is an area characterized by northwest-trending normal faults with moderately well-developed, tilted,

fault-block basins and ranges. Except for the Big Chino, Verde, and Aubrey faults, which are considered as discrete seismic sources, the area has very similar geologic structure, paleoseismic history, geomorphology, volcanic history, and geophysics throughout the zone. Also the historical seismicity is quite similar throughout; if the 1976 Prescott event and its aftershocks were not shown on the seismicity map, the level of seismicity would be even more consistent. In other words, in areas of low activity, seismicity-based zonations can be controlled by the occurrence of just one event. Considering the periodicity of seismicity in areas of such low-level activity, just one more event in the southeastern part of the Arizona Mountain zone would result in an even distribution of historical seismicity throughout the zone. To prevent having to redraw source boundaries after every new earthquake, source-zone boundaries should be based on a wider group of pertinent characteristics, which is the underlying premise of our method. Again, using the longer time periods represented by the neotectonic regime seems to provide a more-representative and more-realistic model of seismic potential.

The area to the north of the Arizona Mountain zone, around the southern margin of the Colorado Plateau, is divided into two zones (Figure 23). The Algermissen model also has two zones (Figure 39) but the boundaries are quite different from those on Figure 23. The Southwestern Plateau Margin zone is somewhat similar to part of zone 014 and the Southeastern Plateau Margin is similar to zone 008, except zone 008 extends across the Rio Grande Rift apparently representing the Jemez Lineament. Data on the Jemez lineament are such that arguments can be formed from several perspectives and it seems to come down to judgement. There is little geological or seismological evidence that the Jemez Lineament represents a neotectonic feature, and the north-south trending Rio Grande Rift seems to be the dominant feature in the area.

About the only aspect of the Jemez lineament that reflects neotectonics is the young volcanism. This young volcanic activity is also an important element in definition of the Southeastern Plateau Margin zone (Section 6.c.(17), but we see the volcanism as being related to extension and crustal breakup along the southern margin of the Colorado Plateau, and the volcanism east of the Rio Grande Rift as being unrelated to that in Arizona. The fact that the active normal faulting in the Rio Grande Rift is dominant and cuts through the Jemez Lineament supports this interpretation. The northward migration of volcanic activity from the Basin and Range areas of Arizona into the southern margin of the Colorado Plateau has been recognized by many geoscientists (for example, Tanaka et al, 1984; Menges, 1983; Leudke and Smith, 1978; Shoemaker et al, 1978) and fits well into the neotectonic geologic structure which indicates a potential for faulting in the Plateau margin zones associated with the volcanism (but less than in the Arizona Mountain zone).

The Southwestern Plateau Margin zone is also characterized by the young volcanism, as well as abundant neotectonic faulting (Plate 1), and a relatively high level of historical seismicity (Figure 26). The central part of this area is defined as the San Francisco Volcanic Field zone (Section 6.c.(11)). Our analyses of faulting in the area shows a very high abundance of Quaternary faulting (Section 3.c.(2)) which coincides with the areas of highest historical seismicity. We suspect that this higher rate of neotectonic strain is related to the volcanic activity and this has resulted in reactivation of basement faulting and hence higher levels of seismicity in the area. However, as discussed in Section 6.c.(11) and (18), the greater abundance of younger faulting may be as much a result of the presence of young volcanic flows which allow better dating of the faults than it is due

to higher rate of tectonic activity. This is one zone in Arizona where historical seismicity was one of the controlling elements in establishing source zone boundaries and recurrence relationships.

(2) Comparison of Recurrence Relations

We have compared the recurrence relationships to the Algermissen model to determine where differences exist so we could evaluate the effects of the differences on the seismic acceleration contour map. Algermissen et al (1982) made use of the Modified Mercalli Maximum Intensity (I_o) scale rather than the magnitude (M) scale in their recurrence relations. The Gutenberg and Richter (1942) relationship ($M = 1.3 + 0.6I_o$) was used by Algermissen et al for conversions between intensity and magnitude scales. Figure 39 is a composite plot of the recurrence relations from Algermissen et al (1982) after converting their intensity values back to magnitude using the Gutenberg and Richter magnitude-intensity relation. Figures 40a thru 40d shows plots of our recurrence relations compared to the same zones of the Algermissen model. Of course, some of the differences are due to different source zone boundaries. In cases where the zones were different, Figure 40 shows more than one zone. For example, the Arizona Mountain zone described above and in Section 6.c.(1) is compared to zones 005, 006, and 014. Many of the recurrence relations compare favorably and are not discussed in detail. For example, most of the zones in California are similar in both models. This is understandable because the seismicity in California is at a high enough level that it can be considered fairly representative of the neotectonic regime. The California zones that are substantially different are the Southern San Andreas fault zone and the source zone gaps along the

FHWA REGION	STATE	PROJECT NUMBER	REPORT NUMBER
9	ARIZ.	HPR-PL-1(37)344	FWHA-AZ92-344

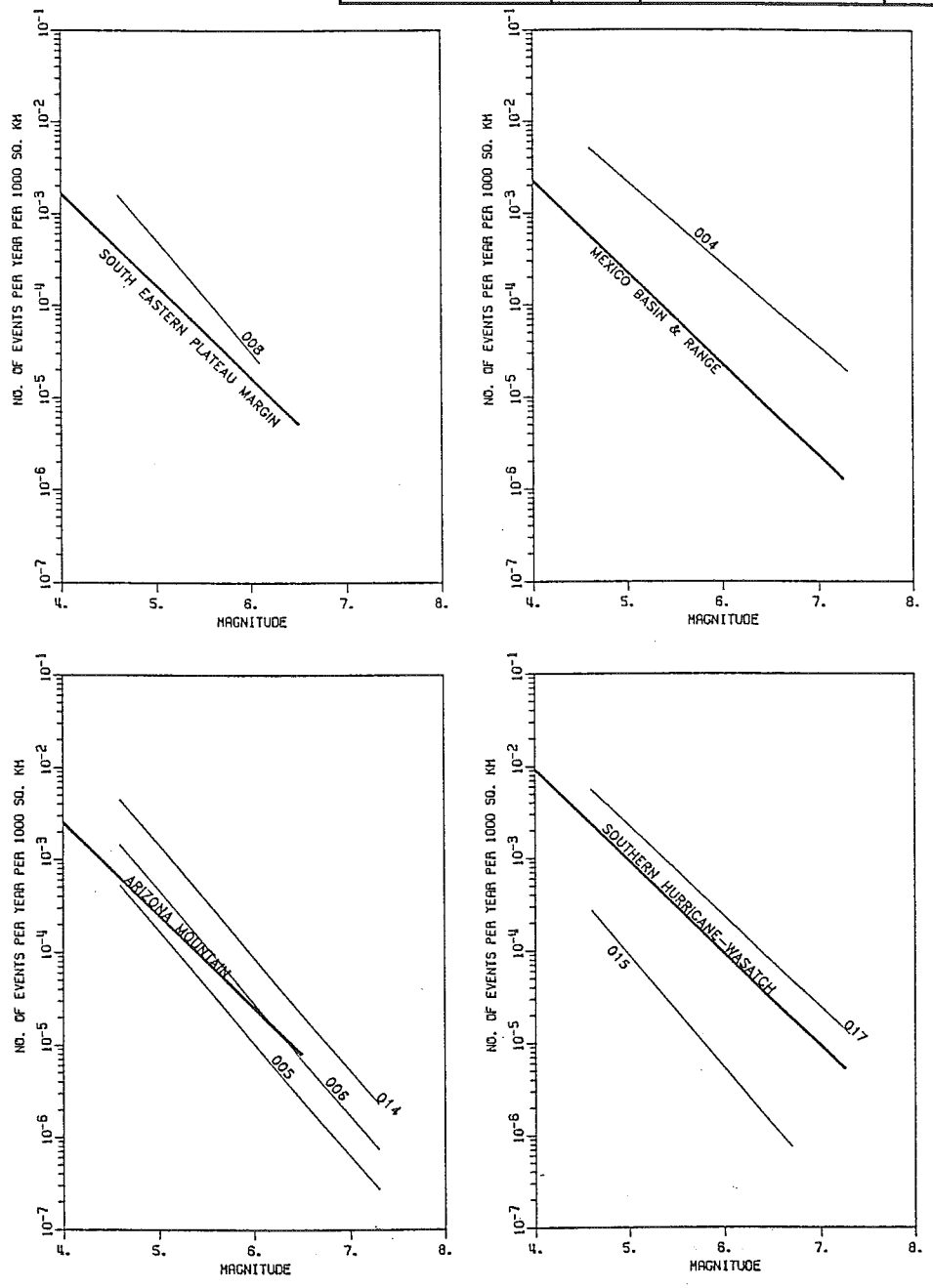

AXIAL CORTEX — RECURRENCE RELATIONSHIP DETERMINED FROM ARIZONA SEISMIC MAP PROJECT

012 — RECURRENCE RELATIONSHIP FROM ALGERMISSEN (1982)

ARIZONA DEPARTMENT OF TRANSPORTATION

ARIZONA TRANSPORTATION RESEARCH CENTER

FIGURE 40a
COMPARISON OF RECURRENCE RELATIONSHIPS

FHWA REGION	STATE	PROJECT NUMBER	REPORT NUMBER
9	ARIZ.	HPR-PL-1(37)344	FWHA-AZ92-344

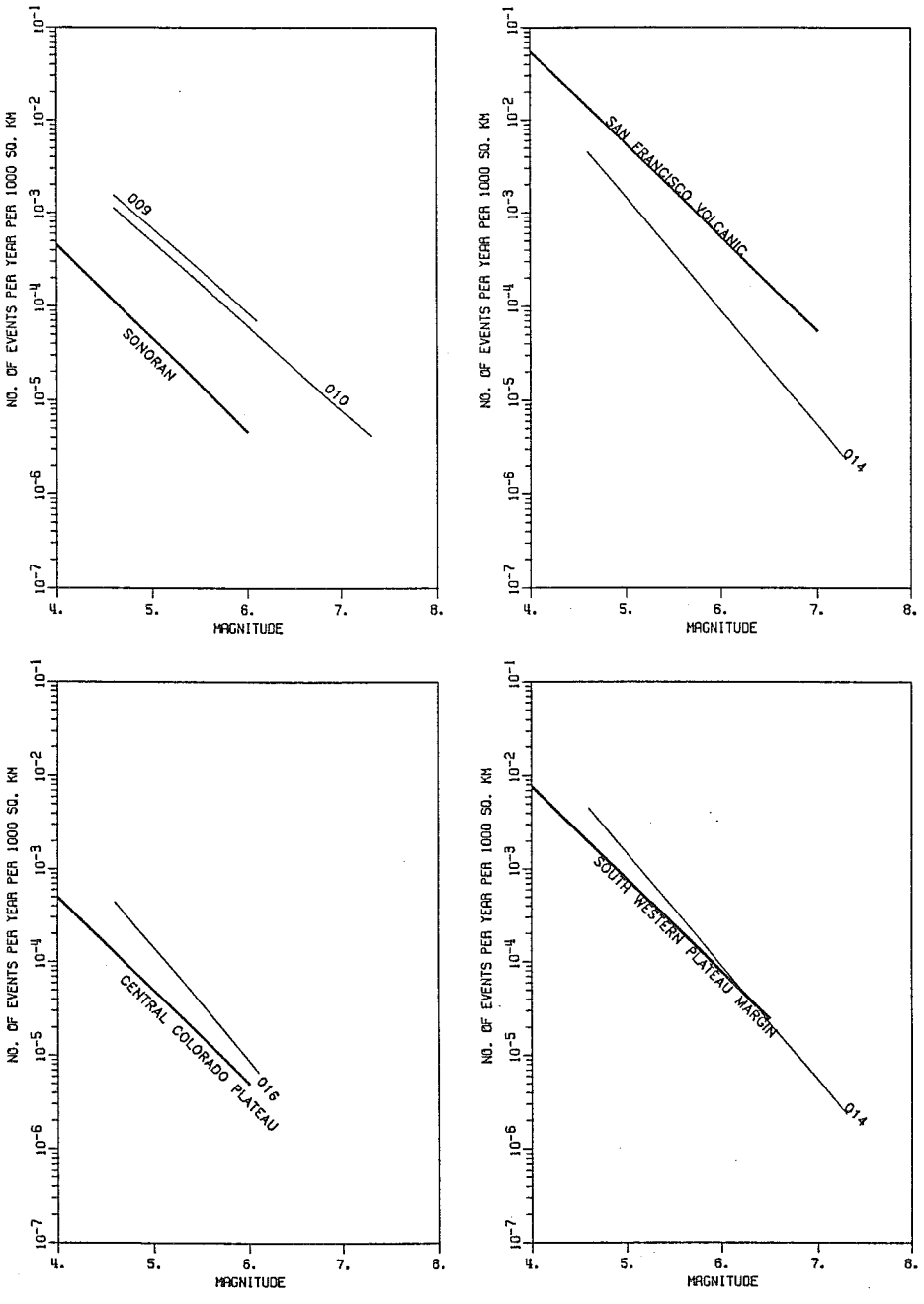

AXIAL CORTEX — RECURRENCE RELATIONSHIP DETERMINED FROM ARIZONA SEISMIC MAP PROJECT

012 — RECURRENCE RELATIONSHIP FROM ALGERMISSEN (1982)

ARIZONA DEPARTMENT OF TRANSPORTATION

ARIZONA TRANSPORTATION RESEARCH CENTER

FIGURE 40b
COMPARISON OF RECURRENCE RELATIONSHIPS

FHWA REGION	STATE	PROJECT NUMBER	REPORT NUMBER
9	ARIZ.	HPR-PL-1(37)344	FWHA-AZ92-344

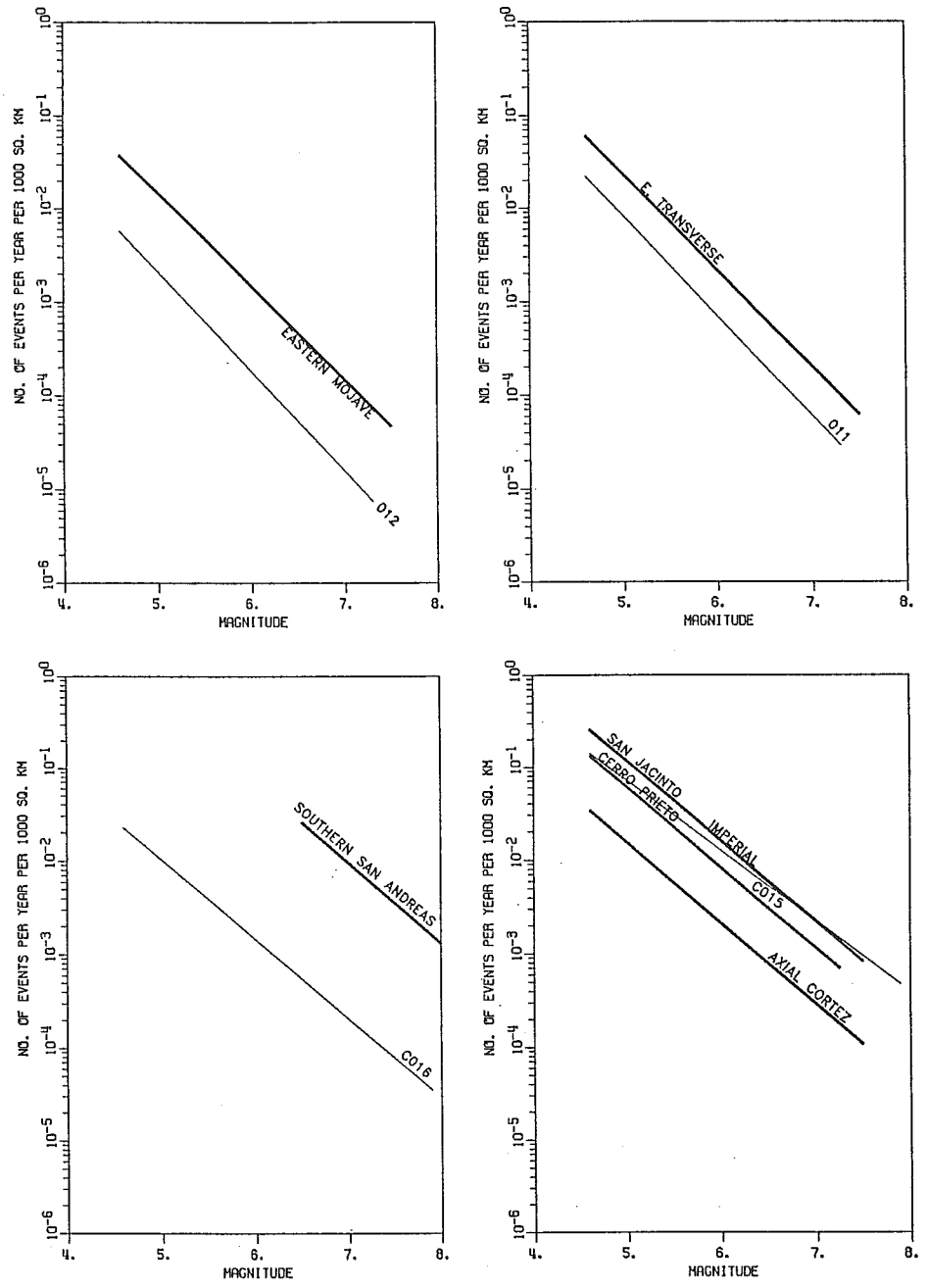

AXIAL CORTEX — RECURRENCE RELATIONSHIP DETERMINED FROM ARIZONA SEISMIC MAP PROJECT

012 — RECURRENCE RELATIONSHIP FROM ALGERMISSEN (1982)

ARIZONA DEPARTMENT OF TRANSPORTATION

ARIZONA TRANSPORTATION RESEARCH CENTER

FIGURE 40c
COMPARISON OF RECURRENCE RELATIONSHIPS

FHWA REGION	STATE	PROJECT NUMBER	REPORT NUMBER
9	ARIZ.	HPR-PL-1(37)344	FWHA-AZ92-344

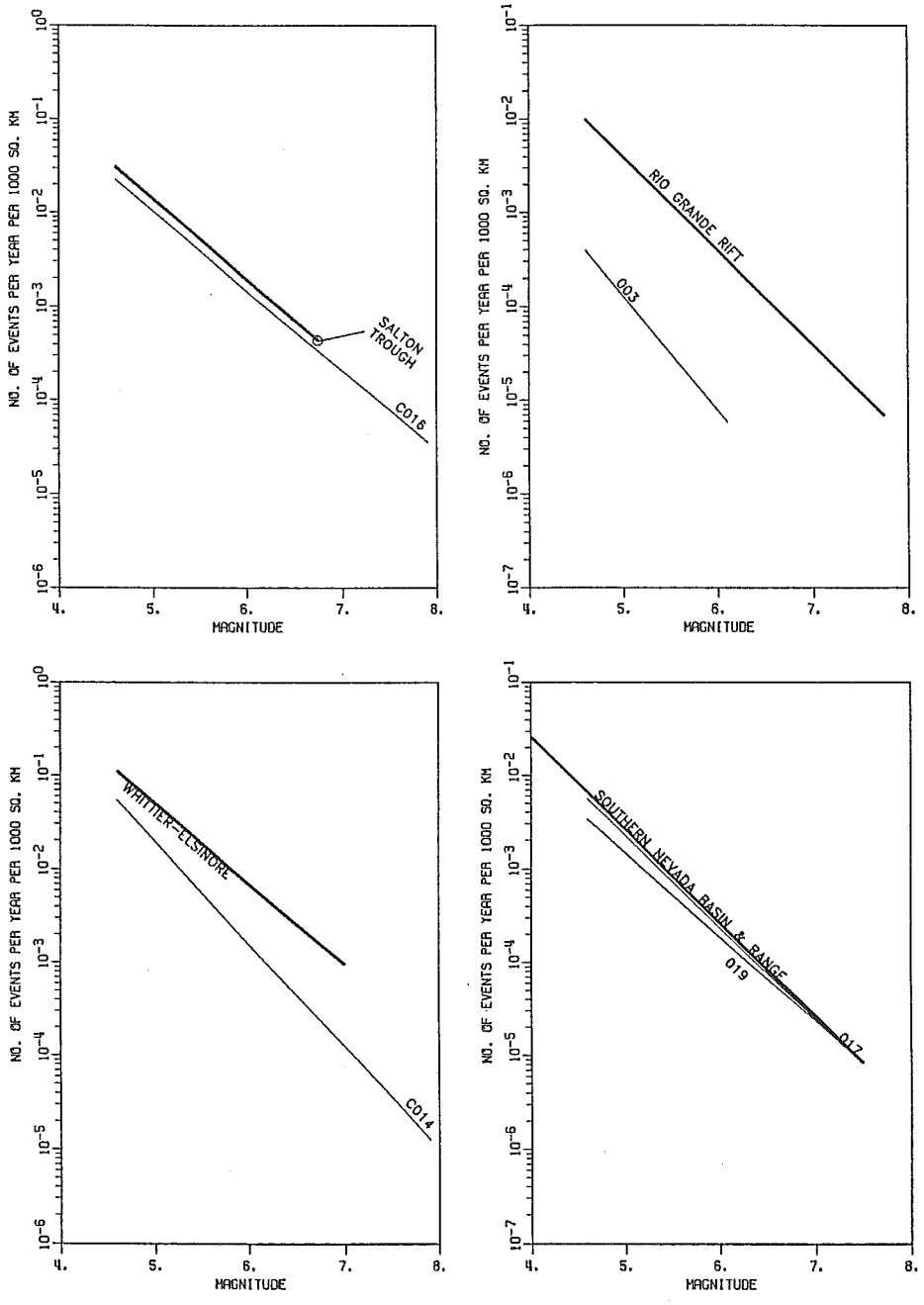

AXIAL CORTEX — RECURRENCE RELATIONSHIP DETERMINED FROM ARIZONA SEISMIC MAP PROJECT

012 — RECURRENCE RELATIONSHIP FROM ALGERMISSEN (1982)

ARIZONA DEPARTMENT OF TRANSPORTATION

ARIZONA TRANSPORTATION RESEARCH CENTER

FIGURE 40d
COMPARISON OF RECURRENCE RELATIONSHIPS

California-Mexico border (Figure 39) which were discussed in the preceding section.

As discussed in Section 6.c.(10), there has been little historical seismicity associated with the Southern San Andreas fault. Geological and geophysical information was used to establish the zone, and the recurrence relations were based on paleoseismic input to moment slip-rate calculations (Section 7.b.(4)).

The two differences that change the ground motion contours the most are the Mexico Basin and Range zone in the southeastern corner of the state and the Southern Hurricane-Wasatch zone, the Hurricane fault, and Toroweap fault in the northwestern corner of the state. The final ground motion contour maps (Plate 2a through 2d) essentially have reversed these two areas from those on the Algermissen et al (1982; 1990) contour maps. Under the Algermissen model, the southeast corner of the state had the potential for the highest acceleration and the northwest was the lowest. On Plates 2a through 2d, these contributions are reversed with one of the highest inputs coming from the northwestern part of the state. Geologic investigations in the past decade, as discussed in Section 6.c.(19) and 7.b.(1), have revealed that both the Hurricane and the Toroweap fault, as well as other faults in the northwest (for example, the Washington fault) have had major ruptures within geologically recent time and the recurrence intervals on these faults are only a few thousand years (Jackson, 1990; Menges and Pearthree, 1983; Anderson and Christenson, 1990; Hecker, 1992). On the other hand, investigations in the southeastern area, Sections 6.c. (9) and 7.b.(2), have shown that, even though faults have ruptured in relatively recent geologic times, the recurrence intervals are on the order of 10^5 years (Bull and Pearthree,

1988; Pearthree and Calvo, 1987; Pearthree, 1991, personal communication). If it wasn't for the 1887 earthquake and its aftershocks, the southeastern part of the state would not have much more seismicity than the Arizona Mountain or Southwestern Plateau Margin zones. Again, this illustrates how much control one event can have in areas of low or moderate activity when only historical seismicity is considered.

In summary, there are many small differences and a few major differences between the seismic zonation and recurrence relationships assigned for this investigation and the Algermissen model (1982, 1990). Although judgements certainly were involved, the primary control over the zones for this investigation was paleoseismic and other geologic information. If the basic premises that the earthquake record is too short and that earthquakes are caused by fault displacements are accepted, then the results of this investigation should be representative of the seismic hazard for the Arizona area.

8. PROBABILISTIC MODEL

One of the objectives of this project was to incorporate more-refined local geological and seismological data into the development of the acceleration contour map for Arizona. To minimize uncertainties arising from probabilistic modeling procedures, the SEISRISK III computer program (Bender and Perkins, 1987) was used to conduct the probabilistic analyses. This is basically the same program used in the development of the "Probabilistic earthquake acceleration and velocity maps for the United States and Puerto Rico" (Algermissen et. al., 1990). The Acceleration Map for 90-percent non-exceedance in 50 years from the Algermissen study was adopted by AASHTO for bridge design (Buckle, 1991). The principal differences between the new map developed from this project and the corresponding Acceleration Coefficient map adopted by AASHTO, would therefore, emanate from application of the newly acquired geological and seismological data.

The methods used in most probabilistic seismic hazard analyses were based on the principals first defined by Cornell (1968). Variations in the fundamental assumptions and the basic elements used in various existing probabilistic models such as those of Bender and Perkins (1987), Cornell (1968), and McGuire (1976) are minor. However, the basic elements of a probabilistic analysis are briefly reviewed in this section. Detailed documentation of the SEISRISK III program has been adequately covered by Bender and Perkins (1987). Documentation of the input parameters and results of the probabilistic analyses are presented in Sections 8.c and 9.

a. General Approach

The principal elements in a probabilistic analysis are illustrated in Figure 41. There are three basic input components:

- o configuration of seismic source zones (area and line sources),
- o recurrence relationships, and
- o attenuation relationships.

The configuration of seismic source zones for this study and the corresponding recurrence relationships are discussed in Sections 6 and 7. The attenuation relationships used in the analyses are presented in the following section, followed by a discussion of the basic assumptions implicit in the probabilistic method and interpretation of results of a probabilistic analysis.

b. Attenuation Relations

An attenuation relation is an expression of the dependency of a given ground-motion parameter with the size of an earthquake (usually in terms of Magnitude), and the distance between the site and the seismic source. The ground motion parameters are typically peak ground acceleration (PGA) or peak ground velocity (PGV). Although, other factors such as local soil conditions will affect ground motion, the independent variables in most

FHWA REGION	STATE	PROJECT NUMBER	REPORT NUMBER
9	ARIZ.	HPR-PL-1(37)344	FWHA-AZ92-344

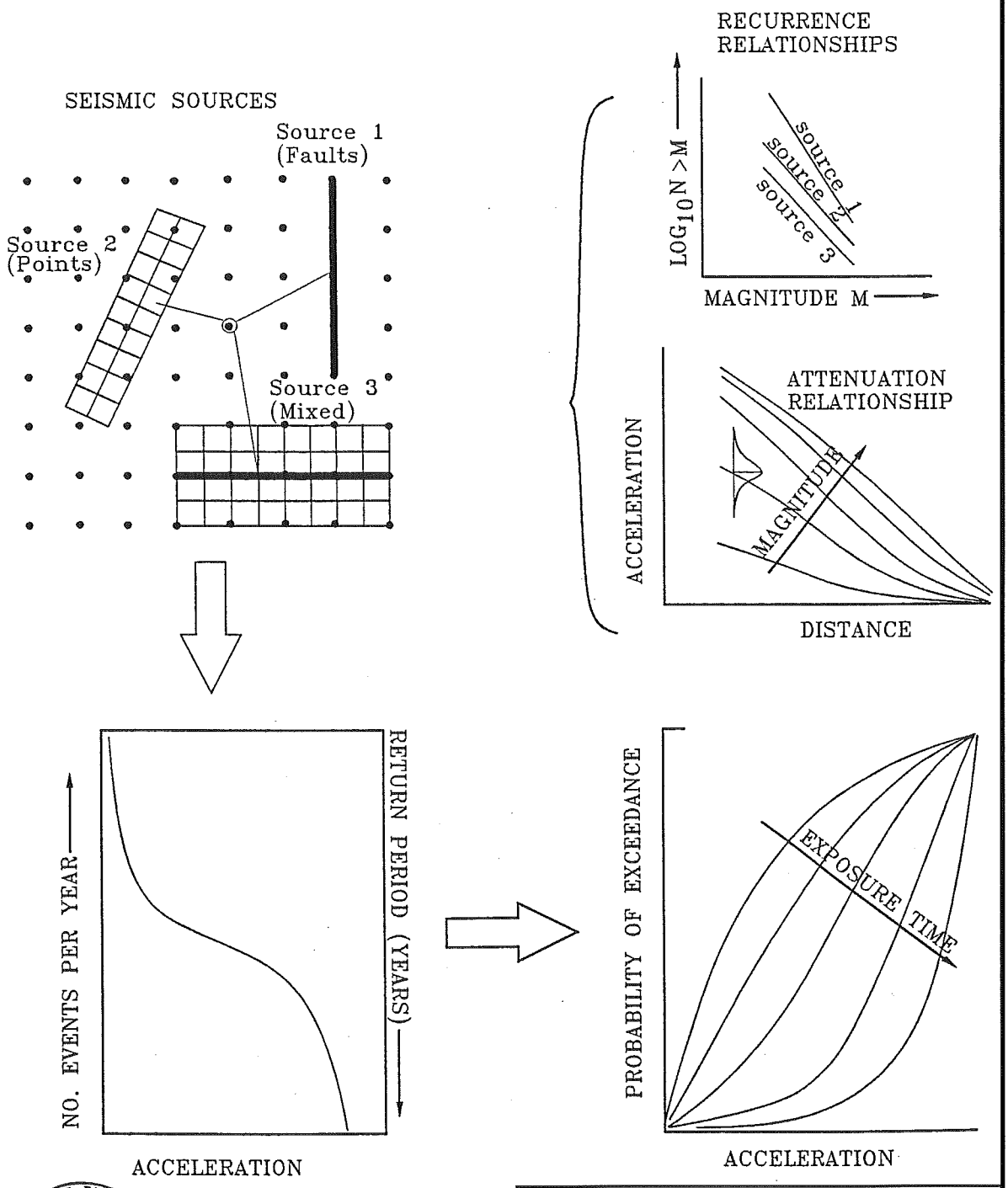

ARIZONA DEPARTMENT OF TRANSPORTATION
ARIZONA TRANSPORTATION RESEARCH CENTER

FIGURE 41
PRINCIPAL ELEMENTS IN A PROBABILISTIC HAZARD MODEL

cases are limited to earthquake magnitude and source-site distance. Most attenuation relationships in use today are based on regression analysis of ground motion records.

The AASHTO design specifications utilize the response spectrum method for bridge design. Therefore, a design response spectrum is the ultimate product representing the intensity of the earthquake loading necessary for bridge design. As shown in Figure 42, a response spectrum is the relationship between the spectral acceleration and the natural period of vibration of a single-degree-of-freedom system for a given or assumed value of damping. The acceleration coefficient serves as an anchor point of the response spectrum curve shapes in the AASHTO design specification.

(1) A_a versus A_v and AASHTO Acceleration Coefficient, A Maps

Many factors are considered in the construction of a design response spectrum, including the structural period and the site soil condition. In seismic design guidelines for buildings (e.g. ATC-3-06 and NEHRP provisions), two acceleration coefficient maps are used to define the level of the response spectrum: an Effective Peak Acceleration Coefficient, A_a map, and an Effective Peak Velocity-Related Acceleration Coefficient, A_v map. Both maps are based on a 90-percent probability of non-exceedance in 50 years. The A_a coefficient is based on an attenuation relationship for PGA and is appropriate as an anchor point at zero-second period in the response spectrum curve shape and defines the peak spectral accelerations (2.5 or 2.0 A_a) for design of structures which have a short fundamental period (less than

FHWA REGION	STATE	PROJECT NUMBER	REPORT NUMBER
9	ARIZ.	HPR-PL-1(37)344	FWHA-AZ92-344

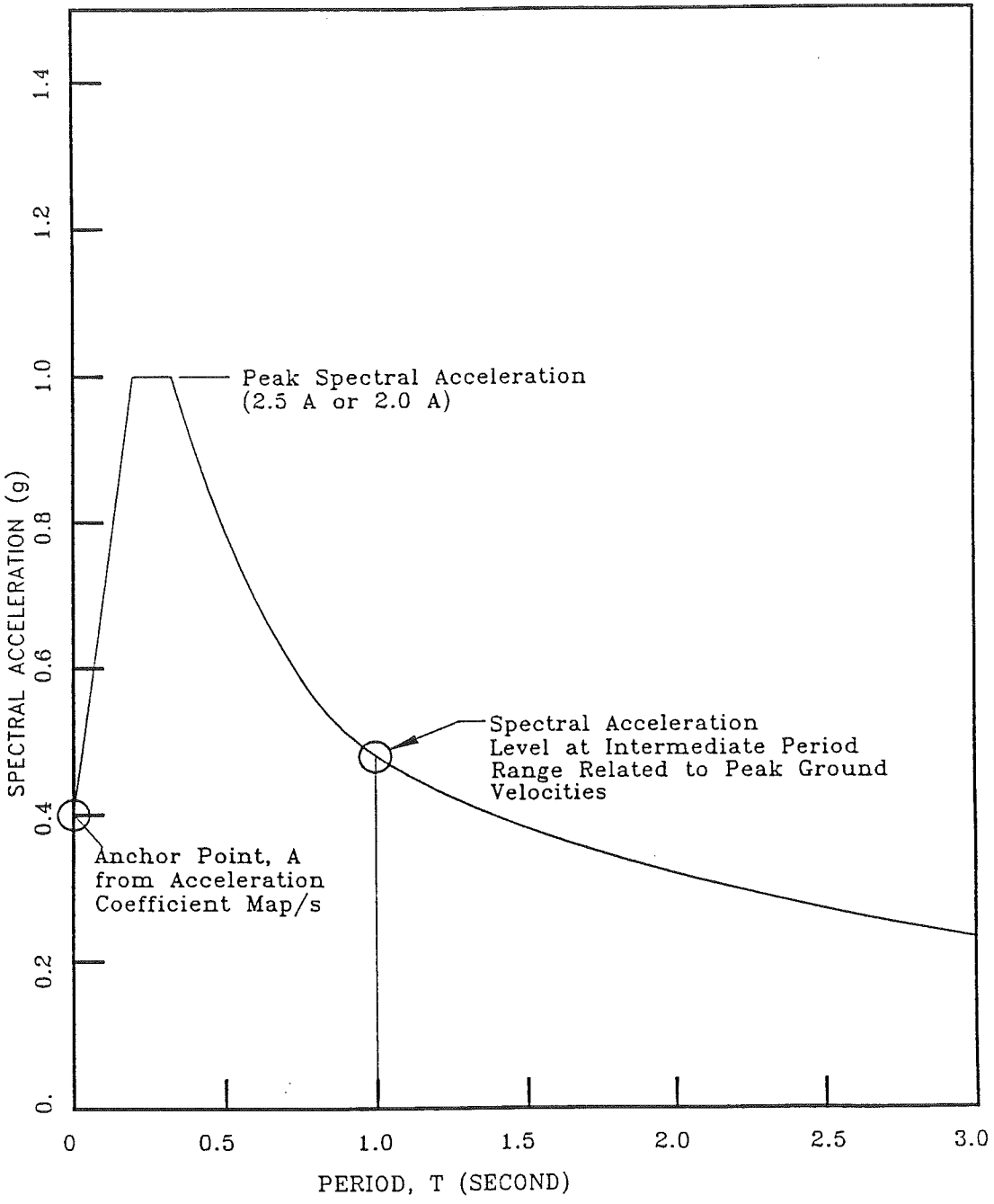

ARIZONA DEPARTMENT OF TRANSPORTATION

ARIZONA TRANSPORTATION RESEARCH CENTER

FIGURE 42

ELEMENTS IN THE AASHTO DESIGN RESPONSE SPECTRUM

about 0.5 second). The A_v coefficient has no physical meaning in itself; it is merely an anchor point for the response spectrum curve shape such that the resultant spectral acceleration curve would have more appropriate values at longer periods (around 1 second). The peak ground velocity (PGV)is a better measure of the spectral acceleration levels at longer periods based on observations of characteristics of earthquake records. Therefore, A_v coefficients are based on attenuation relationships for PGV. A conversion factor is needed to relate PGV which has the units of velocity (e.g. inches per second) to A_v which is dimensionless (in terms of fraction of the gravitational acceleration, g). In the original AASHTO acceleration coefficient A map (AASHTO, 1983), the A coefficient (fraction of g) was based on the ATC-3-06 A_v map (ATC, 1978) where A_v was obtained by dividing estimated peak ground velocities (expressed in inches/second) by 30 (thirty). The conversion factor (30) reflects the consensus of the group of geoscientists and engineers on the Applied Technology Council (ATC) committee which developed the ATC-3-06 guideline. We emphasize that the A_a and A_v coefficients should not be regarded as independent parameters. They are related to the form of the response spectrum curve shape and the procedure to account for local site effects (Site Factor).

Due to the above complexities and the need to fit the resultant coefficients to a format suitable for use in the existing AASHTO procedure which is based on a single acceleration coefficient at bedrock, we elected to adopt the same peak bedrock acceleration attenuation relationship developed by Schnabel and Seed (1973) which were used in the 1990 Algermissen map showing bedrock acceleration contours for the western United States.

This map has been adopted in the AASHTO guide specifications (Buckle, 1991) to anchor the design spectrum curve shape.

(2) Future Trend-Spectral Acceleration Attenuation Relations

In recent years, there have been significant advancements in the development of attenuation relationships that suggest other technical approaches for the development of design spectra and some of these are being considered by various agencies. As a result of these activities, some fundamental changes in the methodology of dynamic response analyses are being considered by the Structural Engineers Association of California (SEOAC) and Building Seismic Safety Council (BSSC) committees responsible for revisions to the NEHRP seismic design recommendations. These changes will probably be adopted by the highway bridge design profession eventually. Although it is not possible for us to anticipate the eventual development in this area, a discussion of the trend of development in the attenuation relationships and their implications on the acceleration contour maps is provided below.

The future trend in the acceleration coefficient maps will be driven by recent developments of attenuation relationships. Since the development of the Schnabel and Seed peak bedrock acceleration attenuation relation (Schnabel and Seed, 1973), there has been significant increase in the number of strong ground motion records and it is now possible to conduct more meaningful statistical analyses. A comprehensive review of attenuation relationships is given by Joyner and Boore (1988). The following excerpt

from Joyner and Boore provides some indications on the future development on the subject.

> "The response spectrum is the best representation of ground motion because it takes account of the natural frequencies of structures. The conventional practice of using peak acceleration to scale standard response spectral shapes is likely to lead to error, except at high frequencies, because the shapes of response spectra depend strongly on magnitude and local geologic site conditions. Magnitude, distance, and site conditions are the principal variables used in predicting future ground motions. A number of predictive relationships derived from regression analyses of strong-motion data are available for horizontal peak acceleration, velocity, and response spectral values."

In summary, A_a and A_v coefficients will likely be replaced by spectral acceleration coefficients and in the future, A_a and A_v maps will probably be replaced by spectral acceleration maps at various periods. Since A_a is generally taken as peak ground acceleration in practice (equal to spectral acceleration at zero-second period), a peak acceleration or an A_a map will still be usable as the spectral acceleration map for zero period. However, A_v maps will become obsolete and will be replaced by spectral acceleration maps at longer period ranges. This trend is true for building as well as highway bridge design. Spectral acceleration contour maps for the contiguous U.S. at two periods (0.3 and 1 second) have already been developed and presented for review in the 1991 edition of NEHRP Recommended Provisions for the Development of Seismic Regulations for New Buildings, (BSSC, 1991). Many

engineers feel that these maps should be adopted for building design in the 1994 NEHRP Provisions.

(3) Bedrock Versus Soil

Another issue relates to the use of bedrock as the design basis. At the time of the development of the original acceleration coefficient map (Algermissen et al., 1982) there were very few attenuation relationships available. The bedrock condition was chosen to avoid the complexity of the local site soil response issue. This is unfortunate in two respects:

- The Schnabel and Seed bedrock attenuation relationship is based largely on empirical data, but there are very few rock site records as compared to soil site records.

- In most applications, foundation conditions are associated with soil sites rather than bedrock sites.

In the most recent spectral acceleration contour maps (BSSC, 1991), the bedrock acceleration scenario has been abandoned and the maps are based on Joyner and Boore's spectral attenuation for soil sites (1982 and 1991). The development of using spectral acceleration rather than A_a or A_v, and soil rather than bedrock will necessitate some change in the overall format of the design procedure in the future.

(4) Adopted Attenuation Relationships

All the above developments might have some bearing on the AASHTO acceleration contour maps in the future. However, the discussed activities are still in a state of flux; therefore, we adopted the same attenuation relationships used for the PGA maps developed by Algermissen et al. (1990). The PGA (A) which in practice is equivalent to A_a, was adopted by AASHTO for bridge design in 1991 (Buckle, 1991). The PGA attenuation relationship is the Schnabel and Seed acceleration for rock (See Figure 43).

Peak ground velocity (PGV) maps were also prepared as part of the probabilistic studies conducted. The adopted PGV attenuation relationship for these analyses is Perkin's (1980) PGV attenuation relationship for the western U.S. (See Figure 44). The A_v coefficient (in g) corresponding to the PGV was obtained by dividing PGV (in/sec) by 30. Comparison of the two attenuation relationships (Figure 45) allows the following observations.

- The slopes of the acceleration versus distance curves are generally flatter for A_v than A (A_a) at far-field distances (over 100 km), indicating that A_v attenuates at a slower rate than A (A_a). This is consistent with our knowledge of ground-motion characteristics.

- In near field (say at 1 km) the A (A_a) coefficient is higher than the A_v coefficient for a comparable small-magnitude earthquake (magnitudes below 6.6), whereas the reverse is observed for a

FHWA REGION	STATE	PROJECT NUMBER	REPORT NUMBER
9	ARIZ.	HPR-PL-1(37)344	FWHA-AZ92-344

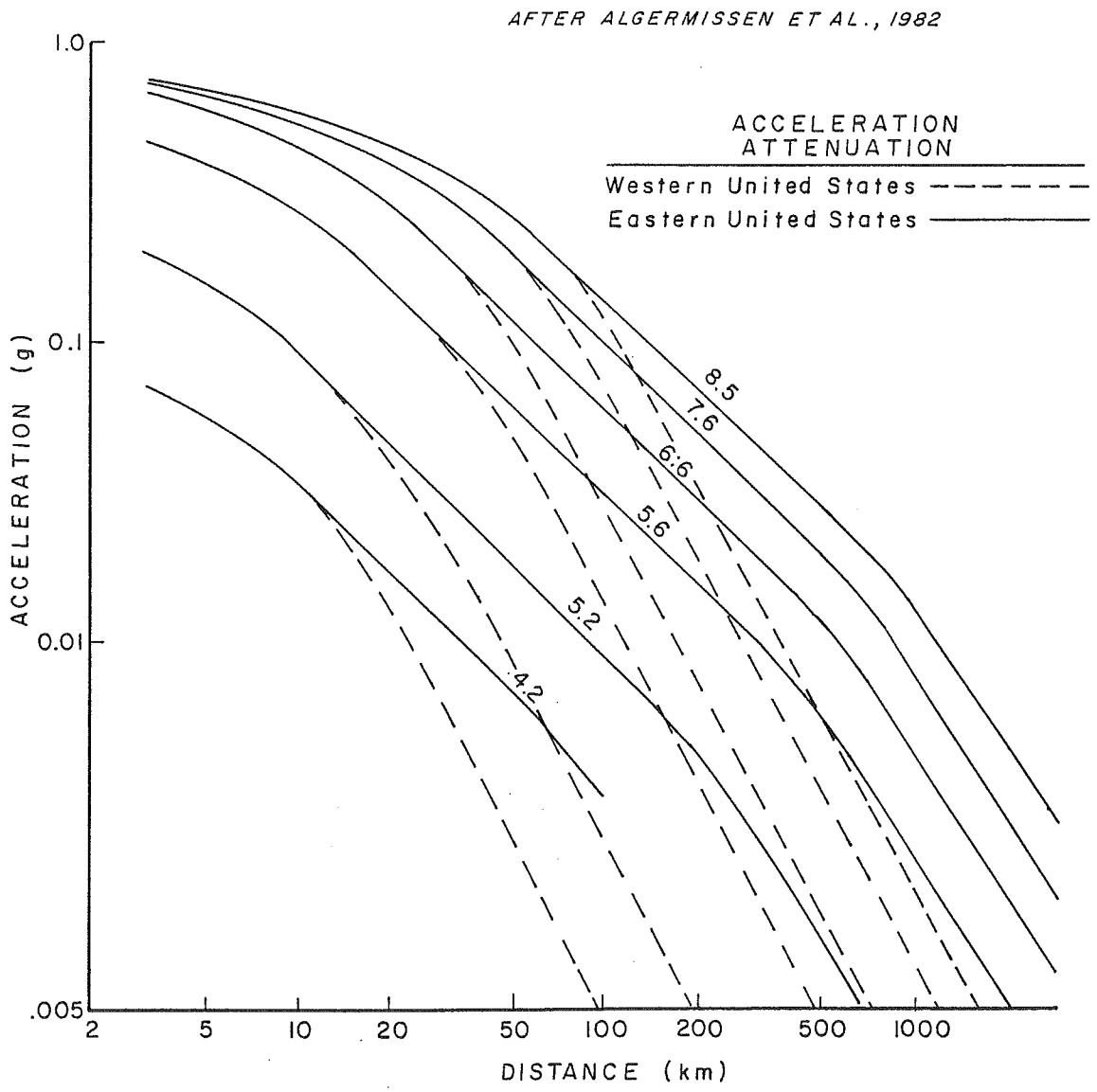

ARIZONA DEPARTMENT OF TRANSPORTATION
ARIZONA TRANSPORTATION RESEARCH CENTER

FIGURE 43
ACCELERATION ATTENUATION RELATION FOR ROCK

FHWA REGION	STATE	PROJECT NUMBER	REPORT NUMBER
9	ARIZ.	HPR-PL-1(37)344	FWHA-AZ92-344

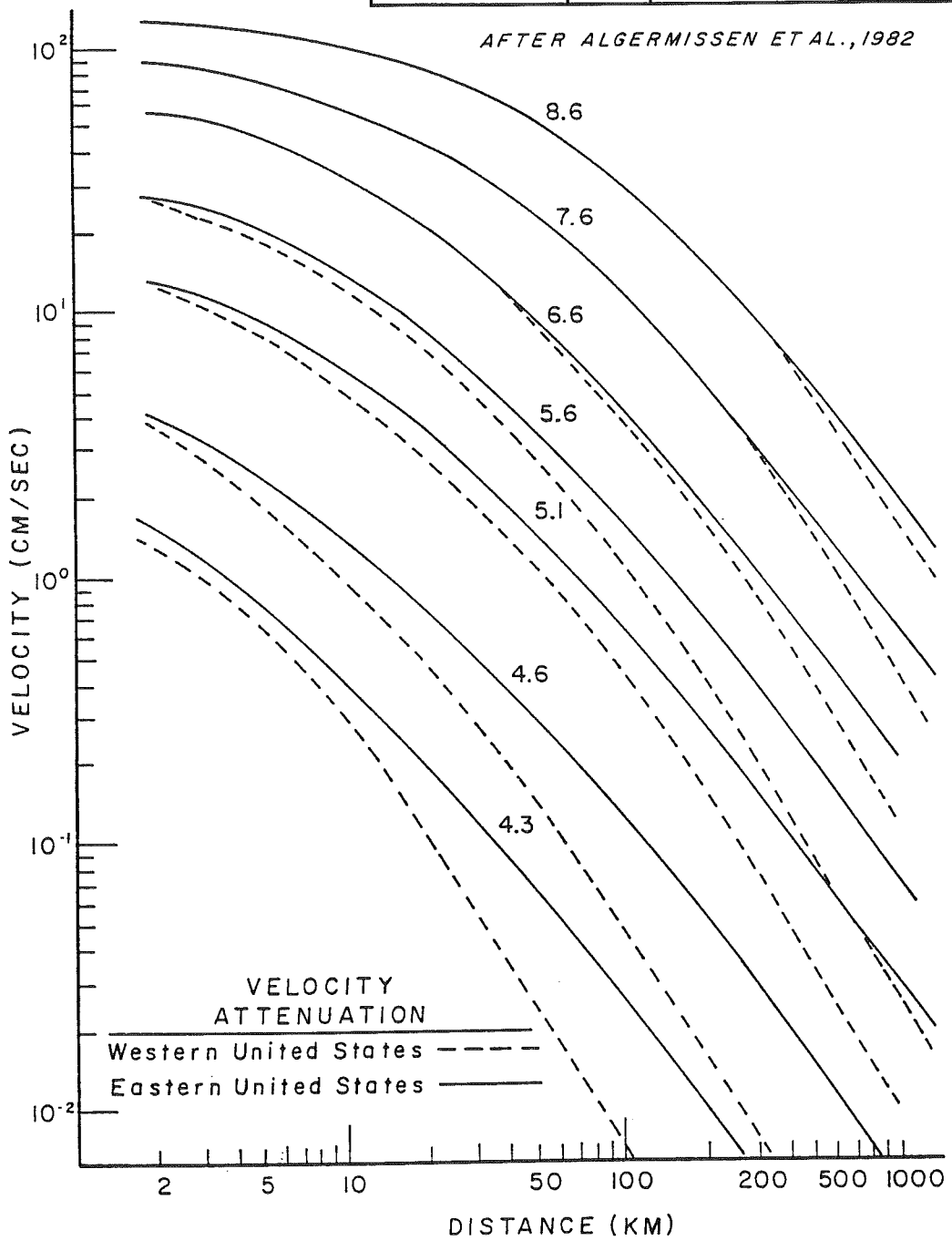

ARIZONA DEPARTMENT OF TRANSPORTATION
ARIZONA TRANSPORTATION RESEARCH CENTER

FIGURE 44
VELOCITY ATTENUATION RELATIONSHIPS

FHWA REGION	STATE	PROJECT NUMBER	REPORT NUMBER
9	ARIZ.	HPR-PL-1(37)344	FWHA-AZ92-344

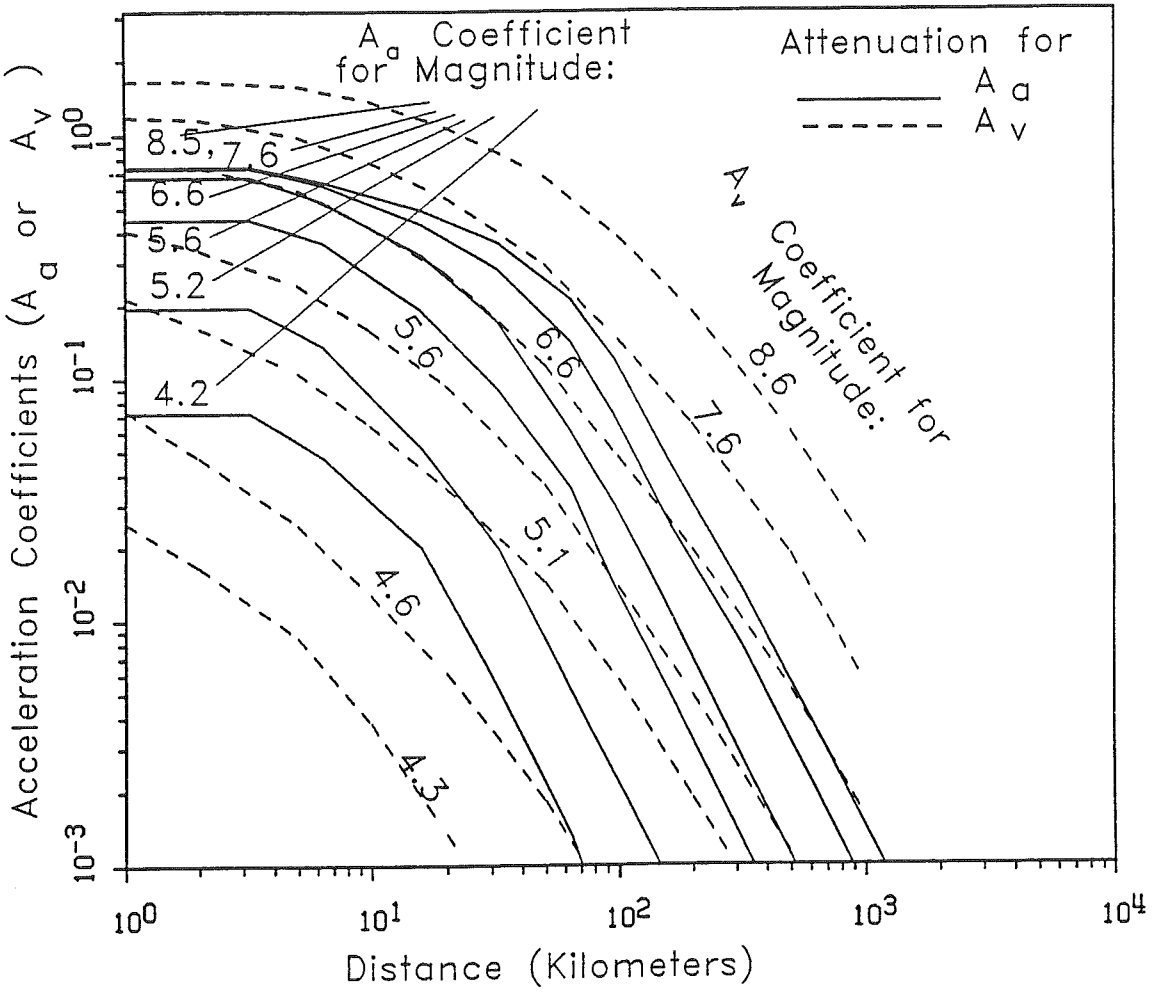

ARIZONA DEPARTMENT OF TRANSPORTATION
ARIZONA TRANSPORTATION RESEARCH CENTER

FIGURE 45
COMPARISON OF PEAK HORIZONTAL ACCELERATION, PGA (Aa) WITH Av

comparable large-magnitude earthquake. This is also consistent with the knowledge that for smaller magnitude earthquakes, the high-frequency content (related to PGA) would be more dominant, whereas for larger magnitude earthquakes, the lower frequency content (related to PGV) would be more dominant.

- At high acceleration levels (combination of short distances and large magnitude), A (A_a) coefficients are almost independent of magnitude in the large-magnitude range (larger than 6.5) due to the limit of soil strength or ground saturation effects. However, A_v coefficients (velocities or long-period motions) appear to be more dependent on magnitude even in the large-magnitude range. This is consistent with the characteristics that soil sites generally have a higher capacity for transmitting longer period motions.

- A (A_a) is roughly equal to A_v for a magnitude 6.6 earthquake.

A prevalent notion among many engineers is that the A_v map leads to higher acceleration coefficients than the A (A_a) map. Observations from the A (A_a) and A_v comparison (Figure 45), indicate that this is not always true. For low seismicity areas such as Arizona, the controlling design earthquake would be smaller magnitude earthquakes at near field, and A_v could be lower than A (A_a).

c. Probabilistic Model

In addition to (1) source zones, (2) recurrence relationships, (3) attenuation relationships, and (4) location of the site relative to the source zones, the SEISRISK III program requires the following input parameters:

1 - the variability (standard deviation) of the attenuation relationships,

2 - the uncertainty in the location of the boundary of area source zones,

3 - the uncertainty in the fault rupture length, and

4 - the site location/s for analysis.

Items (2) and (3) generally do not lead to significant overall changes in the solutions (Bender, 1986). They were introduced primarily to avoid abrupt changes in the solutions across the boundaries of area source zones and at end points of linear faults. The variability of the attenuation relationships (Item 1), however, can lead to significant changes in the solution (Bender, 1984). Additional discussions on the sensitivity of the solution to this parameter are presented in Section 9.c (SEISRISK III-Sensitivity of Solutions).

Given the above input, the SEISRISK III program solves for the annual rate of occurrence (Number of earthquakes per year) at various acceleration levels. In this project, the analyses were conducted at 55 acceleration intervals, ranging from 0.01 to 1.0 g. At each site location, the annual number of earthquakes at each acceleration interval were integrated for all the seismic sources. The yearly or annual exceedance rate, E(a) defined as the number of earthquakes per year exceeding a given acceleration a, is the sum of the annual rate of occurrence at all the acceleration intervals above the acceleration value a. The results are commonly presented as a yearly exceedance rate for various acceleration levels as shown in Figure 46. The inverse of the annual exceedance rate is the return period (number of years between events) of a design earthquake corresponding to the acceleration level.

(1) Poisson Distribution

The yearly exceedance-acceleration relationship, E(a), can be used to determine the probability associated with the exceedance of any acceleration for a given exposure duration. This process requires an assumption of how earthquakes are distributed in time. Consistent with the earlier work conducted for the AASHTO acceleration map, a Poisson distribution is assumed for this study. This is equivalent to assuming that earthquakes have no "memory"; that is, each earthquake occurs randomly (or independently) of any other earthquake and the time that has elapsed since the previous event is not considered in the evaluation. This implies that if an earthquake occurred today, it would have absolutely no influence on the

FHWA REGION	STATE	PROJECT NUMBER	REPORT NUMBER
9	ARIZ.	HPR-PL-1(37)344	FWHA-AZ92-344

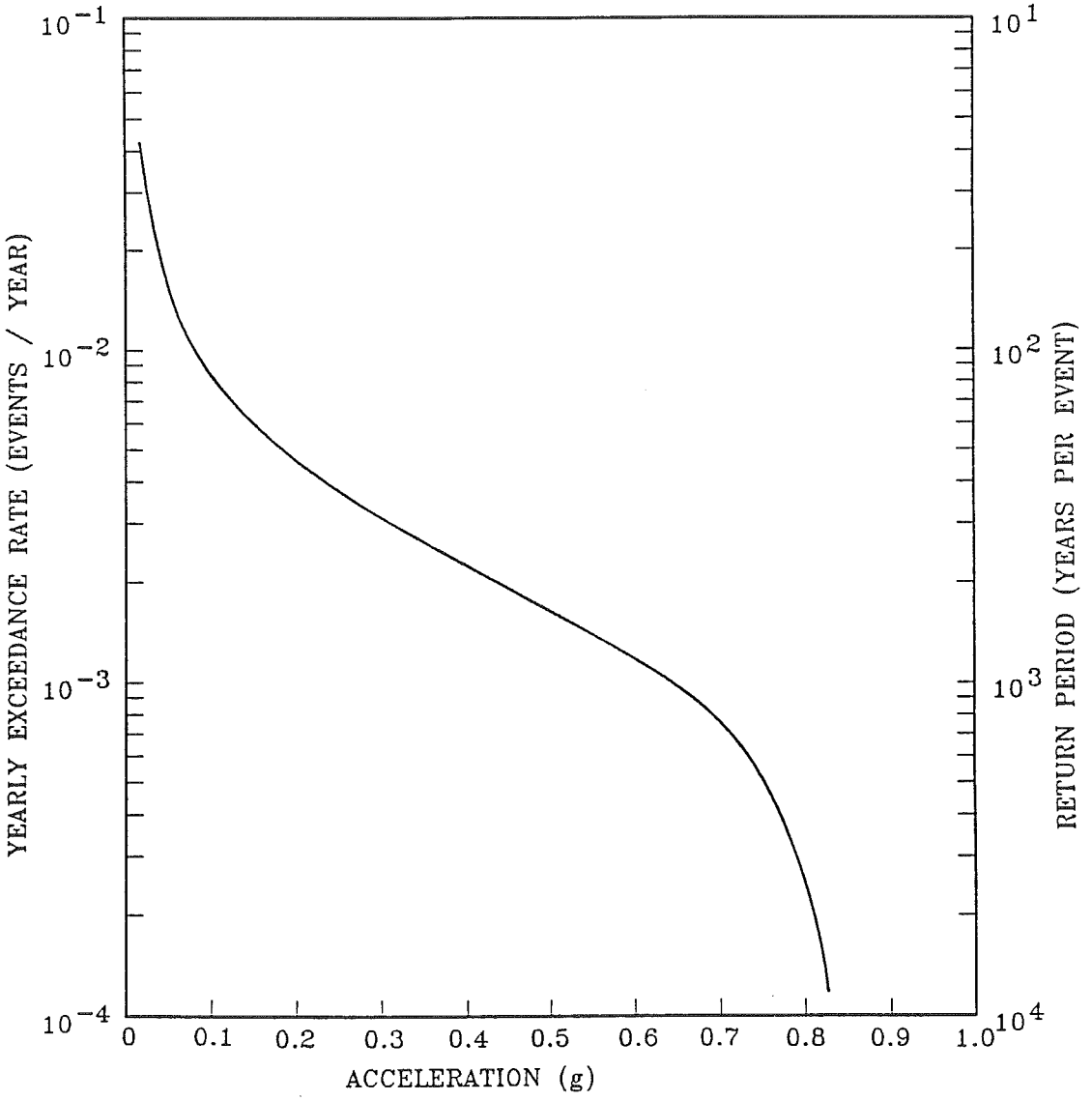

ARIZONA DEPARTMENT OF TRANSPORTATION
ARIZONA TRANSPORTATION RESEARCH CENTER

FIGURE 46
ANNUAL EXCEEDANCE RATE/RETURN PERIOD VERSUS ACCELERATION

next event. Obviously, this is not consistent with foreshock and aftershock experience, as well as physical explanations for earthquakes such as seismic-gap and strain-release theories.

Using a Poisson distribution, the three parameters: (1) probability, P(a,T), of not being exceeded at a given acceleration a, (2) an exposure time (T), and (3) a yearly exceedance rate, E(a) are related to each other by the following expression:

$$P(a,T) = \exp[\ -E(a)\ .\ T\ ],$$

where exp is the exponential function.

The above expression is equivalent to the following:

$$E(a) = \frac{-\log_e[\ P(a,T)\ ]}{T}$$

where $\log_e$ is the natural logarithm function.

By specifying any two of the three parameters in the two expressions (probability of non-exceedance and the yearly exceedance rate), the third parameter can be solved. For example, the AASHTO criteria specifies that the design acceleration should be at a 90-percent confidence level (90 percent probability of not being exceeded) for an exposure of 50 years. This will lead to the following set of parameters:

$$T = 50$$

$$P(a,50) = 0.9$$

For the above parameters, $E(a) = \frac{-\log_e[\ 0.9\ ]}{50} = 0.002107$ event per year.

The corresponding return period of the design earthquake is = 1 / 0.002107 = 475 years per event.

Similarly, for a 90 percent non-exceedance and a 250-year exposure, the annual exceedance rate would be 0.000421 events per year and the corresponding return period is 2,373 years per event.

9. SEISRISK III SOLUTIONS

a. Calibration Comparison with Algermissen's Study

As stated in Section 8, the SEISRISK III computer program was used in our analyses. At the onset of the project, a calibration analysis was undertaken to ensure that the 1990 Algermissen study could be duplicated by using identical source zones, recurrence relationships, and attenuation relationships. The source zones used in Algermissen's study and the corresponding recurrence relationships were documented by Algermissen et al (1982). Discussions with Dr. Perkins, one of the principal investigators in the USGS study, indicated that the differences between the 1982 and the 1990 acceleration coefficient maps are primarily the results of refinements in the SEISRISK computer program. Results from our calibration run are compared to the 1990 Algermissen PGA contour lines in Figure 47. On Figure 47, the acceleration solutions from our study are posted at the grid points as integers in percent g. The contour lines represent g values from the Algermissen's study for the contiguous U.S (1990). There are two areas where minor differences can be observed:

- At the southeast corner of Arizona, the Algermissen map suggested that the peak ground acceleration is 18-percent g compared to 19-percent g in our calibration run.

- the 7.5-percent g contour line in north-central Arizona in

Algermissen's study differs slightly from our study. Our 7.5-percent g contour line would have covered a somewhat wider area.

Communications with Dr. David Perkins of U.S. Geological Survey regarding the differences were very helpful throughout the project. The following discussion provides some of the reasons for the observed differences. Other than the fact that the Algermissen et al map used a slightly different version of the program, and there are some differences in the discretization procedure (grid spacing and choice of central-magnitude values in inputting the recurrence relationships), they did not use area source models exclusively for the two areas where the observed discrepancies occur (zone 004 at southeast corner, and zone 014 at north-central Arizona). They added dummy parallel faults to the two area zones. The dummy faults are parallel to each other at some standard distance. They attributed the larger magnitude earthquakes (center magnitude 6.1 or higher) to the dummy faults. The details of this procedure are not documented in the available publications.

The discussion above reveals that the differences are very minor. In essence our use of the SEISRISK III program gave solutions virtually identical to the Algermissen et al (1990) study and the current AASHTO criteria, where input data were replicated. The principal differences between results from this project (as presented in later sections) and the Algermissen study are not a result of different probabilistic methods, but emanate from application of the newly acquired geologic and seismicity data as well as more-detailed analysis in the Arizona area.

FHWA REGION	STATE	PROJECT NUMBER	REPORT NUMBER
9	ARIZ.	HPR-PL-1(37)344	FWHA-AZ92-344

TABULATED COEFFICIENTS IN PERCENT g FROM CALIBRATION ANALYSIS
CONTOUR LINES FROM ALGERMISSEN ACCELERATION MAP (MF-2120), 1990

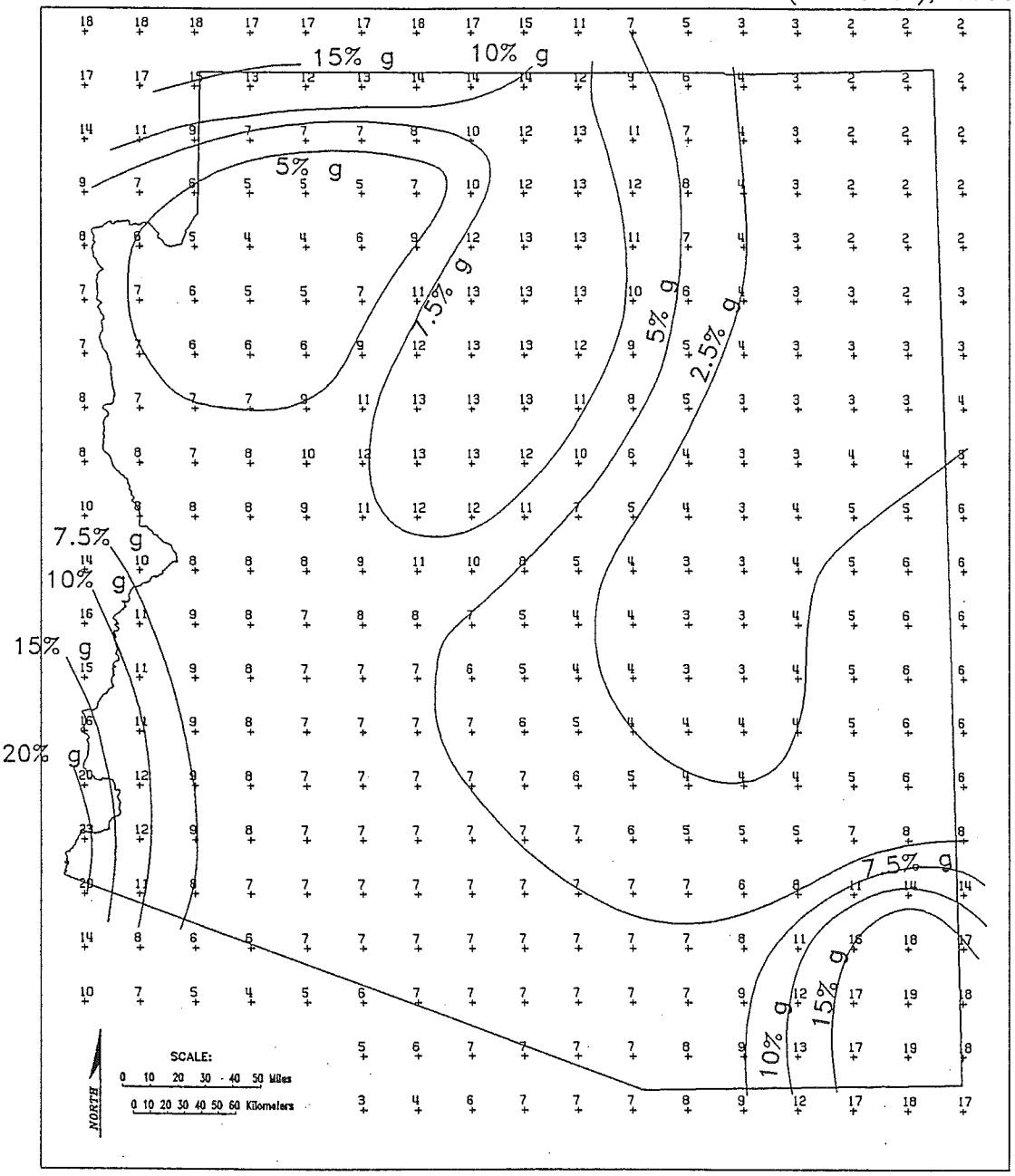

ARIZONA DEPARTMENT OF TRANSPORTATION
ARIZONA TRANSPORTATION RESEARCH CENTER

FIGURE 47
COMPARISON OF CALIBRATION RUN WITH ALGERMISSEN'S CONTOURS 90% NON-EXCEEDANCE OVER 50 YEARS

b. Results of Analyses

In this project, analyses were conducted over an 81 X 81 grid (6,561 grid points) or at a 0.1-degree interval. The boundaries for our analyses were latitude 30 to 38 degrees north and longitude 108 to 116 degrees west. Although the analyses were conducted for a more-extensive area than Arizona, solutions for outside the state are not rigorously constrained as the Arizona area and are not presented herein due to the source zone limits adopted in our analyses.

Results of the probabilistic analyses are presented in two formats in this report: (1) direct posting of the acceleration coefficients at the grid points and (2) maps of contour lines of equal acceleration levels based on the grid-point solutions. Our analysis included several sensitivity analyses to evaluate the sources of accelerations and the effects of various limitations and judgements. Some of these sensitivity analyses are presented in the following sections using the grid-point posting format. Four acceleration contour maps are provided as Plates 2a thru 2d. These are:

- o Plate 2a - Map of Horizontal Acceleration (PGA) at Bedrock for Arizona with 90-Percent Probability of Non-Exceedance in 50 years.

- o Plate 2b - Map of Horizontal Acceleration (PGA) at Bedrock for Arizona with 90-Percent Probability of Non-Exceedance in 250 years.

- o Plate 2c - Map of Horizontal Velocity (PGV) (and corresponding A_v) at Bedrock for Arizona with 90-Percent Probability of Non-Exceedance in 50 years.

- o Plate 2d - Map of Horizontal Velocity (PGV) (and corresponding A_v) at Bedrock for Arizona with 90-Percent Probability of Non-Exceedance in 250 years.

The maps for 90-percent probability non-exceedance in 250 years were prepared for comparative purposes to illustrate the sensitivity of the acceleration coefficients to lower levels of risk.

As discussed above, the Horizontal Velocity and its corresponding A_v value arises from the use of Perkins' (1980) velocity attenuation relationship. The contour lines can be expressed in terms of both velocity (inches per second) as well as acceleration (A_v) values (in g). Annotations for both are provided in the A_v maps (Plates 2c and 2d). Overlain on each of the four contour maps are state lines, county lines, highway networks with mileposts annotated at every ten miles, and geographical names. The contour lines are at 0.01 g intervals with contour annotations at every 0.05 g intervals as specified in our scope of work.

c. Sensitivity of the Solutions

To provide a measure of the effect of various input parameters, results from several sensitivity analyses are presented below. The SEISRISK

- o Plate 2c - Map of Horizontal Velocity (PGV) (and corresponding A_v) at Bedrock for Arizona with 90-Percent Probability of Non-Exceedance in 50 years.

- o Plate 2d - Map of Horizontal Velocity (PGV) (and corresponding A_v) at Bedrock for Arizona with 90-Percent Probability of Non-Exceedance in 250 years.

The maps for 90-percent probability non-exceedance in 250 years were prepared for comparative purposes to illustrate the sensitivity of the acceleration coefficients to lower levels of risk.

As discussed above, the Horizontal Velocity and its corresponding A_v value arises from the use of Perkins' (1980) velocity attenuation relationship. The contour lines can be expressed in terms of both velocity (inches per second) as well as acceleration (A_v) values (in g). Annotations for both are provided in the A_v maps (Plates 2c and 2d). Overlain on each of the four contour maps are state lines, county lines, highway networks with mileposts annotated at every ten miles, and geographical names. The contour lines are at 0.01 g intervals with contour annotations at every 0.05 g intervals as specified in our scope of work.

c. Sensitivity of the Solutions

To provide a measure of the effect of various input parameters, results from several sensitivity analyses are presented below. The SEISRISK

III solutions are presented in grid-point posting format to allow direct comparisons between individual runs. To avoid overcrowding on the figures, results are posted at every third grid point, or roughly at 0.3-degree spacing intervals even though the analyses were conducted at finer spacings. Results from five SEISRISK III runs are presented in Figures 48 thru 53 for the following cases:

- Figure 48 - PGA for 90-percent non-exceedance in 50 years from all seismic sources. This is the solution used to develop Plate 2a.

- Figure 49 - PGA for 90-percent non-exceedance in 50 years from non-Arizona sources.

- Figure 50 - PGA for 90-percent non-exceedance in 50 years for zero standard deviation (no uncertainty) in acceleration attenuation relationship.

- Figure 51 - PGA for 90-percent non-exceedance in 250 years. This is the solution used to develop Plate 2b.

- Figure 52 - A_v for 90-percent non-exceedance in 50 years. This is the solution used to develop Plate 2c.

- Figure 53 - A_v for 90-percent non-exceedance in 250 years. This is the solution used to develop Plate 2d.

FHWA REGION	STATE	PROJECT NUMBER	REPORT NUMBER
9	ARIZ.	HPR-PL-1(37)344	FWHA-AZ92-344

Coefficients in percent g

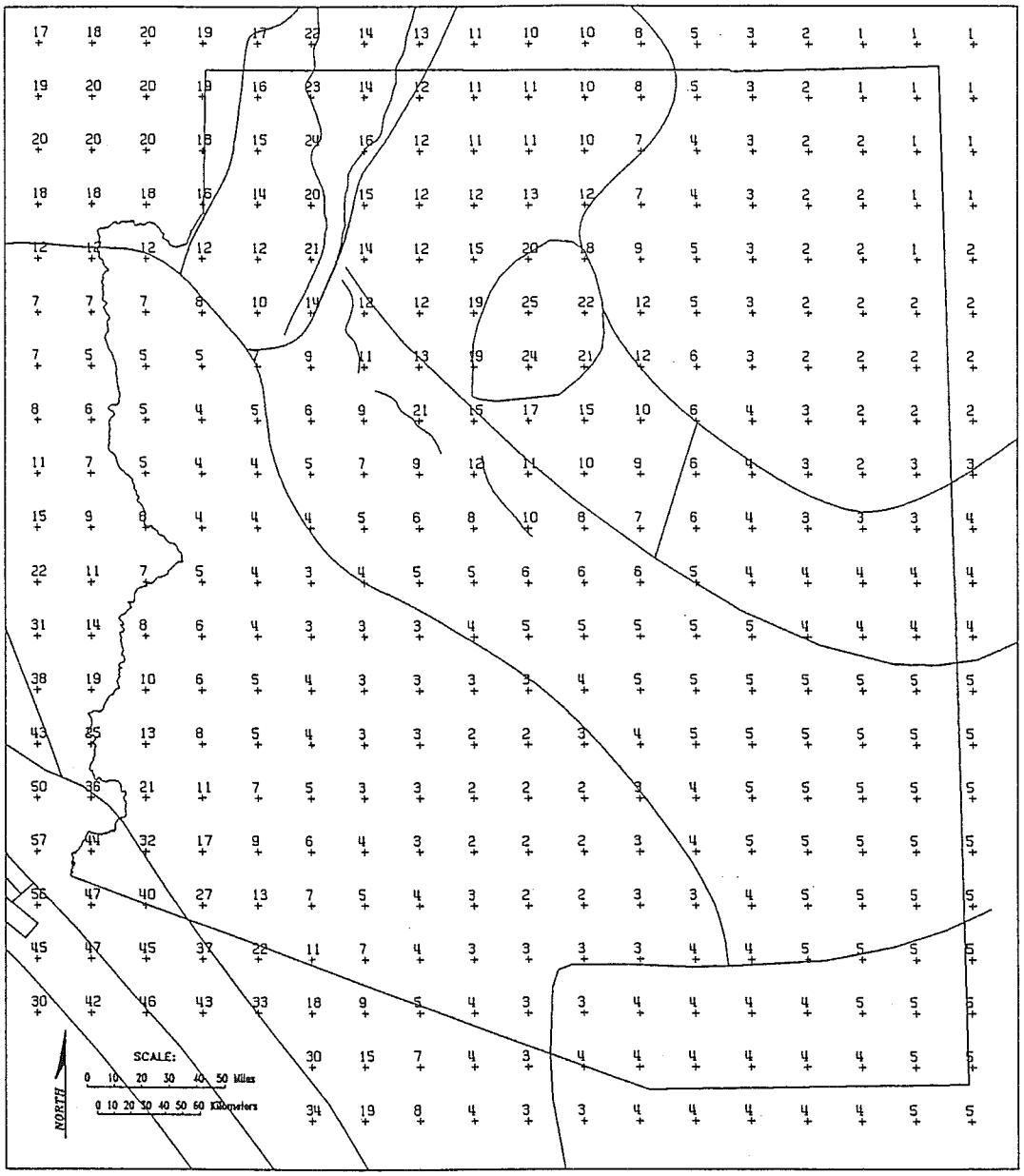

ARIZONA DEPARTMENT OF TRANSPORTATION

ARIZONA TRANSPORTATION RESEARCH CENTER

FIGURE 48

PGA FOR 90% NON-EXCEEDANCE
IN 50 YEARS FROM ALL SEISMIC SOURCES

FHWA REGION	STATE	PROJECT NUMBER	REPORT NUMBER
9	ARIZ.	HPR-PL-1(37)344	FWHA-AZ92-344

Coefficients in percent g

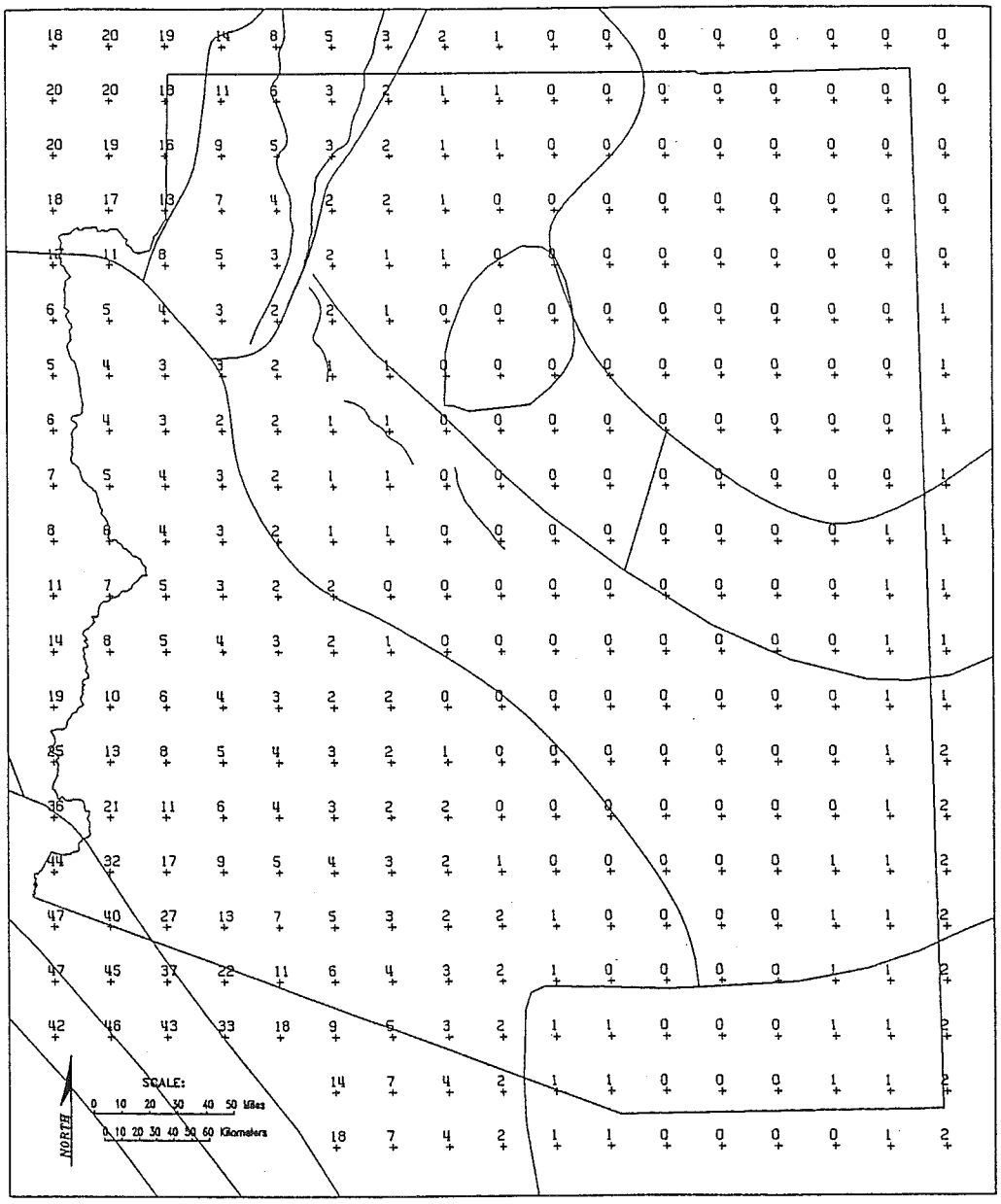

ARIZONA DEPARTMENT OF TRANSPORTATION
ARIZONA TRANSPORTATION RESEARCH CENTER

FIGURE 49
PGA FOR 90% NON-EXCEEDANCE
IN 50 YEARS FROM NON ARIZONA SOURCES

FHWA REGION	STATE	PROJECT NUMBER	REPORT NUMBER
9	ARIZ.	HPR-PL-1(37)344	FWHA-AZ92-344

Coefficients in percent g

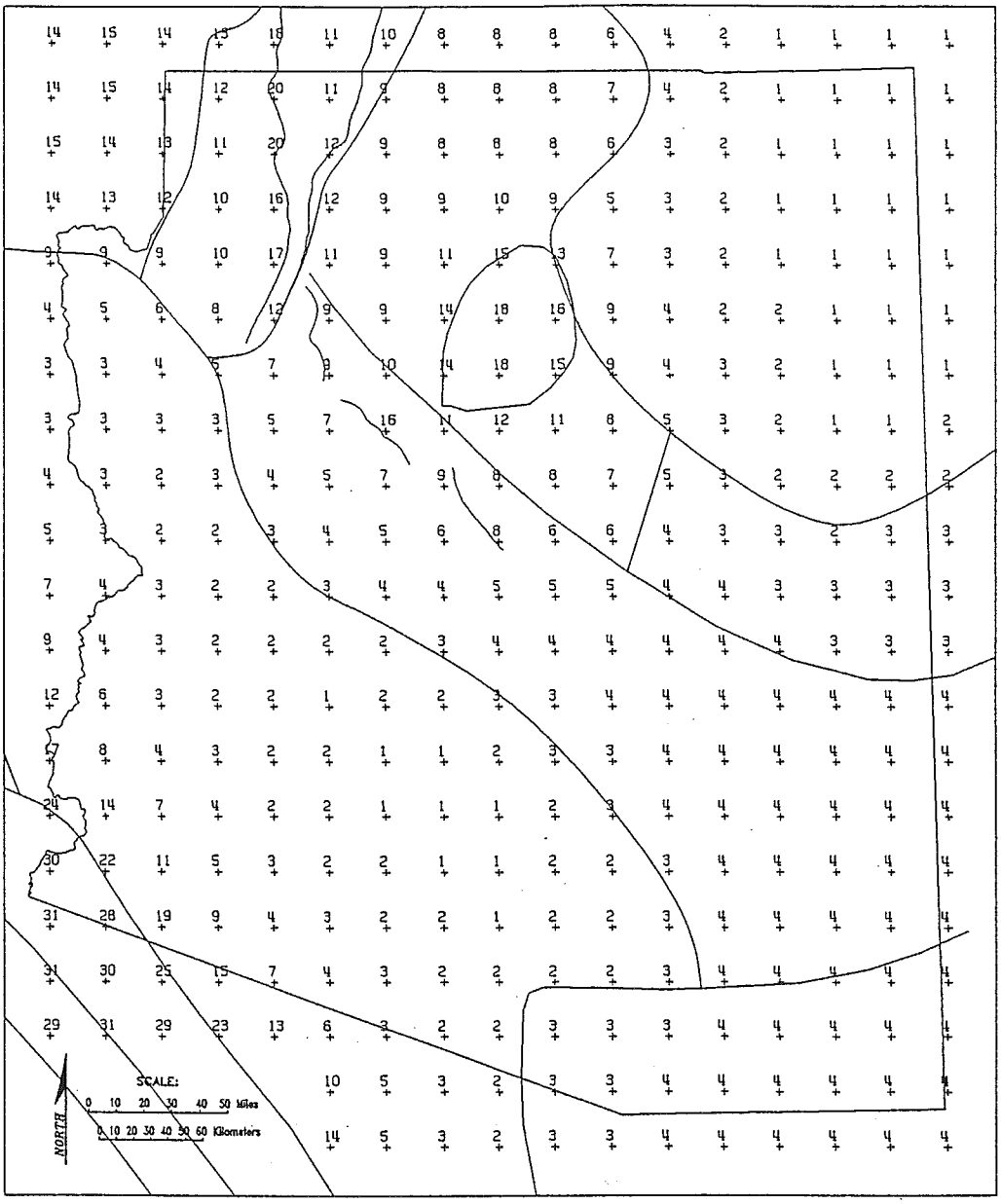

ARIZONA DEPARTMENT OF TRANSPORTATION

ARIZONA TRANSPORTATION RESEARCH CENTER

FIGURE 50

PGA FOR 90% NON-EXCEEDANCE IN 50 YEARS FOR ZERO STANDARD DEVIATION IN ACCELERATION ATTENUATION

FHWA REGION	STATE	PROJECT NUMBER	REPORT NUMBER
9	ARIZ.	HPR-PL-1(37)344	FWHA-AZ92-344

Coefficients in percent g

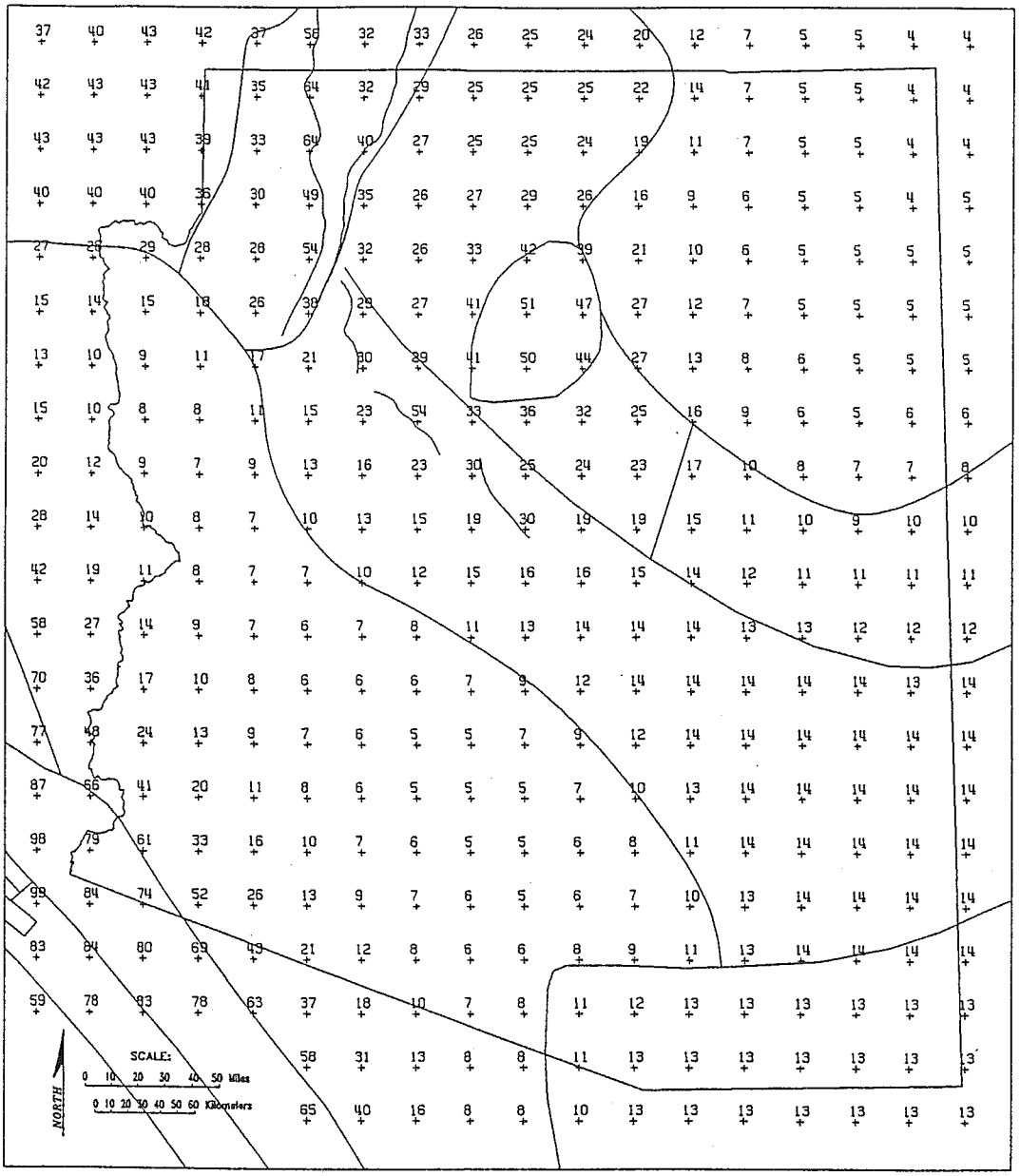

ARIZONA DEPARTMENT OF TRANSPORTATION

ARIZONA TRANSPORTATION RESEARCH CENTER

FIGURE 51

PGA FOR 90% NON-EXCEEDANCE IN 250 YEARS

FHWA REGION	STATE	PROJECT NUMBER	REPORT NUMBER
9	ARIZ.	HPR-PL-1(37)344	FWHA-AZ92-344

Coefficients in percent g

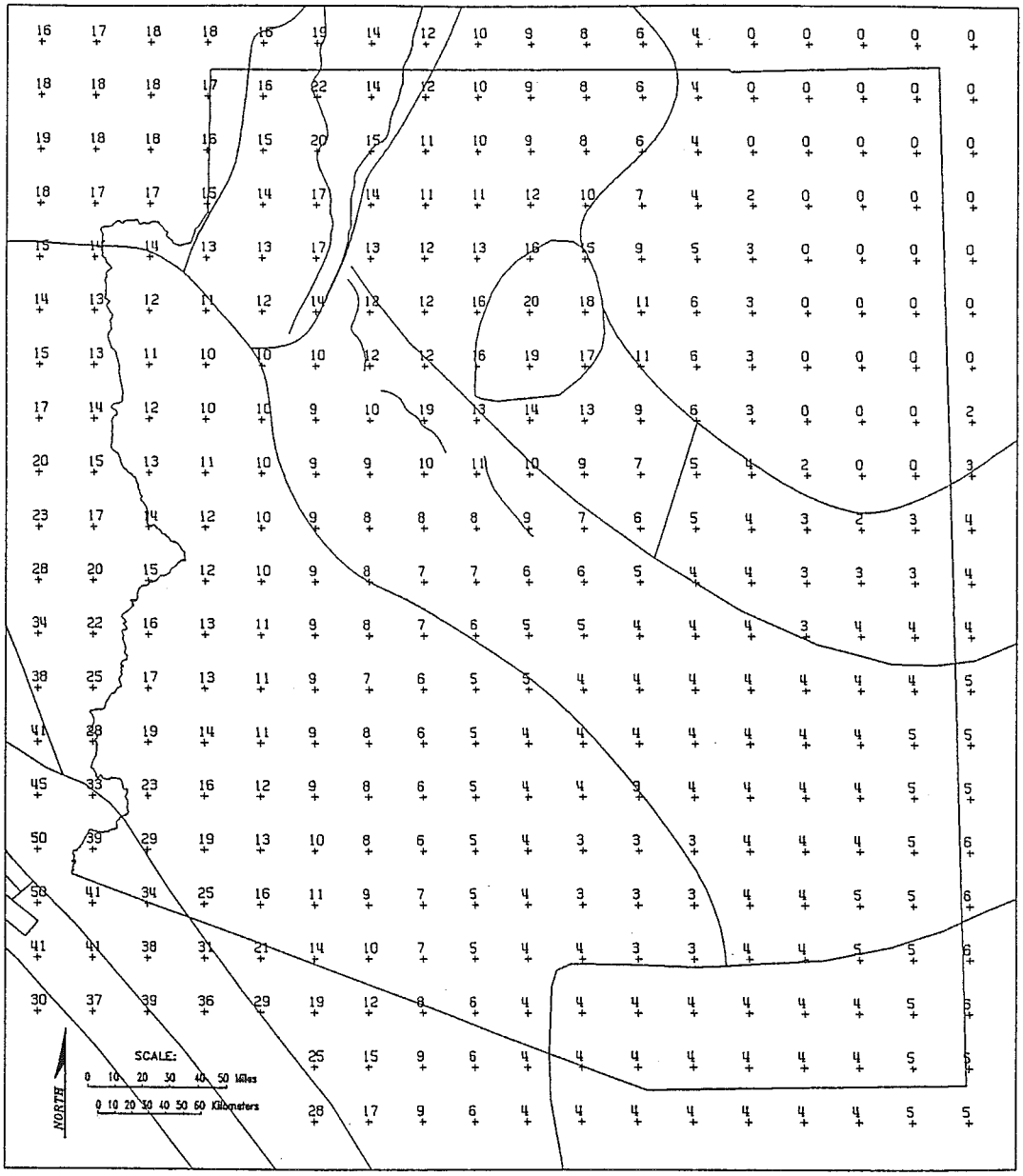

ARIZONA DEPARTMENT OF TRANSPORTATION

ARIZONA TRANSPORTATION RESEARCH CENTER

FIGURE 52

Av FOR 90% NON-EXCEEDANCE IN 50 YEARS

FHWA REGION	STATE	PROJECT NUMBER	REPORT NUMBER
9	ARIZ.	HPR-PL-1(37)344	FWHA-AZ92-344

Coefficients in percent g

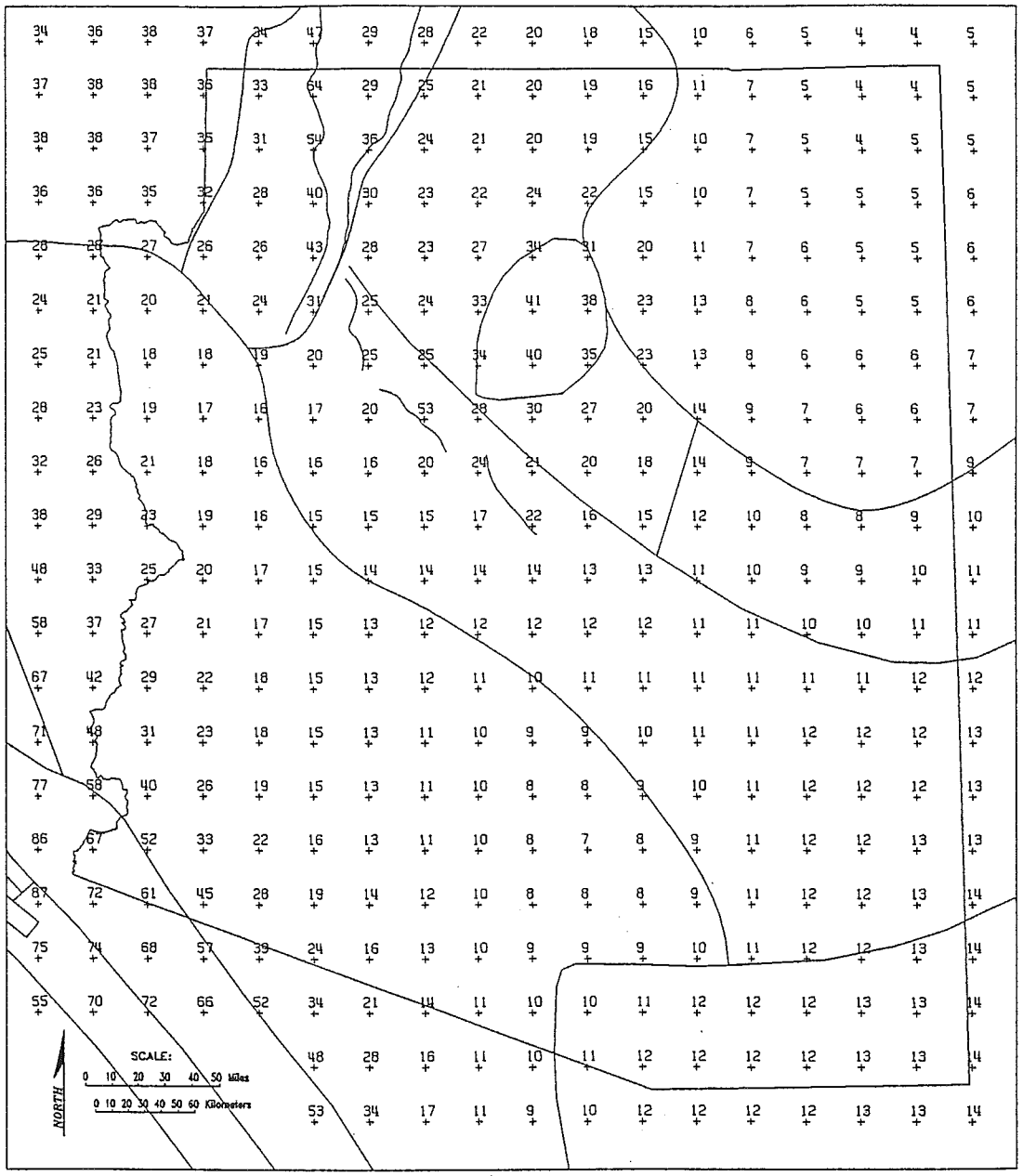

ARIZONA DEPARTMENT OF TRANSPORTATION

ARIZONA TRANSPORTATION RESEARCH CENTER

FIGURE 53

Av FOR 90% NON-EXCEEDANCE IN 250 YEARS

At the southwestern part of the state, the very inactive Sonoran zone is adjacent to the relatively active Salton Periphery zone and the very active Imperial Fault zone in California. The acceleration level is influenced largely by the California earthquakes. Comparison between Figure 49 and 48 illustrates this aspect. Our sensitivity analysis indicates that the Sonoran zone basically has no contribution to the acceleration level. A breakdown of the contribution of the resultant 0.47g at the southwestern part of the state from various seismic sources are: (1) 0.31g from the California fault zones (including Southern San Andreas fault zone, San Jacinto fault zone, Imperial fault zone, Cerro Prieto zone, Axial Cortez zone, and Eastern Transverse Range zone) and (2) 0.16g from the Salton Periphery zone.

Algermissen's study indicated an acceleration value of about 0.3g at the southwest corner of Arizona as compared to our 0.47g. The difference is in part due to our assignment of a higher seismicity level for the California sources as shown in the comparison of the recurrence relationships for non-Arizona sources in Figures 40c and 40d. In addition, some of the difference in the two solutions can be attributed to gaps in seismic source zones along the California-Arizona-Mexico border in Algermissen's model (Figure 39). The Algermissen seismic sources came from two separate studies: one for the contiguous United States except coastal and one for coastal and southern California. The latter study was conducted by Thenhaus et al (1980) entitled, Probabilistic Estimates of Maximum Seismic Horizontal Ground Motion on Rock in Coastal California and the Adjacent Outer Continental Shelf. The map resulting from combination of the source zone maps from these two studies

is presented as Figure 39. Examination of this figure reveals two gaps (in our Salton Periphery and Axial Cortez Zones) not included in any source zones (at the southern tips of California zones C016, C015 and C018). This results in zero input from areas with a significant earthquake potential. This is probably unintentional considering the high historical seismicity in those areas. Our analysis assigned a moderate to high earthquake potential to these areas as well as the area south of the Mexico border and this accounts for much of the increases of acceleration values in southwestern Arizona.

(2) Uncertainty in the Attenuation Relationship

One of the major features of a probabilistic hazard analysis is the ability to allow the activity rate of the seismic sources and the level of uncertainty in the input data to be factored into the decision process. As discussed previously, SEISRISK III allows consideration of uncertainties in three areas, including: (1) the attenuation relationship, (2) the boundaries of source zones and (3) locations of the end points of the fault rupture. Of the above three parameters, uncertainties of the attenuation relationship has been found to have one of the most significant impacts on the solution.

Because the attenuation relationship is based on strong ground motion records, there is considerable scatter in the empirical data about the mean-value relationship shown in Figures 43 and 44. The degree of scatter (uncertainty) is expressed in terms of the standard deviation σ. Many design codes based on deterministic approaches (e.g. the maximum credible earthquake

approach adopted for nuclear power plants and dams), specify an 84th percentile confidence level (mean plus one standard deviation) for design. A greater uncertainty expressed as a higher value in the standard deviation will lead to a higher design acceleration level.

In a probabilistic earthquake-hazard analysis, uncertainty of acceleration in an attenuation relation can be accounted for by assuming a statistical distribution with a standard deviation to denote the amount of scatter in the relation rather than as a set of unique mean-value acceleration-magnitude curves. However, the role of the standard deviation in a probability analysis is fundamentally different than a mean-plus-one standard deviation (84th percentile confidence level) in a deterministic approach. In a probabilistic analysis, the level of risk is defined by the adopted return period (related to the percent non-exceedance over a given exposure duration) and it is unchanged for various standard deviation values. Incorporating acceleration uncertainties merely relates to better accounting or bookkeeping of the statistical scatter in the analysis. Similar to the deterministic approach, adopting a higher value in standard deviation for the attenuation relationship will result in a higher acceleration for design. However, the increase would depend on many factors, including the site and source models, recurrence relationship, and the acceleration level.

The SEISRISK III program assumes that the attenuation relationship follows a log-normal distribution, or that the $\log_e$ (acceleration) is normally distributed with a standard deviation σ. The standard deviation is a constant, independent of magnitude and distance. The standard deviation, σ,

adopted by various researchers ranges from 0.3 to 0.62 depending on the earthquake records selected for the analysis. The standard deviation (natural log basis) adopted in this study is 0.62, which is the same as the standard deviation used in the Algermissen el at study (1990). The 84^{th} percentile acceleration would be 1.86 of the mean acceleration value irrespective of the acceleration level. Research of more-specific conditions (e.g. only near-field earthquakes or single-hypothetical events (Campbell, 1985) and from only one earthquake and one specific soil condition (Seed and Idriss, 1982) suggests a lower standard deviation value of about 0.3. For σ of 0.3, the 84^{th} percentile will be about 1.35 of the mean value. Based on discussions with several experts, a σ of 0.62 is considered conservative, especially at high acceleration levels. In many design codes, uncertainties related to other aspects such as local site effects are considered separately from the attenuation relationship. Therefore the standard deviation should be based only on uncertainties associated with intra-earthquake variability (i.e. only from source effects). The 0.62 standard deviation arises from statistical scatter of a wider range of earthquakes (large and small magnitudes, near- and far-field) in a study by Joyner and Boore (1988). The assumption that the standard deviation is independent of the magnitude of ground acceleration ignores the acceleration saturation effect as evidenced in many attenuation relationships (e.g. the Schnabel and Seed bedrock acceleration relationship in Figure 43) and could lead to unrealistic results for high acceleration levels (combination of long return periods and high seismicity areas).

Figure 50 presents the solution of the 50-year peak horizontal acceleration coefficient solution for a zero standard deviation in the acceleration attenuation relationship. Comparison of this figure with Figure 48, which represents a σ of 0.62, indicates that the ratio between the two solutions (Figure 48 and Figure 50) could range from 1.5 for areas of high acceleration level to 1.0 for areas of low acceleration level. Therefore, the choice of the standard deviation value has very significant implications in design practice.

(3) 250-Year Exposure Scenario

Figures 51 and 53 present the solutions for a longer return period scenario (2,373-year return period corresponding to a 90-percent probability non-exceedance in 250 years) for the PGA and A_v solutions, respectively. Comparison of the two figures with the corresponding 50-year exposure solutions (Figures 48 and 52) indicates that the ratio of the acceleration coefficients between a 250-year and a 50-year scenario ranges from about 1.8 to as much as 4.0. At high acceleration areas (such as southwest Arizona), the ratio is smaller suggesting some ground-acceleration saturation effects in the mean-value Schnabel and Seed bedrock acceleration attenuation relationship. However, the acceleration level at the southwest corner of Arizona is very high (about 0.8 g) and can be attributed to the assumption that the standard deviation in the acceleration value in the attenuation relationship is independent of the acceleration level (see earlier discussion in Section 9.c. Many experts feel that this assumption ignores the acceleration saturation effects and could lead to unrealistic

results for high acceleration ranges. Some of the experts have suggested a magnitude dependent standard deviation approach, or the standard deviation value would be smaller for a larger magnitude earthquake, to account for the constraint on accelerations from ground saturation effects.

(4) A_v Acceleration

Figures 52 and 53 present the A_v solutions for 50- and 250-year exposure scenarios, respectively. Comparison of the two figures with the corresponding peak horizontal acceleration solutions (Figures 48 and 51) indicates that the A_v coefficients are actually lower than the peak horizontal acceleration (A) coefficients for Arizona. As discussed above in the comparison of the two attenuation relationships, for low seismicity areas, a 50-year, 90-percent non-exceedance (475-year return period) event corresponds to a near-field, small, design-earthquake scenario. Higher frequency effects would be more dominant than long-period effects for such conditions. Therefore, the peak horizontal acceleration coefficient would be higher than the A_v coefficients.

In some of the earlier A_v maps such as the one in ATC-3-06 (1978), where attenuation relationships for long-period motions or peak velocities were not available, the A_v attenuation relationships were based on PGA relationships at near-field distances, but the slope of the acceleration versus distance curves were artificially flattened at far-field distances. This generally leads to the conclusion that the A_v map provides higher acceleration coefficients than the A_a map. Such an A_v attenuation relationship is an

overly simplified expression of the characteristics of ground motion and has been responsible for some of the misconceptions regarding the A_v effects. The A_v coefficients tend to be higher than the peak horizontal acceleration coefficient for a combination of long return periods and source zones capable of large maximum earthquakes.

10. CONCLUSIONS AND RECOMMENDATIONS

a. Conclusions

As a result of this project, the seismic hazard in Arizona is quantified by the following work products:

- A fault map of Arizona showing seismic source zone boundaries.
- Recurrence relationships for each of the seismic source zones.
- Four maps of horizontal accelerations and velocities at bedrock with 90-percent probability of non-exceedance in 50 years and 250 years.

Electronic digital data files (AUTOCAD™) for the above maps are delivered to ADOT with this report as one of the deliverables. In addition, an implementation manual was compiled and used in a 1-day seminar for ADOT personnel on the application of the above work products for design.

The use of the horizontal acceleration contour map with 90-percent probability of non-exceedance in 50 years is recommended for AASHTO-based design of highway bridges. The analysis procedures and the basis for this map are consistent with the Algermissen et al (1990) acceleration contour map for the contiguous United States adopted by AASHTO (Buckle, 1991). The differences emanate from the more-detailed regional geological and

seismological information compiled and developed in the course of this project. The PGA map is recommended for design because it would be compatible to the current acceleration map adopted by AASHTO. Also, the PGA map generally gives a higher coefficient than the A_v map for Arizona and therefore the PGA map would be somewhat more conservative. The other maps (the A_v maps and the 250 year maps) are presented for additional information.

In contrast to the previous studies which are based largely on relatively incomplete historical seismicity data, our work is heavily dependent on both seismicity and geologic data in the region. The major difference between the new acceleration contour map (90-percent non-exceedance in 50 years) and the corresponding Algermissen et al map are:

- In northwestern and north-central regions of Arizona (the Southern Hurricane-Wasatch and the San Francisco Volcanic Field seismic source zones), the acceleration levels from our map are significantly higher than those from Algermissen's map. The relatively higher acceleration values are considered appropriate in view of the significant number of potentially active faults in these areas as shown on the fault map of Arizona (Plate 1).

- In the southwestern corner of Arizona, the acceleration levels from our map are higher than those from Algermissen et al map. Our analysis indicates that the higher acceleration levels are caused largely by the California source zones. In Algermissen et al study, there are gaps in the California-Mexico-Arizona

border areas in their source zones which could have resulted in artificially low acceleration levels in southwest Arizona. Part of the differences are also due to higher recurrence rates for the California sources in our model.

- Acceleration levels from our map are either comparable to or lower than Algermissen's map over the remaining parts of Arizona, especially over the southern and southeastern part of Arizona. The reduction of acceleration levels in this region is due in part from incorporating more recent analyses which relocated some of the historical earthquakes from within Arizona to south of the Arizona border and in part from the results of our geologic studies which showed a relatively long recurrence intervals (in excess of 100,000 years) of a typical fault in southeastern Arizona. In the Arizona-New Mexico-Mexico border area, accelerations from our study indicate values of 0.05g as compared to 0.18g from Algermissen's map.

b. Recommendations

Due to current on-going developments by both SEOAC and BSSC committees on the national acceleration coefficient maps, several areas for future improvements or up dating of the acceleration coefficient maps from our study may be warranted in the future. Those areas have been discussed in the report. They are:

- Refinements on the aspects of standard deviation value, to allow a lower standard deviation value for regions of higher acceleration levels to better account for the acceleration saturation effects due to limitation of soil strengths.

- Refinements on the aspects of spectral acceleration instead of PGA coefficients to follow the current developments in the 1991 edition of the NEHRP provisions.

- Refinements on the aspects of soil site versus bedrock site.

The above developments are in a state-of-flux and it is not possible to speculate on some of the details such as the adopted attenuation relation and its appropriate standard deviation value. Some forms of spectral acceleration maps for soil sites (BSSC, 1991) rather than the existing peak bedrock acceleration maps have already been developed and are currently under review. Some consensus may be reached in the next (1994) NEHRP Provisions.

Incorporating the discussed developments in the attenuation relationship would be relatively easy since much of the geological and seismological database as well as the source zones boundaries and recurrence relationships would not be affected by the developments. The appropriate time for refinements on the above aspects would be when there is some consensus in the design community on the subject matter (e.g. in the 1994 NEHRP Provisions).

11. REFERENCES CITED

Albee, A.L. and Smith, J.L., 1966; Earthquake Characteristics and Fault Activity in Southern California; Engineering Geology in Southern California; Association of Engineering Geologists, Arcadia, California, 389 p.

Algermissen, S.T., Perkins, D.M., Thenhaus, P.C., Hanson, S.L., and Bender B.L.; 1990; Probabilistic Earthquake Acceleration and Velocity Maps for the United States and Puerto Rico, Miscellaneous Field Studies Map MF-2120.

Algermissen, S.T., Perkins, D.M., Thenhaus, P.C., Hanson, S.L., and Bender; B.L.; 1982; Probabilistic Estimates of Maximum Acceleration and Velocities in Rock in the Contiguous United States; United States Geological Survey; Open-File Report 82-1033; 107 p.

Algermissen, S.T.; 1969; Seismic Risk Studies in the United States; Proceedings of the Fourth World Conference on Earthquake Engineering; v. 1.

Allen, C.R., and Meisling, K.E.; 1982; Neotectonics of the North Frontal Fault System of the San Bernardino Mountains, Southern California, in Summaries of Technical Reports; v. 14; United States Geological Survey; Open-File Report 82-840; p. 101-103.

American Association of State Highway and Transportation Officials (AASHTO); 1983; Guide Specifications for Seismic Design of Highway Bridges," Washington, D.C.

Anderson, J.G.; 1979; Estimating the Seismicity from Geological Structure for Seismic Risk Studies; Bulletin of the Seismology Society of America; v. 69; n. 1; p. 135-158.

Anderson, R.E. and Christenson, G.C.; 1989; Quaternary Faults, Folds, and Related Volcanic Features of the Cedar City 1° x 2° Quadrangle, Utah; Utah Geological and Mineral Survey Miscellaneous Paper 89-6; 29 p.

Anderson, R.E., and Mehnert, H.H., 1979; Reinterpretations of the History of the Hurricane Fault; in Utah, in Newman, G.W., and Goode, H.D., eds.; 1979 Basin and Range Symposium; Rocky Mountain Association Geological and Utah Geological Association; p. 145-165.

Applied Technology Council; 1984; ATC 3-06, Amended, Tentative Provisions for the Development of Seismic Regulations for Buildings, Second Printing.

Applied Technology Council; 1978; ATC 3-06, Tentative Provisions for the Development of Seismic Regulations for Buildings.

Arabasz, W.J. and Smith, R.B.; 1979; Seismicity, Tectonics, and Crustal Structure in Utah; Important Aspects from New Data, in Earthquake Studies in Utah 1850 to 1978; Salt Lake City, Utah, University of Utah

Seismograph Stations; p. 395-408.

Arabasz, W.J. and Smith, R.B.; 1979; The November 1971 Earthquake Swarm near Cedar City, Utah, in Arabasz, W.J., Smith R.B., and Richins, W.D., editors; Earthquake Studies in Utah, 1850-1978; Salt Lake City, Utah, University of Utah Seismograph Stations; Department of Geology and Geophysics; p. 423-432.

Arizona Nuclear Power Project (ANPP); 1979; Final Safety Analysis Report; Section 2.5.

Arizona Public Service Company; 1974; Palo Verde Nuclear Generating Station Preliminary Safety Analysis Report with Amendments; v. 2 and 3.

Astiz, L. and Allen, C.R.; 1983; Seismicity of the Garlock Fault, California; Seismological Society of America; Bulletin; v. 73; n. 6; p. 1721-1734.

BSSC; 1991; 1991 Edition; NEHRP Recommended Provisions for the Development of Seismic Regulations for New Buildings, Part 1, Provisions, Part 2, Commentary.

Baksi, A.K.; 1974; K-Ar Study of the SP flow; Canadian Journal of Earth Science; v. 11; p. 1350-1356.

Bender, B. and Perkins, D.M.; 1987; SEISRISK III; A Computer Program for Seismic Hazards Estimation; United States Geological Survey Bulletin

1772; 48 p.

Bender, B.; 1986; Modeling Source Zone Boundary Uncertainty in Seismic Hazard Analysis; Seismological Society of America Bulletin; v. 76; April n. 2; p. 329-341.

Bender, B.; 1984; Incorporating Acceleration Variability into Seismic Hazard Analysis; Seismological Society of America Bulletin; v. 74; August, n. 4; p. 1451-1462.

Birkeland, P.W.; 1984; Soils and Geomorphology; Oxford University Press; 372 p.

Bohannon, R.G., and Howell, D.G.; 1982; Kinematic Evolution of the Junction of the San Andreas, Garlock, and Big Pine Faults, California; Geology; v. 7,; p. 358-363.

Bohannon, R.G.; 1979; Strike-slip Faults of the Lake Mead Region of Southern Nevada, in Cenozoic Paleogeography of the Western United States; Society of Economic Paleontologists and Mineralogists, Pacific Section; Pacific Coast Paleogeography Symposium 3; p. 129-139.

Bonilla, M.G., Mark, R.K., and Lienkaemper, J.J.; 1984; statistical Relations Among Earthquake Magnitude, Surface Rupture Length, and Surface Fault Displacement; Seismological Society of America; Bulletin; v. 74; p. 2379-2411.

Bridwell, R.J.; 1976; Lithospheric Thinning and the Late Cenozoic Thermal and Tectonic Regime of the Northern Rio Grande Rift; New Mexico Geological Society Guidebook; 27th Field Conference; Vermego Park; p. 283-292.

Brumbaugh, D.S.; 1992; Written Communication; Arizona Earthquake Catalog.

Brumbaugh, D.S.; 1991; Instrumental Magnitudes of Early Arizona Earthquakes; Seismological Research Letters; v. 62; p. 51.

Brumbaugh, D.S.; 1989; Summary of Earthquake Activity in Arizona for 1988 in Arizona Geology; Arizona Geological Survey; v. 19; n. 1; p. 8.

Brumbaugh, D.S.; 1980; Analysis of the Williams, Arizona Earthquake of November 4, 1971; Seismological Society of America; Bulletin; v 70; n. 3; p. 885-891.

Brune, J.N.; 1968; Seismic Moment, Seismicity and Rate of Slip along Major Fault Zones; Journal of Geophysical Research; v. 75; p. 777-784.

Buckle, I.G.; 1991; Seismic Design Criteria for Highway Bridges, Proceedings, Third Bridge Engineering Conference, Denver, Colorado, March, 1991; Transportation Research Board Record; n. 1290; v. 2; p. 80-94.

Bucknam, R.C., & Anderson, R.E.; 1979; Estimation of Fault-Scarp Ages from a Scarp-Height-Slope-Angle Relationship; in Geology; v. 7; p. 11-14.

Bull, W.B., and Pearthree, P.A.; 1988; Frequency and Size of Quaternary Surface Ruptures of Pitaycachi Fault, Northeastern Sonora Mexico; Bulletin of the Seismologic Society of America; v. 78.

Bull, W.B., and McFadden, L.D.; 1977, Tectonic Geomorphology North and South of the Garlock Fault, California, in Doehring, D.O., ed.; Geomorphology in Arid Regions, Proceedings; 8th Annual Geomorphology Symposium; State University of New York, Binghamton; p. 115-138.

Bull, W.B.; 1974; Reconnaissance of the Colorado River Terraces near the Yuma Dual Purpose Nuclear Plant; in Woodward McNeil & Associates; Geotechnical Investigation; Yuma Dual-Purpose Nuclear Plant; Appendix F, Part 1; 31 p. (prepared for Salt River Project, Phoenix, AZ).

Bullard, E.F. and Lettis, W.R.; 1990; Characteristics of Quaternary Surface Deformation in the Vicinity of the 1987 Whittier Narrows Earthquake, Los Angeles, California; Geological Society of America; Abstracts with Programs; v. 22; p. 11.

Burford, R.O., and Gilmore, T.D.; 1982; Vertical Tectonics, in Summaries of Technical Reports; v. 14; United States Geological Survey; Open-File Report 82-840; p. 29-31.

California Division of Mines and Geology; 1975; Recommended Guidelines of Determining the Maximum Credible and the Maximum Probable Earthquakes; Department of Conservation; Note 43; Sacramento, California.

Campbell, K.M.; 1985; Strong Motion Attenuation Relations; A Ten-year Perspective; Earthquake Spectra, v. 1; n. 4; August, 1985.

Campbell, K.W.; 1983; Bayesian Analyses of Extreme Earthquake Occurrences, Part II; Application to the San Jacinto Fault Zone of Southern California; Bulletin of the Seismological Society of America; v. 73; p. 1099-1115.

Cape, C.D., McGeary, S., and Thompson, G.A.; 1983; Cenozoic Normal Faulting and the Shallow Structure of the Rio Grande Rift near Socorro, New Mexico; Geological Society of America; Bulletin; v. 94; p. 3-14.

Carter, B.; 1982; Meogene Displacement on the Garlock Fault; California; EOS; v. 63; p. 1124.

Cash, D.J.; 1984; The Los Alamos National Laboratory Northern New Mexico Seismic Network and Seismicity, in Proceedings of the Conference on DOE Ground Motion and Seismic Programs On, Around, and Beyond the NTS, Vortman, L.J. (ed.); Sandia National Laboratories, Report SAND 83-2625, p. 345-356.

Christenson, G.E. & Purcell, C.; 1985; Correlation and Age of Quaternary Alluvial-fan Sequences, Basin and Range Province, Southwestern United States; Geological Society of America; Special Paper 203; p. 115-122.

Coffman, J.L., and Von Hake, C.A.; 1973; Earthquake History of the United States; United States Department of Commerce; National Oceanic and Atmospheric Administration, and United States Geological Survey; Publication 41-1; 207 p.

Cordell, L.; 1978; Regional Geophysical Setting of the Rio Grande Rift; Geological Society of America; Bulletin; v. 89; p. 1073-1090.

Cornell, C.A.; 1968; Engineering Seismic Risk Analysis; Seismological Society of America Bulletin; v. 58; p. 1583-1606.

Crone, A.J., Machette, M.N., Bonilla, M.G., Lienkaemper, J.J., Pierce, K.L., Scott, W.E., and Bucknam, R.C.; 1987; Surface Faulting Accompanying the Borak Peak Earthquake and Segmentation of the Lost River Fault, Central Idaho; Seismological Society of America Bulletin; v. 77; p. 739-770.

Cummings, D.; 1980; Mechanics of Fault Deformation and Seismo-tectonic Zoning, Mojave Desert Area, California; in Geology and Mineral Wealth of the California Desert; Ryland-Cummings, Inc.; South Coast Geological Society, Santa Ana, California; p. 101-120.

Damon, P.E., Shafiqullah, Muhammad, and Leventhal, J.S.; 1974; K-Ar Chronology for the San Francisco Volcanic Field and Rate of Erosion of the Little Colorado River, in Karlstrom, T.N. V., Swann, G.A., and Eastwood, R.L., eds., Geology of Northern Arizona with Notes on Archaeology and Paloclimate; Part I, Regional Studies; Geological

Society of America Annual Meeting; Rocky Mountain Section, 27th, Flagstaff, Arizona; p. 221-235.

Davis, G.A., and Burchfiel, B.C.; 1973; Garlock Fault; An Intercontinental Transform Structure, Southern California; Geological Society of America; Bulletin; v. 84; p. 1407-1422.

Demsey, K.A., and Pearthree, P.A.; 1990; Late Quaternary Surface-Rupture History of the Sand Tank Fault and Associated Seismic Hazard for the Proposed Superconducting Super Collider Site, Maricopa County, Arizona; Arizona Geological Survey Open-File Report 90-1.

Dewey, J.W.; 1982; Reanalysis of Instrumentally Recorded United States Earthquakes; Plateau Uplifts, in United States Geological Survey; Open-File Report 82-840; p. 3-4.

Dibblee, T.W. Jr.; 1980; Geologic Structure of the Mojave Desert in Geology and Mineral Wealth of the California Desert; South Coast Geological Society; p. 69-100.

Dibblee, T.W., Jr.; 1967; Evidence of Major Lateral Displacement on the Pinto Mountain Fault, Southeastern California; Geological Society of America; Abstract with Programs; 63rd Annual Meeting; p. 32.

Dohrenwend, J.C., Menges, C.M., Schell, B.A., and Moring, B.C.; 1992; Reconnaissance Photogeologic Map of Young Faults in the Las Vegas 1°

x 2° Quadrangle, Nevada, California, and Arizona; United States Geological Survey; Miscellaneous Field Investigations Map MF 2182.

Dokka, R.K., and Glazner, A.F.; 1982; Late Cenozoic Tectonic and Magmatic Evolution of the Central Mojave Desert, California; in Geologic Excursions in the California Desert; Guidebook prepared for Geological Society of America Cordilleran Section Meeting; p. 1-30.

DuBois, S.M., Sbar, M.L., and Nowak, T.A.; 1982; Historical Seismicity in Arizona; Arizona Bureau of Geology and Mineral Technology; University of Arizona; Open-File Report 82-21; p. 199.

DuBois, S.M., & Smith, A.W.; 1980; The 1887 Earthquake in San Bernardino Valley, Sonora; State of Arizona; Bureau of Geology and Mineral Technology; The University of Arizona; Historic Accounts and Intensity Patterns in Arizona; Special Paper n. 3; p. 112.

DuBois, S.M.; 1979; Earthquakes; Arizona Bureau of Geology and Mineral Technology; Field Notes; v. 9; n. 1; p. 1-9.

Eaton, G.P., Wahl, R.R., Prostka, H.J., Mobey, D.R., and Kleinkopf, M.D.; 1978; Regional Gravity and Tectonic Pattern; Their Relation to Late Cenozoic Epierogeny and Lateral Spreading in the Western Cordillera, in Cenozoic Tectonics and Regional Geophysics of the Western Cordillera; Geological Society of America; Memoir 152; p. 51-91.

Eberhart-Phillips, D., Richardson, R.M., Sbar, M.L., and Herrmann, R.B.; 1981; Analysis of the 4 February 1976 Chino Valley, Arizona, Earthquake; Bulletin of the Seismological Society of America; v. 71; n. 3; p. 787-801.

Freeman, K.J., Fuller, S., and Schell, B.A., 1986; The Use of Surface Faults for Estimating Design earthquakes; Implications of the 28 October 1983 Idaho Earthquake; Bulletin of the Association of Engineering Geologists; v. XXIII, p. 325-332.

Fuis, G.S.; 1982; Crustal Structure of the Mojave Desert, California; Geological Society of America; Abstract with Programs; v. 14; p. 164.

Garfunkel, Z.; 1974; Model for the Late Cenozoic Tectonic History of the Mojave Desert, California, and for its Relation to Adjacent Regions; Geological Society of America; Bulletin; v. 85; p. 1931-1944.

Gawthrop, W.H., and Carr, W.J.; 1988; Location Refinement of Earthquakes in the Southwestern Great Basin; 1931-1974, and Seismotectonic Characteristics of Some of the Important Events; United States Geological Survey; Open-File Report 88-560.

Geological Society of America; Decade of North American Geology (DNAG); Earthquake Catalog.

Gile, L.H., 1986; Late Holocene Displacement along the Organ Mountains Fault in Southern New Mexico, a summary; New Mexico Geology; v. 8; p. 1-4.

Gile, L.H., Hawley, J.W., and Grossman, R.B.; 1981; Soils and Geomorphology in the Basin and Range Area of Southern New Mexico Guidebook to the Desert Project; New Mexico Bureau of Mines & Mineral Resources; Memoir 39; 222 p.

Golombek, M.; 1981; Structure and Tectonics of the Pajarito Fault Zone in the Espanola Basin of the Rio Grande Rift, Northern New Mexico; Geological Society of America; Abstracts with Programs; v. 13; p. 461.

Gonzales, M.A.; 1991; Neotectonic Analysis of Rift-Margin Faults in the Abiquiu Embayment of the Rio Grande Rift, Northern New Mexico; New Mexico Geology; v. 13; n. 4; p. 94.

Goodfellow, G.E.; 1888; The Sonora Earthquake; Science; v. 11; p. 162-166.

Greensfelder, R.W., Kintzer, F.C., and Somerville, M.R.; 1980; Seismotectonic Regionalization of the Great Basin, and Comparison of Moment Rates Computed from Holocene Strain and Historic Seismicity, in Earthquake Hazards Along the Wasatch and Sierra-Nevada Frontal Fault Zones; United States Geological Survey; Open-File Report 80-801; p. 433-493.

Gutenberg, B., and Richter, C.; 1956; Magnitude and Energy of Earthquakes; Anneli de Geofisica; v. 9; n. 1; p. 1.

Gutenberg, B., and Richter, C.; 1956; Seismicity of the Earth and Associated Phenomena; Hefner Publishing Company; 310 p.

Gutenberg, B.; 1945; Amplitudes of Surface Waves and Magnitudes of Shallow Earthquakes; Bulletin of the Seismological Society of America; Bulletin; v. 35; n. 1; p. 3.

Hait, M.H. Jr. and Scott, W.E.; 1978; Holocene Faulting; Lost River Range, Idaho; Abstract; Geological Society of America; Abstract Programs; v. 10; p. 217.

Hamblin, W.K.; 1965; Origin of "Reverse Drag" on the Downthrown Side of Normal Faults; Geological Society of America Bulletin; v. 76; p. 1145-1164.

Hamblin, W.K. and Best, M.G.; 1979; Patterns and Rates of Recurrent Movement Along the Wasatch-Hurricane-Sevier Fault Zone During Late Cenozoic Time; United States Geological Survey; Summaries of Technical Reports; V. VIII; p. 126-127.

Hamblin, W.K., Damon, P.E., and Bull, W.B.; 1981; Estimates of Vertical Crustal Strain Rates Along the Western Margin of the Colorado Plateau; Geology; v. 9; p. 293-298.

Hamilton, W., and Myers, W.B.; 1966; Cenozoic Tectonics of the Western United States; Reviews of Geophysics; v. 4; p. 509-549.

Hanks, T.C., R.C. Bucknam, K.R. Lajoie, and R.E. Wallace; 1984; Modification of Wave-cut and Faulting-Controlled Landforms; Journal of Geophysical Research; v. 89; p. 5771-5790.

Hanks, T.C. and Kanamori, H.; 1979; A Moment Magnitude Scale; Journal of Geophysical Research; v. 84; p. 2348-2350.

Harmsen, S.C., and Rogers, A.M.; 1986; Inferences About the Local Stress Field from Focal Mechanisms; Applications to Earthquake in the Southern Great Basin of Nevada; Bulletin of the Seismological Society of America; v. 76; p. 1560-1572.

Heaton, T.H., Fumiko, T. and Mori, A.W.; 1984; Estimating Ground Motions Using Recorded Accelerograms; unpublished manuscript.

Hecker, S.; 1992; (in prep); Fault Map of Utah; Utah Geological Survey.

Herd, D.G. and McMasters, C.R.; 1982; Surface Faulting in the Sonora, Mexico, Earthquake of 1887; Geological Society of America; Abstracts with Programs 14; p. 172.

Herrmann, R.B., Dewey, J.W., and Park, S.; 1980; The Dulce, New Mexico Earthquake of 23 January 1966; Seismological Society of America; Bulletin; v. 70; n. 6; p. 2171-2183.

Hileman, J.A., Allen, C.R., and Nordquist, V.M.; 1973; Seismicity of the Southern California Region 1 January 1932 to 31 December 1972; California Institute of Technology, Pasadena, California.

Holm, R.F.; 1987; Geomorphic Evidence for Youngest Dated Faults in North-Central Arizona in The Mountain Geologist; v. 24; n. 1; January 1987; p. 19-25.

Holm, R.F., and Ulrich, G.E., 1987; Late Cenozoic Volcanism in the San Francisco and Mormon Volcanic Fields, Southern Colorado Plateau, Arizona; Arizona Bureau of Geology and Mineral Technology; Special Paper 5; p. 85-94.

Hope, R.A.; 1969; The Blue Cut Fault, Southeastern California; United States Geological Survey Professional Paper 650-D; p. 116-121.

Howard, K.A., Arron, J.M., Brabb, E.E., Brock, M.R., Gower, H.D., Hunt, S.J., Milton, D.J., Muehlberger, W.R., Nakata, J.K., Plafker, KG., Prowell, D.C., Wallace, R.E., and Witkind, I.J.; 1978; Preliminary Map of Young Faults in the United States as a Guide to Possible Fault Activity; United States Geological Survey Miscellaneous; Field Studies Map MF-916.

Howell, B.F., Jr.,; 1974; Seismic Regionalization in North America Based on Average Regional Seismic Hazard Index; Seismological Society of America; Bulletin; v. 64; p. 1509-1528.

Humphrey, J.R., & Wong, I.G.; 1983; Recent Seismicity Near Capitol Reef National Park, Utah, and its Tectonic Implications; Geology; v. 11; p. 447-451.

Jackson, G.W.; 1990; The Toroweap Fault: One of the Most Active Faults in Arizona in Arizona Geology; v. 20; n. 3; p. 7-10; Fall 1990; Arizona Geological Survey, Tucson, Arizona.

Jackson, G.W.; 1990; Tectonic Geomorphology of the Toroweap Fault, Western Grand Canyon, Arizona; Implications for Transgression of Faulting on the Colorado Plateau; Arizona Geological Survey; Open-File Report 90-4; p. 66.

Jennings, C.W.; 1975; Fault Map of California with Locations of Volcanoes, Thermal Springs, and Thermal Wells; California Division Mines and Geological Data Map n. 1; Scale 1:750,000.

Johnson, C.; 1980; Southern California Cooperative Seismic Network, in Summaries of Technical Reports; v. 10; United States Geological Survey; Open-File Report 80-842; p. 375-381.

Joyner, W.B., and Boore, D.M.; 1988; Measurement, Characterization, and Prediction of Strong Ground Motion, Proceedings, Earthquake Engineering and Soil Dynamics II - Recent Advances in Ground-Motion Evaluation; June, Park City, Utah; Geotechnical Special Publication; n. 20.

Kirkham, R.M. and Rogers, W.P.; 1985; Colorado Earthquakes Data and Interpretations, 1867 to 1985; Colorado Geological Survey; Bulletin 46.

King, G., and Stein, R.; 1984; Surface Folding, Deformation Rate, and Earthquake Repeat time in a Reverse Faulting Environment; in Coalinga, California Earthquake of May 2, 1983; Earthquake Engineering Research Institute Report 84-03; p. 61-69;

King, R.E.; 1939; Geological Reconnaissance in Northern Sierra Madre Occidental of Mexico; Geological Society of America Bulletin; v. 50; p. 1625-1722.

Longwell, C.R.; 1960; Possible Explanation of Diverse Structural Patterns in Southern Nevada; American Journal of Science; v. 258-A; p. 192-203.

Luedke, R.G., and Smith, R.L.; 1978; Map Showing Distribution, Composition, and Age of Late Cenozoic Volcanic Centers in Arizona and New Mexico; United States Geological Survey; Map 1-1091-A.

Lundberg, P.A.; 1986; A Brief Geologic History and Field Guide to the Jerome District, Arizona; in Geology of Central and Northern Arizona; Geological Society of America; Rocky Mountain Section, Field Trip Guidebook; p. 127-139.

Machette, M.N., Personius, S.F., Nelson, A.R., Schwartz, D.P., and Lund, W.R.; 1989; Segmentation Models and Holocene Movement History of the

Wasatch Fault Zone, Utah, in Schwartz, D.P., and Sibson, R.H., eds., Workshop on "Fault Segmentation and Controls of Rupture Initiation and Termination"; Proceedings of Conference XLV; United States Geological Survey; Open-File Report 89-315; p. 229-245.

Machette, M.N., Personius, S.F., Menges, C.M., and Pearthree, P.A.; 1986; Map Showing Quaternary and Pliocene Faults in the Silver City 1° x 2° Quadrangle and the Douglas 1° x 2° Quadrangle, Southeastern Arizona and Southwestern New Mexico; United States Geological Survey; Miscellaneous Field Studies Map 1465-C.

Machette, M.N., and Colman, S.M.; 1983; Age and Distribution of Quaternary Faults in the Rio Grande Rift; Evidence From Morphometric Analysis of Fault Scarps; Geological Society of America; Abstracts with Programs; v. 15; p. 320.

Machette, M.N. and McGimsey, R.G.; 1982; Quaternary and Pliocene Faults in the Socorro and Western part of the Fort Sumner 1° x 2° Quadrangles, New Mexico; United States Geological Survey Miscellaneous Field Studies Map MF 1465-A.

Machette, M.N.; 1978; Dating Quaternary Faults in the Southwestern United States Using Buried Calcic Paleosols; United States Geological Survey Journal of Research; v. 6; p. 369-381.

Malde, H.E.; 1971; Geologic Investigation of Faulting near the National Reactor Testing Station, Idaho, with section on Micro-Earthquake Studies; A.M. Pitt and J.P. Eaton, Editors; United States Geological Survey; Open-File Report; 167 p.

Martin, E.R., 1990; Structural and Stratigraphic Expression of Late Cenozoic Extensional Tectonism, Eastern and Northern Payson Basin, Central Arizona; Northern Arizona University; Master of Science Thesis; 138 p.

Mayer, J., and Foland, K.A.; 1991; Magmatic-Tectonic Interaction During Early Rio Gande Rift Extension at Questa, New Mexico; Geological Society of America; Bulletin; v. 103; p. 993-1006.

Mayer, L.; 1984; Dating Quaternary Fault Scarps formed in Alluvium using Morphologic Parameters; Quaternary Research; v. 22; p. 300-313.

McGuire, R.K.; 1976; Fortran Computer Program for Seismic Risk Analysis; United States Geological Survey; Open-File Report 76-67; 93 p.

McKee, E.H., and Anderson, C.A.; 1971; Age and Chemistry of Tertiary Volcanic Rocks in North-Central Arizona and Relation of the Rocks to the Colorado Plateau; Geological Society of America Bulletin; v. 82; p. 2767-2782.

Menges, C.M. and Pearthree, P.A.; 1983; Map of Neotectonic (Latest Pliocene-Quaternary) Deformation in Arizona; Bureau of Geology and Mineral Technology; Open File Report 83-22.

Menges, C.M.; 1983 (revised 1984); The Neotectonic Framework of Arizona: Implications for the Regional Character of Basin-Range Tectonism; State of Arizona; Arizona Bureau of Geology and Mineral Technology; (Part of final report, Contract #14-08-0001-19861); Open-File Report 83-19; p. 109.

Mokhtar, T.A.; 1979; The Relationship Between the Seismicity and Late Cenozoic Tectonics in Arizona; University of Arizona; Masters Thesis; p. 53.

Moore, R.T., Wilson, E.D., and O'Haire, R.T.; 1960; Geologic Map of Coconino County, Arizona; Arizona Bureau of Mines and University of Arizona.

Moore, R.B., and Wolfe, K.W.; 1987; Geologic Map of the East part of the San Francisco Volcanic Field; North Central Arizona; United States Geological Survey Miscellaneous Field Studies Map MF-1960.

Morgan, P., and Seager, W.R.; 1983; Thermal, Mechanical and Tectonic Evolution of the Southern Rio Grande Rift; Geological Society of America; Abstracts with Programs; p. 320.

Morrison, R.B.; 1985; Pliocene/Quaternary Geology, geomorphology, and Tectonics of Arizona; in Geological Society of America Special Paper 203; p. 123-146.

Muehlberger, E.W., 1988; The Structure and Stratigraphy of the Western Half of the Payson Basin, Gila County, Arizona; Northern Arizona University; Masters Thesis; 85 p.

Muir, S.G., Schell, B.A., and Farley, T.; 1981; Quaternary Faults in East-central Nevada and West-central Utah; Association of Engineering Geologists Annual Meeting; Abstracts with Programs; p. 46.

Nakata, J.K., Wentworth, C.M., and Machette, M.N.; 1982; Quaternary Fault Map of the Basin and Range and Rio Grand Rift Provinces, Western United States; United States Geological Survey; Open-File Report 82-579; Scale 1:2,500,000.

Nash, D.B.; 1980; Morphologic Dating of Degraded Normal Fault Scarps; Journal of Geology; v. 88; p. 353-360.

Nations, J.D., and Brumgaugh, D.S., 1992; Evidence for pre-27.2 ma Subsidence of Tonto Basin, Central Arizona; Geological Society of America; Abstracts with Programs; v. 24; p. 46.

Oakeshott, G.B.; 1971; California's Changing Landscapes; A Guide to the Geology of the State; McGraw-Hill Book Company, New York; 388 p.

Pearthree, P.A. and Calvo, S.S.; 1987; The Santa Rita Fault Zone; Evidence for Large Magnitude Earthquakes with very Long Recurrence Intervals; Basin and Range Province of Southeastern Arizona; Bulletin of the Seismological Society of America; v. 77; p. 97-116.

Pearthree, P.A.; 1986; Late Quaternary Faulting and Seismic Hazard in Southeastern Arizona and Adjacent Portions of New Mexico and Sonora, Mexico; Arizona Bureau of Geology and Mineral Technology; University of Arizona; Open-File Report 86-8; p 17.

Perkins, D.M.; 1980; Outer Continental Shelf Seismic Risk, in Summaries of Technical Reports, v. IX; United States Geological Survey; Open-File Report 80-6; p. 166-168.

Perkins, D.M., Ziony, J.I., and Algermissen, S.T.; 1980; Probabilistic Estimates of Maximum Seismic Horizontal Ground Motion on Rock in Coastal California and the Adjacent Outer Continental Shelf; United States Geological Survey; Open-File Report 80-924.

Piety, L.A. and Anderson, L.W; 1991; The Horseshoe Fault, Evidence for Prehistoric Surface-Rupturing Earthquakes in Central Arizona in Arizona Geology; v. 21; n. 3; p. 1-8;

Prescott, W.H., Savage, J.C., Lisowski, and King, N.; 1982; Crustal Strain, in Summaries of Technical Reports; v. 14; United States Geological Survey; Open-File Report 82-840; p. 304-308.

Racine, D., O'Donnell, A., Burnetti, J., Klouda, P., Marshall, M., Tobin, Ed., Megyesi, I., and Wagner, R.; 1979; A Seismicity Study of the Southwest Region of the United States; Alexandria Laboratories; Teledyne Geotech for Army Corps of Engineer and Nuclear Regulatory Commission; Contract No. DACW-0979-C-0052; AL-79-5.

Ranney, W.; 1989; The Verde Valley; A Geological History; Museum of Northern Arizona Plateau; v. 60; n. 3.

Reiter, L., 1990; Earthquake Hazard Analysis, Issues and Insights: Columbia University Press, New York.

Richins, W.D., Zandt, G., and Arabasz, W.J.; 1981; Swarm Seismicity along the Hurricane Fault Zone during 1980-1981; A Typical Example for SW Utah; EOS; Transactions of the American Geophysical Union (abs.); v. 62; n. 45; p. 966.

Richter, C.; 1959; Seismic Regionalization; Seismological Society of America Bulletin; v. 49; p. 12-162.

Richter, C.; 1935; An Instrumental Earthquake Scale; Bulletin of the Seismological Society of America; v. 25; n. 1; p. 1-32.

Rieter, M., Edwards, C.L., Hartman, H., and Weidman, D.; 1975; Terrestrial Heat Flow Along the Rio Grande Rift, New Mexico and Southern Colorado; Geological Society of America Bulletin; v. 86; p. 811-818.

Rogers, A.M.; 1977; A Preliminary Assessment of the Seismic Hazard of the Nevada Test Site Region; Seismological Society of America; Bulletin; v. 67; p. 1587-1606.

Rogers, A.M., Harmsen, S.C., and Carr, W.J.; 1981; Southern Great Basin Seismological Data Report for 1980 and Preliminary Data Analysis; United States Geological Survey; Open-File Report 81-10086.

Rogers, A.M., and Lee, W.H.K.; 1976; Seismic Study of Earthquakes in the Lake Mead, Nevada-Arizona Region; Bulletin of the Seismological Society of America; v. 66; n. 5; p. 1657-1681.

Ryall, A.; 1977; Earthquake Hazard in the Nevada Region; Bulletin of the Seismological Society of America; v. 67; p. 517-532.

Sanford, A.R., Olsen, K.H., Jaksha, L.H., 1981, Seismicity of New Mexico 1849 through 1988 in Hays, W.W., ed.; Proceedings of the Conference on Evaluation of Regional Seismic Hazards and Risk, August 25-27; 1980; Santa Fe, New Mexico; United States Geological Survey; Open-File Report 81-437; p. 74-89.

Sanford, A.R., Budding, A.J., Hoffman, J.P., Alptekin, O.S., Rush, C.A., and Toppozada, T.R.; 1972; Seismicity of the Rio Grande Rift in New Mexico; New Mexico Bureau of Mines, Circular 120; 19 p.

Sauk, W.A., and Sumner, J.S.; 1970; Residual Aeromagnetic Map of Arizona; Tucson, Arizona; Department of Geosciences, University of Arizona; Scale 1:1,000,000.

Scarborough, R.B., Menges, C.M., and Pearthree, P.A.; 1983(ca); Late Pliocene-Quaternary (Post 4 M.Y.) Faults, Folds, and Volcanic Rocks in Arizona; Arizona Bureau of Geology and Mineral Technology; Map 22.

Schell, B.A.; 1991; Seismotectonic Zonation and Seismic Hazard Analyses in Southern California; Earthquake Engineering Research Institute; Proceedings of the Fourth International Conference on Seismic Zonation; v. 2; p. 19-26.

Schell, B.A.; 1982; Distribution and Style of Faults in the Great Basin and Their Relationship to Magnitude and Frequency of Earthquakes; American Geophysical Union, Chapman Conference on Fault Behavior and the Earthquake Process.

Schell, B.A.; 1978; Seismotectonic Microzoning for Earthquake Risk Reduction; Proceedings of Second International Conference on Microzonation; p. 571-585.

Schell, B.A., Erickkson, L.G., Murphy, B.E., Boylan, D., Kling M. and Gregory, J.L.; 1985; Application of Seismotectonic Zoning to Regional Site Screening, Characterization, and Selection; Association of Engineering Geologists Annual Meeting; Abstracts with Program; p. 74.

Schell, B.A. and Muir, S.; 1982; Young Faults and Lineaments in the Southern Great Basin of Nevada and Utah; Geological Society of America; Abstracts with Programs; v. 14; p. 231.

Schell, B.A., and Wilson, K.L.; 1982; Regional Neotectonic Analysis of the Sonoran Desert; United States Geological Survey; Open-File Report 82-57; 70 p.

Schell, B.A., Farley, T., and Muir, S.G.; 1981; Fault-Rupture and Earthquake Hazards in East-central Nevada and West-central Utah; Association of Engineering Geologists Meeting; Programs with Abstracts; p. 52.

Schnabel, P. and Seed, H.B.; 1973; Acceleration in Rocks for Earthquakes in the Western United States; Bulletin of the Seismological Society of America; v. 63; p. 501-516.

Schwartz, D.P., and K.L. Coppersmith; 1984; Fault Behavior and Characteristic Earthquakes; Examples from the Wasatch and San Andreas Fault Zones; Journal of Geophysical Research; v. 89; p. 5681-5698.

Scott, W.E., K.L. Pierce, and M.H. Hait, Jr.; 1985; Quaternary Tectonic Setting of the 1983 Borah Peak Earthquake, Central Idaho; Bulletin of the Seismological Society of America; v. 75; p. 1053-1066.

Seed, H.B., and Idriss, I.M.; 1982; Ground Motions and Soil Liquefaction

During Thenhaus; Earthquakes; Earthquake Engineering Research Institute Monograph Series.

Shackleton, N.J. and Opdyke, N.D.; 1973; Oxygen Isotope and Paleomagnetic Stratigraphy of Equatorial Pacific Core V28-238: Oxygen Isotope Temperature and Ice Volumes on a 10^5 Year and 10^6 Year Scale; Quaternary Research; v. 3; n. 1; p. 39-55.

Shafiqullah, M., Damon, P.E., Lynch, D.J., Reynolds, S.J., Rehrig, W.A., & Raymond R.H.; 1980; K-Ar Geochronology and Geologic History of Southwestern Arizona and Adjacent Areas; Arizona Geological Society Digest; v. XII; p. 201-260.

Shoemaker E.M., Squires, R.L., and Abrams, M.J.; 1978; Bright Angel and Mesa Butte Fault Systems of Northern Arizona; in Smith, R.B.; and Eaton, G.P., eds.; Cenozoic Tectonics and Regional Geophysics of the Western Cordillera; Geological Society of America; Memoir 152; p. 341-368.

Sieh, K.E., Stuiver, M., and Brillinger, D.; 1989; A More precise Chronology of Earthquakes Produced by the San Andreas Fault in Southern California; Journal of Geophysical research; v. 94; B1; p. 603-623.

Slemmons, D.B.; 1982; Determination of Design Earthquake Magnitudes of Microzonation; Proceedings of Third International Earthquake Microzonation Conference; v. 1; p. 119-130.

Smith, R.B., and Lindh, A.G.; 1978; Fault-plane Solutions of the Western United States, a compilation; Geological Society of America; Memoir 152; p. 170-110.

Smith, R.B., and Sbar, M.L.; 1974; Contemporary Tectonics and Seismicity of the Western United States with Emphasis on the Intermountain Seismic Belt; Geological Society of America Bulletin; v. 85; p. 1205-1218.

Sowers, J.M., Amundson, R.G., Chadwick, O.A., Harden, J.W., Jull, A.J.T., Ju, T.L., McFadden, L.D., Rehees, M.C., Taylor, E.M., Szabo, B.J., Robinson, S.W.; 1988; Geomorphology and Pedology on the Kyle Canyon Alluvial Fan, Southern Nevada, in This Extended Land, Geological Journeys in the Southern Basin and Range; Geological Society of America Field Trip Guidebook; p. 137-157.

Soule, C.H.; 1978; Tectonic Geomorphology of Big Chino; M.S. Thesis; The University of Arizona; p. 1-102.

Stover, C.W., Reagor, B.G., and Algermissen, S.T.; 1988; Seismicity Map of the State of New Mexico; United States Geological Survey; Miscellaneous Field Studies Map MF-2035;

Stover, C.W., Reagor, B.G., and Algermissen, S.T.; 1986; Seismicity Map of the State of Arizona; United States Geological Survey; Miscellaneous Field Studies Map MF-1852; Scale 1:1,000,000.

Sturgal, J.R. and Irwin, T.D.; 1971; Earthquake History of Arizona and New Mexico; 1850-1966; Arizona Geological Society Digest; v. 9; p. 1-37.

Sumner, J.R.; 1977; The Sonora Earthquake of 1887; Bulletin of the Seismological Society of America; v. 67; p. 1219-1223.

Taggart, J., and Baldwin, F.; 1982; Earthquake Sequence of 1938-1939 in Magollon Mountains, New Mexico; New Mexico Geology; v. 4; p. 49-52.

Tanaka, K.L., Shoemaker, G.E., Ulrich, G.E., and Wolfe, E.W.; 1986; Migration of Volcanism in the San Francisco Volcanic Field, Arizona; Geological Society of America Bulletin; v. 97; p. 129-141.

Tanaka, K.L., Ulrich, G.E. and Shoemaker, E.M.; 1984; Magneto-stratigraphy of the San Francisco Volcanic Field, Arizona; Geological Society of America; Abstracts with Programs; v. 16; p. 257.

Thenhaus, P.C. and Wentworth, C.M.; 1982; Map Showing Zones of Similar Ages of Surface Faulting and Estimated Maximum Earthquake Size in the Basin and Range Province and Selected Adjacent Areas; United States Geological Survey; Open-File Report 82-742; 18 p.

Thenhaus, P.C., Perkins, D.M., Ziony, J.I., and Algermissen, S.T.; 1980; Probabilistic Estimates of Maximum Seismic Horizontal Ground Motion on Rock in coastal California and the Adjacent Outer Continental Shelf; United States Geological Survey; Open-File Report 80-924; 69 p.

Towle, J.N.; 1980; New Evidence for Magmatic Intrusion Beneath the Rio Grande Rift, New Mexico; Geological Society of America Bulletin; v. 91; Part L; p. 626-630.

Townley, S.D., and Allen, M.W.; 1939; Descriptive Catalog of Earthquakes of the Pacific Coast of the United States; 1769 to 1928; Bulletin of the Seismological Society of America; v. 29; p. 1-20.

Van Wormer, J.D., and Ryall, A.S.; 1980; Sierra Nevada-Great Basin Boundary zone; Earthquake Hazard Related to Structure, Active Tectonic Processes, and Anomalous Patterns of Earthquake occurrence; Bulletin of the Seismological Society of America; v. 70; n. 5; p. 1557-1572.

Van Wormer, J.D., and Ryall, A.S.,; 1980; Estimation of Maximum Magnitude and Recommended Seismic Zone Changes in the Western Great Basin; Bulletin of the Seismological Society of America; v. 70; n. 5; p. 1573-1581.

Van Wormer, J.D., and Ryall, A.S.; 1980; Seismicity related to Structure and Active Tectonic Processes in the Western Great Basin, Nevada and Eastern California; in Earthquake Hazards along the Wasatch and Sierra Nevada Frontal Fault Zones; United States Geological Survey; Open-File Report 80-80; p. 37-61.

Wallace, T.C., and Pearthree, P.A.; 1989; Recent Earthquakes in Northern Sonora; Arizona Geology; v. 19;, n. 3; p. 6-7.

Wallace, T.C. Domitrovic, A.M., and Pearthree, P.A.; 1988; Southern Arizona Earthquake Update; Arizona Geology; v. 18;, n. 4; p. 6-7.

Wallace, R.E.; 1987; Grouping and Migration of Surface Faulting and Variations in Slip Rates on Faults in the Great Basin Province; Bulletin of the Seismological Society of America; v. 77; p. 868-876;

Wallace, R.E.; 1977; Profiles and Ages of Young Fault Scarps, North-central Nevada; Geological Society of America Bulletin; v. 88; p. 1267-1281.

Warren, D.H.; 1969; A Seismic-Refraction Survey of Crustal Structure in Central Arizona; Geological Society of America Bulletin; v. 80; p. 257-282.

West, R.E., and Sumner, J.S.; 1973; Bouguer Gravity Anomaly Map of Arizona; Tucson, Arizona; Department of Geosciences, University of Arizona; Scale 1:1,000,000.

Williams, P.L., and Sieh, K.E.; 1987; Decreasing Activity of the Southernmost Sam Andreas Fault During the Past Millenia; Geological Society of America; Abstracts with Programs; v. 19; p. 891.

Witcher, J.C., 1981; Thermal Springs of Arizona; Arizona Bureau of Geology and Mineral Technology; Fieldnotes; v. 11; n. 2; p 1-4.

Wolfe, E.W., Ulrich, G.E., and Newhall, C.G.; 1987; Geologic Map of the Northwest Part of the San Francisco Volcanic Field, North-Central Arizona; United States Geological Survey Miscellaneous Field Studies Map M-F-1987;

Wolfe, E.W., Ulrich, G.E., Holm. R.F., Moore, R.B., and Newhall, C.G.; 1987; Geologic Map of the Central Part of the San Francisco Volcanic Field, North-Central Arizona; United States Geological Survey Miscellaneous Field Studies Map MF 1959.

Wong, I.G., Cash, D.J., Jaksha, L.H.; 1984; The Crownpoint, New Mexico, Earthquakes of 1986 and 1977; Bulletin of the Seismological Society of America; v. 74; p. 2435-2449.

Wood, H.O. and Neuman, F.; 1931; Modified Mercalli Intensity Scale of 1931; Bulletin of the Seismological Society of America; v. 21; p. 277-283.

Working Group on California Earthquake Probabilities; 1988; Probabilities of Large Earthquakes Occurring In California on the San Andreas Fault; United States Geological Survey; Open-File Report 88-398; 62 p.

Wyss, M.; 1979; Estimating Maximum Expectable Magnitude of Earthquakes from Fault Dimensions; Geology; v. 7; p. 336-340.

Young, R.A., Pierce, H.W., and Faulds, J.E.; 1987; Geomorphology and Structure of the Colorado Plateau/Basin and Range Transition Zone, Arizona in Geologic Diversity of Arizona and its Margins; Excursions to Choice Area; Arizona Bureau of Geology and Mineral Technology Special Paper 5; p. 182-196.

APPENDIX A

SUMMARY OF FAULTS AND FAULT ZONES

Seismic Source Zone or Fault		Length (miles)		Displacement		Earthquake
Number	Name/Location	Zone	Longest Segment	Latest Age (1)	Slip Rate	Maximum Credible
1	Hurricane Fault/ NW AZ, Cedar City, Utah to Peach Spring, AZ	160	43	H	0.3-0.5 mm/yr.	7.5-7.75
2	Toroweap/Colorado Plateau, UT & AZ	265	-	h	0.06-0.4 mm/yr.	7.5-7.75
3	West Kaibab/Colorado Plateau, UT-AZ border to Colorado River	41	-	Qy	-	7.5
4	Sinyala/Grand Canyon Kaibab fault to Coconino Plateau	34	-	?	5 m/ 200 my	7.5
5	Grand Wash/ NW AZ to SW Utah	60	-	L	-	7.5
6	Washington/ NW AZ to SW Utah	40	35	Qy	0.01 mm/yr.	7.5
7	Mainstreet Valley Mainstreet Valley, NW AZ 12 mi.W. of Hurricane Fault	35		?	-	7.5
8	Dellenbaugh NW AZ	45	-	Q	0.02 to 0.10 mm/yr	7.25
9	Aubrey Fault/Aubrey Cliffs, N. of Seligman AZ to Toroweap Fault	32	12	H	0.01 to 0.03 mm/yr	7.25
10	West Aubrey N. Aubrey Valley, NW AZ	6	-	Q	-	6.5

Notes: Age of Latest Movement — Approx. Age (myBP)

h - late to mid Holocene	0.005
H - early Holocene to latest Pleistocene	0.005 - 0.02
L - late Pleistocene	0.02 - 0.15
M - mid Pleistocene	0.15 - 0.7
Qy - Late Quaternary; undifferentiated	≤ 0.5
E - early Pleistocene	0.7 - 2
Q - Quaternary; undifferentiated	≤ 2
P - known Pliocene	2 - 5
? - Age Uncertain but Neotectonic	

SUMMARY OF FAULTS AND FAULT ZONES

Seismic Source Zone or Fault		Length (miles)		Displacement		Earthquake
Number	Name/Location	Zone	Longest Segment	Latest Age (1)	Slip Rate	Maximum Credible
11	Passport Graben S. Prospect V., NW AZ	6	-	Q	-	6.5
12	Robbers Roost Fault/ N. Aubrey Valley, AZ	6	2	Qy	-	6.5
13	Pica Graben W. Aubrey V., NW AZ	6	-	Qy	-	6.5
14	Yampai Graben/ Grand Cyn Cavern Area AZ	5	-	Q	-	6.5
15	Audley Escarpment/ 15 mi. E. of Peach Springs AZ	11	-	Q	-	6.5
16	Seventy Four Plains/ Near Audley; S. of Route 66	3	-	Qy	-	6.5
17	Seligman/6 mi. S. of of Seligman, AZ crosses I-40	12	-	H	0.01-0.14 mm/yr.	7
18	Big Chino Fault/NE Side Big Chino Valley, N. of Prescott, AZ	35	18	H	0.06 to 0.12 mm/yr.	7.25
19	W. Chino Valley N-Central Big Chino Valley, NW AZ	5	-	Qy	-	6.5
20	Orchard/12 mi. NW of Cottonwood, AZ	9	-	?		6.75

Notes:

Age of Latest Movement	Approx. Age (myBP)
h - late to mid Holocene	0.005
H - early Holocene to latest Pleistocene	0.005 - 0.02
L - late Pleistocene	0.02 - 0.15
M - mid Pleistocene	0.15 - 0.7
Qy - Late Quaternary; undifferentiated	≤ 0.5
E - early Pleistocene	0.7 - 2
Q - Quaternary; undifferentiated	≤ 2
P - known Pliocene	2 - 5
? - Age Uncertain but Neotectonic	

SUMMARY OF FAULTS AND FAULT ZONES

Seismic Source Zone or Fault		Length (miles)		Displacement		Earthquake
Number	Name/Location	Zone	Longest Segment	Latest Age (1)	Slip Rate	Maximum Credible
21	Railroad/Verde River, 9 miles NNW of Cottonwood AZ	12	-	?	-	6.75
22	Verde Fault/SW side Verde Valley, Yavapai County, AZ	38	17	H/L	0.01 to 0.05 mm/yr.	7.25
23	Paulden/Chino Valley 6 mi. S. of Paulden, AZ	4	1	L/M	-	6.5
24	Williamson Valley Grabens/ Bet. Simmons & Skull Valley, NNW of Prescott	11	1	L/M	-	6.75
25	Prescott Valley Grabens/ 10 mi. NNW of Prescott, AZ	5	1	L/M	0.07 to 0.2	6.5
26	Juniper Mountains Faults/ W. of Juniper Mountains, E. of Aquarius Mountains Mount Hope	21	7	?	-	6.75
27	Big Sandy/Hwy 93, 25 mi. SE of Kingman, AZ	8	-	?	-	6.75
28	Hualapai Mountains/ E. of Hualapai Mountains 22 mi. E. of Kingman, AZ	22	7	?	-	6.5
29	Sheep Mountain Fault/ NE Flank Gila Mountains Yuma County, AZ	6	2	?	-	-
30	Algodones/SW corner AZ	7	-	H	0.04 to 0.1 mm/yr.	6.5

Notes:

Age of Latest Movement	Approx. Age (myBP)
h - late to mid Holocene	0.005
H - early Holocene to latest Pleistocene	0.005 - 0.02
L - late Pleistocene	0.02 - 0.15
M - mid Pleistocene	0.15 - 0.7
Qy - Late Quaternary; undifferentiated	≤ 0.5
E - early Pleistocene	0.7 - 2
Q - Quaternary; undifferentiated	≤ 2
P - known Pliocene	2 - 5
? - Age Uncertain but Neotectonic	

SUMMARY OF FAULTS AND FAULT ZONES

Seismic Source Zone or Fault		Length (miles)		Displacement		Earthquake
Number	Name/Location	Zone	Longest Segment	Latest Age (1)	Slip Rate	Maximum Credible
31	Cargo Muchacho/S. end Cargo Muchacho Mountains 6 mi. NW Yuma, AZ	1	-	L	-	6.5
32	Lost Trigo/Colorado River Trough, 4 mi. S. of Cibola	6	-	E	0.009 mm/yr	6.5
33	Blythe Graben/McCoy Wash, CA, 9 mi. NW of Blythe, CA	4	-	H	0.05 to 0.1	6.5
34	Needles Graben 9 miles East of Needles, CA	8	3	H	0.1 to 0.3 mm/yr	6.5
35	Chemhuevi Graben/ West side Colorado River, CA	3	-	H	0.07 mm/yr	6.5
36	Sand Tank Fault/ 7 mi. ESE of Gila Bend AZ	2	-	H	0.01 to 0.04 mm/yr.	6.5
37	Merriwhitica W. Grand Canyon Area NW AZ	25	-	?	-	7.0
38	Peach Springs Graben/ N Route 66 near Peach springs, AZ	8	-	?	-	7.0
39	Big Spring (Kaibab)/ Kaibab Plateau, N. of Grand Canyon, AZ	36	-	?	-	7.5
40	Moquitch Canyon (Kaibab)/ Kaibab Plateau	16	-	?	-	7.25

Notes:

Age of Latest Movement	Approx. Age (myBP)
h - late to mid Holocene	0.005
H - early Holocene to latest Pleistocene	0.005 - 0.02
L - late Pleistocene	0.02 - 0.15
M - mid Pleistocene	0.15 - 0.7
Qy - Late Quaternary; undifferentiated	≤ 0.5
E - early Pleistocene	0.7 - 2
Q - Quaternary; undifferentiated	≤ 2
P - known Pliocene	2 - 5
? - Age Uncertain but Neotectonic	

SUMMARY OF FAULTS AND FAULT ZONES

Seismic Source Zone or Fault		Length (miles)		Displacement		Earthquake
Number	Name/Location	Zone	Longest Segment	Latest Age (1)	Slip Rate	Maximum Credible
41	Demotte, Kaibab Plateau N. of Grand Canyon, AZ	30	-	Q	-	7.25
42	Bright Angel Grand Canyon, AZ	37	-	?	-	7.5
43	Vishnu Fault, Coconino Plateau, S. Grand Canyon, AZ	19	8	?	-	7.25
44	Cataract Creek Fault Set/ Coconino Plateau, W. of Hwy 64	33	14	?	-	7.25
45	Sand Creek/ Central Coconino Plateau, NW AZ	21	-	?	-	7.25
46	Rose Well/Central Coconino Plateau, AZ	29	17	?	-	7.5
47	Muav Fault Kaibab Plateau N. of W Grand Canyon, AZ	27	-	?	-	7.25
48	Summit Valley/Kaibab Plateau, E. West Kaibab Fault, No. AZ	19	10	?	-	7.25
49	Mohawk/Colorado Plateau, near Toroweap Faults	29	-	?	-	7.25
50	Detrital Valley/W. side Detrital Valley, E. of Hwy 93, NW AZ	9	1	?	-	6.75

Notes:

Age of Latest Movement	Approx. Age (myBP)
h - late to mid Holocene	0.005
H - early Holocene to latest Pleistocene	0.005 - 0.02
L - late Pleistocene	0.02 - 0.15
M - mid Pleistocene	0.15 - 0.7
Qy - Late Quaternary; undifferentiated	≤ 0.5
E - early Pleistocene	0.7 - 2
Q - Quaternary; undifferentiated	≤ 2
P - known Pliocene	2 - 5
? - Age Uncertain but Neotectonic	

SUMMARY OF FAULTS AND FAULT ZONES

Seismic Source Zone or Fault		Length (miles)		Displacement		Earthquake
Number	Name/Location	Zone	Longest Segment	Latest Age (1)	Slip Rate	Maximum Credible
51	Virgin Mountains Frontal Fault system/NW Flank of Virgin Mountains, NW AZ&SE NV	65	20	H	0.01-0.06 mm/yr.	7.25
52	Wheeler Fault & Graben/ Hualapai Wash, NW AZ	34	-	M	0.02 mm/yr.	6.75
53	Echo Bay (Valley of Fire)/ E. Flank Muddy Mountains W. of Overton Arm, NV	7	3	L	-	6.75
54	Bitter Springs Fault Crosses Bitter Spring Valley Bet. Muddy & Black Mountains	7	-	L	-	6.75
55	Coyote Spring/E. Side Coyote Spring Valley, SE NV	10	-	L	-	6.75
56	Littlefield Mesa Scarps/ NW corner AZ-NV-UT	13	2	E	-	6.5
57	Hungry Valley Set/AZ-NV border Bet. Virgin Mountains & Lake Mead	40	6	?	-	6.5
58	Black Ridge/NW Flank of Black Ridge & Bajada of Virgin Mountains, SE NV	16	4	M/E	-	6.75
59	Mormon Mesa Scarps/ N. of Overton Arm Lake Mead area	9	5	Q	-	6.75
60	Toquop Wash/W. side of Toquop Wash, N. side Virgin Valley, SE NV	19	2	Q		6.75

Notes:

Age of Latest Movement		Approx. Age (myBP)
h	late to mid Holocene	0.005
H	early Holocene to latest Pleistocene	0.005 - 0.02
L	late Pleistocene	0.02 - 0.15
M	mid Pleistocene	0.15 - 0.7
Qy	Late Quaternary; undifferentiated	$\leq$ 0.5
E	early Pleistocene	0.7 - 2
Q	Quaternary; undifferentiated	$\leq$ 2
P	known Pliocene	2 - 5
?	Age Uncertain but Neotectonic	

SUMMARY OF FAULTS AND FAULT ZONES

Seismic Source Zone or Fault		Length (miles)		Displacement		Earthquake
Number	Name/Location	Zone	Longest Segment	Latest Age (1)	Slip Rate	Maximum Credible
61	East Morman Mountains/ W side of East Mormon Mountains SE NV	9	2	L	-	7.0
62	Tramp Ridge/N end Tramp Ridge, SE NV	11	-	Q	-	6.75
63	California Wash/ S. Nevada	19	-	L	-	7.25
64	Moapa/W. side California Wash, Moapa Indian Reserv., SE NV	15	-	L	-	7.0
65	Dry Lake Range Fault/ W. side Dry Lake Range E I-15, SE NV	7	-	M/E	-	7.0
66	South Dry Lake Valley/ Sub-parallel to I-15, SE NV	6	-	Q	-	6.75
67	Gypsum Wash/ S end Dry Lake Range, SE Nevada	4	3	M/E	-	6.75
68	Frenchman Mountain/ W. side of Frenchman Mountain, E. of Las Vegas, SE NV	12	-	Qy	-	7.0
69	Arrow Canyon Range/ S. Nevada	16	-	L	-	7.25
70	Meadow Mountain/W. side Meadow Mountains, NNE Las Vegas, SE NV	16	-	L	-	7.25

Notes:

Age of Latest Movement	Approx. Age (myBP)
h - late to mid Holocene	0.005
H - early Holocene to latest Pleistocene	0.005 - 0.02
L - late Pleistocene	0.02 - 0.15
M - mid Pleistocene	0.15 - 0.7
Qy - Late Quaternary; undifferentiated	≤ 0.5
E - early Pleistocene	0.7 - 2
Q - Quaternary; undifferentiated	≤ 2
P - known Pliocene	2 - 5
? - Age Uncertain but Neotectonic	

SUMMARY OF FAULTS AND FAULT ZONES

Seismic Source Zone or Fault		Length (miles)		Displacement		Earthquake
Number	Name/Location	Zone	Longest Segment	Latest Age (1)	Slip Rate	Maximum Credible
71	Transector Fault/S. end Valley Bet. Arrow Canyon Range & Las Vegas Range, NNE Las Vegas, NV	3	-	L	-	6.5
72	Kane Springs Wash/NE margin of Meadows Valley Mountain, NNE Las Vegas, NV	22	-	L	-	7.25
73	Sheep Range Fault/E. side Sheep Range, NV	19	-	L	-	7.25
74	Maynard Lake Fault/S. end Delamar Valley to N. end Sheep Range, SE NV	19	-	L?	-	7.25
75	Mead slope/Fortification Hill, Lake Mead, 12 mi. NE Boulder City, NV	3	-	L	-	6.5
76	Railroad Pass Fault/ SE margin Black Hills, 5 mi. W. Boulder City NV	<1	-	L	-	6.5
77	River Mountains Fault/ W. Las Vegas Bay, Lake Mead, W. River Mountains, NV	3	-	?	-	6.5
78	Boulder City Fault/E. Boulder City, S. Hwy 93 near Jct. Hwy 41, NV	2	-	?	-	6.5
79	Grapevine Mesa North/ N. end Grapeuine Mesa, E. Lake Mead, NW AZ	5	-	Qy	-	6.5
80	Gold Basin Fault/ Western Grapeuine Mesa NW AZ	4	-	?	-	6.5

Notes:

Age of Latest Movement	Approx. Age (myBP)
h - late to mid Holocene	0.005
H - early Holocene to latest Pleistocene	0.005 - 0.02
L - late Pleistocene	0.02 - 0.15
M - mid Pleistocene	0.15 - 0.7
Qy - Late Quaternary; undifferentiated	≤ 0.5
E - early Pleistocene	0.7 - 2
Q - Quaternary; undifferentiated	≤ 2
P - known Pliocene	2 - 5
? - Age Uncertain but Neotectonic	

SUMMARY OF FAULTS AND FAULT ZONES

Seismic Source Zone or Fault		Length (miles)		Displacement		Earthquake
Number	Name/Location	Zone	Longest Segment	Latest Age (1)	Slip Rate	Maximum Credible
81	Garnet Mountain Fault/ SE Grapevine Mesa	4	<1	?	-	6.5
82	Grapevine Mesa South/ Grapevine Mesa, S. Lake Mead, NW AZ	4	-	?	-	6.5
83	Rampart Cave/ NW AZ	8	3	?	-	6.75
84	Separation/ Separation Cyn, W. Grand Canyon, NW AZ	18	-	?	-	7.0
85	Kelly Point/ W. Grand Canyon, NW AZ	12	8	?	-	7.0
86	Blue Mountain W. Grand Canyon, NW AZ	13	-	?	-	7.0
87	Unamed fault set E. of Grand Wash Cliffs, @ Colorado River, NW AZ	21	8	?	-	6.75
88	Hidden Canyon Graben/ E. of Grand Wash Cliffs, NW AZ	16	-	?	-	7.0
89	Gyp Pocket-Dutchman Draw Set/ Bet. Main St. & Hurricane Faults near Utah border	19	14	?	-	7.0
90	Uinkaret Volcanic Field/ Uinkaret Plateau, N. Grand Canyon, E. Hurricane Fault, AZ	22	15	Q	-	7.0

Notes:

Age of Latest Movement	Approx. Age (myBP)
h - late to mid Holocene	0.005
H - early Holocene to latest Pleistocene	0.005 - 0.02
L - late Pleistocene	0.02 - 0.15
M - mid Pleistocene	0.15 - 0.7
Qy - Late Quaternary; undifferentiated	≤ 0.5
E - early Pleistocene	0.7 - 2
Q - Quaternary; undifferentiated	≤ 2
P - known Pliocene	2 - 5
? - Age Uncertain but Neotectonic	

SUMMARY OF FAULTS AND FAULT ZONES

Seismic Source Zone or Fault		Length (miles)		Displacement		Earthquake
Number	Name/Location	Zone	Longest Segment	Latest Age (1)	Slip Rate	Maximum Credible
91	Date/26 mi. NW of Wickenburg near town of Date	2	-	?	-	6.5
92	Wagoner/20 mi. NE of Wickenburg, AZ	4	-	?	-	6.5
93	Lake Pleasant/N. of Lake Pleasant, 36 mi. NNW of Phoenix, AZ	3	-	?	-	6.5
94	Paria Plateau Fault Scarps/6 mi. to 24 mi. W Page, AZ	24	2	?	-	6.75
95	Rainbow Plateau Fault Scarps/24 mi. E Page, AZ	18	4	?	-	6.75
96	Kaibito Plateau Fault Scarps, 24 mi. SE Page, AZ	26	4	?	-	6.75
97	Hot NaNa Fault Scarps/ 24 mi. SW of Page, AZ	14	4	?	-	6.5
98	Fence Fault 36 mi. SW Page, AZ	15	5	?	-	7.0
99	Eminence Break Fault Scarp & Graben/28 mi. to 50 mi. SE Page, AZ	23	-	?	-	7.5
100	Marble Platform Fault Set/ E end Grand Canyon 50+ mi. N Flagstaff, AZ	42	19	?	-	7.25

Notes:

Age of Latest Movement	Approx. Age (myBP)
h - late to mid Holocene	0.005
H - early Holocene to latest Pleistocene	0.005 - 0.02
L - late Pleistocene	0.02 - 0.15
M - mid Pleistocene	0.15 - 0.7
Qy - Late Quaternary; undifferentiated	$\leq$ 0.5
E - early Pleistocene	0.7 - 2
Q - Quaternary; undifferentiated	$\leq$ 2
P - known Pliocene	2 - 5
? - Age Uncertain but Neotectonic	

SUMMARY OF FAULTS AND FAULT ZONES

Seismic Source Zone or Fault		Length (miles)		Displacement		Earthquake
Number	Name/Location	Zone	Longest Segment	Latest Age (1)	Slip Rate	Maximum Credible
101	Walhalla Plateau Fault Set/ E. Grand Canyon, N AZ	14	5	?	-	6.75
102	Big Snake Graben/ E End Grand Canyon 12 mi. SW Moencopi, AZ	20	13	?	-	7.0
103	Shadow Mountain Grabens/ 56 mi. N Flagstaff, AZ	7	3	L/M	0.02 mm/yr.	6.75
104	Mesa Butte Fault Zone & Graben - South/North Segment 32/40 mi. N Flagstaff, AZ	29	-	M	0.07 mm/yr.	6.75
105	Cameron Graben, 5 mi. W Cameron, AZ	6	3	M	0.04 mm/yr.	6.5
106	Black Point Fault Set 48 mi. NE Flagstaff, AZ	8		M	-	6.75
107	Black Point Monocline Fault 37 mi. NE Flagstaff, AZ	4	-	M	-	6.5
108	Doney Mountain Faults/ 30 mi. NE Flagstaff, AZ	6	3	Qy	-	6.75
109	Wupatki Fault Set/ 24 mi. NE Flagstaff, AZ	4	3	Qy	-	6.5
110	Campbell Francis Wash Fault Set/40 mi. N Flagstaff, AZ	14	5	M	-	6.5

Notes:

Age of Latest Movement	Approx. Age (myBP)
h - late to mid Holocene	0.005
H - early Holocene to latest Pleistocene	0.005 - 0.02
L - late Pleistocene	0.02 - 0.15
M - mid Pleistocene	0.15 - 0.7
Qy - Late Quaternary; undifferentiated	$\leq$ 0.5
E - early Pleistocene	0.7 - 2
Q - Quaternary; undifferentiated	$\leq$ 2
P - known Pliocene	2 - 5
? - Age Uncertain but Neotectonic	

SUMMARY OF FAULTS AND FAULT ZONES

Seismic Source Zone or Fault		Length (miles)		Displacement		Earthquake
Number	Name/Location	Zone	Longest Segment	Latest Age (1)	Slip Rate	Maximum Credible
111	SP Fault Set/30 mi. N Flagstaff, AZ	11	7	M	-	6.75
112	Cedar Ranch/Mesa Butte Area 32 mi. N Flagstaff, AZ	7	-	M		7.0
113	Double Top Fault Set/ Coconino Plateau, Mesa Butte Area 30+ mi. NW Flagstaff, AZ	10	-	?	-	6.75
114	Lockwood Canyon Fault/ Mesa Butte Area 40 mi. NW Flagstaff, AZ	10	-	?	-	6.75
115	Gray Mountain Fault Set/ Gray Mountain area, 44 mi. NNW Flagstaff, AZ	24	7	?	-	6.75
116	Sinagua Valley, San Fancisco Mt., N of Flagstaff, AZ	25	2	M	0.03 to 0.07 mm/yr	6.75
117	Bill Williams/ West of Flagstaff, AZ	7.5	4	E/M		6.75
118	Garland Prairie Fault 11 mi. E Williams, AZ	2	1	Q	-	6.5
119	Bellemont Fault/ 10 mi. W Flagstaff, AZ	6	-	L/M	-	6.5
120	Dutton Hill Fault Scarps/ 14 mi. SW Flagstaff, AZ	8	2	?	-	6.5

Notes:

Age of Latest Movement	Approx. Age (myBP)
h - late to mid Holocene	0.005
H - early Holocene to latest Pleistocene	0.005 - 0.02
L - late Pleistocene	0.02 - 0.15
M - mid Pleistocene	0.15 - 0.7
Qy - Late Quaternary; undifferentiated	$\leq$ 0.5
E - early Pleistocene	0.7 - 2
Q - Quaternary; undifferentiated	$\leq$ 2
P - known Pliocene	2 - 5
? - Age Uncertain but Neotectonic	

SUMMARY OF FAULTS AND FAULT ZONES

Seismic Source Zone or Fault		Length (miles)		Displacement		Earthquake
Number	Name/Location	Zone	Longest Segment	Latest Age (1)	Slip Rate	Maximum Credible
121	Oak Creek Fault Zone - North Segment/5 mi. W Flagstaff, AZ	15	7.5	M/E		7.0
122	Flagstaff Fault Set/Along I-17, S Flagstaff, AZ	13	5	?	-	6.5
123	Munds Park Fault Zone 18 mi. S Flagstaff, AZ	15	8	?	-	6.75
124	Mormon Lake Fault Zone/ E side Mormon Lake, 20 mi. SE Flagstaff, AZ	10	8	?	-	6.75
125	Lake Mary Fault Zone/ Lake Mary area, 7 mi. to 17 mi. SE Flagstaff, AZ	12	9	?	-	6.75
126	Walnut Canyon Fault Set/ Walnut Canyon area, E Flagstaff, AZ	21	5	?	-	6.5
127	Unnamed Faults/ E of Flagstaff, S of Merrian Crater, AZ	2.5	-	M	-	6.5
128	Leupp Fault Set/ Two Guns area, E Flagstaff, AZ	32	8	?	-	6.75
129	Chavez Mountain Faults/ 40 mi. SE Flagstaff, AZ SE side Chavez Mountain	25	10	?	-	6.75
130	Turret Peak Fault/ 22 mi. S Camp Verde, AZ	7	-	Qy	-	6.75

Notes:

Age of Latest Movement	Approx. Age (myBP)
h - late to mid Holocene	0.005
H - early Holocene to latest Pleistocene	0.005 - 0.02
L - late Pleistocene	0.02 - 0.15
M - mid Pleistocene	0.15 - 0.7
Qy - Late Quaternary; undifferentiated	≤ 0.5
E - early Pleistocene	0.7 - 2
Q - Quaternary; undifferentiated	≤ 2
P - known Pliocene	2 - 5
? - Age Uncertain but Neotectonic	

SUMMARY OF FAULTS AND FAULT ZONES

Seismic Source Zone or Fault		Length (miles)		Displacement		Earthquake
Number	Name/Location	Zone	Longest Segment	Latest Age (1)	Slip Rate	Maximum Credible
131	East Verde River Fault/ 14 mi. W Payson, AZ	7	-	?	-	6.75
132	Deadman Creek Fault Zone 30 mi. NE Carefree, AZ	11	-	?	-	6.75
133	Horseshoe Dam Fault (Tangle Peak Fault)/18 mi. NE Carefree, AZ	13	7-8	L/M	0.007 mm/yr	6.75
134	Seven Springs Fault/ 13 mi. N Carefree, AZ	3	-	?	-	6.5
135	Carefree Fault/ 5 mi. E Carefree, AZ	8	4	?	-	6.5
136	Alder Creek Fault Zone/ 26 mi. NW Roosevelt Dam, AZ	7	4	Qy	-	6.5
137	Tonto Basin - Northwest/ SW Side of Roosevelt Res.	9	3	?	-	6.5
138	Tonto Basin - Central (Punkin Center Fault)/10 mi. NW Roosevelt Dam, AZ	3	2	?	-	6.5
139	Two Bar Mtn. (North & South)/ 2 mi. SE Roosevelt Dam AZ	2	-	?	-	6.5
140	Gold Gulch Fault-W Branch/ SW Side Roosevelt Res. 11-24 mi. NW Globe, AZ	6	-	?	-	6.5

Notes:

Age of Latest Movement	Approx. Age (myBP)
h - late to mid Holocene	0.005
H - early Holocene to latest Pleistocene	0.005 - 0.02
L - late Pleistocene	0.02 - 0.15
M - mid Pleistocene	0.15 - 0.7
Qy - Late Quaternary; undifferentiated	$\leq$ 0.5
E - early Pleistocene	0.7 - 2
Q - Quaternary; undifferentiated	$\leq$ 2
P - known Pliocene	2 - 5
? - Age Uncertain but Neotectonic	

SUMMARY OF FAULTS AND FAULT ZONES

Seismic Source Zone or Fault		Length (miles)		Displacement		Earthquake
Number	Name/Location	Zone	Longest Segment	Latest Age (1)	Slip Rate	Maximum Credible
141	Sugarloaf Peak Fault 20 mi. W Roosevelt Dam, AZ	6	3	H		6.75
142	Rolls Fault/20 mi. SW Roosevelt Dam, AZ	6	3	L/M & E/P	-	6.5
143	Miami Fault/W side Miami, FL	12	-	?	-	6.75
144	Picketpost Mountain Fault/ 7 mi. W Superior, AZ	2	-	?	-	6.5
145	China Wash Scarp/ 6 mi.NE Florence, AZ	3	-	?	-	6.5
146	Muscal Creek Mescal Mountains, 16 mi. SE Globe, AZ	3	-	?	-	6.5
147	Antelope Flat Scarps/ 28 mi. E Globe, AZ	3	-	?	-	6.5
148	Mammoth Fault/22 mi. SE Hayden, AZ	9	-	?	-	6.5
149	San Manuel Fault/ 8 mi. E San Manuel, AZ	4	2	?	-	6.5
150	Santa Rita Fault Scarps 20 mi. to 44 mi. S. Tucson, AZ	34	2	L	0.035 mm/yr.	7.5

Notes:

Age of Latest Movement	Approx. Age (myBP)
h - late to mid Holocene	0.005
H - early Holocene to latest Pleistocene	0.005 - 0.02
L - late Pleistocene	0.02 - 0.15
M - mid Pleistocene	0.15 - 0.7
Qy - Late Quaternary; undifferentiated	≤ 0.5
E - early Pleistocene	0.7 - 2
Q - Quaternary; undifferentiated	≤ 2
P - known Pliocene	2 - 5
? - Age Uncertain but Neotectonic	

SUMMARY OF FAULTS AND FAULT ZONES

Seismic Source Zone or Fault		Length (miles)		Displacement		Earthquake
Number	Name/Location	Zone	Longest Segment	Latest Age (1)	Slip Rate	Maximum Credible
151	Greaterville Fault/ E Flank Mt. Wrightson Pima County, NNE Nogales, AZ	5	-	?	-	6.5
152	Patagonia Fault/ near Patagonia, AZ	4	2	?	-	6.5
153	Patagonia Mountains Fault Zone/ 10 mi. NE Nogales, AZ	4	2	?	-	6.5
154	Sierra Vista Fault/ S San Pedro Valley, 6-11 mi. SE Sierra Vista, AZ	10	1	L	0.02 to 0.03 mm/yr	7.0
155	California Wash Monocline & Faults/9 mi. S. Benson, AZ	5	-	?	-	6.5
156	Swisshelm Mountains Fault/ 10 mi. E. Elfrida, AZ E Side Swisshelm Mts.	12	6	E	-	6.75
157	Pedregosa Fault/ W Side San Bernardino V. 20 mi. NE Douglas, AZ	15	8	E/M	0.04 to 0.40 mm/yr	6.75
158	Guadalupe Canyon Fault/ 28 mi. E. Douglas, AZ Guadulupe Mts, AZ/NM Border SE AZ	3	-	E	-	6.5
159	Bunk Robinson Peak/Outlaw Mountain Fault/E Side San Bernardino V., SE AZ	10	3	E	0.04 to 0.40 mm/yr	7.0
160	Joe Glenn Ranch Fault E Side Pedregosa Mts., SE AZ	5	-	E	-	6.75

Notes:

Age of Latest Movement	Approx. Age (myBP)
h - late to mid Holocene	0.005
H - early Holocene to latest Pleistocene	0.005 - 0.02
L - late Pleistocene	0.02 - 0.15
M - mid Pleistocene	0.15 - 0.7
Qy - Late Quaternary; undifferentiated	$\leq$ 0.5
E - early Pleistocene	0.7 - 2
Q - Quaternary; undifferentiated	$\leq$ 2
P - known Pliocene	2 - 5
? - Age Uncertain but Neotectonic	

SUMMARY OF FAULTS AND FAULT ZONES

Seismic Source Zone or Fault		Length (miles)		Displacement		Earthquake
Number	Name/Location	Zone	Longest Segment	Latest Age (1)	Slip Rate	Maximum Credible
161	Pitaycachi and Chiriones Fault/30 mi. SE Douglas, AZ State of Sonora, Mexico	50	-	Historical	0.01 to 0.03 mm/yr	7.5
162	Grays Ranch Fault Scarp/ 24 mi. SE Portal, AZ	10	1	M	-	7.0
163	Gillespie Mountain Fault/ 28 mi. SE Portal, AZ	15	3	H	-	7.25
164	Cowboy Pass Fault/ San Simon Valley AZ-NM Border	7	-	Q	-	6.75
165	Washburn Ranch Fault/ W Side Animas Valley SW NM	10	5	H	0.005 to 0.02 mm/yr.	7.0
166	Animas Valley Fault/ E Side N. Animas Valley SW NM	13	5	L	-	7.25
167	Black Mountain Fault/ W. Side of Black Mtn., 12 mi. SE Duncan, AZ	6	-	Q	-	6.75
168	Pearson Mesa Fault/ Northern Animas Valley, SW New Mexico, 8 mi SE of Duncan, AZ	3	-	L	-	6.5
169	Rim Rock Fault/ W Side Summit Mts. 6 mi. NE Duncan, AZ	8	-	L	-	6.75
170	Ward Canyon Fault 20 mi. NW Duncan, AZ SE AZ	10	5	M	-	6.75

Notes:

Age of Latest Movement	Approx. Age (myBP)
h - late to mid Holocene	0.005
H - early Holocene to latest Pleistocene	0.005 - 0.02
L - late Pleistocene	0.02 - 0.15
M - mid Pleistocene	0.15 - 0.7
Qy - Late Quaternary; undifferentiated	≤ 0.5
E - early Pleistocene	0.7 - 2
Q - Quaternary; undifferentiated	≤ 2
P - known Pliocene	2 - 5
? - Age Uncertain but Neotectonic	

SUMMARY OF FAULTS AND FAULT ZONES

Seismic Source Zone or Fault		Length (miles)		Displacement		Earthquake
Number	Name/Location	Zone	Longest Segment	Latest Age (1)	Slip Rate	Maximum Credible
171	Maverick Hill W Side Summit Mts. 15 mi. N of Duncan AZ	16	5	E	-	6.75
172	Buena Vista/ 9 mi. E. Safford, AZ	2	-	L	-	6.5
173	Cactus Flats Fault San Simon Valley 3 mi. S. Safford, AZ	5	2	M/E	-	6.5
174	Safford Fault/E Side of Pinaleno Mts./5 mi. to 22 mi. S. of Safford, AZ	20	10	L	-	7.0
175	Rice Mesa Fault/ 31 mi. NE Clifton, AZ	5	-	E/P	-	6.5
176	Mogollon Fault zone/ 40 mi. NEE Clifton, AZ	40	8	?	-	7.0
177	Deep Creek Mesa Scarp/ 40 mi. NE Clifton, AZ	4	3	?	-	6.5
178	Alma Mesa Fault/ 32 mi. NE Clifton, AZ	9	3	Q	-	6.75
179	Sprucedale Fault/30 mi. S. Springerville, AZ	12	8	?	-	6.75
180	Big Lake Fault & Graben/ 20 mi. S Springerville, AZ	14	8	?	-	6.75

Notes:

Age of Latest Movement	Approx. Age (myBP)
h - late to mid Holocene	0.005
H - early Holocene to latest Pleistocene	0.005 - 0.02
L - late Pleistocene	0.02 - 0.15
M - mid Pleistocene	0.15 - 0.7
Qy - Late Quaternary; undifferentiated	$\leq$ 0.5
E - early Pleistocene	0.7 - 2
Q - Quaternary; undifferentiated	$\leq$ 2
P - known Pliocene	2 - 5
? - Age Uncertain but Neotectonic	

SUMMARY OF FAULTS AND FAULT ZONES

Seismic Source Zone or Fault		Length (miles)		Displacement		Earthquake
Number	Name/Location	Zone	Longest Segment	Latest Age (1)	Slip Rate	Maximum Credible
181	Coyote Creek Fault/ 9 mi. NE Springerville, AZ	5	2	?	-	6.5
182	St. John's Fault Set 16 mi. N Springerville, AZ	6	-	Q	-	6.5
183	St. Johns Fault Set-Main Zone/30 mi. NW Springerville, AZ	18	5	Q	-	6.75
184	Piute Mesa Fault Scarps/ AZ-UT Border 48 mi. E Page, AZ	8	3	?	-	6.5
185	Kendrick Peak Fault/ 20 mi. NW Flagstaff, AZ	2	-	L	-	6.5
186	Andrus Valley Fault/ Shivwitz Plateau, N. West Grand Canyon, AZ	25	6	?	-	7.0

Notes:

Age of Latest Movement	Approx. Age (myBP)
h - late to mid Holocene	0.005
H - early Holocene to latest Pleistocene	0.005 - 0.02
L - late Pleistocene	0.02 - 0.15
M - mid Pleistocene	0.15 - 0.7
Qy - Late Quaternary; undifferentiated	$\leq$ 0.5
E - early Pleistocene	0.7 - 2
Q - Quaternary; undifferentiated	$\leq$ 2
P - known Pliocene	2 - 5
? - Age Uncertain but Neotectonic	

APPENDIX B

GLOSSARY

Alluviation: The subaerial deposition or formation of alluvium or alluvial features (such as cones or fans) at places where stream velocity is decreased or stream flow is checked; the process of aggradation or of building-up of sediments by a stream along its course, or of covering or filling a surface with alluvium.

Alluvium: A general term for clay, silt, sand, gravel, or similar unconsolidated sedimentary material deposited as a cone or fan at the base of a mountain slope.

Andesitic: Pertaining to a dark-colored, fine grained extrusive rock of intermediate composition.

Angle of Repose: The maximum angle of slope (measured from a horizontal plane) at which loose, cohesionless material will come to rest on a pile of similar material. Commonly about 35 degrees for sand.

Angular: Having sharp angles or borders of a sedimentary particle showing very little or no evidence of abrasion, with all of its edges and corners sharp.

Antithetic Fault: A fault that is subsidiary to a major fault, formed in the same stress regime, is oriented at a high angle to the major fault, and (for

strike-slip faults) has a sense of displacement opposite that of the major fault or (for normal faults) dips in the opposite direction. Commonly involves rotated fault-bonded blocks so that the net slip on each fault is greater than it would be without rotation.

Aseismic Creep: Slow crustal movement without accompanying earthquakes.

Axial Rift: A narrow cleft, fissure, or other opening made by cracking or splitting apparently of tensional origin.

Bajada: A broad, continuous alluvial slope or gently inclined detrital surface extending from the base of mountain ranges out into and around an inland basin, formed by the lateral coalescence of a series of separate but confluent alluvial fans.

Basalt: A general term for dark-colored mafic igneous rocks, commonly extrusive but locally intrusive (e.g. as dikes), composed chiefly of calcic plagioclase and clinopyroxene; the fine-grained equivalent of gabbro.

Base-Level: The level below which a stream cannot erode its bed. The surface toward which external forces strive, at which neither erosion nor deposition takes place. The theoretical limit or lowest level toward which erosion of the Earth's surface constantly progresses but seldom, if ever, reaches.

Basement: The undifferentiated complex of rocks that underlies the rocks of interest in an area. Commonly crystalline, igneous, and/or metamorphic rocks of Precambrian age.

Basin and Range: Said of a topography, landscape, or physiographic province characterized by a series of tilted fault blocks forming longitudinal, asymmetric ridges or mountains and intervening basins.

Bedding: The arrangement of a sedimentary rock in beds or layers of varying thickness and character.

Bedrock: A general term for the rock, usually solid, that underlies soil or other unconsolidated, surficial material.

Bimodal: Characterized by two localized modes each have a higher frequency of occurrence that are immediately adjacent individuals or classes.

Bolson: In deserts of Southwestern U.S., an extensive flat alluvium-floored basin or depression, into which drainage from the surrounding mountains flows with gentle gradients toward a playa or central depression; an interior basin, or a basin with internal drainage.

Butte: A conspicuous, usually isolated, generally flat-topped hill or small mountain with relatively steep slopes or precipitous cliffs, often capped with a resistant layer of rock and bordered by talus, and representing an erosion remnant carved from flat-lying rocks.

Caprock: Usually used for hard, resistant, surficial, generally flat-lying rock.

Carbonate: A sediment formed by the organic or inorganic precipitation from aqueous solution of carbonates of calcium, magnesium, or iron, e.g. limestone and dolomite.

Cementation: The diagenetic process by which coarse clastic sediments are turned into hard rock.

Chronology: Arranging events in their proper sequence in time; also, considering or measuring time in discrete units.

Cinder Cone: A conical hill formed by the accumulation of cinders and other volcanically ejected fragments.

Clasts: An individual constituent, grain, or fragment of a sediment or rock, produced by the mechanical breakdown or weathering of a larger rock mass.

Cohesion: Shear strength of a rock not related to inter-particle friction.

Colluvium: A general term applied to any loose, heterogeneous, and incoherent mass of soil material and/or rock fragments deposited by rainwash, sheetwash, or slow continuous downslope creep, usually collecting on or at the base of gentle slopes or hillsides.

Conglomerate: A coarse-grained clastic sedimentary rock, composed of rounded to subangular fragments larger than 2 mm in diameter (granules, pebbles, cobbles, boulders) set in a fine-grained matrix of sand or silt, and commonly cemented by calcium carbonate, iron oxide, silica, or hardened clay.

Consolidation: Any process whereby loosely aggregated, soft, or liquid earth materials become firm and coherent rock.

Cretaceous: The final period of the Mesozoic era (after the Jurassic and before the Tertiary period of the Cenozoic era), thought to have covered the span of time between 135 and 65 million years ago; also, the corresponding system of rocks.

Cross-Bedding: Cross-stratification in which the cross-beds are more than 1 cm in thickness; imparted to sediments due to wind or water currents.

Cross-Cutting Relationship: A principle or law stating that a disrupted pattern of rock is older than the cause of disruption of the rock.

Crust: The outermost layer or shell of the Earth, defined according to various criteria, including seismic velocity, density and composition.

Cumulative Soil: A soil that has received influxes of new material at the same time that soil formation is going on.

Deposits: Earth material of any type, either consolidated or unconsolidated, that has accumulated by some natural process or agent.

Detritus: A collective term for loose rock and mineral material that is worn off or removed by mechanical means, as by disintegration or abrasion, such as sand, silt, and clay, derived from older rocks and moved from its place of origin.

Dip: The angle that a surface, e.g. a bedding or fault plane, makes with the horizontal, measured perpendicular to the strike.

Dip-Slip: In a fault, the component of the movement or slip that is parallel to the dip of the fault.

Disaggregate: Separation or reduction of an aggregate into its component parts.

Displacement: A general term for the relative movement to the two sides of a fault.

Disseminated: Said of a mineral deposit in which the desired minerals occur as scattered particles in the rock.

Downcutting: Stream erosion in which the cutting is directed in a downward direction.

Drag: The bending of strata on either side of a fault, caused by the friction of the moving blocks along the fault surface; also, the bends or distortions so formed.

Earthquake: A sudden motion or trembling in the Earth caused by the abrupt release of slowly accumulated strain.

Epicenter: The point on the Earth's surface that is directly above the focus of an earthquake.

Erosion: The general process or the group of processes whereby the materials of the Earth's crust are loosened, dissolved, or worn away, and simultaneously moved from one place to another, by natural agencts, which include weathering, solution, corrosion, and transportation, but usually exclude mass wasting.

Escarpment: A long, more or less continuous cliff or relatively steep slope facing in one general direction, breaking the continuity of the land by separating two level or gently sloping surfaces, and produced by erosion or by faulting.

Evaporite Deposits: A sedimentary rock composed primarily of minerals produced from a saline solution as a result of extensive or total evaporation of the solvent.

Fault Zone: A fault that is expressed as a zone of numerous small fractures or of breccia or fault gouge. A Fault zone may be as wide as hundreds of meters.

Fault Plane: The actual surface along which relative fault displacement occurs.

Fault: A fracture or a zone of fractures along which there has been displacement of the sides relative to one another parallel to the fracture.

Fluvial: Of or pertaining to a river or rivers.

Focal Mechanism: A method of determining the type and sense of fault displacement associated with an earthquake.

Focal Depth: The depth at which of an earthquake originates. (see Hypocenter)

Folds: A curve or bend of a planar structure such as rock strata, bedding planes, foliation or cleavage.

Formation: A body of rock identified by lithic characteristics and stratigraphic position.

Friable: A rock or mineral that is easily broken, pulverized, or reduced to small gains or powder.

Frontal Fault: A fault bounding the front of a mountainous region.

Gabbro: A group of dark-colored, basic intrusive igneous rocks composed principally of basic plagioclase (commonly labradorite or bytownite) and clinopyroxene (augite), with or without olivine and orthopyroxene; also, any member of that group. It is the approximate intrusive equivalent of basalt.

Geothermal Anomaly: A departure from the expected or normal geothermal gradient.

Geomorphology: The study of shape and origin of landforms.

Graben: An elongate, relatively depressed crustal unit or block that is bounded by faults on its long sides.

Gravel: An unconsolidated, natural accumulation of rounded rock fragments resulting from erosion, consisting predominantly of particles larger than sand, such as boulders, cobbles, pebbles, granules, or any combination of these fragments.

Heat Flow Units: A measurement of terrestrial heat flow equivalent to 10^{-6} $cal/cm^2/sec$.

Holocene: An epoch of the Quaternary period, from the end of the Pleistocene, approximately 10,000 years ago, to the present time; also, the corresponding series of rocks and deposits.

Hypocenter: Focus; the initial rupture point of an earthquake, where strain energy is first converted to elastic wave energy.

Igneous Rocks: An assemblage of temporally and spatially related igneous rocks of the same general form of occurrence (plutonic, hypabyssal, or volcanic) characterized by possessing in common certain chemical, mineralogic, and textural features or properties so that the rocks together exhibit a continuous variation.

Imbrication: A sedimentary fabric characterized by disk-shaped or elongate fragments dipping in a preferred direction at an angle to the bedding.

Indurated: Said of a rock or soil hardened or consolidated by pressure, cementation, or heat.

Intensity: Earthquake intensity. A measure of an earthquakes's size by its effect on people and buildings.

Intermontaine: Situated between or surrounded by mountains, mountain ranges, or mountainous regions.

Joint: A surface of fracture or parting in a rock, without displacement; the surface is usually plane and often occurs with parallel joints to form part of a joint set.

Jurassic: The second period of the Mesozoic era (after the Triassic and before the Cretaceous), thought to have covered the span of time between 190 and 135 million years ago; also, the corresponding system of rocks.

Lacustrine: Pertaining to, produced by, or formed in a lake or lakes; e.g. "lacustrine sands" deposited on the bottom of a lake, or a "lacustrine terrace" formed along its margin.

Laminae: A thin plate, sheet, or layer.

Laramide: A period of deformation from late Cretaceous time until about the end of the Paleocene epoch.

Left-Lateral Fault: A fault on which the displacement is left-lateral separation.

Limestone: A sedimentary rock consisting chiefly (more than 50% by weight) of calcium carbonate, primarily in the form of the mineral calcite, and with or without magnesium carbonate. Limestones are formed by either organic or inorganic processes and may be detrital, chemical, oolitic, earthy, crystalline, or recrystallized.

Lineament: A linear feature of regional extent that is believed to reflect crustal structure such as fault lines, aligned volcanoes, and straight stream courses.

Liquefaction: The loss of cohesion or transformation of loosely packed water-saturated sediment into a fluid-like mass due to vibrations acting upon the sediments.

Lithogenesis: The origin and formation of rocks, especially sedimentary.

Lithologic: The study of rocks. Pertaining to physical and chemical characteristics of rocks such as the texture, cementation, hardness, porosity, composition, etc.

Lithosphere: The solid portion of the Earth, as compared with the atmosphere and hydrosphere. It includes the crust and part of the upper mantle and is of the order of 60 miles (100 km) in thickness.

Loam: A rich, permeable soil composed of a friable mixture of relatively equal and moderate proportions of clay, silt, and sand particles, and usually containing organic matter.

Magma: Naturally occurring molten or ductile material, generated within the Earth and capable of intrusion and extrusion, from which igneous rocks are thought to have been derived through solidification and related processes.

Magnitude: Earthquake magnitude. A measure of the energy released during an earthquake.

Massive: A stratified rock that occurs in very thick, homogeneous beds, or of a stratum that is imposing by its thickness.

Matrix: The finer-grained material enclosing, or filling the spaces between, the larger grains or particles of a sediment or sedimentary rock; the natural material in which a sedimentary particle or fossil is embedded, as opposed to the fossil itself.

Mesa: An isolated nearly level landmass standing distinctly above the surrounding country, bounded by abrupt or steeply sloping erosion scarps on all sides, and capped by layers of resistant, nearly horizontal rock.

Mesozoic: An era of geologic time, from the end of the Paleozoic to the beginning of the Cenozoic, or from about 225 to about 65 million years ago.

Metamorphic Rocks: Any rock derived from pre-existing rocks by mineralogical, chemical and/or structural changes, essentially in the solid state, in response to marked changes in temperature, pressure, shearing stress, and chemical environment, generally at depth in the Earth's crust.

Metasedimentary Rock: Sedimentary rock that shows evidence of having been subjected to metamorphism.

Metavolcanic Rock: An informal term for volcanic rocks that show evidence of having been subjected to metamorphism.

Microseismicity: Small magnitude earthquakes below the level of detection by humans; generally less than about Richter magnitude of 2.

Microzones: A smaller seismotectonic zone with unique seismogenic characteristics within a seismotectonic province.

Miocene: An epoch of the upper Tertiary period, after the Oligocene and before the Pliocene; the corresponding worldwide series of rocks, considered to be a period when the Tertiary is designated as an era.

Mississippian: A period of the Paleozoic era (after the Devonian and before the Pennsylvanian), thought to have covered the span of time between 345 and 320 million years ago; also, the corresponding system of rocks.

Moho: Abbreviated form of Mohorovičić discontinuity, suggested by Birch. The boundary surface or sharp seismic-velocity discontinuity that separates the Earth's crust from the subjacent mantle.

Moment-Magnitude: A calculated earthquake magnitude determined from analysis of the physical size of an earthquake.

Monocline: A local steepening in an otherwise uniform gentle dip; a steplike fold in rock.

Morphology: The external structure, form and arrangement of rocks in relation to the development of landforms.

Mottling: Variation of color in sediments and soils, as represented by localized spots, patches, blotches, or shades of color.

Mudstone: A blocky or massive, fine-grained sedimentary rock in which the proportions of clay and silt are approximately equal.

Neotectonic: (see Tectonic) Modern tectonics; tectonics involving active faulting, folding, and crustal deformation. In this report, chiefly late Pliocene to the present time.

Normal Fault: A fault with vertical displacement in which the downdropped block moves downward relative to the other block. The angle of the fault plane is usually 45°-90°.

Oblique Fault: A fault that strikes oblique to, rather than parallel or perpendicular to, the strike of the constituent rocks or dominant structure.

Orogenic: The process of formation of mountains.

Orthogonal: Pertaining to or composed of right angles; representation of an object formed by the perpendicular intersection of planes.

Outcrop: That part of a geologic formation or structure that appears at the surface of the Earth.

Paleotectonic: Geologic and tectonic features that formed during a previous episode of geologic deformation. Also said of the time period when these features formed.

Paleozoic: An era of geologic time, from the end of the Precambrian to the beginning of the Mesozoic, or from about 570 to about 225 million years ago.

Pavement: A natural residual concentration of wind-polished, closely packed pebbles, boulders, and other rock fragments.

Pebble: A small, roundish worn stone; a rock fragment larger than a granule and smaller than a cobble.

Pediment: A broad gently sloping rock-floored erosion surface or plain of low relief, typically developed by subaerial agents in an arid or semiarid region at the base of an abrupt and receding mountain front or plateau escarpment, and underlain by bedrock.

Pedogenic: Pertaining to weathering and formation of soils on rocks and sediment.

Pennsylvanian: A period of the Paleozoic era (after the Mississippian and before the Permian), thought to have covered the span of time between 320 and 280 million years ago; also, the corresponding system of rocks.

Permian: The last period of the Paleozoic era (after the Pennsylvanian), thought to have covered the span of time between 280 and 225 million years ago; also, the corresponding system of rocks.

Photogrammetry: The art and science of obtaining measurements from photographic images; measurements relate not only to size, shape, and position, but also to color or tone, texture, and patterns of distribution of these elements.

Physiography: A description of the physical form, substance, and arrangement, surficial of geologic landforms such as mountains, valleys, plains.

Piedmont: Lying or formed at the base of a mountain or mountain range such as an area, plain, slope, glacier.

Plate Subduction: The process of one lithospheric plate descending beneath another.

Playa: A dry, vegetation-free, flat area at the lowest part of an undrained desert basin, underlain by stratified clay, silt, or sand, and commonly soluble salts.

Pleistocene: An epoch of the Quaternary period, between about 10,000 years before the present and about 2 million years before present.

Pliocene: An epoch of the Tertiary period, after the Miocene and before the Pleistocene. Between about 5.5 million years and 2 million years before present.

Pluton: An igneous intrusion.

Pluvial: The period between glacial periods.

Potassium/Argon Age: The age of a mineral or rock in years, based on measurement of the ratio of radiogenic argon-40 to potassium-40 and the known radioactive decay rate of potassium-40 to argon-40.

Precambrian: All geologic time, and its corresponding rocks, before the beginning of the Paleozoic.

Quartzite: A very hard, possibly metamorphosed, sandstone consisting chiefly of quartz grains that have been so completely and solidly cemented with secondary silica, or recrystallized, that the rock breaks across or through the grains rather than around them.

Quaternary: The second period of the Cenozoic era which includes the Pleistocene and Holocene Epochs; following the Tertiary Period beginning about two million years ago and extending to the present.

Recurrence Interval: The average time interval between occurrences of an earthquake event of a given magnitude.

Relief: The physical shape, configuration, or general unevenness of a part of the Earth's surface, considered with reference to variations of height and slope or to irregularities of the land surface.

Reverse Fault: A fault on which the hanging wall appears to have moved upward relative to the footwall. The dip of the fault is usually greater than 45°. There is dip separation but there may or may not be dip slip.

Rhyolite: A group of extrusive igneous rocks, typically porphyritic and commonly exhibiting flow texture, with phenocrysts of quartz and alkali feldspar in a glassy to cryptocrystalline groundmass; also, any rock in that group; the extrusive equivalent of granite.

Rifting: The process of tensional extension of the earth's crust forming a trough bounded by normal faults; a belt of strike-slip faults of regional extent.

Right-Lateral Strike-Slip Fault: A fault on which the displacement is right-lateral separation in the direction of strike.

Sandstone: A medium-grained clastic sedimentary rock composed of abundant rounded or angular fragments of sand size set in a fine-grained matrix (silt or clay) and more or less firmly united by a cementing material.

Scarp: A line of cliffs produced by faulting or by erosion.

Sediment: Solid fragmental material that originates from weathering of rocks and is transported or deposited by air, water, or ice, or that accumulates by other natural agents, such as chemical precipitation from solution or secretion by organisms.

Seismicity: The phenomenon of Earth movements.

Seismogenic Crust: The seismically active portion of the earth's crust. Generally the upper brittle portion of the earth's crust above the softer, plastic, or ductile lower part of the crust.

Seismogram: The record made by a seismograph.

Seismograph: An instrument that detects, magnifies, and records vibrations of the Earth, especially earthquakes.

Seismotectonic: (see Tectonic) Tectonics involving earthquakes.

Shale: A fine-grained detrital sedimentary rock, formed by the consolidation of clay, silt, or mud. A thinly laminated or fissile claystone, siltstone, or mudstone.

Shear: A deformation resulting from stresses that cause or tend to cause contiguous parts of a body to slide relatively to each other in a direction parallel to their plane of contact.

Siltstone: An indurated silt having the texture and composition of shale but lacking its fine lamination or fissility; a rock whose composition is intermediate between those of sandstone and shale and at least two-thirds is material of silt size.

Slickensides: A polished and smoothly striated surface that results from movement and friction along a fault plane.

Slip Rates: The rate of relative displacement of formerly adjacent points on opposite sides of a fault, measured across the fault surface.

Soil-Profile: A vertical section of a soil that displays all its horizons.

Splay: One of a series of minor faults at the extremities of a major fault.

Spreading Center: A plate boundary where two or more plates diverge generally by horizontal extension or rifting.

Strata: A tabular or sheetlike body or layer of sedimentary rock, visually separable from other layers above and below.

Stratigraphy: Concerned with the succession and age of rock strata and also their form, distribution, lithologic composition, fossil content, geophysical, and geochemical properties.

Stream-Terrace: A series of level surfaces in a stream valley, flanking and more or less parallel to the stream channel, originally occurring at or below, but now above, the level of the stream, and representing the dissected remnants of an abandoned flood plain, stream bed, or valley floor produced during a former stage of erosion or deposition.

Strike: The direction or trend taken by a structural surface such as a bedding or fault plane, as it intersects the horizontal.

Subangular: Somewhat angular, free from sharp angles but not smoothly rounded.

Subparallel: Designating two or more straight but nearly coplanar lines that do not intersect; almost parallel.

Subrounded: Partially rounded; a sedimentary particle showing considerable but incomplete abrasion and an original general form that is still discernible, and having many of its edges and corners noticeably rounded off to smooth curves.

Subsidence: The sudden sinking or gradual downward settling of the Earth's surface with little or no horizontal motion; may be caused by natural geologic processes, such as solution, thawing, compaction slow crustal warping, or withdrawal of fluid from beneath a solid crust, or from sediments.

Superposition: The order in which rocks are placed or accumulated in beds one above the other, the highest bed being the youngest.

Surficial Deposits: Unconsolidated and residual, alluvial, or glacial deposits lying on bedrock or occurring on or near the Earth's surface; generally unstratified and represents the most recent of geologic deposits.

Tectonic: Pertaining to the forces involved in, or the resulting large-scale crustal deformation.

Tectonic Geomorphology: The science of using geomorphology to analyze tectonic process.

Tertiary: The first period of the Cenozoic era (after Cretaceous of the Mesozoic era and before Quaternary), thought to have covered the span of time between 65 and about two million years ago; divided into five epochs (the Paleocene, Eocene, Oligocene, Miocene, Pliocene).

Texture: The general physical appearance or character of a rock, including the geometric aspects of, and the mutual relations among, its component particles or crystals.

Topography: The general configuration of a land surface or any part of the Earth's surface, including its relief and the position of its natural and man-made features.

Transform Fault: A special variety of strike-slip fault, along which the displacement suddenly stops or changes form. Many transform faults are associated with mid-oceanic ridges, where the actual slip is opposite from the apparent displacement across the fault. A plate boundary that ideally shows pure strike-slip displacement.

Transition Zone: A region within the state of Arizona separating the Colorado Plateau Physiographic Province to the north and the Basin and Range Physiographic Province to the south.

Triassic: The first period of the Mesozoic era (after the Permian and before the Jurassic), thought to have covered the span of time between 225 and 1990 million years ago; also, the corresponding system of rocks.

Trough: Any long, narrow depression in the Earth's surface, such as one between hills or with no surface outlet for drainage; may be bounded by faults.

Uplift: A structurally high area in the crust, produced by positive movements that raise or upthrust the rocks, as in a dome or arch.

Vesicular: The texture of a rock, especially a lava, characterized by abundant vesicles formed as a result of the expansion of gases during the fluid stage of the lava.

Volcanic Flows: Lava flow.

Volcanics: Pertaining to the activities, structures, or rock types of a volcano.

Volcanism: The processes by which molten rock and its associated gases rise into the crust and are extruded onto the Earth's surface and into the atmosphere.

Wedge: The shape of a stratum, vein, or intrusive body that thins out.

Volcanotectonic: Crustal deformation related to volcanism.

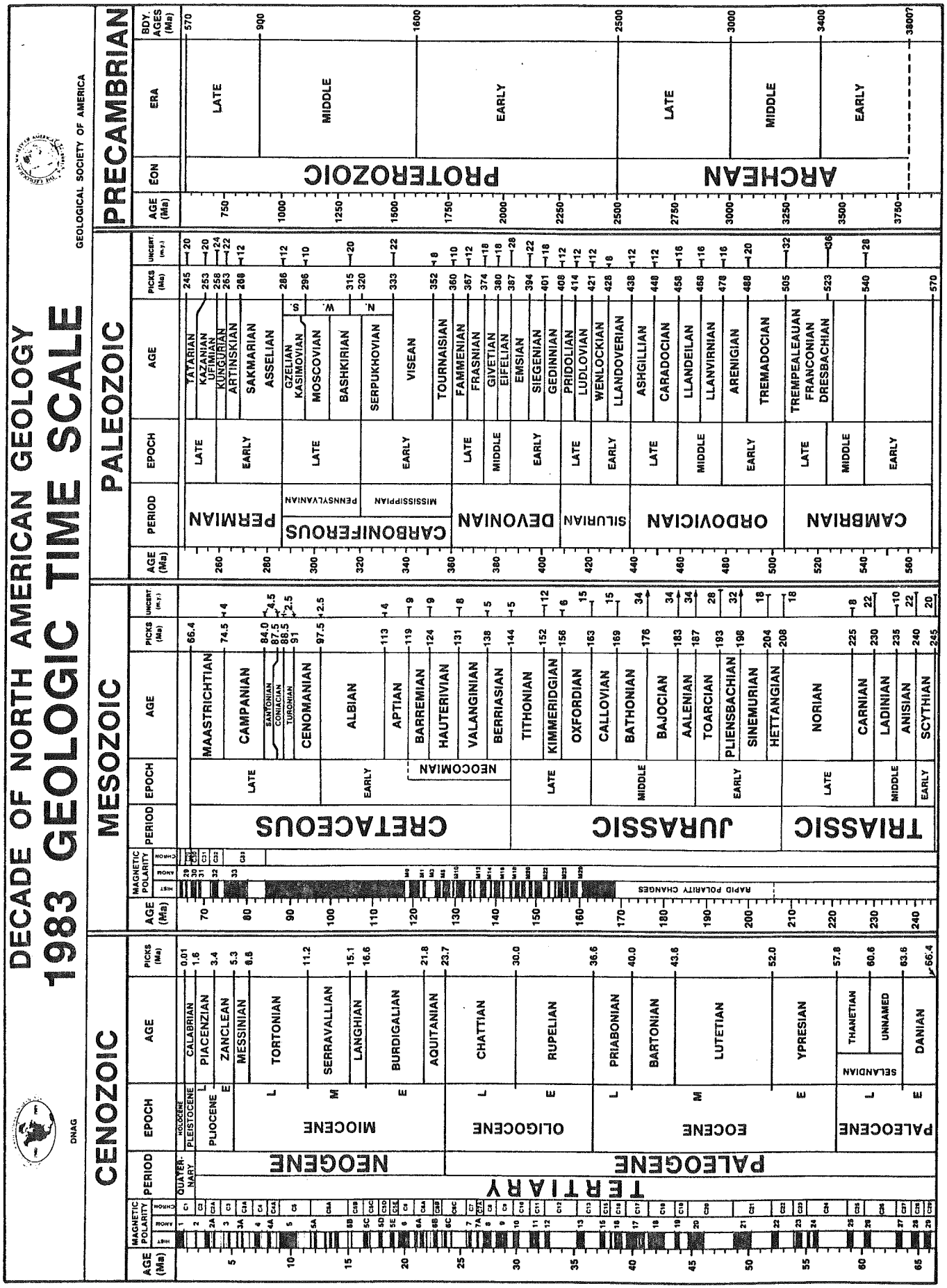
DECADE OF NORTH AMERICAN GEOLOGY
1983 GEOLOGIC TIME SCALE
GEOLOGICAL SOCIETY OF AMERICA
DNAG
CENOZOIC
MESOZOIC
PALEOZOIC
PRECAMBRIAN
AGE (Ma)
EON
ERA
BDY. AGES (Ma)
PERIOD
EPOCH
AGE
PICKS (Ma)
UNCERT (m.y.)
MAGNETIC POLARITY
QUATERNARY
TERTIARY
NEOGENE
PALEOGENE
HOLOCENE
PLEISTOCENE
PLIOCENE
MIOCENE
OLIGOCENE
EOCENE
PALEOCENE
SELANDIAN
CRETACEOUS
JURASSIC
TRIASSIC
PERMIAN
CARBONIFEROUS
PENNSYLVANIAN
MISSISSIPPIAN
DEVONIAN
SILURIAN
ORDOVICIAN
CAMBRIAN
PROTEROZOIC
ARCHEAN
LATE
MIDDLE
EARLY
NEOCOMIAN
CALABRIAN
PIACENZIAN
ZANCLEAN
MESSINIAN
TORTONIAN
SERRAVALLIAN
LANGHIAN
BURDIGALIAN
AQUITANIAN
CHATTIAN
RUPELIAN
PRIABONIAN
BARTONIAN
LUTETIAN
YPRESIAN
THANETIAN
UNNAMED
DANIAN
MAASTRICHTIAN
CAMPANIAN
SANTONIAN
CONIACIAN
TURONIAN
CENOMANIAN
ALBIAN
APTIAN
BARREMIAN
HAUTERIVIAN
VALANGINIAN
BERRIASIAN
TITHONIAN
KIMMERIDGIAN
OXFORDIAN
CALLOVIAN
BATHONIAN
BAJOCIAN
AALENIAN
TOARCIAN
PLIENSBACHIAN
SINEMURIAN
HETTANGIAN
NORIAN
CARNIAN
LADINIAN
ANISIAN
SCYTHIAN
TATARIAN
KAZANIAN
UFIMIAN
KUNGURIAN
ARTINSKIAN
SAKMARIAN
ASSELLIAN
GZELIAN
KASIMOVIAN
MOSCOVIAN
BASHKIRIAN
SERPUKHOVIAN
VISEAN
TOURNAISIAN
FAMMENIAN
FRASNIAN
GIVETIAN
EIFELIAN
EMSIAN
SIEGENIAN
GEDINNIAN
PRIDOLIAN
LUDLOVIAN
WENLOCKIAN
LLANDOVERIAN
ASHGILLIAN
CARADOCIAN
LLANDEILAN
LLANVIRNIAN
ARENIGIAN
TREMADOCIAN
TREMPEALEAUAN
FRANCONIAN
DRESBACHIAN
RAPID POLARITY CHANGES

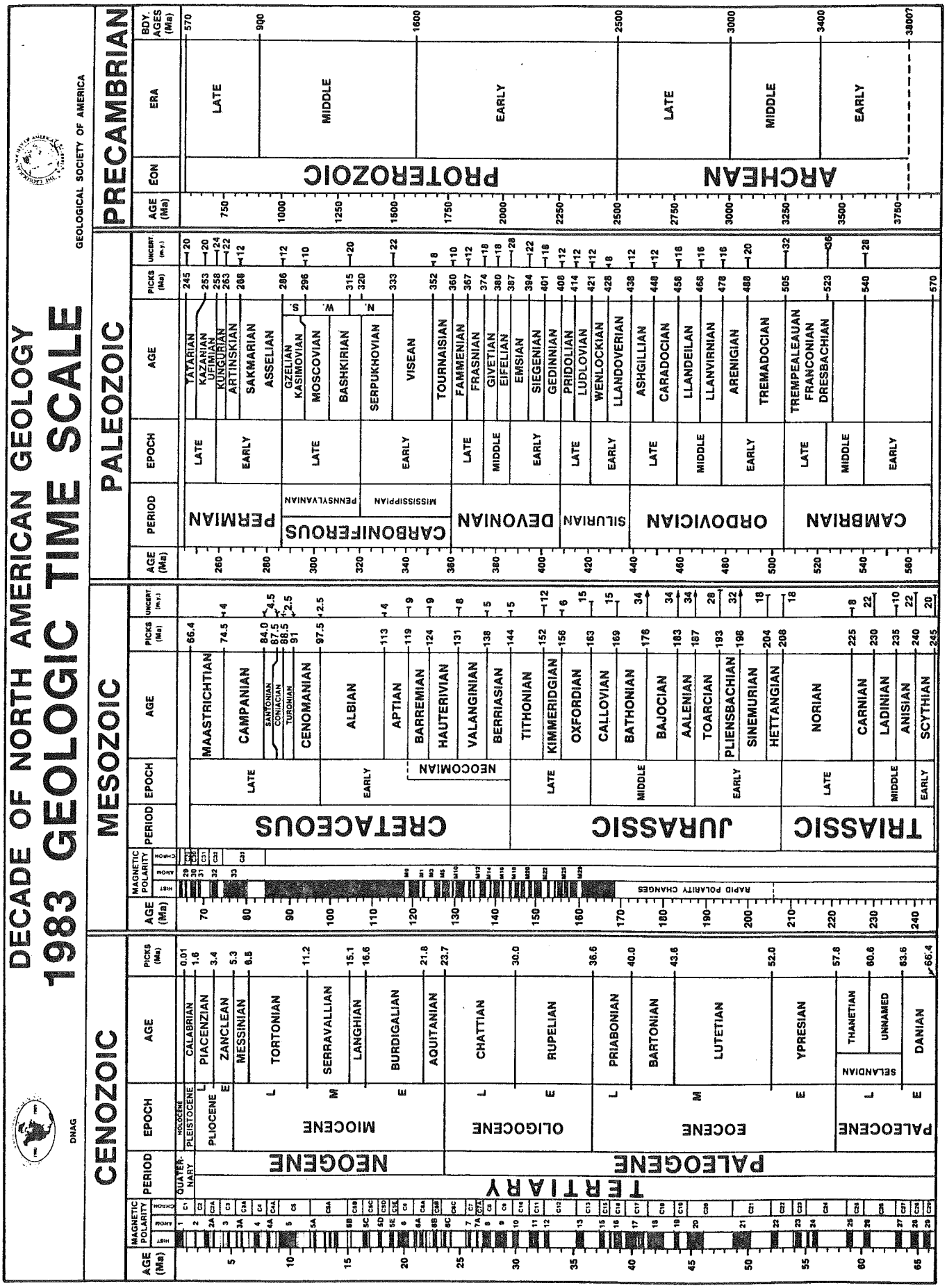
DECADE OF NORTH AMERICAN GEOLOGY
1983 GEOLOGIC TIME SCALE
GEOLOGICAL SOCIETY OF AMERICA
DNAG
CENOZOIC
MESOZOIC
PALEOZOIC
PRECAMBRIAN
AGE (Ma)
MAGNETIC POLARITY
PERIOD
EPOCH
AGE
PICKS (Ma)
UNCERT (m.y.)
QUATERNARY
HOLOCENE
PLEISTOCENE
PLIOCENE
MIOCENE
OLIGOCENE
EOCENE
PALEOCENE
NEOGENE
PALEOGENE
TERTIARY
CALABRIAN
PIACENZIAN
ZANCLEAN
MESSINIAN
TORTONIAN
SERRAVALLIAN
LANGHIAN
BURDIGALIAN
AQUITANIAN
CHATTIAN
RUPELIAN
PRIABONIAN
BARTONIAN
LUTETIAN
YPRESIAN
SELANDIAN
THANETIAN
UNNAMED
DANIAN
CRETACEOUS
JURASSIC
TRIASSIC
LATE
EARLY
NEOCOMIAN
MAASTRICHTIAN
CAMPANIAN
SANTONIAN
CONIACIAN
TURONIAN
CENOMANIAN
ALBIAN
APTIAN
BARREMIAN
HAUTERIVIAN
VALANGINIAN
BERRIASIAN
TITHONIAN
KIMMERIDGIAN
OXFORDIAN
CALLOVIAN
BATHONIAN
BAJOCIAN
AALENIAN
TOARCIAN
PLIENSBACHIAN
SINEMURIAN
HETTANGIAN
NORIAN
CARNIAN
LADINIAN
ANISIAN
SCYTHIAN
RAPID POLARITY CHANGES
PALEOZOIC
PERMIAN
CARBONIFEROUS
DEVONIAN
SILURIAN
ORDOVICIAN
CAMBRIAN
PENNSYLVANIAN
MISSISSIPPIAN
MIDDLE
YATARIAN
KAZANIAN
UFIMIAN
KUNGURIAN
ARTINSKIAN
SAKMARIAN
ASSELIAN
GZELIAN
KASIMOVIAN
MOSCOVIAN
BASHKIRIAN
SERPUKHOVIAN
VISEAN
TOURNAISIAN
FAMMENIAN
FRASNIAN
GIVETIAN
EIFELIAN
EMSIAN
SIEGENIAN
GEDINNIAN
PRIDOLIAN
LUDLOVIAN
WENLOCKIAN
LLANDOVERIAN
ASHGILLIAN
CARADOCIAN
LLANDEILAN
LLANVIRNIAN
ARENIGIAN
TREMADOCIAN
TREMPEALEAUAN
FRANCONIAN
DRESBACHIAN
PRECAMBRIAN
PROTEROZOIC
ARCHEAN
BDY. AGES (Ma)
ERA
EON

SOUTHERN NEVADA BASIN & RANGE ZONE

SOUTHERN HURRICANE – WASATCH ZONE

SOUTHWESTERN PLATEAU MARGIN ZONE

CENTRAL COLORADO PLATEAU ZONE

HURRICANE FAULT

TOROWEAP FAULT

AUBREY

BIG CHINO

VERDE

ARIZONA MOUNTAINS ZONE

SONORAN ZONE

SALTON PERIPHERY ZONE

AXIAL CORTEZ ZONE

EASTERN TRANSVERSE RANGES ZONE

SAN FRANCISCO VOLCANIC ZONE

SOUTHEASTERN PLATEAU MARGIN ZONE

MEXICO BASIN & RANGE ZONE

Littlefield
Fredonia
Page
North Rim
Grand Canyon
Hoover Dam
Bullhead City
Kingman
Williams
Flagstaff
Winslow
Holbrook
Sedona
Cottonwood
Chino Valley
Clarkdale
Jerome
Prescott
Camp Verde
Lake Havasu City
Snowflake
Taylor
St. Johns
Show Low
Pinetop
Springerville
Eagar
Payson
Parker
Wickenburg
Surprise
Goodyear
Phoenix
Tempe
Mesa
Apache Junction
Buckeye
Globe
Miami
Superior
Kearny
Winkelman
Florence
Gila Bend
Casa Grande
Eloy
Mammoth
Yuma
Wellton
Somerton
San Luis
Thatcher
Safford
Clifton
Duncan
Marana
Why
Tucson
South Tucson
Robles Jct.
Lukeville
Willcox
Benson
Tombstone
Sierra Vista
Bisbee
Douglas
Patagonia
Nogales
Sasabe

COCONINO
NAVAJO
APACHE
YAVAPAI
MOHAVE
LA PAZ
MARICOPA
YUMA
PINAL
PIMA
GILA
GRAHAM
GREENLEE
COCHISE
SANTA CRUZ

SCALE:

10 0 10 20 30 40 Miles

10 0 10 20 30 40 50 Kilometers

NORTH

EXPLANATION

Quaternary–Age Fault, letters in circle indicate age of most recent displacement according to table below; numbers represent fault identification no. used in accompanying report.

			Approximate Age (million years before present)
Q– Quaternary < 2 my B.P.	Qy– late Quaternary < 0.5 my B.P.	h – Late to mid Holocene	< 0.005
		H – Early Holocene to Late Pleistocene	0.005– 0.02
		L – Late Pleistocene	0.02 – 0.15
		M – Mid Pleistocene	0.15 – (0.5–0.7)
		E – Early Pleistocene	(0.5–0.7) – 2

Neotectonic Fault of uncertain age, generally of late Pliocene or older Pleistocene age

Highway with milepost markers every ten miles

Seismic source zone boundary

Development of Seismic Maps for Arizona
Report Number: FHWA–AZ92–344
ADOT Contract No: HPR–PL–1(37)344

	Name	Date	ARIZONA DEPARTMENT OF TRANSPORTATION
Drawn			ARIZONA TRANSPORTATION RESEARCH CENTER
Checked			
Team Leader			PLATE 1

FHWA REGION	STATE	PROJECT NUMBER	REPORT NUMBER
9	ARIZ.	HPR–PL–1(37)344	FHWA–AZ92–344

REGISTERED GEOLOGIST CERTIFICATE NO. 10338 KENNETH M. EUGE ARIZONA, U.S.A. Date signed 9-8-92

REGISTERED PROFESSIONAL ENGINEER (CIVIL) CERTIFICATE NO. 25158 IGNATIUS P. LAM ARIZONA, U.S.A. Date signed 9/3/92

DEPARTMENT OF TRANSPORTATION STATE OF ARIZONA DOT

Prepared by

Geological Consultants
2333 West Northern Avenue, Suite 1A
Phoenix, Arizona 85021

&

Earth Mechanics, Inc.
17660 Newhope Street, Suite E
Fountain Valley, California 92708

GEOLOGICAL CONSULTANTS

Earth Mechanics, Inc.
Geotechnical and Earthquake Engineering

FAULT MAP OF ARIZONA AREA

By

Bruce A. Schell, Kenneth M. Euge, and Ignatius Po Lam, 1992

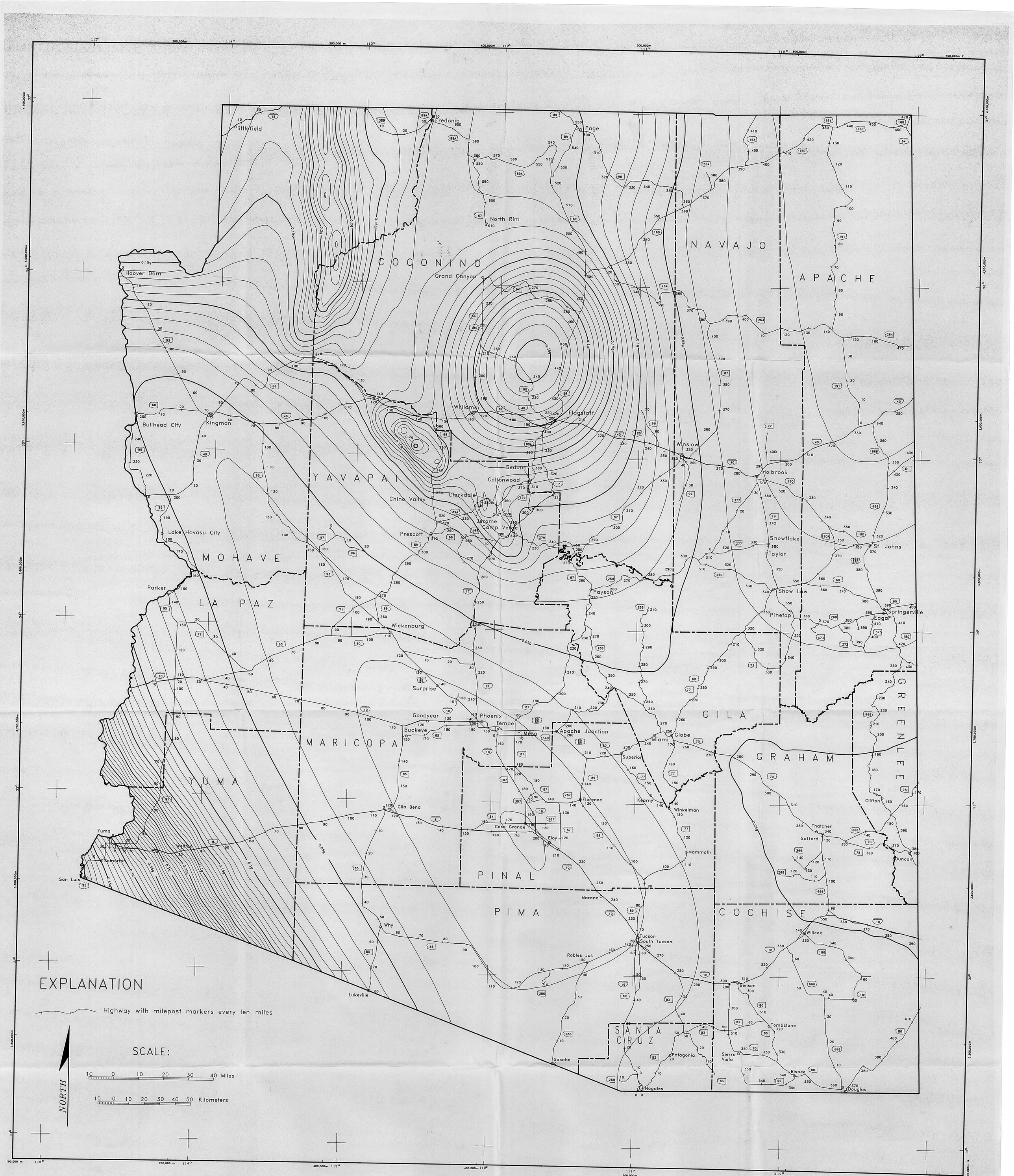

Development of Seismic Maps for Arizona
Report Number: FHWA-AZ92-344
ADOT Contract No: HPR-PL-1(37)344

Prepared by

Geological Consultants
2333 West Northern Avenue, Suite 1A
Phoenix, Arizona 85021

GEOLOGICAL CONSULTANTS

&

Earth Mechanics, Inc.
17660 Newhope Street, Suite E
Fountain Valley, California 92708

Earth Mechanics, Inc.
Geotechnical and Earthquake Engineering

DEPARTMENT OF TRANSPORTATION — DOT — STATE OF ARIZONA

	Name	Date
Drawn		
Checked		
Team Leader		

ARIZONA DEPARTMENT OF TRANSPORTATION
ARIZONA TRANSPORTATION RESEARCH CENTER

PLATE 2a

FHWA REGION	STATE	PROJECT NUMBER	REPORT NUMBER
9	ARIZ.	HPR-PL-1(37)344	FHWA-AZ92-344

REGISTERED GEOLOGIST — CERTIFICATE NO. 10339 — KENNETH M. EUGE — Date Signed 9-2-92 — ARIZONA, U.S.A.

REGISTERED PROFESSIONAL ENGINEER (CIVIL) — CERTIFICATE NO. 25158 — IGNATIUS P. LAM — Date Signed 8/31/92 — ARIZONA, U.S.A.

MAP OF HORIZONTAL ACCELERATION AT BEDROCK FOR ARIZONA
with 90 Percent Probability of Non-Exceedance in 50 Years

By
Ignatius Po Lam, Bruce A. Schell and Kenneth M. Euge, 1992

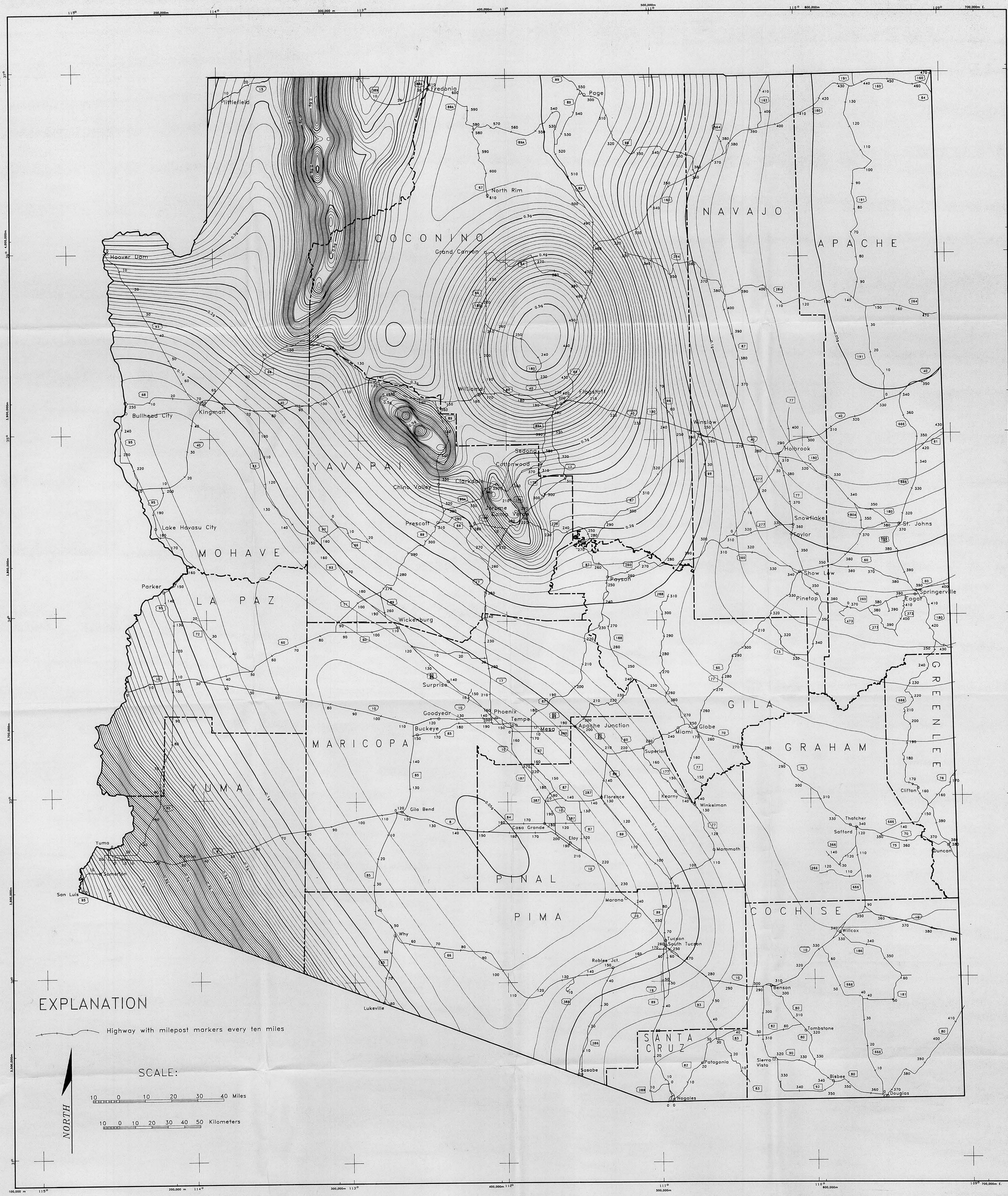

EXPLANATION

Highway with milepost markers every ten miles

NORTH

SCALE:

10 0 10 20 30 40 Miles

10 0 10 20 30 40 50 Kilometers

Development of Seismic Maps for Arizona
Report Number: FHWA-AZ92-344
ADOT Contract No: HPR-PL-1(37)344

Prepared by

Geological Consultants
2333 West Northern Avenue, Suite 1A
Phoenix, Arizona 85021

GEOLOGICAL CONSULTANTS

&

Earth Mechanics, Inc.
17660 Newhope Street, Suite E
Fountain Valley, California 92708

Earth Mechanics, Inc.
Geotechnical and Earthquake Engineering

DEPARTMENT OF TRANSPORTATION DOT STATE OF ARIZONA

	Name	Date
Drawn		
Checked		
Team Leader		

ARIZONA DEPARTMENT OF TRANSPORTATION
ARIZONA TRANSPORTATION RESEARCH CENTER

PLATE 2b

FHWA REGION	STATE	PROJECT NUMBER	REPORT NUMBER
9	ARIZ.	HPR-PL-1(37)344	FHWA-AZ92-344

REGISTERED GEOLOGIST CERTIFICATE NO. 10338 KENNETH M. EUGE Date Signed 9-8-92 ARIZONA, U.S.A.

REGISTERED PROFESSIONAL ENGINEER (CIVIL) CERTIFICATE NO. 25158 IGNATIUS P. LAM Date Signed 8/31/92 ARIZONA, U.S.A.

MAP OF HORIZONTAL ACCELERATION AT BEDROCK FOR ARIZONA
with 90 Percent Probability of Non-Exceedance in 250 Years

By

Ignatius Po Lam, Bruce A. Schell and Kenneth M. Euge, 1992

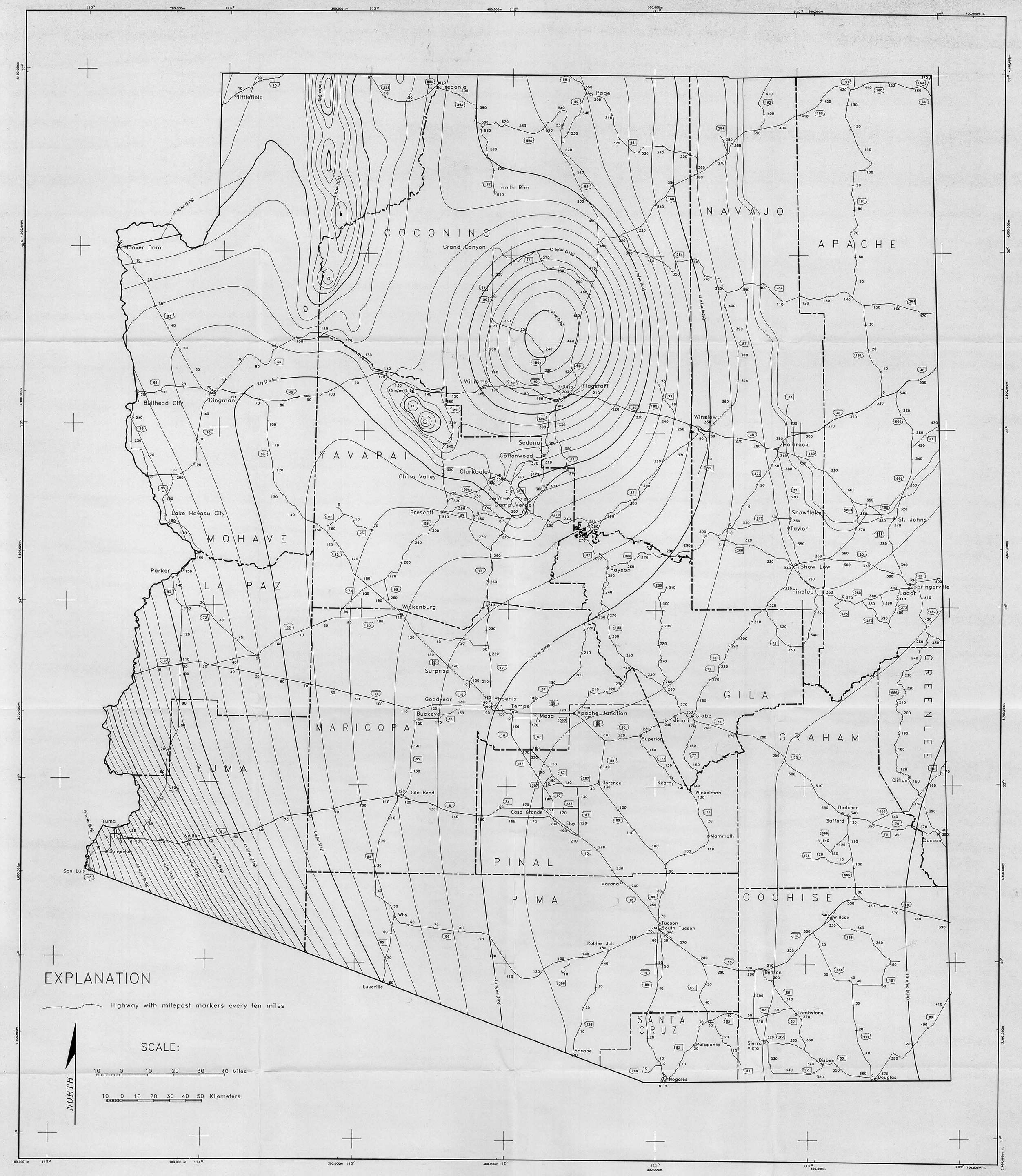

EXPLANATION

Highway with milepost markers every ten miles

NORTH

SCALE:

10 0 10 20 30 40 Miles

10 0 10 20 30 40 50 Kilometers

Development of Seismic Maps for Arizona
Report Number: FHWA-AZ92-344
ADOT Contract No: HPR-PL-1(37)344

Prepared by

Geological Consultants
2333 West Northern Avenue, Suite 1A
Phoenix, Arizona 85021

GEOLOGICAL CONSULTANTS

&

Earth Mechanics, Inc.
17660 Newhope Street, Suite E
Fountain Valley, California 92708

Earth Mechanics, Inc.
Geotechnical and Earthquake Engineering

DEPARTMENT OF TRANSPORTATION DOT STATE OF ARIZONA

	Name	Date
Drawn		
Checked		
Team Leader		

ARIZONA DEPARTMENT OF TRANSPORTATION
ARIZONA TRANSPORTATION RESEARCH CENTER

PLATE 2c

FHWA REGION	STATE	PROJECT NUMBER	REPORT NUMBER
9	ARIZ.	HPR-PL-1(37)344	FHWA-AZ92-344

REGISTERED GEOLOGIST CERTIFICATE NO. 10338 KENNETH M. EUGE Date Signed 8-3-92 ARIZONA, U.S.A.

REGISTERED PROFESSIONAL ENGINEER (CIVIL) CERTIFICATE NO. 25158 IGNATIUS P. LAM Date Signed 8/3/92 ARIZONA, U.S.A.

MAP OF HORIZONTAL VELOCITY (A_v) AT BEDROCK FOR ARIZONA with 90 Percent Probability of Non-Exceedance in 50 Years

By

Ignatius Po Lam, Bruce A. Schell and Kenneth M. Euge, 1992

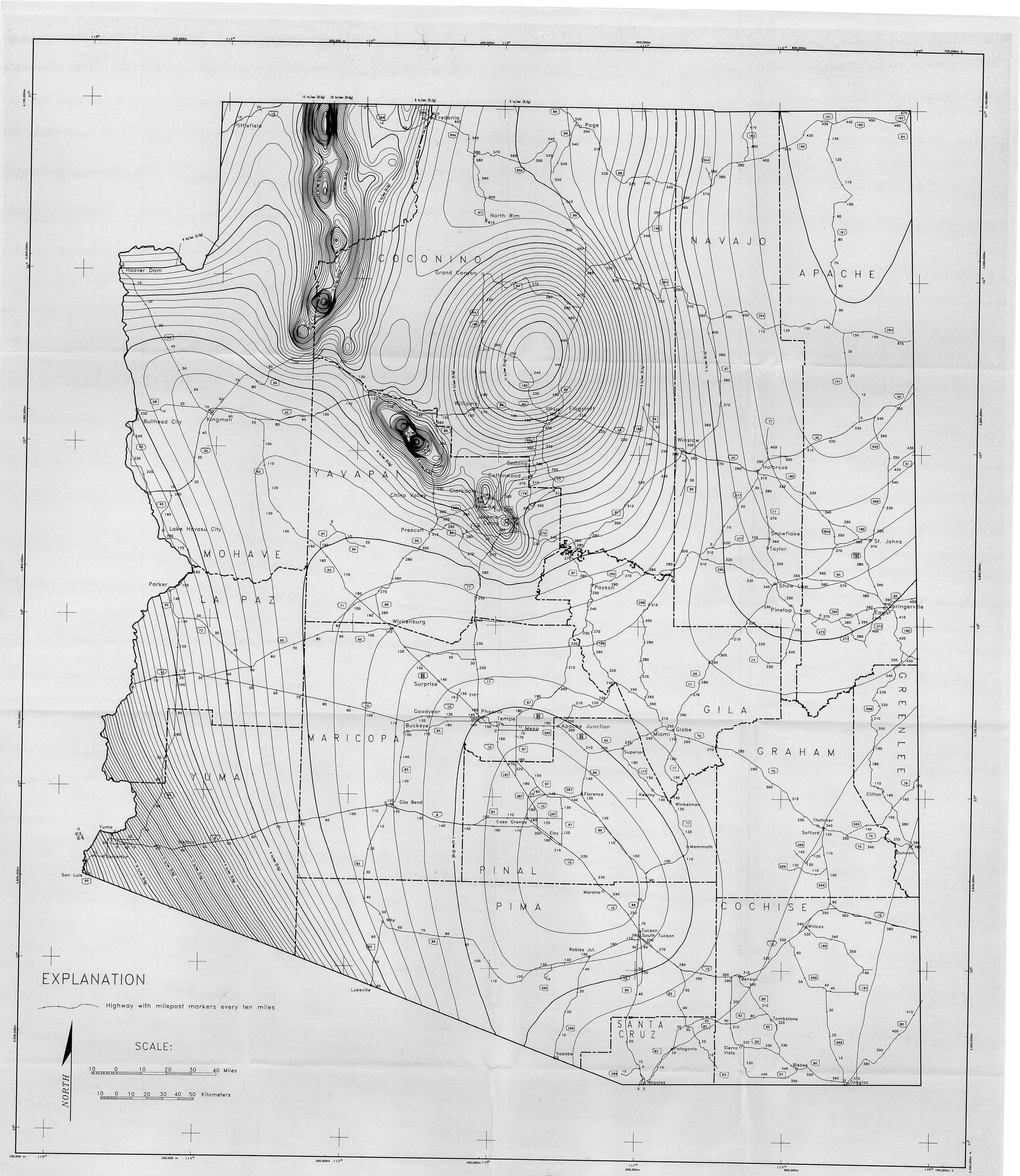

Development of Seismic Maps for Arizona
Report Number: FHWA-AZ92-344
ADOT Contract No: HPR-PL-1(37)344

Prepared by

Geological Consultants
2333 West Northern Avenue, Suite 1A
Phoenix, Arizona 85021

GEOLOGICAL CONSULTANTS

&

Earth Mechanics, Inc.
17660 Newhope Street, Suite E
Fountain Valley, California 92708

Earth Mechanics, Inc.
Geotechnical and Earthquake Engineering

	Name	Date
Drawn		
Checked		
Team Leader		

ARIZONA DEPARTMENT OF TRANSPORTATION
ARIZONA TRANSPORTATION RESEARCH CENTER

PLATE 2d

FHWA REGION	STATE	PROJECT NUMBER	REPORT NUMBER
9	ARIZ.	HPR-PL-1(37)344	FHWA-AZ92-344

REGISTERED GEOLOGIST CERTIFICATE NO. 10338 KENNETH M. EUGE Date Signed 4-8-92 ARIZONA, U.S.A.

REGISTERED PROFESSIONAL ENGINEER (CIVIL) CERTIFICATE NO. 25158 IGNATIUS P. LAM Date Signed 8/31/92 ARIZONA, U.S.A.

MAP OF HORIZONTAL VELOCITY (CORRESPONDING A_v) AT BEDROCK FOR ARIZONA with 90 Percent Probability of Non-Exceedance in 250 Years

By

Ignatius Po Lam, Bruce A. Schell and Kenneth M. Euge, 1992